

Protein recognition and degradation via the N-end rule pathway

H a b i l i t a t i o n s s c h r i f t

zur Erlangung des akademischen Grades

doctor rerum naturalium habilitatus (Dr. rer. nat. habil.)

vorgelegt der

Naturwissenschaftlichen Fakultät I
Biowissenschaften

der Martin-Luther-Universität Halle-Wittenberg

von

Herrn Dr. rer. nat. Nico Dissmeyer

geboren am 11. Mai 1979 in Detmold

Gutachter/in

1. Professor Sacha Baginsky, Halle
2. Professor Claus Schwechheimer, Freising
3. Professor Michael J. Holdsworth, Nottingham

Halle (Saale), 10. September, 2018

„Wir wissen noch nicht, warum wir das hier machen, aber in Zukunft werden wir das verstehen.“

Joseph Beuys.

CONTENTS

CONTENTS	5
ABSTRACT	7
1 PART I – BIOLOGY OF THE N-END RULE	9
1.1 INTRODUCTION PART I – BIOLOGY	9
1.1.1 Proteases prime targets for recognition by the N-end rule	9
1.2 OBJECTIVES PART I – BIOLOGY	17
1.3 RESULTS PART I – BIOLOGY	18
1.3.1 PROTEOLYSIS1 is a highly specific N-end rule E3 Ubiquitin ligase	19
1.3.2 Core regulator of cell differentiation is the first PROTEOLYSIS1 target	33
1.3.3 Cysteine dioxygenation enables subsequent arginylation in the N-end rule pathway	47
1.4 OUTLOOK PART I – BIOLOGY	57
2 PART II – BIOTECHNOLOGY OF THE N-END RULE	59
2.1 INTRODUCTION PART II – BIOTECHNOLOGY	59
2.1.1 Conditional expression and degradation as genetic tools	59
2.1.2 Manipulation of biological processes via conditional proteolysis	86
2.2 OBJECTIVES PART II – BIOTECHNOLOGY	97
2.3 RESULTS PART II – BIOTECHNOLOGY	97
2.3.1 Phenotypes on demand via switchable target protein degradation in multicellular organisms	98
2.4 OUTLOOK PART II – BIOTECHNOLOGY	115
3 CONCLUSION	117
REFERENCES	119
ACKNOWLEDGEMENT	121
ERKLÄRUNG	123
CURRICULUM VITAE	125

ABSTRACT

The activity and abundance of proteins within a cell are precisely controlled to ensure the physiological regulation of cellular processes. Protein quality control systems sense proteins that need to be removed from the cell. In eukaryotes, this can be achieved by targeting specific proteins for degradation by the Ubiquitin-proteasome system. The N-end rule pathway is a subset of the Ubiquitin-proteasome system and targets proteins for degradation mainly depending on the identity of a protein's N-terminal residue or its post-translational modifications involving a hierarchical cascade of highly specific enzymes. This cascade comprises E3 Ubiquitin protein ligases, aminoacyltransferases, deamidases and dioxygenases.

My main interest is on protein homeostasis (proteostasis) mediated by posttranslational protein modifications via these highly diverse enzymes and includes enzymatic mechanisms and their regulation, substrate identification and genetics of the N-end rule modification system, its role in stress conditions and development and harnessing the N-end rule pathway for genetic and biotechnological applications.

Here, I describe molecular principles as well as recently found functions and applications of the N-end rule pathway. I highlight on the one hand a potentially predominant role in break-down of regulatory proteins and targets undergoing proteolytic cleavage as part of their posttranslational modification. On the other hand, I demonstrate distinct applications for the N-end rule pathway in multicellular organisms that can be used as tools in genetic and biotechnological contexts. A focus is on our current understanding of N-end rule substrate formation by protease cleavage and the roles and bottlenecks of state-of-the-art techniques in substrate identification and characterization of the role of the N-end rule in physiological processes.

1 PART I – BIOLOGY OF THE N-END RULE

1.1 INTRODUCTION PART I – BIOLOGY

A fundamental question of research on proteostatic control via the N-end rule pathway is – besides revealing the actual identity of *in vivo* targets – how substrates are generated, detected, experimentally confirmed and what the biological cause is. In the following chapter, the current understanding of substrate formation via proteolytic cleavage, state-of-the-art of analytical methods and experimental caveats are described.

1.1.1 Proteases prime targets for recognition by the N-end rule

This publication deals with the current understanding on N-end rule substrate generation, current methods on analysing N-terminal modifications and mapping the so-called neo-N-termini of proteolytic events and highlight the difficulties and bottlenecks of identifying and characterizing N-end rule substrate candidates.

Publication:

Dissmeyer N*, Rivas S, Graciet E.* Life and death of proteins after protease cleavage: protein degradation by the N-end rule pathway.
New Phytol, in print.



Tansley insight

Life and death of proteins after protease cleavage: protein degradation by the N-end rule pathway

Authors for correspondence:
Emmanuelle Graciet
Tel: +353 1 708 6255
Email: Emmanuelle.Graciet@nuim.ie

Nico Dissmeyer
Tel: +49 345 5582 1710
Email: nico.dissmeyer@ipb.halle.de

Received: 30 November 2016
Accepted: 4 April 2017

Nico Dissmeyer^{1,2}, Susana Rivas³ and Emmanuelle Graciet⁴

¹Independent Junior Research Group on Protein Recognition and Degradation, Leibniz Institute of Plant Biochemistry (IPB), Weinberg 3, Halle (Saale) D-06120, Germany; ²ScienceCampus Halle – Plant-based Bioeconomy, Betty-Heimann-Strasse 3, Halle (Saale) D-06120, Germany; ³LIPM, Université de Toulouse, INRA, CNRS, Castanet-Tolosan 31 326, France; ⁴Department of Biology, Maynooth University, Maynooth, Co. Kildare, Ireland

Contents

Summary	1	V. Concluding remarks	4
I. Introduction: conservation and diversity of N end rule pathways	1	Acknowledgements	6
II. Defensive functions of the N end rule pathway in plants	2	References	6
III. Proteases and degradation by the N end rule pathway	2		
IV. New proteomics approaches for the identification of N end rule substrates	4		

Summary

The N end rule relates the stability of a protein to the identity of its N terminal residue and some of its modifications. Since its discovery in the 1980s, the repertoire of N terminal degradation signals has expanded, leading to a diversity of N end rule pathways. Although some of these newly discovered N end rule pathways remain largely unexplored in plants, recent discoveries have highlighted roles of N end rule mediated protein degradation in plant defense against pathogens and in cell proliferation during organ growth. Despite this progress, a bottleneck remains the proteome wide identification of N end rule substrates due to the prerequisite for endoproteolytic cleavage and technical limitations. Here, we discuss the recent diversification of N end rule pathways and their newly discovered functions in plant defenses, stressing the role of proteases. We expect that novel proteomics techniques (N terminomics) will be essential for substrate identification. We review these methods, their limitations and future developments.

New Phytologist (2017)
doi: 10.1111/nph.14619

Key words: arginylation, cysteine oxidation, N degron, N end rule pathway, N recognins, N terminomics, proteases, ubiquitin proteasome system.

I. Introduction: conservation and diversity of N-end rule pathways

The control of protein stability plays a key role in the regulation of all cellular processes and, in eukaryotes, is largely controlled by the ubiquitin proteasome system (UPS). The N end rule pathway, a subset of the UPS, relates the *in vivo* half life of a protein to the nature of its N terminal amino acid residue and some of its

post translational modifications (PTMs). Removal of the initiator Met residue by methionine aminopeptidases (MetAPs) or cleavage of pre proproteins (i.e. proteins that bear signal peptides and/or that require cleavage for their activation or degradation) by endoproteases exposes new N terminal residues, potentially directing the resulting protein fragments for degradation by the N end rule pathway (Fig. 1). In eukaryotes, the N end rule pathway comprises different branches that mediate the degradation

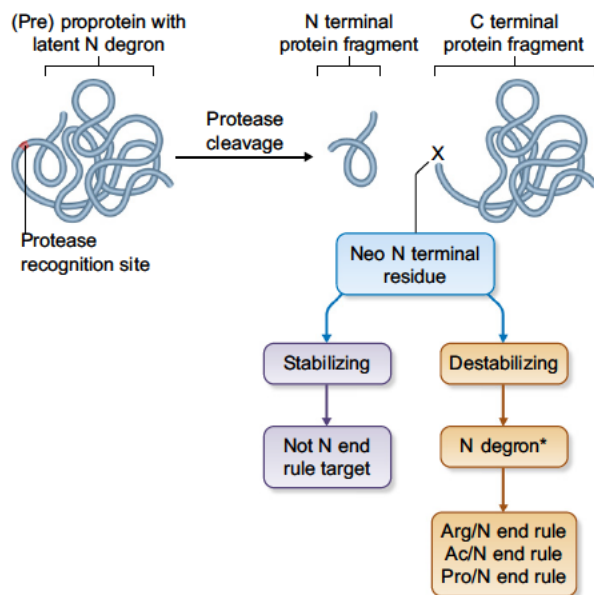


Fig. 1 Role of proteases in the generation of N end rule substrates. Endoproteolytic cleavage of a pre proprotein results in the exposure of a new N terminal or 'neo N terminal' residue. This endoproteolytic event can expose to the solvent a 'latent' or 'dominant' N terminal degradation signal, or N degron, that was previously buried in the internal sequence of the protease recognition site. Neo N terminal residues may be either 'stabilizing' or 'destabilizing' based on the Arg/ or Ac/ or Pro/N end rule and may hence serve to target the protein fragment for degradation by the N end rule pathway. However, not all N terminal destabilizing residues lead to a functional N degron (denoted by an asterisk) and degradation of the target protein. Additional structural and sequence features, such as flexibility of the N terminal region, presence of Lys side chains as ubiquitin acceptor sites and charge or hydrophobicity of residues close to the neo N terminal, are also critical for an N end rule target. Furthermore, the N terminal methionine residue of a protein may serve directly as a destabilizing residue, so that endoproteolytic cleavage is not always a prerequisite.

of proteins whose N terminal residues are acetylated (Ac/N end rule) and non acetylated, respectively (reviewed by Varshavsky, 2011; Gibbs *et al.*, 2016). Together, these two branches of the N end rule pathway can recognize all existing N terminal amino acid residues and some of their modifications. This includes the initiator Met residue that is typically found at the N terminus of proteins (Hwang *et al.*, 2010; Kim *et al.*, 2014).

Recent findings have led to an expansion of the acetylation independent branch, which now comprises the 'classic' Arg/N end rule (described in more detail below) and the newly found Pro/N end rule pathway (Chen *et al.*, 2017). The latter was discovered in yeast and targets for degradation proteins with Pro at first or second position through the activity of Gid4, a subunit of the GID ubiquitin ligase (Santt *et al.*, 2008) that targets gluconeogenic enzymes in yeast (Hammerle *et al.*, 1998; Chen *et al.*, 2017). While it is not yet known whether the Pro/N end rule is present in multicellular eukaryotes, components of the Arg/ and Ac/N end rule pathways appear to be mostly conserved (reviewed by Varshavsky, 2011; Tasaki *et al.*, 2012; Lee *et al.*, 2016). For example, the hierarchical organization of the Arg/N end rule

pathway is overall the same in eukaryotes (Fig. 2): N terminal primary destabilizing residues can be directly bound by E3 ligases called N recognins; secondary destabilizing residues require conjugation of Arg (a primary destabilizing residue) by the conserved Arg transferases (ATEs); and tertiary destabilizing residues are first enzymatically or chemically transformed into secondary destabilizing residues before arginylation by ATEs.

The evolutionary conservation of different N end rule pathways is further underlined by the recent suggestion that chloroplasts (Rowland *et al.*, 2015; Zhang *et al.*, 2015) and mitochondria (Vogtle *et al.*, 2009; Calvo *et al.*, 2017) might also have organelle specific N end rule pathways that resemble that of prokaryotes.

II. Defensive functions of the N-end rule pathway in plants

While the recent diversification of N end rule pathways in eukaryotes has expanded the repertoire of destabilizing residues and modifications that serve as N terminal degradation signals (or N degrons), in plants, functions of the Ac/ and Arg/N end rule pathways are just emerging. In particular, these pathways have been involved in plant responses to a variety of developmental and environmental signals (reviewed by Gibbs *et al.*, 2014, 2016; Lee *et al.*, 2016). The most recent discoveries include their role in the control of plant defense responses. First, the stability of the Nod like immune receptors (NLRs) SUPPRESSOR OF NPR1, CONSTITUTIVE1 (SNC1) and RESISTANCE TO *Pseudomonas syringae* pv. *maculicola* (RPM1) is regulated through N terminal acetylation (Xu *et al.*, 2015). It is tempting to speculate that the Ac/N end rule pathway might participate in NLR homeostasis, as NatA mediated acetylation of the first Met residue of SNC1 contributes to its degradation. Second, a new role for the Arg/N end rule pathway was uncovered in activating the production of defense related metabolites, such as glucosinolates and the phytohormone jasmonic acid (de Marchi *et al.*, 2016). It was additionally shown that the Arg/N end rule pathway positively regulates defenses against a wide range of bacterial and fungal pathogens with different lifestyles and, more particularly, that the ATEs regulate the timing and amplitude of the defense program against avirulent bacteria (de Marchi *et al.*, 2016). That study also led to the discovery of the first physiological function of the PRT1 N recognin, which appears to act as a positive regulator of plant defenses (de Marchi *et al.*, 2016). Third, a recent report highlighted a link between the known functions of the Arg/N end rule pathway in the degradation of key transcriptional regulators of the hypoxia response (the ERFVII transcription factors; Gibbs *et al.*, 2016) and *Arabidopsis* infection by the protist *Plasmodiophora brassicae*, which triggers clubroot development (Gravot *et al.*, 2016). Their study suggests strongly that Arg/N end rule driven hypoxia responses may be a general feature of pathogen induced gall development in plants.

III. Proteases and degradation by the N-end rule pathway

Despite recent progress in our understanding of the Ac/ and Arg/N end rule pathways in plants, elucidation of the underlying

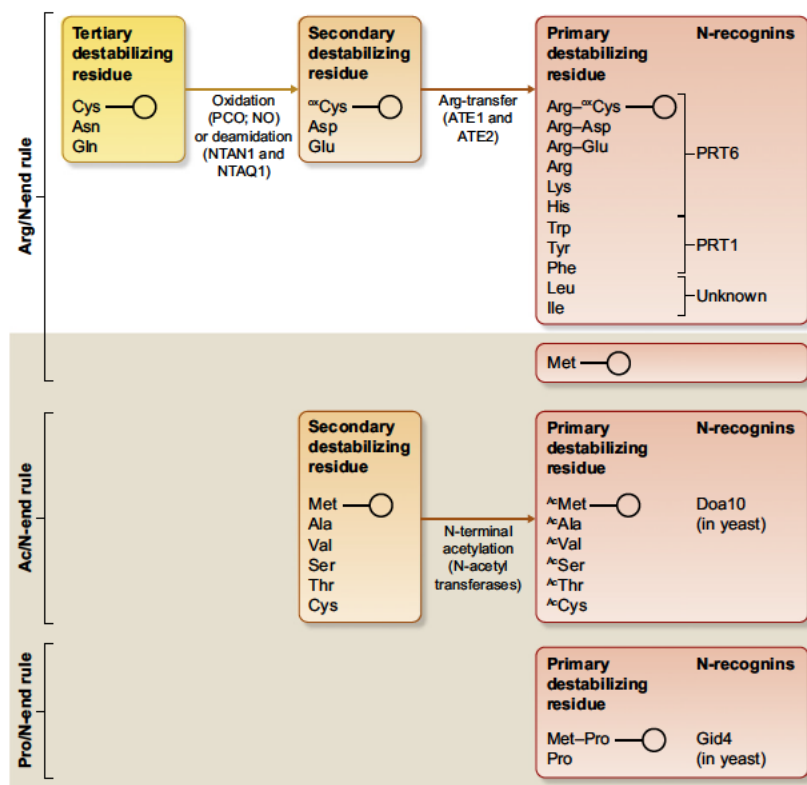


Fig. 2 Canonical N end rule pathways. The neo N terminus of a protein may be a tertiary (yellow), secondary (orange) or primary (red) destabilizing residue. One potential outcome of the exposure of neo N termini is their modification involving deamidation or Cys oxidation, arginylation, acetylation and finally ubiquitylation, followed by degradation of the protein by the Arg/, Ac/ or Pro/N end rule pathways. Protein fragments starting with primary destabilizing residues can be recognized and bound by so called N recognins, which belong to the class of E3 ubiquitin ligases. *In vivo* studies with artificial N end rule reporter substrates in plants show that PRT6 is specific for positively charged or Type 1 residues (Garzon *et al.*, 2007) and that PRT1 recognizes aromatic hydrophobic or Type 2 residues (Potuschak *et al.*, 1998). Furthermore, *in vitro* ubiquitylation assays of fluorescently labeled artificial N end rule substrates confirmed the specificity of PRT1 and its E3 ligase activity (Mot *et al.*, 2017). Note that the degradation of proteins with N terminal Met, as well as through the Ac/ and Pro/N end rule (all represented on a beige background) have not yet been demonstrated to exist in plants, but are found in yeast (Hammerle *et al.*, 1998; Chen *et al.*, 2017). In yeast, the Ac/N end rule requires the activity of the E3 ligase Doa10. The Ac/N end rule is also found in animals (Hwang *et al.*, 2010; Varshavsky, 2011). Circles denote the C terminal protein fragments after endoproteolytic cleavage. NO, nitric oxide; PCO, PLANT CYSTEINE OXIDASE.

molecular mechanisms has remained largely elusive due to technical difficulties for the proteome wide identification of N end rule substrates and the complex mechanisms that lead to their formation. Indeed, most Arg/N end rule substrates identified in yeast and animals are generated through protease cleavage (Figs 1, 2; Rao *et al.*, 2001; Ditzel *et al.*, 2003; Piatkov *et al.*, 2012a,b; Brower *et al.*, 2013; reviewed by Tasaki *et al.*, 2012), making it difficult to predict N end rule substrates without detailed knowledge of protease cleavage sites and substrates. Moreover, an N terminal destabilizing residue is not necessarily sufficient for the generation of an N degron. Indeed, the accessibility of the N terminal residue for N recognin binding, the properties of the residues neighboring the N terminus and the proximity of a Lys residue that may be ubiquitylated are also important (Tasaki *et al.*, 2012; Wadas *et al.*, 2016; Mot *et al.*, 2017). The complexity of an N degron probably explains why many proteins with a presumed N terminal destabilizing residue appear to be relatively abundant and stable in plant cells (Li *et al.*, 2017).

As highlighted by two recent proteomics studies, endoproteolytic events that can lead to N end rule mediated degradation of protein fragments are prevalent in plant cells. The first study (Zhang *et al.*, 2015) used quantitative proteomics to identify N end rule substrates that were expected to accumulate in Arg/N end rule mutants compared to the wild type. The second study (Venne *et al.*, 2015) aimed at advancing techniques to characterize and quantify neo N termini for dissecting proteolytic events. Despite using different methods, the majority of N terminal fragments identified in these studies were the result of a protease cleavage or of initiator Met excision, suggesting that most intracellular proteins are endoproteolytically processed. However, most of the newly exposed N terminal residues were not destabilizing based on the Arg/N end rule, suggesting that: (1) many proteolytic fragments are not substrates of the Arg/N end rule pathway; and (2) fragments starting with destabilizing residues may not be detected, possibly because of their rapid Arg/N end rule dependent degradation. Moreover, N terminal

acetylation accounted for 55% of the N terminal fragments identified, with most of these appearing to be acetylated co-translationally. These results hence also highlight the potential relevance of the Ac/N end rule pathway in plants (Zhang *et al.*, 2015).

How can N end rule substrates be identified given the prerequisite for protease cleavage? One possibility is to use knowledge of protease substrates and cleavage sites. The latest example of an N end rule substrate identified using such information is that of the organ size regulator BIG BROTHER, which is cleaved by the protease DA1 in *Arabidopsis*. The resulting C terminal fragment then appears to be targeted for degradation by the N recognin PRT1 (Dong *et al.*, 2017). It is also worth noting that the recently discovered defensive functions of the Ac/ and Arg/N end rule pathways are coherent with a potential role of defense related plant proteases (including MetAPs) in generating N end rule substrates. One example highlighting the connection between proteases and the generation of N end rule substrates during plant pathogen interactions is the cleavage of the central *Arabidopsis* defense regulator RPM1 INTERACTING PROTEIN4 (RIN4) by the *P. syringae* protease effector AvrRpt2, which leads to RIN4 fragments with potential N terminal destabilizing residues (Chisholm *et al.*, 2005; Eschen Lippold *et al.*, 2016). Although no *in vivo* evidence has been provided to date, it has been suggested that AvrRpt2 derived RIN4 fragments could be degraded by the Arg/N end rule pathway (Takemoto & Jones, 2005). Yet another example is the list of potential N end rule substrates generated following cleavage by METACASPASE9 in *Arabidopsis* (Tsiatsiani *et al.*, 2013). However, similarly to RIN4, *in vivo* evidence that any of these fragments are degraded by the N end rule pathways is still lacking.

Other putative N end rule substrates may be predicted using the primary sequence of proteins starting with Met Cys, as MetAPs may excise the initial Met residue, exposing the Cys at the N terminus of the protein. The resulting N terminal Cys residue may then be oxidized through either a chemical reaction or the activity of Cys oxidases (Fig. 2). The latter, termed PLANT CYSTEINE OXIDASES (PCOs), have so far only been found in plants (Weits *et al.*, 2014) and generate N terminal Cys sulfinic acid (White *et al.*, 2016), which can act as an N degron.

Finally, novel developments that further highlight the role of proteases in the generation of N end rule substrates in plants include the potential existence of a chloroplast specific N end rule (Nishimura & van Wijk, 2015). Indeed, recent studies show that following cleavage of the chloroplast transit peptide, destabilizing residues (of the prokaryotic N end rule pathway) are under represented in nuclear encoded chloroplast proteins (Rowland *et al.*, 2015; Zhang *et al.*, 2015). Together with the recent discovery of a chloroplast ortholog of the bacterial ClpS N recognin (Nishimura *et al.*, 2013), these results suggest that stromal processing peptidases may play a role in the generation of chloroplast N end rule substrates (Rowland *et al.*, 2015). Strikingly, a mitochondrion specific N end rule with similarities to the prokaryotic N end rule could also exist (Vogtle *et al.*, 2009; Calvo *et al.*, 2017).

IV. New proteomics approaches for the identification of N-end rule substrates

Given the pre eminent role of proteases in the generation of N end rule substrates, recent attempts at discovering new N end rule substrates in plants have relied on novel proteomics techniques, termed N terminomics, that were initially developed to characterize proteolytic events and identify newly exposed neo N terminal residues and their PTMs (e.g. acetylation, oxidation, deamidation, arginylation) (Fig. 3). These novel N terminomics techniques address some of the limitations of shotgun proteomics approaches, which had been developed to compare global protein abundance (e.g. in a wild type vs a mutant plant), but could not provide information on the identity of N terminal residues and potential N end rule substrates (Majovsky *et al.*, 2014).

N terminomics approaches are based on targeted enrichment of N terminal peptides through chemical labeling of α amine groups of N terminal residues, which makes them distinguishable from internal amines derived from sample treatment by proteases (Huesgen & Overall, 2012). This specific N terminal labeling reduces the complexity of the peptide mixtures and allows the identification of the true N termini of mature proteins. N terminomics approaches use various strategies to separate N terminal peptides from internal ones. COmbined FRActional Diagonal Chromatography (COFRADIC; Gevaert *et al.*, 2003) and Charge based FRActional Diagonal Chromatography (ChaFRADIC; Venne *et al.*, 2013) rely on different chromatographic techniques to enrich for N terminal peptides. Terminal Amine Isotopic Labeling of Substrates (TAILS; Kleifeld *et al.*, 2010; Rowland *et al.*, 2015; Zhang *et al.*, 2015) allows the capture of N terminal peptides via chemical modification. Other techniques include Stable Isotope Protein N terminal Acetylation Quantification (SILProNAQ; Bienvenu *et al.*, 2015) and Proteomic Identification of protease Cleavage Sites (PICS; Schilling *et al.*, 2011). Importantly, these techniques can be coupled with immunoprecipitation approaches, for example using antibodies raised against artificial peptides harboring specific destabilizing N terminal residues, to further enrich samples for N end rule substrates (Hoernstein *et al.*, 2016). As these techniques develop further, we expect that they will greatly contribute to our understanding of the molecular mechanisms underlying the functions of the N end rule pathway in plants.

V. Concluding remarks

How the regulation of protein stability contributes to developmental processes and to plant responses to environmental cues remains a key question. In recent years, the N end rule pathway has emerged as an important regulator of these processes. Despite this progress, the number of known N end rule substrates remains small, largely due to the complex proteolytic mechanisms that lead to their formation. Indeed, specific endogenous or exogenous triggers, such as a stress or developmental cues, that lead to endoproteolytic cleavage and exposure of N terminal destabilizing residues are often required to generate N end rule substrates. Hence, these substrates might only be generated in specific

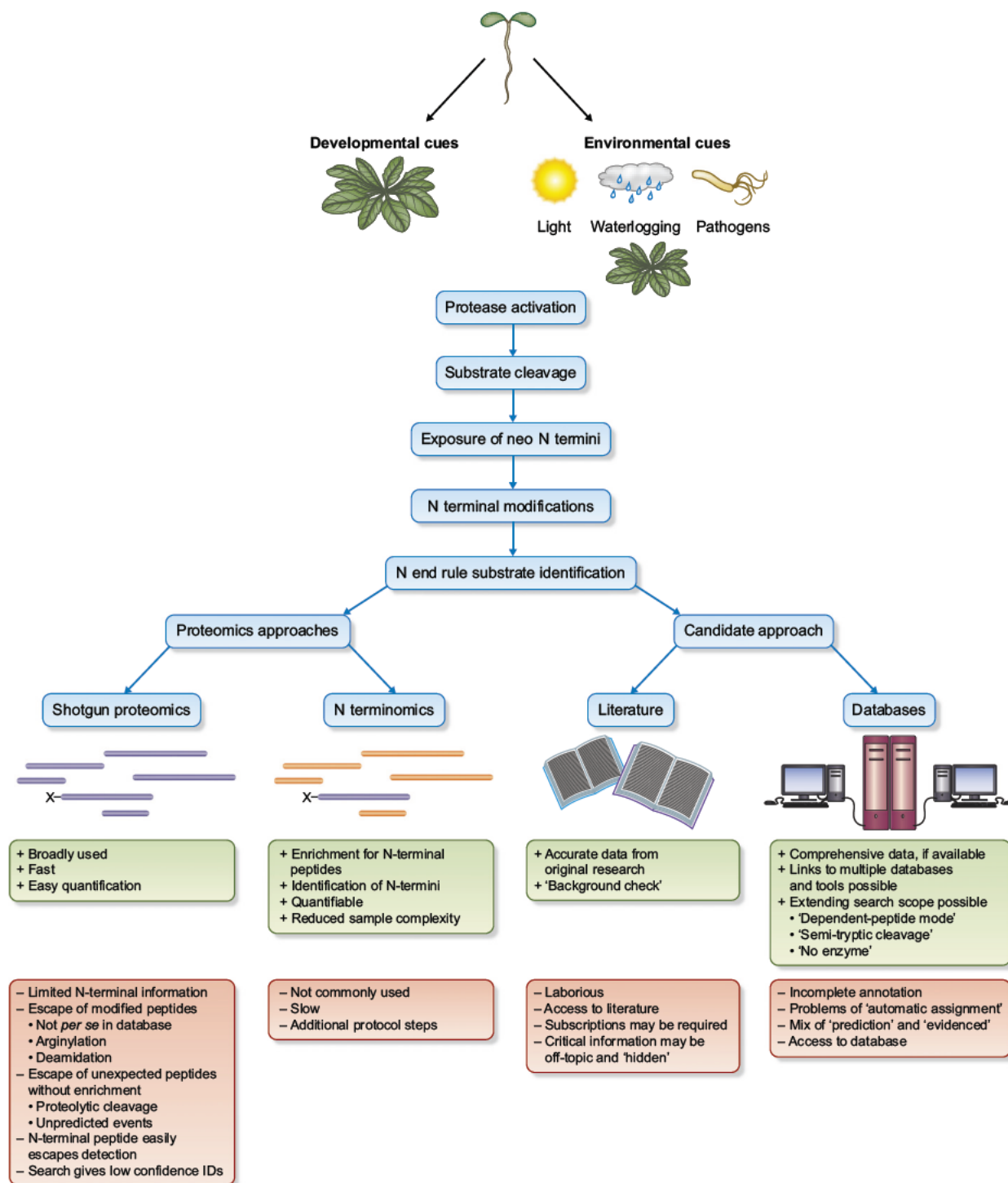


Fig. 3 Approaches used to identify N end rule substrate candidates. Endoproteolytic cleavage of (pre)proteins plays an important role in the generation of N end rule substrates. The activity of proteases is tightly regulated and may depend on both developmental and environmental cues. Hence, specific N end rule substrates may exist only in specific conditions or at specific developmental stages. As primary protein sequence information alone is mostly insufficient to predict N end rule substrates, more complex proteomics methods have been recently applied. These include shotgun proteomics and more specific N terminomics approaches. In addition, scanning through the literature or searching through databases can lead to the identification of putative N end rule substrates. Pros and cons of the different methods are highlighted in green and red, respectively.

conditions, and probably accumulate in a transient and/or in a cell type specific manner. Other key limitations include the lack of knowledge of protease cleavage sites and resulting neo N termini in plants, as well as technical limitations of proteomics approaches. For example, insufficient sensitivity of current proteomics methods and protocols, together with the nature and low abundance of the PTMs to be detected (i.e. acetylation, oxidation, deamidation, arginylation) have hampered N end rule substrate discovery. Method optimization for the identification of N end rule substrates includes the use of various proteases as alternatives to trypsin, which cleaves after Arg. Improving search algorithms that allow us to identify all possible peptides, including unusual ones with mass increments corresponding to specific PTMs, is also essential. Potential loss of information can also be counteracted by adapting search modes to identify more accurately protein fragments that may result from unpredicted cleavage by unknown proteases present in the proteome. We expect that improved proteomics methods will allow the direct identification of proteins with N terminal destabilizing residues, while also increasing the completeness and accuracy of databases for protease cleavage sites, further facilitating the identification of N end rule substrates.

In summary, the N end rule pathway represents a central and emerging field of investigation to understand the role of protein degradation in plants. Importantly, it also has a potential for applications in agronomy. For example, it has been shown that mutants of ATEs or PRT6 accumulated ERFVII transcription factors that act as master regulators of the hypoxia response. This accumulation correlated with increased tolerance to waterlogging (Gibbs *et al.*, 2011, 2016; Riber *et al.*, 2015; Mendiondo *et al.*, 2016). Furthermore, easy manipulation of turnover rates of recombinant target proteins by using temperature inducible N degrons (Faden *et al.*, 2016) indicates that the N end rule pathway may also be a valuable tool for biotechnological applications in the future.

Acknowledgements

We thank Wolfgang Hoehenwarter (Leibniz Institute of Plant Biochemistry, Halle), Ines Lassowskat (University of Münster) and Saskia Venne (Leibniz Institute for Analytical Sciences, Dortmund) for helpful comments. Work in E.G.'s lab is funded by a Science Foundation Ireland award to E.G. (13/IA/1870) and the Virtual Irish Centre for Crop Improvement (VICCI; grant 14/S/819 from the Department of Agriculture Food and the Marine). N.D. is supported by a grant for a junior research group by the ScienceCampus Halle Plant based Bioeconomy, by grant LSP TP2 1 of the Research Focus Program 'Molecular biosciences as a motor for a knowledge based economy' from the European Regional Development Fund, by grant DI 1794/3 1 of the Deutsche Forschungsgemeinschaft (DFG) and by the DFG Graduate Training Center GRK1026 'Conformational transitions in macromolecular interactions'. Work at the LIPM is supported by the French Laboratory of Excellence project 'TULIP' (ANR 10 LABX 41; ANR 11 IDEX 0002 02). E.G. and N.D. are participants of the COST action BM1307 (PROTEOSTASIS).

References

- Bienvenu WV, Giglione C, Meinel T. 2015. Proteome-wide analysis of the amino terminal status of *Escherichia coli* proteins at the steady-state and upon dephosphorylation inhibition. *Proteomics* 15: 2503–2518.
- Brower CS, Piatkov KI, Varshavsky A. 2013. Neurodegeneration-associated protein fragments as short-lived substrates of the N-end rule pathway. *Molecular Cell* 50: 161–171.
- Calvo SE, Julien O, Clauser KR, Shen H, Kamer KJ, Wells JA, Mootha VK. 2017. Comparative analysis of mitochondrial N-termini from mouse, human, and yeast. *Molecular & Cellular Proteomics* 16: 512–523.
- Chen SJ, Wu X, Wadas B, Oh JH, Varshavsky A. 2017. An N-end rule pathway that recognizes proline and destroys gluconeogenic enzymes. *Science* 355: eaal3655.
- Chisholm ST, Dahlbeck D, Krishnamurthy N, Day B, Sjolander K, Staskawicz BJ. 2005. Molecular characterization of proteolytic cleavage sites of the *Pseudomonas syringae* effector AvrRpt2. *Proceedings of the National Academy of Sciences, USA* 102: 2087–2092.
- Ditzel M, Wilson R, Tenev T, Zachariou A, Paul A, Deas E, Meier P. 2003. Degradation of DIAP1 by the N-end rule pathway is essential for regulating apoptosis. *Nature Cell Biology* 5: 467–473.
- Dong H, Dumenil J, Lu FH, Na L, Vanhaeren H, Naumann C, Klecker M, Prior R, Smith C, McKenzie N *et al.* 2017. Ubiquitylation activates a peptidase that promotes cleavage and destabilization of its activating E3 ligases and diverse growth regulatory proteins to limit cell proliferation in Arabidopsis. *Genes & Development* 31: 197–208.
- Eschen-Lippold L, Jiang X, Elmore JM, Mackey D, Shan L, Coaker G, Scheel D, Lee J. 2016. Bacterial AvrRpt2-like cysteine proteases block activation of the Arabidopsis mitogen-activated protein kinases, MPK4 and MPK11. *Plant Physiology* 171: 2223–2238.
- Faden F, Ramezani T, Mielke S, Almudi I, Nairz K, Froehlich MS, Hockendorff J, Brandt W, Hoehenwarter W, Dohmen RJ *et al.* 2016. Phenotypes on demand via switchable target protein degradation in multicellular organisms. *Nature Communications* 7: 12202.
- Garzon M, Eifler K, Faust A, Scheel H, Hofmann K, Koncz C, Yephremov A, Bachmair A. 2007. PRT6/At5g02310 encodes an Arabidopsis ubiquitin ligase of the N-end rule pathway with arginine specificity and is not the CER3 locus. *FEBS Letters* 581: 3189–3196.
- Gevaert K, Goethals M, Martens L, Van Damme J, Staes A, Thomas GR, Vandekerckhove J. 2003. Exploring proteomes and analyzing protein processing by mass spectrometric identification of sorted N-terminal peptides. *Nature Biotechnology* 21: 566–569.
- Gibbs DJ, Bacardit J, Bachmair A, Holdsworth MJ. 2014. The eukaryotic N-end rule pathway: conserved mechanisms and diverse functions. *Trends in Cell Biology* 24: 603–611.
- Gibbs DJ, Bailey M, Tedds HM, Holdsworth MJ. 2016. From start to finish: amino-terminal protein modifications as degradation signals in plants. *New Phytologist* 211: 1188–1194.
- Gibbs DJ, Lee SC, Isa NM, Gramuglia S, Fukao T, Bassel GW, Correia CS, Corbineau F, Theodoulou FL, Bailey-Serres J *et al.* 2011. Homeostatic response to hypoxia is regulated by the N-end rule pathway in plants. *Nature* 479: 415–418.
- Gravot A, Richard G, Lime T, Lemarie S, Jubault M, Lariagon C, Lemoine J, Vicente J, Robert-Seilantant A, Holdsworth MJ *et al.* 2016. Hypoxia response in Arabidopsis roots infected by *Plasmodiophora brassicae* supports the development of clubroot. *BMC Plant Biology* 16: 251.
- Hammerle M, Bauer J, Rose M, Szallies A, Thumm M, Dusterhus S, Mecke D, Entian KD, Wolf DH. 1998. Proteins of newly isolated mutants and the amino-terminal proline are essential for ubiquitin-proteasome-catalyzed catabolite degradation of fructose-1,6-bisphosphatase of *Saccharomyces cerevisiae*. *Journal of Biological Chemistry* 273: 25000–25005.
- Hoernstein SN, Mueller SJ, Fiedler K, Schuelke M, Vanselow JT, Schuessele C, Lang D, Nitschke R, Igloi GL, Schlosser A *et al.* 2016. Identification of targets and interaction partners of arginyl-tRNA protein transferase in the moss *Physcomitrella patens*. *Molecular & Cellular Proteomics* 15: 1808–1822.
- Huesgen PF, Overall CM. 2012. N- and C-terminal degradomics: new approaches to reveal biological roles for plant proteases from substrate identification. *Physiologia Plantarum* 145: 5–17.

- Hwang CS, Shemorry A, Varshavsky A. 2010. N-terminal acetylation of cellular proteins creates specific degradation signals. *Science* 327: 973–977.
- Kim HK, Kim RR, Oh JH, Cho H, Varshavsky A, Hwang CS. 2014. The N-terminal methionine of cellular proteins as a degradation signal. *Cell* 156: 158–169.
- Kleifeld O, Doucet A, auf dem Keller U, Prudova A, Schilling O, Kainthan RK, Starr AE, Foster LJ, Kizhakkedathu JN, Overall CM. 2010. Isotopic labeling of terminal amines in complex samples identifies protein N-termini and protease cleavage products. *Nature Biotechnology* 28: 281–288.
- Lee KE, Heo JE, Kim JM, Hwang CS. 2016. N-terminal acetylation-targeted N-end rule proteolytic system: the Ac/N-end rule pathway. *Molecules and Cells* 39: 169–178.
- Li L, Nelson CJ, Trosch J, Castleden I, Huang S, Millar AH. 2017. Protein degradation rate in *Arabidopsis thaliana* leaf growth and development. *Plant Cell* 29: 207–228.
- Majovsky P, Naumann C, Lee CW, Lassowski I, Trujillo M, Dissmeyer N, Hoehenwarter W. 2014. Targeted proteomics analysis of protein degradation in plant signaling on an LTQ-Orbitrap mass spectrometer. *Journal of Proteome Research* 13: 4246–4258.
- de Marchi R, Sorel M, Mooney B, Fudal I, Goslin K, Kwasniewska K, Ryan PT, Pfalz M, Kroymann J, Pollmann S *et al.* 2016. The N-end rule pathway regulates pathogen responses in plants. *Scientific Reports* 6: 26020.
- Mendiondo GM, Gibbs DJ, Szurman-Zubrzycka M, Korn A, Marquez J, Szarejko I, Maluszynski M, King J, Axcell B, Smart K *et al.* 2016. Enhanced waterlogging tolerance in barley by manipulation of expression of the N-end rule pathway E3 ligase PROTEOLYSIS6. *Plant Biotechnology Journal* 14: 40–50.
- Mot AC, Prell E, Klecker M, Naumann C, Faden F, Westermann B, Dissmeyer N. 2017. Real-time detection of N-end rule-mediated ubiquitination via fluorescently labeled substrate probes. *New Phytologist*. doi: 10.1111/nph.14497.
- Nishimura K, Asakura Y, Friso G, Kim J, Oh SH, Rutschow H, Ponnala L, van Wijk KJ. 2013. ClpS1 is a conserved substrate selector for the chloroplast Clp protease system in *Arabidopsis*. *Plant Cell* 25: 2276–2301.
- Nishimura K, van Wijk KJ. 2015. Organization, function and substrates of the essential Clp protease system in plastids. *Biochimica et Biophysica Acta* 1847: 915–930.
- Piatkov KI, Brower CS, Varshavsky A. 2012a. The N-end rule pathway counteracts cell death by destroying proapoptotic protein fragments. *Proceedings of the National Academy of Sciences, USA* 109: E1839–E1847.
- Piatkov KI, Colnaghi L, Bekes M, Varshavsky A, Huang TT. 2012b. The auto-generated fragment of the Usp1 deubiquitylase is a physiological substrate of the N-end rule pathway. *Molecular Cell* 48: 926–933.
- Potusachak T, Sary S, Schlogelhofer P, Becker F, Nejjinskaia V, Bachmair A. 1998. PRT1 of *Arabidopsis thaliana* encodes a component of the plant N-end rule pathway. *Proceedings of the National Academy of Sciences, USA* 95: 7904–7908.
- Rao H, Uhlmann F, Nasmyth K, Varshavsky A. 2001. Degradation of a cohesin subunit by the N-end rule pathway is essential for chromosome stability. *Nature* 410: 955–959.
- Riber W, Muller JT, Visser EJ, Sasidharan R, Voeselek LA, Mustroph A. 2015. The greening after extended darkness1 is an N-end rule pathway mutant with high tolerance to submergence and starvation. *Plant Physiology* 167: 1616–1629.
- Rowland E, Kim J, Bhuiyan NH, van Wijk KJ. 2015. The *Arabidopsis* chloroplast stromal N-terminome: complexities of amino-terminal protein maturation and stability. *Plant Physiology* 169: 1881–1896.
- Santt O, Pfirrmann T, Braun B, Juretschke J, Kimmig P, Scheel H, Hofmann K, Thumm M, Wolf DH. 2008. The yeast GID complex, a novel ubiquitin ligase (E3) involved in the regulation of carbohydrate metabolism. *Molecular Biology of the Cell* 19: 3323–3333.
- Schilling O, Huesgen PF, Barre O, auf dem Keller U, Overall CM. 2011. Characterization of the prime and non-prime active site specificities of proteases by proteome-derived peptide libraries and tandem mass spectrometry. *Nature Protocols* 6: 111–120.
- Takemoto D, Jones DA. 2005. Membrane release and destabilization of *Arabidopsis* RIN4 following cleavage by *Pseudomonas syringae* AvrRpt2. *Molecular Plant-Microbe Interactions* 18: 1258–1268.
- Tasaki T, Sriram SM, Park KS, Kwon YT. 2012. The N-end rule pathway. *Annual Review of Biochemistry* 81: 261–289.
- Tsiatsiani L, Timmerman E, De Bock PJ, Vercammen D, Stael S, van de Cotte B, Staes A, Goethals M, Beunens T, Van Damme P *et al.* 2013. The *Arabidopsis* metacaspase9 degradome. *Plant Cell* 25: 2831–2847.
- Varshavsky A. 2011. The N-end rule pathway and regulation by proteolysis. *Protein Science* 20: 1298–1345.
- Venne AS, Solari FA, Faden F, Paretto T, Dissmeyer N, Zahedi RP. 2015. An improved workflow for quantitative N-terminal charge-based fractional diagonal chromatography (ChaFRADIC) to study proteolytic events in *Arabidopsis thaliana*. *Proteomics* 15: 2458–2469.
- Venne AS, Vogtle FN, Meisinger C, Sickmann A, Zahedi RP. 2013. Novel highly sensitive, specific, and straightforward strategy for comprehensive N-terminal proteomics reveals unknown substrates of the mitochondrial peptidase Icp55. *Journal of Proteome Research* 12: 3823–3830.
- Vogtle FN, Wortelkamp S, Zahedi RP, Becker D, Leidhold C, Gevaert K, Kellermann J, Voos W, Sickmann A, Pfanner N *et al.* 2009. Global analysis of the mitochondrial N-proteome identifies a processing peptidase critical for protein stability. *Cell* 139: 428–439.
- Wadas B, Piatkov KI, Brower CS, Varshavsky A. 2016. Analyzing N-terminal arginylation through the use of peptide arrays and degradation assays. *Journal of Biological Chemistry* 291: 20976–20992.
- Weits DA, Giuntoli B, Kosmacz M, Parlanti S, Hubberten HM, Riegler H, Hoefgen R, Perata P, van Dongen JT, Licausi F. 2014. Plant cysteine oxidases control the oxygen-dependent branch of the N-end-rule pathway. *Nature Communications* 5: 3425.
- White MD, Klecker M, Hopkinson R, Weits D, Mueller C, Naumann C, O'Neill R, Wickens J, Yang J, Brooks-Bartlett J *et al.* 2016. Plant cysteine oxidases are dioxygenases that directly enable arginyl transferase-catalyzed arginylation of N-end rule targets. *Nature Communications* 8: 14690.
- Xu F, Huang Y, Li L, Gannon P, Linster E, Huber M, Kapos P, Bienvenut W, Polevoda B, Meinnel T *et al.* 2015. Two N-terminal acetyltransferases antagonistically regulate the stability of a nod-like receptor in *Arabidopsis*. *Plant Cell* 27: 1547–1562.
- Zhang H, Deery MJ, Gannon L, Powers SJ, Lilley KS, Theodoulou FL. 2015. Quantitative proteomics analysis of the Arg/N-end rule pathway of targeted degradation in *Arabidopsis* roots. *Proteomics* 15: 2447–2457.

1.2 OBJECTIVES PART I – BIOLOGY

In my lab, we investigate protein degradation in plants. Since starting my lab in 2011, my main interest is protein homeostasis (proteostasis) mediated by posttranslational protein modifications via the N-end rule pathway. The N-end rule relates the stability of some proteins to the identity of their amino- or N-terminus and is considered to be responsible for targeted protein degradation as part of the Ubiquitin proteasome system.

My research interests include:

- ✓ enzymatic mechanisms and their regulation;
- ✓ substrate identification and genetics of the N-end rule system;
- ✓ its roles under stress conditions versus the normal environment in plant development and fitness using *Arabidopsis* as the model; and
- ✓ harnessing the N-end rule pathway for genetic and biotechnological applications.

The N-end rule plays a pivotal role in plant development, response to endogenous as well as exogenous stresses, and can be beneficially modified for improving recombinant production of proteins of interest *on demand* in various ways and adapt their manufacture to target-specific needs. By using cutting edge approaches and having established key collaborations, we aim to understand the consequences of altering N-end rule substrate concentration in a biological context, thus, our research sets out to link mechanistics of targeted proteolysis with phenotypes.

We developed assays and artificial substrates highly specific for this pathway to identify and characterize novel enzymatic modifiers and approach potential substrates via differential proteomics and knowledge-based pipelines.

Using comparative proteomics of mutants defective in protein degradation (in collaboration with Wolfgang Hoehenwarter, IPB Halle and René Zahedi, ISAS Dortmund), we set out to identify novel degradation targets of the plant N-end rule pathway in an explorative approach. Basic and general differential proteomics by shotgun protocols lead to a good estimate on relative abundance of differentially regulated proteins between wild type and the mutants ([Majovsky et al., J Proteome Res, 2014](#)) and N-terminomics approaches, that is, subproteomics techniques specific for N-termini of proteins and peptides, revealed the overall N-terminal acetylation status of the proteome of N-end rule mutants versus the wild type ([Venne et al., Proteomics, 2015](#)) and helped to identify various neo-N-termini of interest which must have resulted from prior posttranslational protease cleavage ([Naumann et al., under preparation](#)).

In this chapter, I will describe how we analyzed enzyme–substrate interaction of the N-end rule pathway and how we identified novel N-end rule substrates and functions.

1.3 RESULTS PART I – BIOLOGY

Although the *bona fide* N-end rule E3 Ubiquitin ligase PROTEOLYSIS1 (PRT1) was isolated from a forward genetics screen based on protein degradation and is known since 1993, its function remained obscure (Potuschak *et al.*, *Proc Natl Acad Sci U S A*, 1998; Stary *et al.*, *Plant Physiol*, 2003). We demonstrated for the first time that the PRT1 can indeed mediate Ubiquitin transfer and is strongly dependent of the presence of hydrophobic amino acids at the N-terminus and Lysine residues as Ubiquitin acceptor sites further downstream ([Mot *et al.*, *New Phytol*, 2017](#)). In frame of this work, we could establish a real-time fluorescence-based assay for rapid live measurements of polyubiquitination of N-end rule substrates, see chapter 1.3.1.

In order to address different functional aspects of the N-end rule, we have established several more molecular tools in the lab, mainly based on peptides we synthesize in my lab or recombinantly produced chimeric proteins ([Faden *et al.*, *Meth Mol Biol*, 2016](#); [Klecker & Dissmeyer, *Meth Mol Biol*, 2016](#); [Naumann *et al.*, *Meth Mol Biol*, 2016](#)).

We could then identify the first degradation target of PROTEOLYSIS1 *in vivo*, that is the central core regulator of cell differentiation, BIG BROTHER. The ubiquitination-activated peptidase DA1 regulates organ size by limiting cell proliferation and endoreduplication in *Arabidopsis*. Ubiquitylation activates this peptidase to promote cleavage and destabilization of its own activating E3 ligase BIG BROTHER and other growth regulatory proteins ([Dong *et al.*, *Genes Dev*, 2017](#)). Phenotypes associated with limited cell proliferation are caused by genetic and physical interactions within a molecular feedback network. This study was done in collaboration with Dirk Inzé, VIB Plant Systems Biology, Ghent, Belgium, and Michael Bevan, John Innes Center, Norwich, UK, see chapter 1.3.2.

Our work also shed light on a long-discussed molecular link between N-terminal post-translational protein modifications and rapid turn-over of a class of stress-responsive plant transcription factors of the group VII ETHYLENE RESPONSE FACTORS (ERF-VIIs; [White *et al.*, *Nature Comms*, 2017](#)). We demonstrated that N-end rule substrates are indeed modified in a very peculiar way via plant-specific dioxygenases and arginyl tRNA transferases which enables them for degradation under participation of N-end rule E3 Ubiquitin ligases. This work was accomplished in collaboration with Emily Flashman, Chemistry Research Laboratory, University of Oxford, and Tom Grossmann, VU Amsterdam, The Netherlands, see chapter 1.3.3.

PART I – BIOLOGY OF THE N-END RULE

1.3.1 PROTEOLYSIS1 is a highly specific N-end rule E3 Ubiquitin ligase

A research focus is on the molecular basis of protein–protein recognition and targeted protein degradation in the context of proteostasis. Only few details are known of a very small number of enzymatic N-end rule components and neither their substrates nor their mode of action are sufficiently studied. We generated a tool for biochemical studies, fluorescent probes for enzyme kinetics and assays aiming at specificity of posttranslational modifications ([Mot et al., *New Phytol*, 2017](#)). Here, a novel time-resolved approach was used to demonstrate biochemical evidence for highly specific ubiquitination activity of the N-end rule E3 ubiquitin ligase PRT1 – a concept that was hypothesized but not yet proven since the mid 1990s.

Publication:

Mot AC, Prell E, Klecker M, Naumann C, Faden F, Westermann B, **Dissmeyer N***. Real-time detection of N-end rule-mediated ubiquitination via fluorescently labeled substrate probes.

New Phytol. 2017 Mar 9. doi: 10.1111/nph.14497

Real-time detection of N-end rule-mediated ubiquitination via fluorescently labeled substrate probes*

Augustin C. Mot^{1,2}, Erik Prell³, Maria Klecker^{1,2}, Christin Naumann^{1,2}, Frederik Faden^{1,2}, Bernhard Westermann³ and Nico Dissmeyer^{1,2}

¹Independent Junior Research Group on Protein Recognition and Degradation, Leibniz Institute of Plant Biochemistry (IPB), Weinberg 3, Halle (Saale), D-06120, Germany; ²ScienceCampus Halle – Plant-based Bioeconomy, Betty-Heimann-Str. 3, Halle (Saale), D-06120, Germany; ³Department of Bioorganic Chemistry, Leibniz Institute of Plant Biochemistry (IPB), Weinberg 3, Halle (Saale), D-06120, Germany

Summary

Author for correspondence:
Nico Dissmeyer
Tel: +49 345 5582 1710
Email: nico.dissmeyer@ipb.halle.de

Received: 5 December 2016
Accepted: 26 January 2017

New Phytologist (2017)
doi: 10.1111/nph.14497

Key words: activity profiling, E3 ligases, fluorescent dyes, labeling chemistry, N end rule pathway, protein labeling, proteolysis, ubiquitination.

- The N end rule pathway has emerged as a major system for regulating protein functions by controlling their turnover in medical, animal and plant sciences as well as agriculture. Although novel functions and enzymes of the pathway have been discovered, the ubiquitination mechanism and substrate specificity of N end rule pathway E3 ubiquitin ligases have remained elusive. Taking the first discovered *bona fide* plant N end rule E3 ligase PROTEOLYSIS1 (PRT1) as a model, we used a novel tool to molecularly characterize polyubiquitination live, in real time.
- We gained mechanistic insights into PRT1 substrate preference and activation by monitoring live ubiquitination using a fluorescent chemical probe coupled to artificial substrate reporters. Ubiquitination was measured by rapid in gel fluorescence scanning as well as in real time by fluorescence polarization.
- The enzymatic activity, substrate specificity, mechanisms and reaction optimization of PRT1 mediated ubiquitination were investigated *ad hoc* instantaneously and with significantly reduced reagent consumption.
- We demonstrated that PRT1 is indeed an E3 ligase, which has been hypothesized for over two decades. These results demonstrate that PRT1 has the potential to be involved in polyubiquitination of various substrates and therefore pave the way to understanding recently discovered phenotypes of *prt1* mutants.

Introduction

The on/off status of protein function within the cell proteome and the general abundance and specific distribution of proteins throughout the cell compartments are precisely controlled by protein quality control (PQC) mechanisms. These mechanisms ensure that protein functions and activities are directly regulated to maintain the processes critical to the successful survival of any organism. Biochemical analysis of the underlying mechanisms safeguarding proteostatic control is therefore pivotal. Such analysis ranges from the molecular characterization of enzymes involved in PQC and their catalyzed reactions to enzyme substrate and nonsubstrate protein protein interactions. The so called ubiquitin (Ub) 26S proteasome system (UPS) is a master component of PQC, with the key elements being noncatalytic Ub ligases (E3), Ub conjugating enzymes (E2), and Ub activating enzymes (E1).

To investigate an element conferring substrate specificity, we chose PROTEOLYSIS1 (PRT1) in *Arabidopsis thaliana* as a

model E3 ligase, which is a *bona fide* single subunit E3 with an unknown substrate portfolio (Bachmair *et al.*, 1993; Potuschak *et al.*, 1998; Sary *et al.*, 2003). Its biological function remains elusive but it presumably represents a highly specific enzyme with E3 ligase function of the N end rule pathway of targeted protein degradation, which is part of the UPS. A recent study revealed that, upon cleavage by protease DA1 ('large' in chinese 1), the central organ size regulatory protein BIG BROTHER forms a C terminal, Tyr initiated fragment. Its stability depends on the N terminal amino acid Tyr and the function of PRT1 E3 ligase (Dong *et al.*, 2017).

The N end rule relates the half life of a protein to its N terminal amino acid (Bachmair *et al.*, 1986) and causes rapid proteolysis of proteins bearing so called N degrons, N terminal sequences that lead to the degradation of the protein. N degrons are created by endoproteolytic cleavage of protein precursors (proteins) and represent the resulting neo N termini of the remaining C terminal protein moiety, albeit not all freshly formed N termini automatically present destabilizing residues (Fig. 1a).

The N end rule pathway is a vibrant emerging area of research and has a multitude of functions in all kingdoms (Dogan *et al.*, 2010; Varshavsky, 2011; Tasaki *et al.*, 2012; Gibbs *et al.*, 2014a;

*Correction added after online publication 9 March 2017: the title was amended from 'PROTEOLYSIS1 (PRT1)-mediated' to 'N-end rule-mediated'.

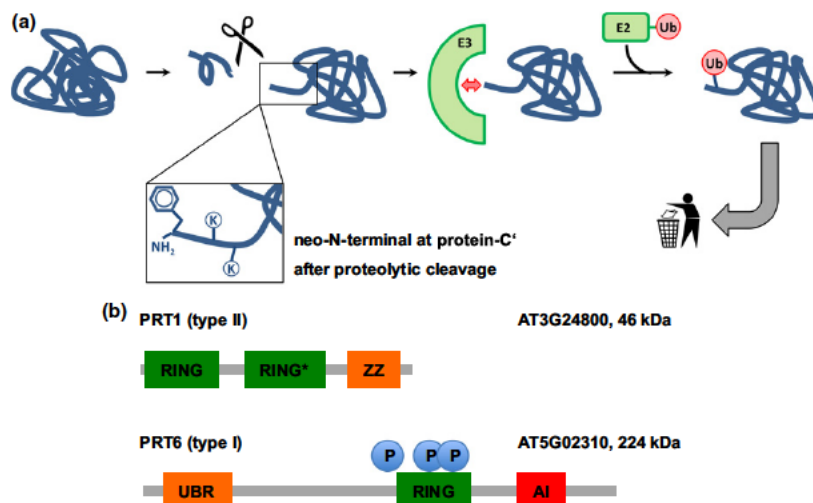


Fig. 1 Generation of N end rule substrates by proteolytic processing and predicted features of the two *bona fide* plant N recognins. (a) Substrates containing N degrons can be generated from (pre)pro proteins as precursor sequences after proteolytic cleavage (indicated by the scissors). The N degron shown here comprises a Phe residue as the primary destabilizing residue at the protein C' and internal lysines for polyubiquitination. These N degrons can be recognized by N end rule E3 Ub ligases (N recognins), which, in turn, associate with Ub conjugating enzymes (E2) carrying Ub, which was previously activated by E1 enzymes. One possible result of ubiquitination is protein degradation and currently, in the context of the N end rule, ubiquitination is assumed to lead to degradation in most cases. (b) The two known *Arabidopsis thaliana* N recognins were identified by their function (PROTEOLYSIS1 (PRT1); 46 kDa) and by homology to the so called UBR box which is the substrate recognition domain of *Saccharomyces cerevisiae* UBR1p (PRT6; 224 kDa). UBR, structural motif involved in binding type I substrates; RING*, composite domain containing RING (Really Interesting New Gene) and CCCH type Zn fingers; ZZ, domain binding two zinc ions, similar to RING; RING, protein-protein interaction domain for E2-E3 interaction; AI, predicted autoinhibitory domain (intramolecular interaction); P, phosphorylation sites confirmed by mass spectrometry (PhosPhAt 4.0; phosphat.uni-hohenheim.de): pThr1136 and pSer1257 (Roitinger *et al.*, 2015) and pThr1335 (Engelsberger & Schulze, 2012).

Gibbs, 2015). Identified substrates are mainly important regulatory proteins and play key roles in animal and human health (Zenker *et al.*, 2005; Piatkov *et al.*, 2012; Brower *et al.*, 2013; Shemorry *et al.*, 2013; Kim *et al.*, 2014), plant stress response and agriculture (Gibbs *et al.*, 2011, 2014a,b; Licausi *et al.*, 2011; Weits *et al.*, 2014; de Marchi *et al.*, 2016; Mendiondo *et al.*, 2016).

In plants, functions of N end rule enzymes are associated with central developmental processes including seed ripening and lipid breakdown, hormonal signaling of abscisic acid (ABA), gibberellin and ethylene, seed dormancy and germination (Holman *et al.*, 2009; Abbas *et al.*, 2015; Gibbs *et al.*, 2015), leaf and shoot morphogenesis, flower induction, apical dominance (Graciet *et al.*, 2009), and the control of leaf senescence (Yoshida *et al.*, 2002). The pathway has been shown to be a sensor for molecular oxygen and reactive oxygen species (ROS) by mediating nitric oxide (NO) signaling and regulating the stress response after hypoxia, for example after flooding and plant submergence (Gibbs *et al.*, 2011, 2014b; Licausi *et al.*, 2011). A novel plant specific class of enzymes, plant cysteine oxidases (PCOs), has been found to be associated with the pathway, indicating the involvement of plant specific molecular circuits, enzyme classes and mechanisms in this pathway (Weits *et al.*, 2014; White *et al.*, 2017). In the moss *Physcomitrella patens*, N end rule mutants are defective in gametophytic development (Schuessele *et al.*, 2016) and protein targets of N end rule mediated posttranslational modifications were discovered (Hoernstein *et al.*, 2016). Also, in

barley (*Hordeum vulgare*), the pathway is connected with development and stress responses (Mendiondo *et al.*, 2016). Very recently, a link between N end rule function and plant pathogen response and innate immunity was found (de Marchi *et al.*, 2016), shedding light on novel functions of the as yet underexplored process of targeted proteolysis. However, to date, the identity of plant N end rule targets still remains obscure and clear evidence from biochemical data obtained in *in vitro* and *in vivo* studies such as N terminal subproteomics or enzymatic assays is still lacking.

A novel *in vivo* protein stabilization tool for genetic studies in developmental biology and biotechnological applications, the low temperature ('lt) degron', works in plants and animals by directly switching the levels of functional proteins *in vivo* (Faden *et al.*, 2016). The method is based on conditional and specific PRT1 mediated protein degradation, a process we studied in depth with the generated fluorescently labeled substrate reporter proteins.

N degrons are by definition recognized and the corresponding protein ubiquitinated by specialized N end rule E3 ligases, so called N recognins (Sriram *et al.*, 2011; Varshavsky, 2011; Tasaki *et al.*, 2012; Gibbs, 2015). In plants, only two of these, namely PRT1 and PRT6, are associated with the N end rule pathway and are assumed to function as N recognins (Fig. 1b). This is in contrast to the high number of proteolytically processed proteins which carry in their mature form N terminal amino acids that could potentially enter the enzymatic N end rule pathway

cascade (Venne *et al.*, 2015). Given that there are > 800 putative proteases in the model plant *A. thaliana*, it is likely that the N end rule pathway plays an important role in protein half lives in a proteome wide manner. Examples are found in the METACASPASE9 degradome, that is, the part of the proteome that is associated with degradation (Tsiatsiani *et al.*, 2013), or the N degradome of *Escherichia coli* (Humbard *et al.*, 2013), with a possibly analogous overlap with endosymbiotic plant organelles (Apel *et al.*, 2010).

PRT1, compared with the *Saccharomyces cerevisiae* N recognin Ubr1 (225 kDa), is a relatively small protein (46 kDa) and is totally unrelated to any known eukaryotic N recognin but has functional similarities to prokaryotic homologs (Fig. 1b). It is therefore perceived as a plant pioneer E3 ligase with both diversified mechanisms and function. Artificial substrate reporters based on mouse dihydrofolate reductase (DHFR) comprising an N terminal phenylalanine generated via the ubiquitin fusion (UFT) technique were used to identify and isolate a *prt1* mutant in a forward mutagenesis screen (Bachmair *et al.*, 1993). In the mutant cells and after MG132 treatment, the F DHFR reporter construct was shown to be stabilized whereas it was unstable in the untreated wild type (Potuschak *et al.*, 1998; Stary *et al.*, 2003). *PRT1* was able to heterologously complement a *Saccharomyces cerevisiae* *ubr1Δ* mutant strain where Phe, Tyr, and Trp initiated β galactosidase test proteins were stabilized. These reporters were rapidly degraded in *ubr1Δ* transformed with *PRT1* (Stary *et al.*, 2003). A new study revealed that cleavage of the E3 ligase BIG BROTHER by protease DA1 forms a C terminal, Tyr initiated fragment. Its stability depends on the N terminal amino acid Tyr and the function of *PRT1* E3 ligase (Dong *et al.*, 2017). However, to date, there have been no more *in vivo* targets or direct functions associated with *PRT1*, but, recently, a potential role of *PRT1* in plant innate immunity was suggested (de Marchi *et al.*, 2016).

The spectrum of N termini possibly recognized by plant N end rule E3 ligases including *PRT1* has not been sufficiently explored. Only Phe starting test substrates were found to be stabilized in a *prt1* mutant, whereas initiation by Arg and Leu still caused degradation (Potuschak *et al.*, 1998; Stary *et al.*, 2003; Garzón *et al.*, 2007). In the light of substrate identification, it is crucial to investigate *PRT1* mechanisms in more detail, because several posttranslationally processed proteins bearing Phe, Trp and Tyr at the neo N termini have been found (Tsiatsiani *et al.*, 2013; Venne *et al.*, 2015) and hence represent putative *PRT1* targets. Elucidating the substrate specificity of *PRT1* will be an important step forward towards substrate identification and placing *PRT1* and the N end rule in a biological context.

We established a technique that allows real time measurements of ubiquitination using fluorescence scanning of SDS PAGE gels and fluorescence polarization. We propose its use as a generic tool for mechanistic and enzymological characterization of E3 ligases as master components of the UPS directing substrate specificity. With a series of artificial test substrates comprising various *bona fide* destabilizing N end rule N termini, substrate specificity was analyzed and revealed the preference of *PRT1* for Phe as a representative of the bulky hydrophobic class of amino acids. The

methods commonly used to assay *in vitro* ubiquitination are based on end time methods where the reaction is stopped at a given time point and analyzed by SDS PAGE followed by immunostaining with anti Ub vs anti target specific antibodies. This detection via western blot often gives rise to the characteristic hallmark of polyubiquitinated proteins, a 'ubiquitination smear' or a more distinct 'laddering' of the posttranslationally Ub modified target proteins. All information about what occurred during the reaction is unknown unless the assay is run at several different time points, which drastically increases both experimental time and reagent consumption. Besides the most common methods used for ubiquitination assessment which involve immunodetection with anti Ub and anti target antibodies, there are few other approaches making use of different reagents. Comparable methods, and their advantages and disadvantages, are listed in Supporting Information Table S1. The novelty offered by the present study is the development of a fluorescence based assay that allows real time measurement of Ub incorporation in solution, eliminating shortcomings of the existing methods, and thus a more real mechanistic investigation. Our method monitors the ubiquitination process live, in real time, using fluorescently labeled substrate proteins and fluorescence based detection assays, namely fluorescence polarization (FP). FP is a spectroscopical technique that allows investigations of the molecular mobility of biomolecules by providing biophysical information on fluorescently labeled molecules. It is used in studies of protein ligand or protein protein interactions, polymer formation, proteolysis etc. Its advantage is that it allows the possibility of visualizing molecular binding and dissociation processes in a direct and instantaneous fashion from 'outside' without affecting the system. This allows us to acquire real time kinetics and information on binding equilibria.

In addition, the protocol was coupled to fast and convenient scanning fluorescence in gel detection. This type of assay can be easily adapted for high throughput measurements of ubiquitination activity and probably also similar protein modification processes involving changes in substrate molecule properties over time *in vitro*. Rather than merely analyzing enzyme substrate or protein protein interactions, the method described here employs FP measurements for the characterization of enzyme activity and parameters affecting the performance of the ubiquitination reaction (Xia *et al.*, 2008; Kumar *et al.*, 2011; Smith *et al.*, 2013).

Materials and Methods

Cloning and expression of recombinant proteins

The *Escherichia coli* flavodoxin (Flv; uniprot ID J7QH18) coding sequence was cloned directly from *E. coli* DNA BL21(DE3) and flanked by an N terminal triple hemagglutinin (HAT) epitope sequence using the primers Flv rvs (5' TTATTTGAGTAAA TTAATCCACGATCC 3') and Flv eK HAT(oh) fwd (5' CTGGTGCTGCAGATATCACTCTTATCAGCGG 3'). The X eK sequences comprising codons for various N terminal amino acids exposed after tobacco etch virus (TEV) cleavage of the expressed X eK Flv fusion protein were cloned from an eK:HAT

template using the primers eK(X) TEV(oh) fwd (5' GAGAATCTTTATTTTCAG_{xxx} CACGGATCTGGAGCTT G 3' with xxx GTT (for Phe), GGG (for Gly), GAG (for Arg), and GTT (for Leu)) and eK HAT flav(oh) rvs (5' CCGCT GATAAGAGTGATATCTGCAGCACCAG 3'). This sequence contains a TEV protease recognition sequence (ENLYFQ[X], with X being the neo N terminal after cleavage, i.e. TEV P1' residue) at the N terminal of the expressed X eK Flv fusion protein. In order to attach Gateway attB sites and fuse the PCR products, a PCR was performed using Flv attB2(oh) rvs (5' GGGACC ACTTTGTACAAGAAAGCTGGGTA TCATTATTTGAGTA AATTAATCCACGATCC 3') and adapter tev fwd (5' GGGG ACAAGTTT TACAAAAAAGCAGGCAGGCTTAGAAAAC CTGTAT TTTCAGGGAATG 3'). A Gateway entry clone was generated by BP recombination reaction (Thermo Fisher Scientific, Waltham, MA, USA) with pDONR201 (Thermo Fisher Scientific). All primer sequences are listed in Table S2. A Gateway LR recombination reaction (Thermo Fisher Scientific) into pVP16 (Thao *et al.*, 2004) (a kind gift from Russell L. Wrobel, University of Wisconsin, Madison, WI, USA) produced the final construct which consisted of an N terminal 8xHis:MBP double affinity tag. The expression vector pVP16::8xHis:MBP:tev:eK:3xHA:Flv was transformed into *E. coli* BL21(DE3) and the fusion protein was expressed by 0.2 mM IPTG (isopropyl β -D-thiogalactopyranoside) induction in LB (lysogeny broth) medium for 16 h at 26°C. Cells were harvested via centrifugation (3500 g at 4°C for 20 min), resuspended in Ni buffer (50 mM sodium phosphate, pH 8.0, and 300 mM NaCl), and treated with 1 mg ml⁻¹ lysozyme (Sigma) in the presence of PMSF (sc 3597; Santa Cruz Biotechnology Inc., Heidelberg, Germany) added to a final concentration of 1 mM followed by sonication (4 min, 40% intensity; 6 min, 60% intensity). The lysate was centrifuged (12 500 g for 30 min), the supernatant was loaded onto an Ni NTA agarose column (Qiagen) equilibrated with Ni buffer, followed by Ni buffer washing, and then the protein was eluted with Ni buffer containing 200 mM imidazole (Merck, Darmstadt, Germany) and loaded onto amylose resin (New England Biolabs, Ipswich, MA, USA). After washing with amylose buffer (25 mM sodium phosphate, pH 7.8, and 150 mM NaCl), the protein was eluted with amylose buffer containing 10 mM maltose. For the TEV digest, the fusion protein was incubated overnight at 4°C with 0.27 μ g μ l⁻¹ TEV protease, expressed from pRK793 (plasmid 8827; Addgene, Cambridge, MA, USA), in 50 mM phosphate, pH 8.0, 0.5 mM EDTA and 1 mM DTT and loaded onto an Ni agarose column (Qiagen) equilibrated with Ni buffer. The flow through containing the tag free X eK Flv substrate was concentrated with an Amicon Ultra 15 (Merck Millipore, Billerica, MA, USA).

PRT1 was cloned, expressed and purified as described previously (Dong *et al.*, 2017).

Chemical labeling

An incubation of 10 μ M purified X eK Flv was carried out for 1 h at room temperature with a 100 μ M concentration of the synthesized thiol reactive fluorogenic labeling dye in 20 mM

Tris Cl, pH 8.3, 1 mM EDTA and 1 mM tris(2 carboxy ethyl) phosphine (TCEP; Thermo Fisher Scientific). The reaction was stopped with 1 mM cysteine hydrochloride, the unreactive dye was removed using 10 kDa cut off Amicon filters (Merck Millipore) in three successive washing steps, and the labeling efficiency was evaluated on the basis of the fluorescence intensity of the labeled dye using a fluorescence plate reader (Infinite M1000; Tecan, Männedorf, Switzerland) and the total protein concentration using an infra red spectrophotometer (Direct Detect; Merck).

Chemical synthesis

The detailed synthesis protocols of the labeling probe NBD NH PEG₂ NH haloacetamide are described in Methods S1. In brief, the following synthesis steps were accomplished: (1) tert butyl {2 [2 (2 aminoethoxy)ethoxy]ethyl} carbamate (NH₂ PEG₂ NHBoc); (2) NBD NH PEG₂ NHBoc; (3) NBD NH PEG₂ NH₂ hydrochloride; (4) NBD NH PEG₂ NH iodoacetamide; (5) NBD NH PEG₂ NH iodoacetamide; (6) NBD NH PEG₂ NH chloroacetamide.

Ubiquitination assay and in-gel fluorescence detection

The X eK Flv fluorescently labeled substrate (X eK Flv NBD), at a total protein concentration (both labeled and unlabeled) of 3.4 μ M, was solved in 25 mM Tris Cl, pH 7.4, 50 mM KCl, 5 mM MgCl₂ and 0.7 mM DTT containing 16 μ M Ub from bovine erythrocytes (U6253; Sigma Aldrich). For ubiquitination, 2 mM ATP (New England Biolabs), 40 nM E1¹⁵, 0.31 μ M E2 (UBC8)¹⁵, and 5 nM E3 (8xHis:MBP tagged or untagged PRT1) were added to the previously mentioned solution in a final volume of 30 μ l and incubated at 30°C for 1 h. The reaction was stopped by adding 5X reductive SDS PAGE loading buffer and incubating for 10 min at 96°C followed by SDS PAGE. The gels were scanned using fluorescence detection on a Typhoon FLA 9500 biomolecular imager (GE Healthcare, Little Chalfont, Buckinghamshire, UK) with a blue excitation laser (473 nm) LD (laser diode) and an LPB (long pass blue) emission filter (510LP), then blotted onto a cellulose membrane and detected with either mouse monoclonal anti Ub antibody (Ub (P4D1), sc 8017; Santa Cruz Biotechnology; 1 : 5000 dilution in blocking solution (150 mM NaCl, 10 mM Tris Cl, pH 8, 3% skim milk powder and 0.1% Tween 20)) or mouse monoclonal anti HA epitope tag antibody (HA.11, clone 16B12: MMS 101R; Covance, Princeton, NJ, USA; 1 : 1000 to 1 : 5000 in blocking solution) and goat anti mouse IgG HRP (1858415; Thermo Scientific™ Pierce™, Waltham, MA, USA; 1 : 2500 to 1 : 5000 dilution in blocking solution). The acquired images of the gels (prior blotting) were analyzed using the GELANALYZER, online available, free densitometric software (<http://Gel.Analyser.com>). Thus, one may use the same gel for both in gel fluorescence detection followed by blotting and immunodetection.

The same gels that underwent detection via fluorescence scanning were blotted and underwent detection with ECL (enhanced chemiluminescence) without further processing such as stripping.

Thus, fluorescent detection can be combined with ECL in one simple workflow. For evaluation of pH dependence, 50 mM Tris Cl was used as a buffering agent at pH 6.75, 7.0, 7.5, 8.0, 8.5 and 9.0.

Real-time ubiquitination assay using fluorescence polarization

For FP, the reaction mixture (24 μ l) containing all the components except the ATP was incubated in a 384 well microplate (cat. no. 3712 or 3764; Corning, Corning, NY, USA) at 30°C in a M1000 infinite plate reader (Tecan) until the temperature was stable (typically after 4–5 min) and the reaction was triggered by adding 6 μ l of 10 mM ATP preheated to 30°C. FP was monitored every 2 min at 562 nm while the excitation wavelength was set to 470 nm. The M1000 fluorescence polarization module was calibrated using 10 nM fluorescein in 10 mM NaOH at FP = 20 mP.

Results

PRT1 is an E3 ubiquitin ligase and prefers bulky N-termini

For the analysis of PRT1 E3 ligase function, that is, recognition of N end rule substrates, we used recombinant PRT1 together with generic substrate reagents with novel detection features combining chemically synthesized fluorophores and recombinant ubiquitination acceptors which were used as live protein modification detectors. To describe the N terminal amino acid specificity of PRT1, the N terminally variable protein parts of the reporters were engineered as N terminal His8:MBP fusions comprising a recognition sequence of TEV protease at the junction to the subsequent generic substrate protein moiety (Figs 2a, S1a). Cleavage by TEV gave rise to small C terminal fragments of the His8:MBP substrate fusions of which the neo N terminal, that is, the P1' residue of the TEV cleavage site, can be altered to all proteinogenic amino acids except proline (Kapust *et al.*, 2002; Phan *et al.*, 2002; Naumann *et al.*, 2016). For a novel fluorescence based approach, we covalently coupled a synthetic fluorescent probe (Fig. 2b) to the artificial substrate protein. The resulting reagent served as the fluorescent protein Ub acceptor in N end rule ubiquitination assays. The architecture of the reagent is as follows: after the cleavable His8:MBP tag, eK, part of *E. coli lacZ* (Bachmair *et al.*, 1986) followed by a triple hemagglutinin epitope tag (3HA) for immunodetection and an *E. coli flavodoxin* (Flv) were combined. The junctions between His8:MBP and eK encode the N termini glycine (Gly (G)), phenylalanine (Phe (F)), arginine (Arg (R)), and leucine (Leu (L)) that become N terminally exposed after TEV cleavage. Flv was chosen as a highly soluble and stable protein and includes flavin mononucleotide as a cofactor. Its semiquinone is fluorescent but not stable enough to be used as a fluorophore for detection in its plain form. Therefore, we decided to additionally label the Flv protein. The G/F/L/R eK Flv constructs contain a single cysteine (Cys101 of Flv) that allowed the labeling of the purified recombinant fusion protein with a novel thiol reactive

probe that comprises an iodoacetamide polyethylene glycol (PEG) linker and the fluorogenic subunit of 4 nitro 2,1,3 benzoxadiazole (NBD; Fig. 2b). We chose the latter in view of its small size compared with other labeling reagents such as large fluorescein moieties and because it can be detected very specifically by both UV absorption and UV fluorescence with low background interference. In principle, if Cys residues are not required for activity, folding or protein interactions, more amenable Cys would lead to higher labeling efficiency. The labeling efficiency was *c.* 30% on average, based on the fluorescence intensity of the labeled substrate, using free NBD as a standard for calibration.

In an *in vitro* ubiquitination assay, we used recombinant UBC8 as a promiscuous E2 conjugating enzyme and UBA1 as an E1 activating enzyme (Stegmann *et al.*, 2012) and show here for the first time E3 ligase activity of PRT1 depending on E1, E2 and ATP (Fig. 2c). PRT1 discriminated a substrate by its N terminal, aiding the transfer of Ub to the substrate and leading to polyubiquitination. After immunostaining with anti Ub antibodies, usually, a typical smear of higher molecular weight compared with the target protein's size is observed or, after probing with target specific antibodies, a more or less distinct laddering, also of high molecular weight, becomes evident. These are the common signs for polyubiquitination and a clear laddering was also visualized by fluorescent scanning in our novel approach. We identified distinct subspecies via in gel detection (Fig. 2c). A classical end time point assay where the reaction was stopped at different reaction time points followed by SDS PAGE and in gel fluorescence detection revealed the kinetics of PRT1 activity using F eK Flv as a substrate (Fig. 2d).

However, real time monitoring of the kinetic profile of the enzymatic reaction is only possible via FP in live detection measurements. The kinetic profile is best fitted with an S shaped curve and a growth curve model of logistic type (Richards' equation) rather than exponentially as expected for simple kinetics (Fig. 2e).

It was previously suggested that PRT1 binds to N degrons carrying bulky destabilizing residues (Stary *et al.*, 2003), but biochemical evidence for that was still lacking. By changing the N terminal residue of the X eK Flv NBD substrate, it was possible to reveal that PRT1 indeed discriminates the substrates according to the N terminal residue, as expected (Figs 2f, S1b,c). While the substrates carrying G, R and L initiated N termini showed poor ubiquitination, F eK Flv NBD was heavily ubiquitinated. Lysines are the general acceptor sites of Ub transfer from E2 to the substrate and are a requirement for any ubiquitination substrate. Their removal was expected to negatively influence the Ub chain formation. There are an additional seven lysine residues present in Flv itself but they are less likely to act as Ub acceptors as they are less accessible (Fig. S1a). While the eK based substrate showed the kinetic curve discussed in the previous paragraph, the control F e Δ K Flv substrate with mutated lysines (expected sites of ubiquitination, Lys15 and Lys17, both replaced by Arg) presented a faster initial rate of ubiquitination but FP values of only half the final value (Fig. 2f). This is in good agreement with the in gel fluorescence detection, where lower degrees of

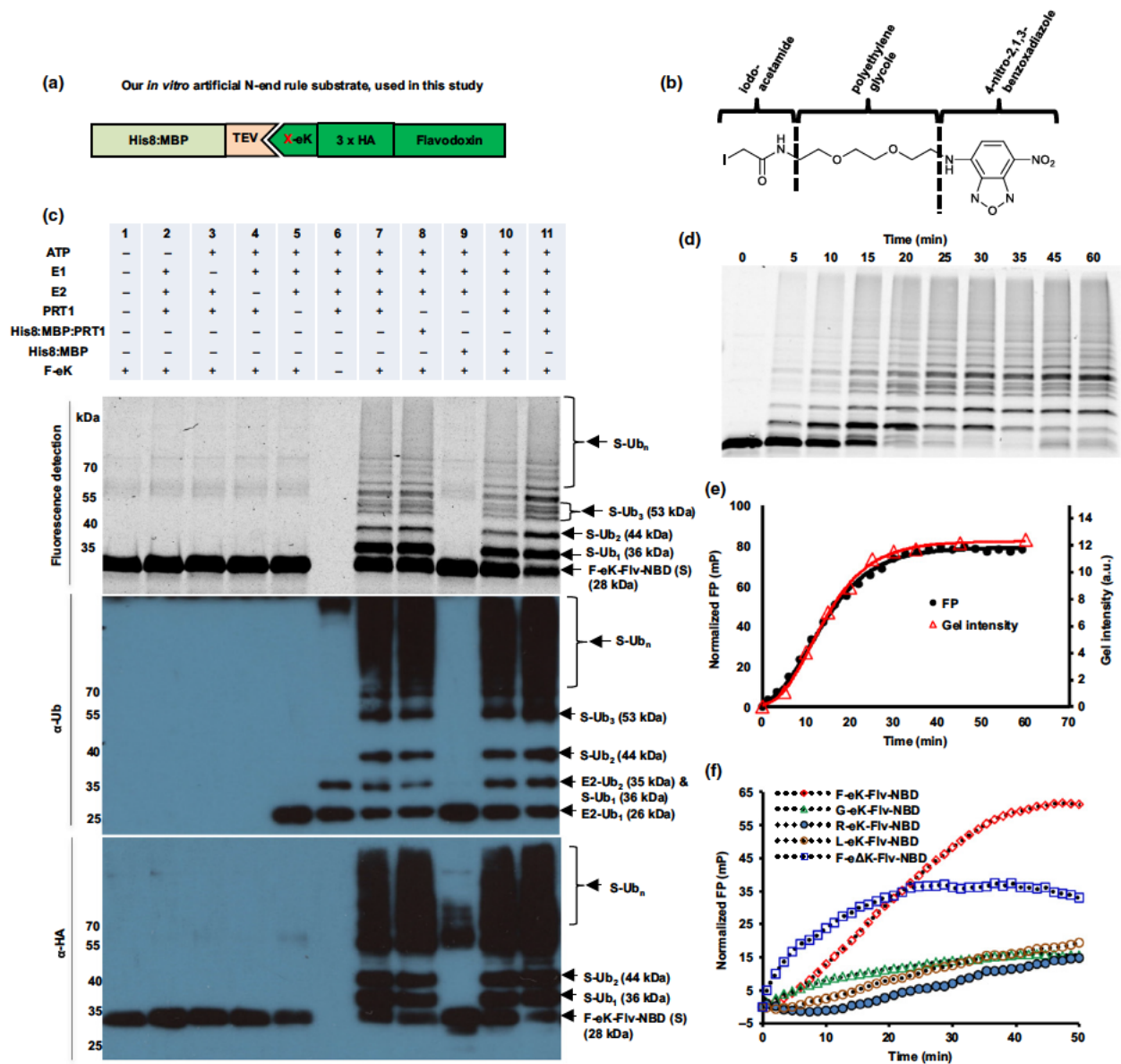


Fig. 2 Fluorescent protein conjugates for monitoring *in vitro* substrate ubiquitination in real time. (a) Design of recombinant fusion proteins used as N end rule substrates. After tobacco etch virus (TEV) cleavage and removal of the His8:MBP affinity tag, the artificial substrate based on *Escherichia coli* flavodoxin (Flv) is initiated with a neo N terminal, here Phe (F), Gly (G), Leu (L) or Arg (R). (b) Skeletal formula of the synthesized thiol reactive fluorescent compound. The substrate was covalently tagged with the reagent composed of iodoacetamide, polyethylene glycol (PEG) linker and 4-nitro-2,1,3-benzoxadiazole (NBD). The reactive iodine containing group on the left couples to the thiol group of internal Cys residues of Flv. NBD serves as a fluorophore with excitation at 470 nm and emission at 520 nm. (c) Detection via fluorescence and immunoblotting of the F-eK-Flv-NBD after *in vitro* ubiquitination. The labeled protein and its ubiquitinated variants were detected via fluorescence scanning directly from the SDS-PAGE gel followed by western blotting and immunodetection with anti-HA and anti-Ub antibodies. Lane 6 shows ubiquitinated E2 and autoubiquitination of PROTEOLYSIS1 (PRT1) as a very high molecular weight 'smear'. Cleaved PRT1 as well as His8:MBP tagged PRT1 were used together with His:UBA1 (E1) and His:UBC8 (E2) (Stegmann *et al.*, 2012). (d, e) Kinetic profiles of PRT1 mediated ubiquitination. F-eK-Flv-NBD ubiquitination was monitored by fluorescence polarization (FP) and in-gel fluorescence scanning. The S-shaped kinetic curve is observed in both in-gel fluorescence scanning detection and fluorescence polarization. (f) N-terminal specificity evaluated by real-time ubiquitination detection. Fluorescently labeled R-eK-Flv, L-eK-Flv, G-eK-Flv, F-eΔK-Flv and F-eK-Flv were comparatively evaluated for their degree of ubiquitination by PRT1.

ubiquitination of F-eΔK-Flv, and reduced mono and di ubiquitination but still clear polyubiquitination were observed (Fig. S1c).

Another observation of the ubiquitination pattern in the in-gel fluorescence image (using three different independent substrate protein purifications of F-eK-Flv-NBD) was that the tri

ubiquitinated form presented three distinct subspecies which eventually led to a multitude of other species at a higher level (Fig. S1b). There was only one species of tri ubiquitinated F eK Flv NBD generated, where two ubiquitination acceptors sites within eK (Lys15 and Lys17) were replaced by Arg (Fig. S1b).

Fluorescently labeled substrate proteins reveal the mechanism of PRT1-mediated ubiquitination

The combination of the proposed two fluorescence based methods allowed fast and efficient *in vitro* investigation of the ubiquitination process via the E3 ligase PRT1 and the optimization of the reaction conditions. As a first approach utilizing the real time

assay in the context of substrate ubiquitination, we studied the effect of changes in pH on the ubiquitination process mediated by PRT1. The pH is an important parameter regulating enzyme activity and is especially important for E3 ligase function as the mechanism implies a nucleophilic attack of the accepting lysine of the substrate on the carbonyl group of the thioester of E2 Ub. This attack is highly dependent on the pH < A classical end time approach revealed the reaction optimum to be clearly above pH 7 but below pH 9, as indicated by the occurrence of polyubiquitinated species of the fluorescent substrate probe F eK Flv NBD (Fig. 3a). However, using our real time FP protocol, we additionally acquired the kinetic profile of the PRT1 mediated ubiquitination process (Fig. 3b) and the maximum polarization values of this reaction that were reached (Fig. 3c). These correlated with

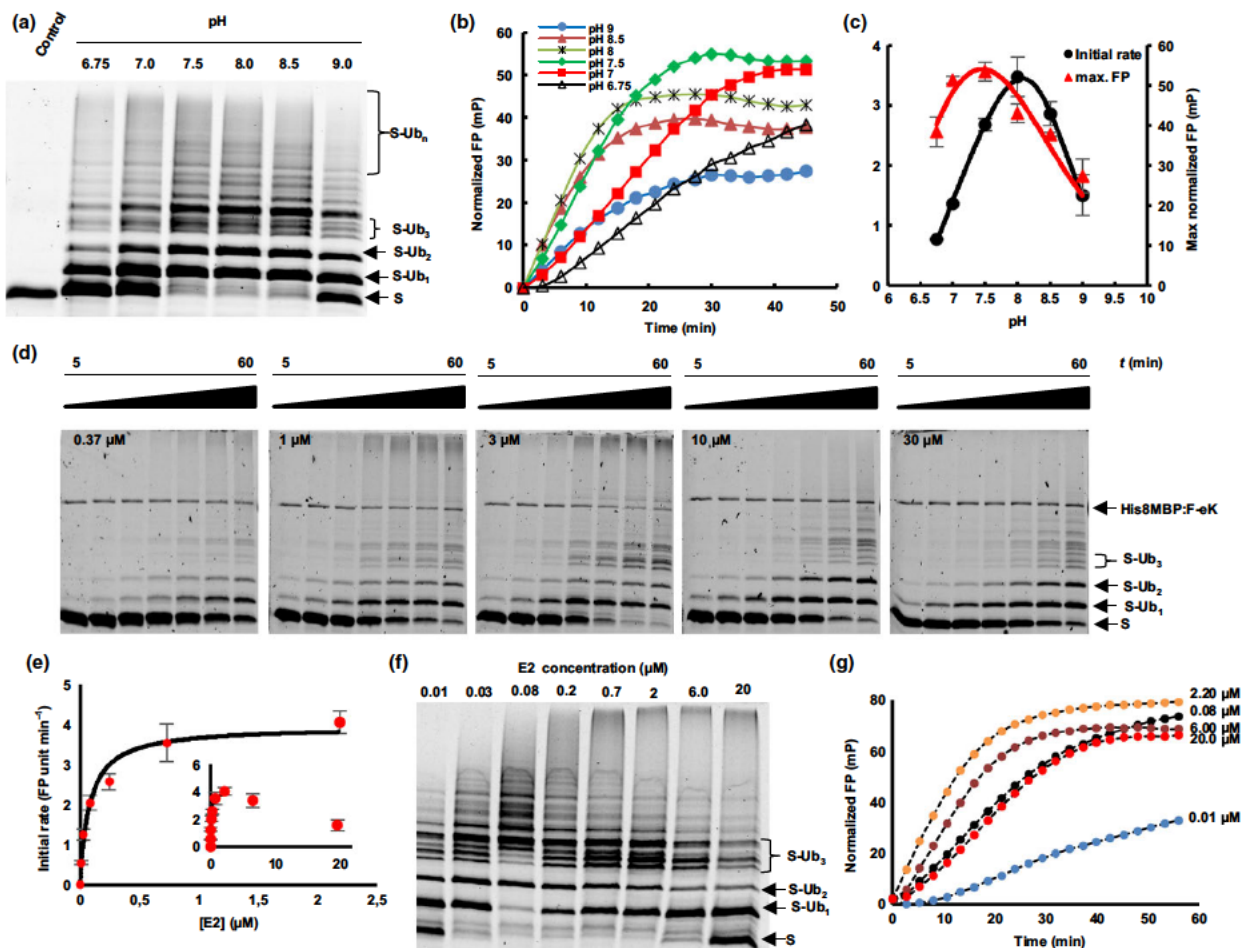


Fig. 3 Applications of fluorescent protein conjugates for monitoring pH dependent ubiquitination and enzymatic parameters of PROTEOLYSIS1 (PRT1) E3 ligase. (a) pH dependent ubiquitination of the F eK Flv substrate. (a) In gel detection of F eK Flv ubiquitinated species after a 1 h reaction at several pH values demonstrating different patterns of polyubiquitination preferences depending on the pH. (b) Kinetic profiles. (c) Initial rates and maximum end time fluorescence polarization (FP) values forming a bell shaped distribution depending on the pH. (d) PRT1 mediated ubiquitination of F eK Flv dependent on the concentration of E2 conjugating enzyme (UBC8). (d) Time dependence of ubiquitination at several E2 concentrations for the first 60 min at 5 nM PRT1; time scale: 5 60 min. (e) Michaelis-Menten curve plotted using the initial rate from FP data suggests an E2 driven inhibition effect. (f) Influence of E2 concentration on the ubiquitination pattern evaluated using in gel fluorescence scanning and (g) kinetic profiles were obtained using FP measurements, with similar conditions as in (d) but with a 10 times higher concentration of PRT1; that is, 50 nM.

the amount of polyubiquitinated species detected in the SDS PAGE gel based end time experiment (Fig. 3a) and the highest initial rate (Fig. 3c), whereas the latter appears to be different from the reaction optimum according to the detected maximum FP. We also had previously observed that F e Δ K Flv ubiquitination presented a faster initial rate but only half of the final FP (Fig. 2f) and lower degrees of final ubiquitination (Fig. S1c). Both bell shaped forms of the pH dependence for the highest initial reaction rate (pH 8.0) and the maximum substrate polyubiquitination rate (pH 7.5) indicated two competing processes that generate a local maximum (Fig. 3c).

A strong decrease of the ubiquitination rate mediated by PRT1 was observed at higher concentrations of the E2 conjugating enzyme UBC8 (> 2 μ M) via both in gel fluorescence (Fig. 3d) and FP (Fig. 3e g). Based on the FP measurements using a concentration of UBC8 of up to 2 μ M, the Michaelis Menten constant (K_M) of substrate ubiquitination by PRT1 at different E2 concentrations was found to be in the submicromolar range, 0.08 ± 0.01 μ M, indicating very tight binding of E2 to PRT1 compared with other RING (Really Interesting New Gene) E3 ligases (Ye & Rape, 2009; Fig. 3e). Moreover, the distribution pattern of the ubiquitinated substrate species at the end of the reaction (Fig. 3f) and the kinetic profiles of ubiquitination (Fig. 3g) are different, depending on the E2 concentration used.

Discussion

The N end rule pathway is a vibrant emerging area of research in plant sciences and agriculture (Gibbs *et al.*, 2011, 2014b; Licausi *et al.*, 2011; Weits *et al.*, 2014; de Marchi *et al.*, 2016; Mendiondo *et al.*, 2016; reviewed in Gibbs *et al.*, 2014a, 2016; Gibbs, 2015; N. Dissmeyer *et al.*, unpublished). Taking the first *bona fide* plant N end rule E3 Ub ligase PRT1 as a model, we have described a novel tool with which to molecularly characterize polyubiquitination live, in real time, and have used it to gain mechanistic insights into PRT1 substrate preference, activation and functional pairing with an E2 conjugating enzyme. To date, the activity and function of enzymatic N end rule pathway components have only been speculated upon, and the field was lacking investigations at the molecular level. Here, we have provided the first molecular evidence of ubiquitination activity of an E3 ligase candidate for the plant N end rule pathway.

In this study, we have demonstrated PRT1 E3 Ub ligase activity and substrate preference by using recombinant PRT1 together with artificial protein substrates in an *in vitro* fluorescence based life ubiquitination assay. We found that, first, the reporter construct based on bacterial Flv chemically coupled to NBD (Fig. 2b) works as a ubiquitination acceptor. Second, this reaction reflects substrate specificity and cannot be considered an *in vitro* artifact, as N terminal amino acids other than Phe rendered the substrate a weaker target for PRT1 (Figs 2f, S1b,c). Third, our test system allowed description of E3 ligase function and target specificity by using variants of labeled substrates.

Similar experiments are usually based on immunochemical and colorimetric detection, incorporation of radioisotopes such as 125 I or 32 P, or fluorescently labeled native or recombinant Ub

(Ronchi & Haas, 2012; Melvin *et al.*, 2013; Lu *et al.*, 2015a,b; Table S1). However, problems of steric hindrance produced by modifying Ub and difficulties in discriminating between auto and substrate ubiquitination if using labeled Ub may occur. Also, artificial experimental set ups such as single molecule approaches or extreme buffer conditions might not represent or support for formation of the required complex ubiquitination machinery (Table S1). Our assay allowed both direct assessment during the actual FP experiment and gel based evaluation after completing SDS PAGE. This renders protein transfer via western blotting and the subsequent time consuming steps of blocking, immunodetection and chemical detection obsolete. The protocol described is rapid and nonradioactive, uses only a small fluorophore as a covalent dye, and works with complete substrate proteins instead of only peptides, and the results produced can be read out live in real time. Moreover, the FP approach provides superimposable kinetic curves with data from classical end time point assays, but faster, with higher resolution in time and using fewer reagents. The advantage of a combination of the two fluorescence based approaches described, that is, the gel based approach and FP, is the possibility of gaining mechanistic insights, which is not possible if only one of the protocols is used. An example is the determination of K_M and the catalytic rate constant (k_{cat}) of the interaction of the E3 ligase PRT1 with E2 conjugating enzymes. This determination included the influence of the E2 concentration on both the ubiquitinated substrate species and the kinetic profile of the ubiquitination reaction.

Using FP coupled to immunoblot analysis, we were able to confirm that PRT1 is an active E3 ligase acting in concert with the E2 conjugating enzyme UBC8. In a buffer system close to physiological conditions, it could be shown that PRT1 not only monoubiquitinates N degron containing substrates, but also mediates polyubiquitination without the aid of further cofactors. Therefore, it was ruled out that PRT1 only monoubiquitinates, which was speculated previously (Stary *et al.*, 2003). Moreover, the action of a type II N recognin as small as PRT1 (46 kDa) is probably sufficient for subsequent target degradation by the proteasome. As PRT1 lacks the conserved ClpS domain that confers affinity to type II substrates in other N recognins, the binding mechanism of PRT1 to its substrate remains an intriguing open question.

Using FP facilitated real time monitoring of the kinetic profile of the PRT1 mediated ubiquitination, we observed an S shaped curve of the reaction (Fig. 2e). One explanation for these kinetics and the presence of an initial lag phase is an increase of the affinity of PRT1 for the monoubiquitinated substrates compared with the nonubiquitinated population. Preferences of E2s and E3s for mono or polyubiquitinated substrates and their influence on ubiquitination velocity were shown previously, but it was also shown that initial ubiquitination greatly enhances the binding affinity of E3s for the substrate in subsequent reactions (Sadowski & Sarcevic, 2010; Lu *et al.*, 2015b). Chain elongation (Ub Ub isopeptide bond formation) can be faster than chain initiation, which might represent the rate limiting step of the reaction, rather than an E1 E2 controlled limiting step. Thus, the chain elongation and chain initiation steps appear to be distinct

processes that have distinct molecular requisites, in agreement with previous findings for other E3s (Petroski & Deshaies, 2005; Deshaies & Joazeiro, 2009). The lag phase is reduced if the rate is increased by a higher concentration of PRT1 (Fig. 2e).

The FP based assay revealed that the kinetic profile of the ubiquitination was dependent on the position and availability of lysines as Ub acceptor sites, as suggested to be characteristic of N-degrons (Bachmair & Varshavsky, 1989). By lowering the overall number of available lysines in the F eΔK Flv NBD substrate (two lysines fewer than in X eK Flv constructs, with 11 Lys in total), the overall ubiquitination was detectably reduced. Differences in the kinetic curves of F eK Flv and F eΔK Flv indicated that a reduction in the number of available Lys residues led to a faster initial rate of ubiquitination, whereas the final FP values reached only half the values obtained in the assay applying the substrate with the full set of Lys residues (Figs 2f, S1c). However, the simple gel based end point assay could not determine if this was attributable to altered velocity of chain initiation vs chain elongation. The initiation per Lys residue was expected to be similar in F eK vs F eΔK Flv substrates, but chain elongation could apparently start more rapidly in F eΔK Flv. This demonstrated that the presence of E2 together with the particular substrate plays a key role in the formation of the molecular assembly facilitating the ubiquitination process. Already, the intermolecular distance between the E3 ligase and the Ub acceptor lysines of the substrate as well as the amino acid residues proximal to the acceptor lysines determine the progress of the reaction and ubiquitination specificity (Sadowski & Sarcevic, 2010). Taking the slower initiation of polyubiquitination of F eK Flv into account, the availability of lysines at the N terminus might interfere with the monoubiquitination of other, more distal lysines and E3 could remain associated with substrates that are monoubiquitinated at the N terminal.

When the F eK Flv NBD substrate fusion protein was subjected to *in vitro* ubiquitination assays, three distinct subspecies of the tri ubiquitinated form were detected vs only one form if F eΔK Flv NBD was used (Fig. S1c). This could be explained by the formation of various ubiquitinated isoforms of the substrate by utilizing different lysine side chains as ubiquitination acceptor sites. These could be either within the sequence of eK (e.g. Lys15 and Lys17) or within Flv (e.g. Lys100 and Lys222, which seem structurally more favored according to the structural model; Fig. S1a). This was further supported by the fact that there is only one species of tri ubiquitinated F eΔK Flv NBD, where two ubiquitination acceptor sites within eK (Lys15 and Lys17) are replaced by Arg (Fig. S1b).

In the analysis of the influence of pH on the function of PRT1 as an E3 Ub ligase, we documented bell shaped forms of pH dependence for the highest initial reaction rate (pH 8.0) and determined the maximum substrate polyubiquitination rate (pH 7.5). These indicated two competing processes that generate a local maximum (Fig. 3c). In the light of recently discussed mechanisms of E3 ligase action (Berndsen & Wolberger, 2014) and the prediction of two RING domains in PRT1 (Stary *et al.*, 2003), higher ubiquitination rates with increased pH could be attributable to deprotonation of the attacking lysine side chain of

the E2 active site. This would facilitate thioester cleavage between E2 and Ub and thereby mediate Ub transfer to the substrate lysines. A similar effect was observed regarding the influence of the acidic residues in close vicinity to the E2 active site, which also cause deprotonation of the lysine side chain of the incoming substrate (Plechanovova *et al.*, 2012). This possibly explains the drastic increase in the initial rate of PRT1 substrate ubiquitination in the range pH 6.8–8 (Fig. 3c). The competing processes leading to the decrease in ubiquitination at pH > 8 could be destabilization of ionic and hydrogen bonds at alkaline pH simply interfering with protein–protein interaction or ATP hydrolysis affecting the Ub charging of E2 by E1. This could also explain the premature leveling of the kinetic curves in the FP measurements at pH > 8 (Fig. 3b) while, at a longer reaction timescale, the maximum FP values would be expected to be the same from pH 6.8 to 7.5.

The apparent k_{cat} of the Ub transfer, more precisely the transfer of the first Ub molecule, which is the rate limiting step, was found to be $1.30 \pm 0.07 \text{ s}^{-1}$. This suggested that, on the one hand, PRT1 had a high turnover number as a result of a highly active catalytic center and, on the other hand, that the E2 concentration influences not only the rate of the Ub transfer to the substrate but also the mechanism itself. Possible causes are the two separate and potentially distinctly favored chain initiation and elongation processes mentioned above. These could result in lowering the rate of the initiation step at higher E2 concentrations, as both the kinetic profile and the formation of ubiquitinated species are affected and also the attacking lysines might be structurally differently favored. This is especially suggested by the variable occurrence of the distinct pattern of tri ubiquitinated substrate species (Fig. 3d,f), as mentioned above and discussed in other systems (Ye & Rape, 2009).

By using fluorescently labeled substrate proteins in the two approaches described, that is, gel based fluorescence scanning after SDS PAGE and FP, we were able to investigate the mechanism of PRT1 mediated ubiquitination and optimize the reaction conditions. The presented work serves as a model for the demonstration of differential mechanisms of substrate recognition and tight interactor binding in the N end rule pathway.

PRT1 is a plant pioneer enzyme lacking homologs in the other kingdoms, albeit small and easy to produce in an active form as a recombinant protein, rendering it an exciting candidate for further functional and structural studies of key functions of one branch of the N end rule pathway. So far, only three research articles mention work on PRT1: the two first brief descriptions (Potuschak *et al.*, 1998; Stary *et al.*, 2003) and one recently published study highlighting the role of the N end rule pathway and in particular a novel function for PRT1 in plant immunity (de Marchi *et al.*, 2016). However, to date, the community lacks proofs demonstrating that PRT1 and other E3 candidates are indeed involved in substrate protein ubiquitination.

The tool described here can be adopted by laboratories investigating N end rule related posttranslational modifications such as deamidation, methionine excision, oxidation, deamidation, arginylation, ubiquitination and degradation. Moreover, we are convinced that it may also be extended to assays for other

posttranslational modifications such as phosphorylation and to other E3 Ub ligases as long as at least one native or artificial substrate protein for the modification of interest is known. Because it makes use of chemical labeling of substrate proteins rather than labeling protein modifiers themselves, such as Ub or phosphate, one common reagent can be used for various modification assays. The approach allows one to measure and track posttranslational protein modification live and in a time resolved manner and has profound implications for our understanding of the interactions of E3 ligases with substrates and nonsubstrates. Concerning the field of the N end rule pathway, this might apply to other candidates for E3 Ub ligases, such as PROTEOLYSIS6 (PRT6) and BIG (AT3G02260), or potential N end rule adapter proteins, such as PRT7 (AT4G23860) (Tasaki *et al.*, 2005; Garzón, 2008; Talloji, 2011). These experiments will be of great interest in the future because phenotypes of biological importance and genetically determined causalities have been described and need to be substantiated at the molecular level. Therefore, we see potential for a broader impact for ubiquitination research, as it is conceivable that the method is transferable to other E3 ligases and enzyme substrate pairs. In the course of our studies, we felt that rapid, easy and cheap protocols were lacking for in depth biochemical analysis of E3 ligase kinetics, and the same holds true for nonradioactive and sterically noninterfering protocols and those where entire proteins and directly labeled substrates can be applied.

In terms of further applications, the kinetic approach allowed collection of data that can assist in setting up high throughput assays, for example for screens of inhibitors and assays assessing the influence of small molecules potentially facilitating or enhancing ubiquitination. In our example, this included testing of the enzymatic parameters of E2 E3 interactions and substrate specificities for PRT1. Similar approaches have used labeling with radionuclides or fluorescent dyes coupled to Ub (Ronchi & Haas, 2012; Melvin *et al.*, 2013; Lu *et al.*, 2015a,b). The latter covalent modification of Ub with fluorescent moieties is often impractical as these groups can sterically hinder the E1 catalyzed activation and E2 dependent transthiolation reactions (Ronchi & Haas, 2012). This in turn can alter the rate limiting step. The use of radioactive isotopes requires at least the running of an SDS PAGE and gel drying or western blotting followed by autoradiography for hours to days (Table S1). Besides the described *in vitro* methods, several protocols and tools were successfully applied *in vivo*, mainly based on translational fusions of fluorescent proteins to degrons of the Ub fusion degradation (UFD) pathway (Hamer *et al.*, 2010; Matilainen *et al.*, 2016), the N end rule pathway (Speese *et al.*, 2003; Faden *et al.*, 2016) or both (Dantuma *et al.*, 2000). Other methods make use of Ub binding systems to achieve various read outs (Marblestone *et al.*, 2012; Matilainen *et al.*, 2013; Table S1).

In conclusion, we describe a system for real time measurements of ubiquitination in solution with combined fluorescence scanning of SDS PAGE gels and fluorescence polarization. This set up was used to establish an artificial substrate protein based detection reagent that can be used to obtain important mechanistic insights into the E2 PRT1 substrate interaction. We

demonstrated that PRT1 is indeed involved in polyubiquitination of substrate proteins depending on their N terminal amino acids and therefore mechanistically investigated PRT1 as a player of the N end rule pathway for the first time.

Acknowledgements

We thank Marco Trujillo for expression clones of UBC8/UBA1, discussions and constant support and Angela Schaks for synthesis. This work was supported by a grant for the junior research group of the ScienceCampus Halle Plant based Bioeconomy to N.D., by grant WE 1467/13 1 from the German Research Foundation (DFG) to B.W., by grant DI 1794/3 1 from the DFG to N.D., by grants from the Leibniz DAAD Research Fellowship Programme of the Leibniz Association and the German Academic Exchange Service (DAAD) to A.C.M. and N.D., and by Ph.D. fellowships from the Landesgraduiertenförderung Sachsen Anhalt awarded to C.N. and F.F. Financial support came from the Leibniz Association, the state of Saxony Anhalt, the DFG Graduate Training Center GRK1026 'Conformational Transitions in Macromolecular Interactions', and the Leibniz Institute of Plant Biochemistry (IPB). A Short Term Scientific Mission (STSM) of the European Cooperation in Science and Technology (COST) program was granted to A.C.M. and N.D. by COST Action BM1307 'European network to integrate research on intracellular proteolysis pathways in health and disease (PROTEOSTASIS)'.

Author contributions

A.C.M. performed the ubiquitination reactions and related analysis. E.P. and B.W. designed and synthesized the fluorescent probe, B.W. supervised the chemical synthesis, M.K. established PRT1 ubiquitination reactions, C.N. cloned and purified PRT1, and F.F. cloned the X eK HAT fragment and performed site directed mutagenesis. N.D. and A.C.M. designed the study, wrote the manuscript under consultation with all co authors and designed the figures. All authors read and approved the final version of the manuscript.

References

- Abbas M, Berckhan S, Rooney DJ, Gibbs DJ, Vicente Conde J, Sousa Correia C, Bassel GW, Marin-de la Rosa N, Leon J, Alabadi D *et al.* 2015. Oxygen sensing coordinates photomorphogenesis to facilitate seedling survival. *Current Biology* 25: 1483–1488.
- Apel W, Schulze WX, Bock R. 2010. Identification of protein stability determinants in chloroplasts. *Plant Journal* 63: 636–650.
- Bachmair A, Becker F, Schell J. 1993. Use of a reporter transgene to generate arabidopsis mutants in ubiquitin-dependent protein degradation. *Proceedings of the National Academy of Sciences, USA* 90: 418–421.
- Bachmair A, Finley D, Varshavsky A. 1986. *In vivo* half-life of a protein is a function of its amino-terminal residue. *Science* 234: 179–186.
- Bachmair A, Varshavsky A. 1989. The degradation signal in a short-lived protein. *Cell* 56: 1019–1032.
- Berndsen CE, Wolberger C. 2014. New insights into ubiquitin E3 ligase mechanism. *Nature Structural & Molecular Biology* 21: 301–307.
- Brower CS, Piatkov KI, Varshavsky A. 2013. Neurodegeneration-associated protein fragments as short-lived substrates of the N-end rule pathway. *Molecular Cell* 50: 161–171.

- Dantuma N, Lindsten K, Glas R, Jellne M, Masucci M. 2000. Short-lived green fluorescent proteins for quantifying ubiquitin/proteasome-dependent proteolysis in living cells. *Nature Biotechnology* 18: 538–543.
- Deshais RJ, Joazeiro CA. 2009. RING domain E3 ubiquitin ligases. *Annual Review of Biochemistry* 78: 399–434.
- Dong H, Dumenil J, Lu F, Na L, Vanhaeren H, Naumann C, Klecker M, Prior R, Smith C, McKenzie N *et al.* 2017. A novel ubiquitin-activated peptidase regulates organ size in *Arabidopsis* by cleaving growth regulators that promote cell proliferation and inhibit endoreduplication. *Genes & Development*, doi: 10.1101/gad.292235.116.
- Dougan D, Truscott K, Zeth K. 2010. The bacterial N-end rule pathway: expect the unexpected. *Molecular Microbiology* 76: 545–558.
- Engelsberger WR, Schulze WX. 2012. Nitrate and ammonium lead to distinct global dynamic phosphorylation patterns when resupplied to nitrogen-starved *Arabidopsis* seedlings. *Plant Journal* 69: 978–995.
- Faden F, Ramezani T, Mielke S, Almudi I, Nairz K, Froehlich MS, Hockendorff J, Brandt W, Hoehenwarter W, Dohmen RJ *et al.* 2016. Phenotypes on demand via switchable target protein degradation in multicellular organisms. *Nature Communications* 7: 12202.
- Garzón M. 2008. *Links between the Ubiquitin-Proteasome system and cell death pathways in Arabidopsis thaliana*. Dissertation, University of Cologne, Cologne, Germany.
- Garzón M, Eifler K, Faust A, Scheel H, Hofmann K, Koncz C, Yephremov A, Bachmair A. 2007. *PRT6/AT5G02310* encodes an *Arabidopsis* ubiquitin ligase of the N-end rule pathway with arginine specificity and is not the *CER3* locus. *FEBS Letters* 581: 3189–3196.
- Gibbs DJ. 2015. Emerging functions for N-terminal protein acetylation in plants. *Trends in Plant Science* 20: 599–601.
- Gibbs DJ, Bacardit J, Bachmair A, Holdsworth MJ. 2014a. The eukaryotic N-end rule pathway: conserved mechanisms and diverse functions. *Trends in Cell Biology* 24: 603–611.
- Gibbs DJ, Bailey M, Tedds HM, Holdsworth MJ. 2016. From start to finish: amino-terminal protein modifications as degradation signals in plants. *New Phytologist* 211: 1188–1194.
- Gibbs DJ, Conde JV, Berckhan S, Prasad G, Mendiondo GM, Holdsworth MJ. 2015. Group VII ethylene response factors coordinate oxygen and nitric oxide signal transduction and stress responses in plants. *Plant Physiology* 169: 23–31.
- Gibbs DJ, Lee SC, Isa NM, Gramuglia S, Fukao T, Bassel GW, Correia CS, Corbineau F, Theodoulou FL, Bailey-Serres J *et al.* 2011. Homeostatic response to hypoxia is regulated by the N-end rule pathway in plants. *Nature* 479: 415–418.
- Gibbs DJ, Md Isa N, Movahedi M, Lozano-Juste J, Mendiondo GM, Berckhan S, Marin-de la Rosa N, Vicente Conde J, Sousa Correia C, Pearce SP *et al.* 2014b. Nitric oxide sensing in plants is mediated by proteolytic control of group VII ERF transcription factors. *Molecular Cell* 53: 369–379.
- Graciet E, Walter F, O'Maoláidigh D, Pollmann S, Meyerowitz E, Varshavsky A, Wellmer F. 2009. The N-end rule pathway controls multiple functions during *Arabidopsis* shoot and leaf development. *Proceedings of the National Academy of Sciences, USA* 106: 13618–13623.
- Hamer G, Matilainen O, Holmberg CI. 2010. A photoconvertible reporter of the ubiquitin-proteasome system *in vivo*. *Nature Methods* 7: 473–478.
- Hoernstein SN, Mueller SJ, Fiedler K, Schuelke M, Vanselow JT, Schuessele C, Lang D, Nitschke R, Igloi GL, Schlosser A *et al.* 2016. Identification of targets and interaction partners of arginyl-tRNA protein transferase in the moss *Physcomitrella patens*. *Molecular & Cellular Proteomics: MCP* 15: 1808–1822.
- Holman T, Jones P, Russell L, Medhurst A, Ubeda Tomas S, Talloji P, Marquez J, Schmuths H, Tung S, Taylor I *et al.* 2009. The N-end rule pathway promotes seed germination and establishment through removal of ABA sensitivity in *Arabidopsis*. *Proceedings of the National Academy of Sciences, USA* 106: 4549–4554.
- Humbard M, Surkov S, De Donatis G, Jenkins L, Maurizi M. 2013. The N-degradome of *Escherichia coli*: limited proteolysis *in vivo* generates a large pool of proteins bearing N-degrons. *Journal of Biological Chemistry* 288: 28913–28924.
- Kapust R, Tozser J, Copeland T, Waugh D. 2002. The P1' specificity of tobacco etch virus protease. *Biochemical and Biophysical Research Communications* 294: 949–955.
- Kim H, Kim R, Oh J, Cho H, Varshavsky A, Hwang C. 2014. The N-terminal methionine of cellular proteins as a degradation signal. *Cell* 156: 158–169.
- Kumar E, Charvet C, Lokesh G, Natarajan A. 2011. High-throughput fluorescence polarization assay to identify inhibitors of Cbl(TKB)-protein tyrosine kinase interactions. *Analytical Biochemistry* 411: 254–260.
- Licausi F, Kosmacz M, Weits DA, Giuntoli B, Giorgi FM, Voesenek LA, Perata P, van Dongen JT. 2011. Oxygen sensing in plants is mediated by an N-end rule pathway for protein destabilization. *Nature* 479: 419–422.
- Lu Y, Lee BH, King RW, Finley D, Kirschner MW. 2015a. Substrate degradation by the proteasome: a single-molecule kinetic analysis. *Science* 348: 1250834.
- Lu Y, Wang W, Kirschner MW. 2015b. Specificity of the anaphase-promoting complex: a single-molecule study. *Science* 348: 1248737.
- Marblestone JG, Laroque JP, Mattern MR, Leach CA. 2012. Analysis of ubiquitin E3 ligase activity using selective polyubiquitin binding proteins. *Biochimica et Biophysica Acta* 1823: 2094–2097.
- de Marchi R, Sorel M, Mooney B, Fudal I, Goslin K, Kwasniewska K, Ryan PT, Pfalz M, Kroymann J, Pollmann S *et al.* 2016. The N-end rule pathway regulates pathogen responses in plants. *Scientific Reports* 6: 26020.
- Matilainen O, Arpalahti L, Rantanen V, Hautaniemi S, Holmberg CI. 2013. Insulin/IGF-1 signaling regulates proteasome activity through the deubiquitinating enzyme UBH-4. *Cell Reports* 3: 1980–1995.
- Matilainen O, Jha S, Holmberg CI. 2016. Fluorescent tools for *in vivo* studies on the ubiquitin-proteasome system. *Methods in Molecular Biology* 1449: 215–222.
- Melvin A, Woss G, Park J, Dumberger L, Waters M, Allbritton N. 2013. A comparative analysis of the ubiquitination kinetics of multiple degrons to identify an ideal targeting sequence for a proteasome reporter. *PLoS ONE* 8: e78082.
- Mendiondo GM, Gibbs DJ, Szurman-Zubrzycka M, Korn A, Marquez J, Szarejko I, Maluszynski M, King J, Axcell B, Smart K *et al.* 2016. Enhanced waterlogging tolerance in barley by manipulation of expression of the N-end rule pathway E3 ligase PROTEOLYSIS6. *Plant Biotechnology Journal* 14: 40–50.
- Naumann C, Mot AC, Dissmeyer N. 2016. Generation of artificial N-end rule substrate proteins *in vivo* and *in vitro*. *Methods in Molecular Biology* 1450: 55–83.
- Petroski MD, Deshaies RJ. 2005. Mechanism of lysine 48-linked ubiquitin-chain synthesis by the cullin-RING ubiquitin-ligase complex SCF-Cdc34. *Cell* 123: 1107–1120.
- Phan J, Zdanov A, Evdokimov A, Tropea J, Peters H, Kapust R, Li M, Wlodawer A, Waugh D. 2002. Structural basis for the substrate specificity of tobacco etch virus protease. *Journal of Biological Chemistry* 277: 50564–50572.
- Piatkov K, Brower C, Varshavsky A. 2012. The N-end rule pathway counteracts cell death by destroying proapoptotic protein fragments. *Proceedings of the National Academy of Sciences, USA* 109: E1839–E1847.
- Plechanovova A, Jaffray EG, Tatham MH, Naismith JH, Hay RT. 2012. Structure of a RING E3 ligase and ubiquitin-loaded E2 primed for catalysis. *Nature* 489: 115–120.
- Potuschak T, Sary S, Schlogelhofer P, Becker F, Nejkaska V, Bachmair A. 1998. PRT1 of *Arabidopsis thaliana* encodes a component of the plant N-end rule pathway. *Proceedings of the National Academy of Sciences, USA* 95: 7904–7908.
- Roitinger E, Hofer M, Kocher T, Pichler P, Novatchkova M, Yang J, Schlogelhofer P, Mechtler K. 2015. Quantitative phosphoproteomics of the *ATAXIA TELANGIECTASIA*-MUTATED (ATM) and *ATAXIA TELANGIECTASIA*-MUTATED AND *RAD3*-RELATED (ATR) dependent DNA damage response in *Arabidopsis thaliana*. *Molecular & Cellular Proteomics: MCP* 14: 556–571.
- Ronchi VP, Haas AL. 2012. Measuring rates of ubiquitin chain formation as a functional readout of ligase activity. *Methods in Molecular Biology* 832: 197–218.
- Sadowski M, Sarcevic B. 2010. Mechanisms of mono- and poly-ubiquitination: ubiquitination specificity depends on compatibility between the E2 catalytic core and amino acid residues proximal to the lysine. *Cell Division* 5: 19.
- Schuessele C, Hoernstein SN, Mueller SJ, Rodriguez-Franco M, Lorenz T, Lang D, Igloi GL, Reski R. 2016. Spatio-temporal patterning of arginyl-tRNA

- protein transferase (ATE) contributes to gametophytic development in a moss. *New Phytologist* 209: 1014–1027.
- Hemorry A, Hwang C, Varshavsky A. 2013.** Control of protein quality and stoichiometries by N-terminal acetylation and the N-end rule pathway. *Molecular Cell* 50: 540–551.
- Smith M, Scaglione K, Assimon V, Patury S, Thompson A, Dickey C, Southworth D, Paulson H, Gestwicki J, Zuiderweg E. 2013.** The E3 ubiquitin ligase CHIP and the molecular chaperone Hsc70 form a dynamic, tethered complex. *Biochemistry* 52: 5354–5364.
- Speese S, Trotta N, Rodesch C, Aravamudan B, Broadie K. 2003.** The ubiquitin proteasome system acutely regulates presynaptic protein turnover and synaptic efficacy. *Current Biology* 13: 899–910.
- Sriram S, Kim B, Kwon Y. 2011.** The N-end rule pathway: emerging functions and molecular principles of substrate recognition. *Nature Reviews Molecular Cell Biology* 12: 735–747.
- Stary S, Yin X, Potuschak T, Schlogelhofer P, Nizhynska V, Bachmair A. 2003.** PRT1 of *Arabidopsis* is a ubiquitin protein ligase of the plant N-end rule pathway with specificity for aromatic amino-terminal residues. *Plant Physiology* 133: 1360–1366.
- Stegmann M, Anderson RG, Ichimura K, Pecenkova T, Reuter P, Zarsky V, McDowell JM, Shirasu K, Trujillo M. 2012.** The ubiquitin ligase PUB22 targets a subunit of the exocyst complex required for PAMP-triggered responses in *Arabidopsis*. *Plant Cell* 24: 4703–4716.
- Talhoji P. 2011.** *Identification of novel components and links in ubiquitin dependent protein degradation pathways of Arabidopsis thaliana*. Dissertation, University of Cologne, Cologne, Germany.
- Tasaki T, Mulder L, Iwamatsu A, Lee M, Davydov I, Varshavsky A, Muesing M, Kwon Y. 2005.** A family of mammalian E3 ubiquitin ligases that contain the UBR box motif and recognize N-degrons. *Molecular and Cellular Biology* 25: 7120–7136.
- Tasaki T, Sriram S, Park K, Kwon Y. 2012.** The N-end rule pathway. *Annual Review of Biochemistry* 81: 261–289.
- Thao S, Zhao Q, Kimball T, Steffen E, Blommel P, Ritters M, Newman C, Fox B, Wrobel R. 2004.** Results from high-throughput DNA cloning of *Arabidopsis thaliana* target genes using site-specific recombination. *Journal of Structural and Functional Genomics* 5: 267–276.
- Tsiatsiani L, Timmerman E, De Bock PJ, Vercammen D, Stael S, van de Cotte B, Staes A, Goethals M, Beunens T, Van Damme P *et al.* 2013.** The *Arabidopsis* METACASPASE 9 degradome. *Plant Cell* 25: 2831–2847.
- Varshavsky A. 2011.** The N-end rule pathway and regulation by proteolysis. *Protein Science* 20: 1298–1345.
- Venne AS, Solari FA, Faden F, Paretto T, Dissmeyer N, Zahedi RP. 2015.** An improved workflow for quantitative N-terminal charge-based fractional diagonal chromatography (ChaFRADIC) to study proteolytic events in *Arabidopsis thaliana*. *Proteomics* 15: 2458–2469.
- Weits D, Giuntoli B, Kosmacz M, Parlanti S, Hubberten H, Riegler H, Hoefgen R, Perata P, van Dongen J, Licausi F. 2014.** Plant cysteine oxidases control the oxygen-dependent branch of the N-end-rule pathway. *Nature Communications* 5: 3425.
- White MD, Klecker M, Hopkinson R, Weits D, Mueller C, Naumann C, O'Neill R, Wickens J, Yang J, Brooks-Bartlett J *et al.* 2017.** Plant cysteine oxidases are dioxygenases that directly enable arginyl transferase-catalyzed arginylation of N-end rule targets. *Nature Communications* 8: 14690.
- Xia Z, Webster A, Du F, Piatkov K, Ghislain M, Varshavsky A. 2008.** Substrate-binding sites of UBR1, the ubiquitin ligase of the N-end rule pathway. *Journal of Biological Chemistry* 283: 24011–24028.
- Ye Y, Rape M. 2009.** Building ubiquitin chains: E2 enzymes at work. *Nature Reviews Molecular Cell Biology* 10: 755–764.
- Yoshida S, Ito M, Callis J, Nishida I, Watanabe A. 2002.** A delayed leaf senescence mutant is defective in arginyl-tRNA:protein arginyltransferase, a component of the N-end rule pathway in *Arabidopsis*. *Plant Journal* 32: 129–137.
- Zenker M, Mayerle J, Lerch M, Tagariello A, Zerres K, Durie P, Beier M, Hulskamp G, Guzman C, Rehder H *et al.* 2005.** Deficiency of UBR1, a ubiquitin ligase of the N-end rule pathway, causes pancreatic dysfunction, malformations and mental retardation (Johanson-Blizzard syndrome). *Nature Genetics* 37: 1345–1350.

Supporting Information

Additional Supporting Information may be found online in the Supporting Information tab for this article:

Fig. S1 Modeled structure of the F eK Flv substrate and PRT1 N terminal specificity.

Table S1 State of the art ubiquitination detection methods

Table S2 Oligonucleotides used in this study

Methods S1 Synthesis of the chemical probe NBD NH PEG₂ NH haloacetamide.

Please note: Wiley Blackwell are not responsible for the content or functionality of any Supporting Information supplied by the authors. Any queries (other than missing material) should be directed to the *New Phytologist* Central Office.

1.3.2 Core regulator of cell differentiation is the first PROTEOLYSIS1 target

The central organ size and cell proliferation regulator BIG BROTHER is cut by the protease DA1 in a double-negative feed-back loop and afterwards recognized by N-end rule E3 ubiquitin ligase PRT1 which leads to its degradation – as its first identified substrate.

Publication:

Dong H, Dumenil J, Lu F, Na L, Vanhaeren H, Naumann C, Klecker M, Prior R, Smith C, McKenzie N, Saalbach G, Chen L, Xia T, Gonzalez N, Seguela M, Inzé D, **Dissmeyer N**, Li Y*, Bevan M*. Ubiquitylation activates a peptidase that promotes cleavage and destabilization of its activating E3 ligases and diverse growth regulatory proteins to limit cell proliferation in Arabidopsis.

Genes Dev. 2017, **31**:197-208

Ubiquitylation activates a peptidase that promotes cleavage and destabilization of its activating E3 ligases and diverse growth regulatory proteins to limit cell proliferation in *Arabidopsis*

Hui Dong,^{1,6} Jack Dumenil,^{1,6} Fu-Hao Lu,^{1,6} Li Na,^{2,6} Hannes Vanhaeren,³ Christin Naumann,⁴ Maria Klecker,⁴ Rachel Prior,¹ Caroline Smith,¹ Neil McKenzie,¹ Gerhard Saalbach,¹ Liangliang Chen,² Tian Xia,² Nathalie Gonzalez,³ Mathilde Seguela,^{1,5} Dirk Inze,³ Nico Dissmeyer,⁴ Yunhai Li,² and Michael W. Bevan¹

¹John Innes Centre, Norwich NR4 7QA, United Kingdom; ²State Key Laboratory of Plant Cell and Chromosome Engineering, CAS Centre of Excellence in Molecular Plant Biology, Institute of Genetics and Developmental Biology, Chinese Academy of Sciences, Beijing 100101, China; ³VIB-UGent Centre for Plant Systems Biology, Ghent University, 9052 Gent, Belgium; ⁴Leibniz Institute of Plant Biochemistry (IPB), D-06120 Halle, Germany

The characteristic shapes and sizes of organs are established by cell proliferation patterns and final cell sizes, but the underlying molecular mechanisms coordinating these are poorly understood. Here we characterize a ubiquitin-activated peptidase called DA1 that limits the duration of cell proliferation during organ growth in *Arabidopsis thaliana*. The peptidase is activated by two RING E3 ligases, Big Brother (BB) and DA2, which are subsequently cleaved by the activated peptidase and destabilized. In the case of BB, cleavage leads to destabilization by the RING E3 ligase PROTEOLYSIS 1 (PRT1) of the N-end rule pathway. DA1 peptidase activity also cleaves the deubiquitylase UBP15, which promotes cell proliferation, and the transcription factors TEOSINTE BRANCHED 1/CYCLOIDEA/PCF 15 (TCP15) and TCP22, which promote cell proliferation and repress endoreduplication. We propose that DA1 peptidase activity regulates the duration of cell proliferation and the transition to endoreduplication and differentiation during organ formation in plants by coordinating the destabilization of regulatory proteins.

[*Keywords:* ubiquitylation; organ size; *Arabidopsis*; ubiquitin activated peptidase; N end rule mediated degradation]

Supplemental material is available for this article.

Received October 17, 2016; revised version accepted January 11, 2017.

The shapes and sizes of organs are established by mechanisms that orient cell proliferation and determine the final numbers and sizes of cells forming the organ. Transplantation experiments showed that some animal organs have an intrinsic mechanism that determines their final size by controlling the duration of cell proliferation (Barry and Camargo 2013), which is controlled in part by the HIPPO/YAP pathway that limits cell proliferation and promotes apoptosis (Pan 2010). However, the mechanisms coordinating cell proliferation and cell size during organ growth remain poorly understood (Johnston and

Gallant 2002). Due to the simpler planar structures of their organs, such as leaves and petals, and the absence of cell movement due to rigid cell walls, plants have some experimental advantages for studying organ growth (Green et al. 2010).

Leaf growth in plants is initiated at shoot meristems (for review, see Sluis and Hake 2015). After specification of boundaries and growth axes, the leaf lamina grows in an initial period of cell division in which cell size is relatively constant, followed by a transition to endoreduplication as associated with cell expansion and differentiation (Breuer et al. 2010; De Veylder et al. 2011). The transition from cell proliferation to cell expansion is spatially and temporally regulated during leaf growth and appears to progress from the tip to the base of the leaf as a cell division arrest

⁵Present address: UMR1318, Institut Jean-Pierre Bourgin, 78000 Versailles, France.

⁶These authors contributed equally to this work.

Corresponding authors: michael.bevan@jic.ac.uk, yhli@genetics.ac.cn
Article Published online ahead of print. Article and publication date are online at <http://www.genesdev.org/cgi/doi/10.1101/gad.292235.116>. Freely available online through the *Genes & Development* Open Access option.

© 2017 Dong et al. This article, published in *Genes & Development*, is available under a Creative Commons License [Attribution 4.0 International], as described at <http://creativecommons.org/licenses/by/4.0/>.

Dong et al.

front (Kazama et al. 2010) accompanied by shifts in gene expression patterns (Efroni et al. 2008; Andriankaja et al. 2012). A key question is how the transition from cell proliferation to cell expansion and differentiation is coordinated to generate a correctly sized organ.

The RING E3 ligases Big Brother (BB) (Disch et al. 2006) and DA2 (Xia et al. 2013) limit the duration of cell proliferation during organ growth. Members of the *DA1* family also limit cell proliferation (Li et al. 2008), and loss of function mutations in *BB* and *DA2* interact synergistically with the *da1 1* allele of *DA1* to increase organ and seed size in *Arabidopsis* (Li et al. 2008; Xia et al. 2013), suggesting that one of their growth limiting activities is mediated by enhancing the growth repressive activity of *DA1* family members. Genetic analyses showed that *DA1* reduced the stability of both *UBP15* (Du et al. 2014), a deubiquitylation enzyme promoting cell proliferation (Liu et al. 2008), and *TEOSINTE BRANCHED 1/CYCLOIDEA/PCF 14* (*TCP14*) and *TCP15* proteins (Peng et al. 2015), which repress endoreduplication by transcriptional control of *RETINOBLASTOMA RELATED 1* (*RBR1*) and *CYCLIN A2;3* (*CYCA2;3*) gene expression (Li et al. 2012).

Here we show that *DA1* is an endopeptidase activated by multiple ubiquitylations mediated by the E3 ligases *BB* and *DA2*. In a feedback mechanism, *DA1* then cleaves *BB* and *DA2*, leading to their destabilization. *DA1* mediated cleavage of *BB* exposed a destabilizing N terminal that was substrate for the N end rule E3 ligase *PROTEOLYSIS 1* (*PRT1*). This mechanism is predicted to transiently activate *DA1* peptidase, which also cleaves *UBP15*, *TCP15*, and the related *TCP22*, leading to their predicted inactivation and destabilization. *DA1* peptidase may therefore contribute to the concerted transition from cell proliferation to endoreduplication and differentiation, limiting organ size.

Results

Genetic and physical interactions of DA1, BB, and DA2

We previously identified genetic interactions between the *da1 1* allele of *DA1* and genes encoding the RING E3 ligases *BB* (Li et al. 2008) and *DA2* (Xia et al. 2013) that led to synergistic increases in seed and organ sizes. In this study, we used the *da1 1* enhancing allele of *BB* called *eod1 2* (Li et al. 2008) and refer to the mutant version as *bb eod1 2* and the wild type version as *BB*. The *da1 1* allele, an R358K change in a highly conserved region, had a negative influence on the functions of *DA1* and the close family member *DAR1*, but the basis of this was not known, which complicated interpretation of *DA1* function. We therefore assessed phenotypes of a loss of function T DNA allele of *DA1* (*da1 ko1*).

Measurements of petal and seed sizes using high resolution scanning showed that the *da1 ko1* T DNA allele led to increased petal (Fig. 1A,B) and seed (Fig. 1C,D) sizes and that it also interacted genetically with the loss of function allele *bb eod1 2* and *da2 1* in both petal size and seed area. This showed that *DA1* can be studied independently of other *DA1* family members. Both the *da1 1*

and *bb eod1 2* mutations increased the maximum growth rate, while the double mutant *da1 1 bb eod1 2* showed a further increased maximum growth rate and continued to grow for ~5 d longer than either single mutant (Fig. 1E). The time at maximum growth rates was slightly earlier in *bb eod1 2* than in Columbia (Col 0), in contrast to *da1 1* and *da1 1 bb eod1 2*, which showed a 3 d retardation of the time of maximum growth rate, and final leaf sizes showed a more than additive increase in the double mutant, as observed previously (Li et al. 2008). These data indicated that *BB* may influence leaf final size at earlier stages of growth than *DA1*. We demonstrated previously that *DA1* and *DA2* physically interact (Xia et al. 2013). Pull down experiments showed that GST tagged *DA1* also interacted with HIS tagged *BB* but not with HIS tagged *BBR* (*BB* related; At3g19910), a close homolog of *BB* (Fig. 1F; Breuninger and Lenhard 2012). These in vitro interactions were verified by *Agrobacterium* mediated coexpression of *BB* GFP and Myc tagged *DA1* in *Nicotiana benthamiana* leaves. Myc *DA1* was detected only in a complex with *BB* GFP and not GFP (Fig. 1G).

DA1 is multiply ubiquitylated by BB and DA2

The interactions of *DA1* with *BB* and *DA2* suggested that *DA1* might be a substrate of these RING E3 ligases, so we conducted in vitro ubiquitylation reactions using *BB*, *DA2*, and *BBR* E3 ligases. Figure 2A shows that *BB* ubiquitylated *DA1* in an E1 and E2 dependent reaction, as did *DA2* (Fig. 2B), while *BBR* did not (Fig. 2C). Supplemental Figure S1 shows that *DA2* also ubiquitylated *DAR1* and *DAR2* but not *DAR3*. The extent of *DA1* ubiquitylation suggested that *DA2* was more efficient at ubiquitylation than *BB*, and the sizes of ubiquitylated *DA1* indicated that between four and seven ubiquitin molecules may be conjugated to *DA1*. Mass spectrometric analyses of ubiquitylated *DA1* prepared in vitro were used to identify peptides containing the characteristic diglycine ubiquitylation signature of a lysine residue (KGG). Analysis of *DA1* ubiquitylated by *DA2* or *BB* identified seven ubiquitylated lysine residues in *DA1*, with four lysines in the C terminal domain of *DA1* (K381, K391, K475, and K591) consistently conjugated with ubiquitin (Supplemental Fig. S2). This number of ubiquitylation sites concurred with the patterns of ubiquitylation observed in Figure 2, A and B, suggesting that *DA1* molecules are multiply ubiquitylated (Haglund et al. 2003; Komander and Rape 2012). Mutation of the consistently ubiquitylated lysines to arginine in *DA1* [termed *DA1(4K 4R)*] did not reduce ubiquitylation by *DA2* in vitro (Fig. 2D), and mass spectrometric analyses showed ectopic ubiquitylation of other lysines across *DA1* (Supplemental Fig. S2B). Therefore, the *DA1* ubiquitylation mechanism has a preference, but not specificity, for certain lysines. These patterns of ubiquitylation are shown in Figure 2D.

DA1 and four other family members have multiple ubiquitin interaction motifs (UIMs) that interact with ubiquitin (Li et al. 2008; Peng et al. 2015). UIMs are part of a larger class of ubiquitin binding domains (UBDs) formed from a single α helix that is often found in multiple

A ubiquitin-activated peptidase and organ growth

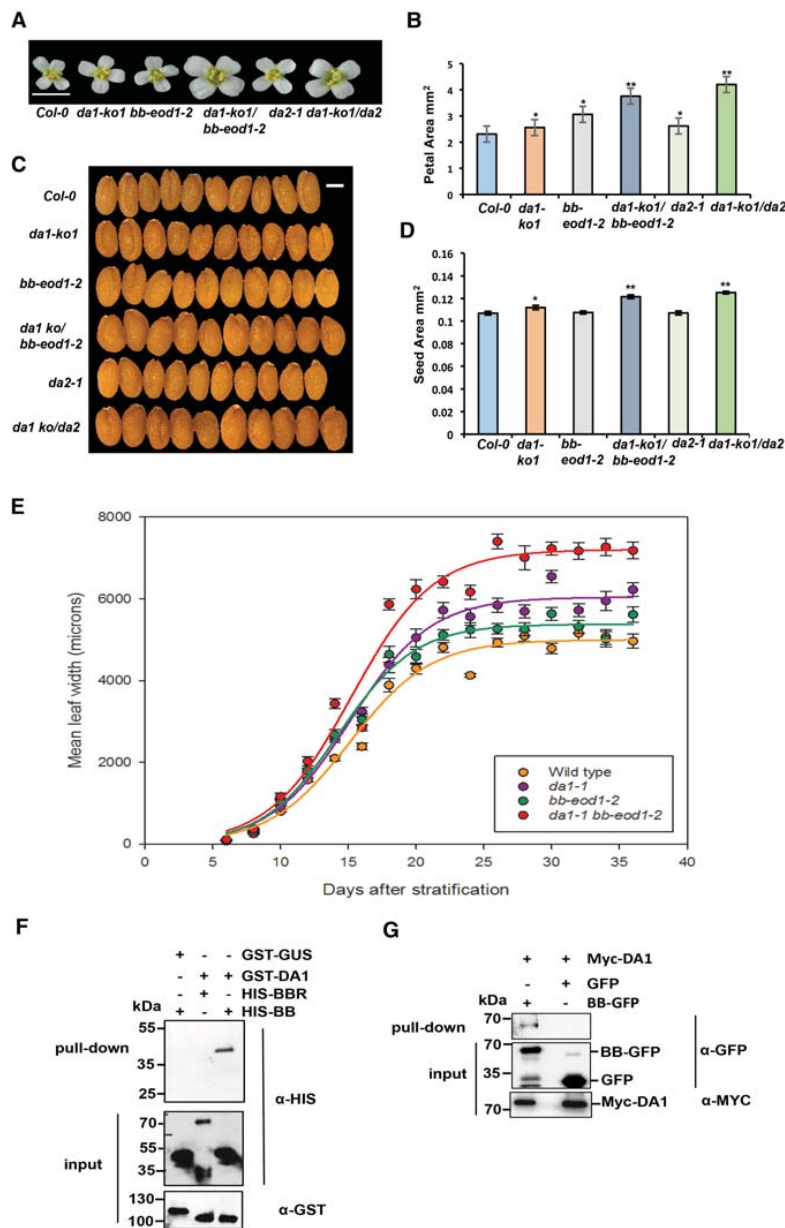


Figure 1. Genetic and physical interactions of DA1, BB, and DA2. (A,B) The single loss-of-function *da1-ko1* allele interacts with *bb-eod1-2* and *da2-1* to increase petal area. (A) An image of flower heads showing the sizes of petals. Bar, 5 mm. (B) Petal areas. The values given are means ($n = 36$) \pm SE. (*) $P < 0.05$; (**) $P < 0.01$ (Student's *t*-test) compared with wild-type Col-0. (C,D) The single loss-of-function *da1-ko1* allele interacts with *bb-eod1-2* and *da2-1* to increase seed area. (C) Ten seeds aligned to reveal size differences. Bar, 2 mm. (D) Seed areas. The values given are means ($n = 50$) \pm SE. (*) $P < 0.05$; (**) $P < 0.01$ (Student's *t*-test) compared with wild-type Col-0. (E) Dynamic growth measurements of leaf 1 width in Col-0, *da1-1*, and *da1-1 bb-eod1-2*. Lines were fitted to data points using the sigmoidal function of sigmaplot 13. (F) DA1 interacts with BB in vitro. GST-DA1 interacted with HIS-BB. GST-DA1 did not interact with HIS-BBR, an E3 ligase closely related to BB. GST-GUS (β -glucuronidase) was used as a negative control. (G) Myc-tagged DA1 interacted with BB-GFP after transient coexpression in *N. benthamiana* leaves. BB-GFP and GFP were coexpressed with Myc-DA1 using *Agrobacterium*-mediated transient expression in *N. benthamiana* leaves. Expressed proteins were purified using GFP trap and immunoblotted.

arrays (Hicke et al. 2005; Husnjak and Dikic 2012). Tandem UIMs have been shown to bind K63 linked ubiquitin chains in the mammalian DNA repair protein RAP80 (Sato et al. 2009). To assess their function in DA1, the N terminal region of DA1 containing mutated UIM1 and UIM2 was fused to GST and expressed in *Escherichia coli*, and conserved Ala and Ser residues, predicted to be in the α helical domain of the UIMs (Supplemental Fig. S3; Kim et al. 2007), were mutated to Gly in both UIMs of GST UIM1+2 and in DA1. GST UIM1+2 bound ubiquitin, and mutation of UIM1 alone did not reduce binding of

ubiquitin, while mutation of UIM2 abolished ubiquitin binding, confirming that the GST UIM1+2 protein bound ubiquitin via its UIM motifs (Supplemental Fig. S3). Figure 2E shows that UIM1+2 conferred BB and DA2 dependent ubiquitylation on GST in vitro, with DA2 again facilitating higher levels of ubiquitylation. Figure 2F shows that mutation of both UIM1 and UIM2 in GST UIM1+2 strongly reduced in vitro ubiquitylation of GST UIM1+2 by BB and DA2. The UIM1 and UIM2 mutations in DA1 also reduced its ubiquitylation in vitro (Fig. 2G), and DA1 with mutated UIMs did not

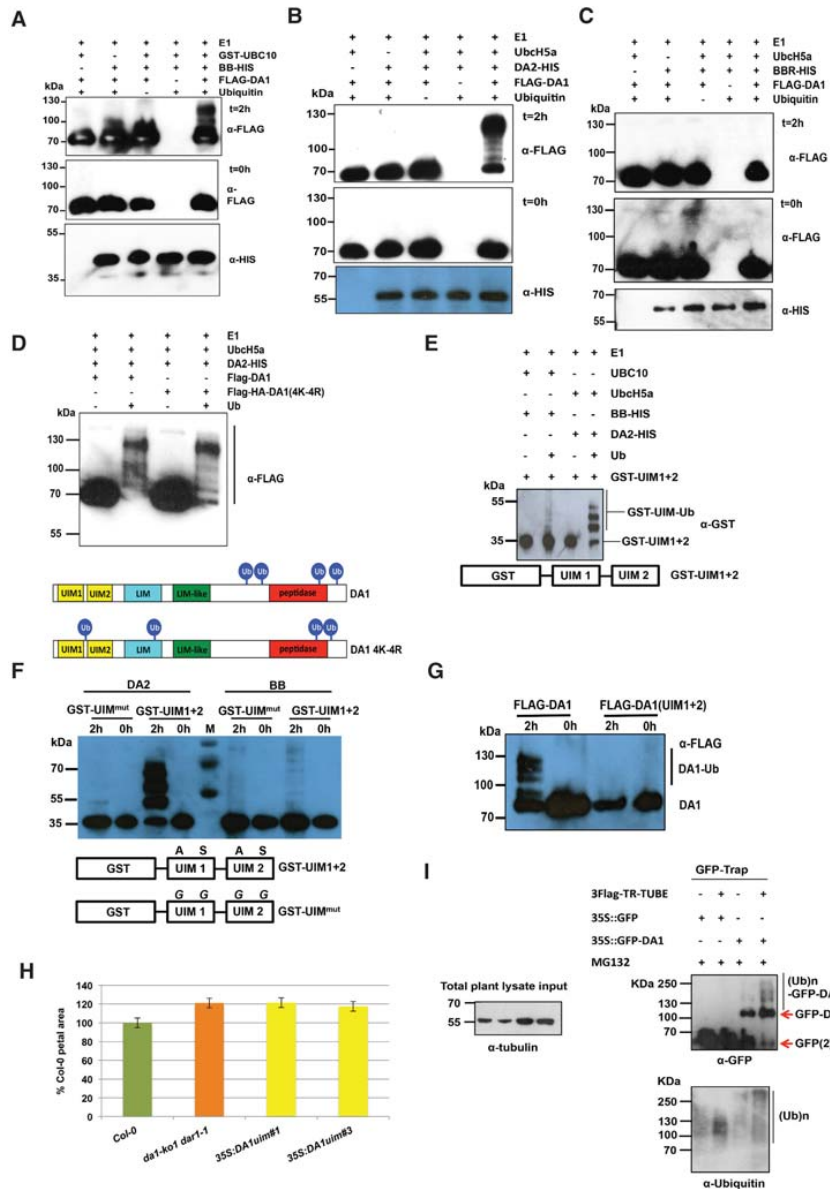


Figure 2. DA1 is multiply ubiquitylated by BB and DA2 in a ubiquitin interaction motif (UIM)-dependent reaction. (A–C) In vitro ubiquitylation of DA1 by the RING E3 ligases BB (A) and DA2 (B), but not BBR (C), in an E1-, E2-, and ubiquitin-dependent reaction. Anti-Flag antibodies detected Flag-ubiquitylated forms of Flag-DA1 ranging from >70 kDa to ~130 kDa. Anti-HIS antibodies detected BB-HIS, DA2-HIS, or BBR-HIS fusion proteins. (D) Both Flag-DA1 and Flag-DA1(4K-4R) are ubiquitylated by DA2 in similar patterns in an in vitro ubiquitylation reaction. In the bottom panel, Ub represents a ubiquitin moiety conjugated to a lysine at the approximate location in DA1 and DA1(4K-4R). Regions of protein similarity with known domains are shown: UIM1 and UIM2 are similar to UIMs, LIM is similar to canonical LIM domains, LIM-like is a related motif found in DA1 family members, and peptidase contains a predicted peptidase active site. (E) An in vitro ubiquitylation reaction with DA2 and BB as E3 ligases and GST-UIM1+2. GST-UIM1+2 is ubiquitylated in a pattern similar to that of DA1 by both DA2 and BB, with DA2 conferring higher levels of ubiquitylation than BB. (F) An in vitro ubiquitylation reaction with DA2 and BB as E3 ligases and GST-UIM1+2 with mutations that reduce ubiquitin binding. Mutated versions of UIM1 and UIM2 strongly reduced DA2- and BB-mediated ubiquitylation of GST-UIM1+2. (G) A time course of Flag-DA1 and Flag-DA1(UIM1+2) with mutations in the UIMs as in E. These strongly reduced DA1 ubiquitylation. (H) DA1(UIM1+2) is not functional in vivo, as it does not complement the large petal phenotype of the *da1-ko1 dar1-1* double mutant. Two independent homozygous T-DNA insertion lines were scored for petal size and compared with wild-type Col-0 and *da1-ko1 dar1-1*. The values given are means ($n = 120$) \pm SE, expressed as the percentage of wild-type Col-0 petal areas. Student's *t*-test showed no significant differences between the transformants and the parental *da1-ko1 dar1-1* line. (I) Transgenic *Arabidopsis* plants expressing a GFP-DA1 fusion protein under the control of the 35S promoter were used to detect DA1 ubiquitylation in vivo. GFP ran as a dimer on the gel due to high protein concentrations. Protein extract input levels are shown using anti-tubulin antibody.

complement the large petal size in the double mutant *da1 ko dar1 1* (Fig. 2H). To detect ubiquitylation in vivo, DA1 was expressed from the constitutive 35S promoter as an N terminal GFP fusion protein and purified from seedling tissues using a GFP trap. Characteristic patterns of DA1 ubiquitylation were detected on purified GFP DA1 (Fig. 2I, right panel). Therefore, DA1 is ubiquitylated by the E3 ligases BB and DA2 in vitro by a UIM1 and UIM2 dependent mechanism, DA1 is ubiquitylated in vivo, and UIMs are required for DA1 function.

DA1 cleaves BB and DA2 with a ubiquitin dependent peptidase activity

A time course of BB HIS incubated with purified Flag DA1 that had been ubiquitylated by BB or incubated with non ubiquitylated Flag DA1 showed that, in the presence of ubiquitylated DA1, a HIS tagged BB fragment of ~35 kDa was produced after 4 h of incubation (Fig. 3A, arrows). When ubiquitylated Flag DA1 was incubated with DA2 HIS, a 25 kDa HIS tagged DA2 cleavage product was also detected after 4 h of incubation (Fig. 3A, arrows). Similar experiments using Flag DA1 ubiquitylated by DA2 showed identical patterns of BB HIS and DA2 HIS cleavage (Fig. 3B). BBR HIS did not show a cleavage product in these conditions. Thus, DA1 ubiquitylated by either BB or DA2 generated cleavage products from both BB and DA2 in vitro.

Examination of the conserved C terminal region of DA1 revealed an extended sequence motif, HEMMHX₁₅EE (Supplemental Fig. S4), which is a zinc aminopeptidase active site found in clan MA endopeptidases (Rawlings et al. 2012). The HEMMH motif was mutated to AEMMA, removing the putative zinc coordinating histidine residues, to form DA1(pep). Figure 3C shows that DA1(pep) and DA1 were ubiquitylated in vitro to an equal extent by both BB and DA2. In an in vitro time course reaction, ubiquitylated DA1(pep) did not generate the 25 kDa HIS tagged DA2 band seen after incubation with ubiquitylated DA1 (Fig. 3D). Coexpression of BB Flag, DA2 Flag, or BBR Flag with HA DA1 or HA DA1(pep) in *da1 ko1 dar1 1* mutant leaf protoplasts showed that HA DA1, but not HA DA1(pep), generated a similar sized 35 kDa BB Flag cleavage product (Fig. 3E, top panel, arrow) as seen in in vitro reactions (Fig. 3A,B). Longer exposure of the same Western blot (Fig. 3E, bottom panel) was required to identify the 25 kDa DA2 Flag cleavage product, which was not generated by coexpression with DA1(pep). Figure 3F shows that the mutation in DA1 abolishing DA1 peptidase activity did not complement the *da1 ko1 dar1 1* large petal phenotype, establishing that DA1 peptidase activity is required for in vivo function. To detect DA1 peptidase activity in vivo, transgenic plants expressing *BB::gsGreen BB* gene fusion and a RING domain mutant version that was predicted to be more stable in vivo due to reduced autopolyubiquitylation (Disch et al. 2006) were generated. Analysis of GFP trap purified proteins (Fig. 3G, left panel) showed a cleavage product of the expected size generated from RING mutant gsGreen protein in two independent transformants. Full length

wild type gsGreen BB was not detected, although low levels of an expected cleavage product were identified. For comparison, the same constructs, together with a noncleavable form (AY GG) (see Fig. 5B, below), were expressed using the 35S promoter in protoplasts with DA1 (Fig. 3G, right panel). This showed the predicted DA1 mediated BB cleavage product, which was not generated in the AY GG version of BB.

A Förster resonance energy transfer (FRET) DA1 peptidase sensor was constructed using eGFP donor and mCherry acceptor pairs (van der Krogt et al. 2008) connected by BB to provide another measure of DA1 peptidase activity in vivo. Cleavage of the fluorophore pair by DA1 would increase the fluorescence lifetime toward that of eGFP BB compared with that of the intact sensor protein by impairing energy transfer between the fluorophores. The peptidase sensor and a control donor sensor were transfected into *da1 ko1 dar1 1* root protoplasts, and fluorescence lifetime imaging (FLIM) was performed. Figure 4A shows that the fluorescence lifetime (τ) of the GFP BB donor control was ~2.48 nsec, while that of an intact donor acceptor pair was ~2.25 nsec, demonstrating efficient FRET. When cotransfected with DA1, the fluorescent lifetime of the donor acceptor pair increased to ~2.38 nsec. Lifetime imaging of typical transfected protoplasts showed a generalized cellular localization of DA1 mediated cleavage. Figure 4B shows that the eGFP BB mCherry donor acceptor pair was cleaved by DA1 peptidase at the expected site in transfected root protoplasts. Therefore, DA1 has a latent peptidase activity that is activated by multiple ubiquitylation mediated by its UIM1+2 domain and the RING E3 ligases BB and DA2, and activated DA1 peptidase then specifically cleaves these two E3 ligases.

Identification of a DA1 peptidase cleavage site in BB

To define the potential functions of DA1 mediated cleavage, the DA1 cleavage site in BB was identified using Edman sequencing of purified cleaved BB HIS. Supplemental Figure S5 shows neo N terminal amino acid sequences that had a unique match to six amino acids in BB (Fig. 5A). This indicated a potential DA1 cleavage site within BB between A₆₀ and Y₆₁, consistent with the sizes of BB and its ~35 kDa cleaved form (Fig. 3A). Two mutant forms of BB were made to assess this potential DA1 cleavage site: a four amino acid deletion surrounding the site (Δ NAYK) and AY changed to GG (AY GG) (Fig. 5B). These proteins were coexpressed in *Arabidopsis da1 ko1 dar1 1* mesophyll protoplasts as C terminal Flag fusion proteins with HA DA1 and HA DA1(pep). Figure 5B shows that the mutant BB Flag proteins were not cleaved by DA1, establishing that DA1 peptidase activity cleaved BB between A₆₀ and Y₆₁. A cleaved form of BB, called MY61 BB, was also made with an initiator Met followed by Y₆₁ (Fig. 5B). MY61 BB was expressed using the 35S promoter in *da1 ko1 bb eod1 2* mutant *Arabidopsis*. Its lack of complementation of *bb eod1 2* (Fig. 5C) showed that DA1 peptidase mediated cleavage reduced BB activity.

Dong et al.

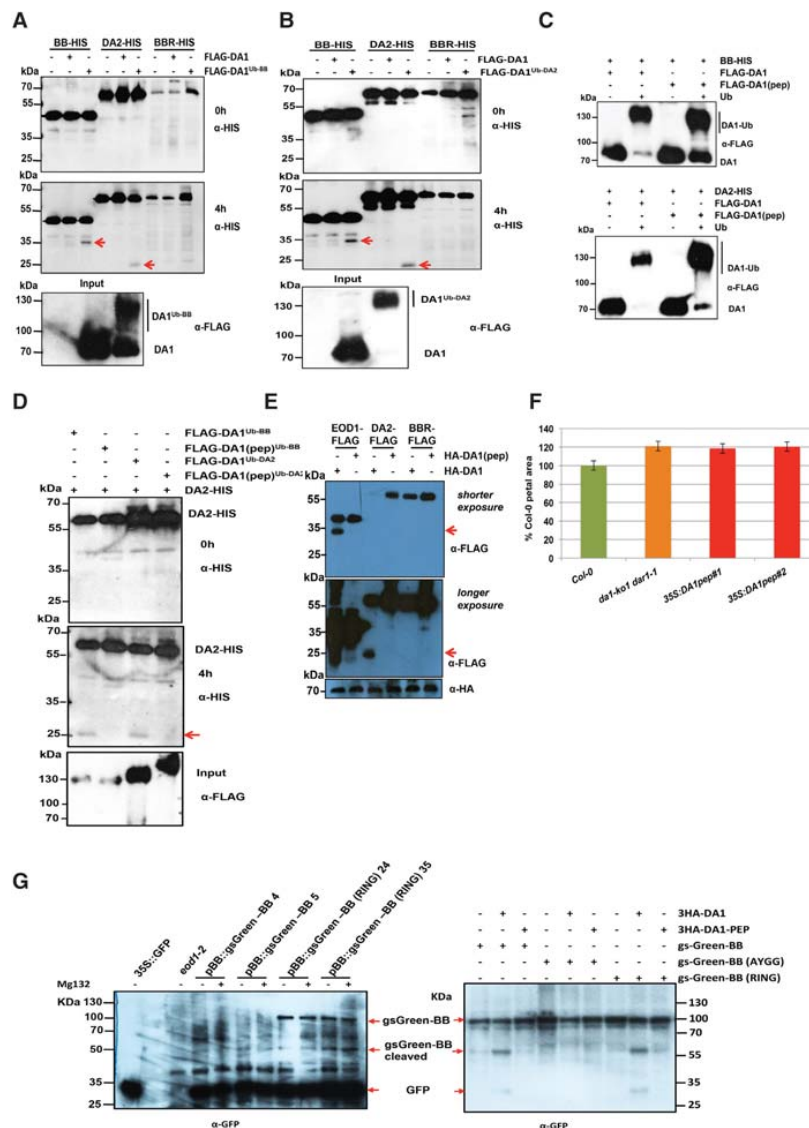


Figure 3. DA1 is an endopeptidase activated by multiple ubiquitylations and cleaves the E3 ligases BB and DA2 that ubiquitylate it. (A,B) Time course of an in vitro reaction of Flag-DA1 or Flag-DA1 ubiquitylated by BB (A) or DA2 (B) with BB-HIS, DA2-HIS, and BBR-HIS. The bottom panels show loading of Flag-DA1 and Flag-DA1^{Ub-BB}. After 4 h, cleavage products (shown by red arrows) of BB and DA2 had been produced by ubiquitylated Flag-DA1 but not Flag-DA1. BBR was not cleaved under these conditions. (C) An in vitro ubiquitylation reaction of DA1 and DA1(pep) using BB-HIS (top panel) and DA2-HIS (bottom panel) as E3 ligases. Ubiquitin-dependent multiple monoubiquitylations of Flag-DA1 and Flag-DA1(pep) by both BB and DA2 were detected. (D) A time course of an in vitro cleavage reaction using DA2-HIS as a substrate (left panels) and Flag-DA1 or Flag-DA1(pep) ubiquitylated by either BB or DA2 (loading shown in the bottom panel). The red arrow in the bottom left panel indicates the DA2 cleavage product at 4 h that was produced only by Flag-DA1^{Ub} and not Flag-DA1(pep)^{Ub}. (E) *Arabidopsis da1-ko1 dar1-1* mesophyll protoplasts were cotransfected with plasmids expressing BB-Flag, DA2-Flag, BBR-Flag, HA-DA1, and HA-DA1(pep). The same-sized cleavage products (red arrows) from BB-Flag and DA2-Flag were detected as seen in A and B above. (Middle panel) Longer exposure of the top immunoblot showed cleaved DA2. The bottom panel shows loading of HA-DA1 and HA-DA1(pep). (F) DA1(pep) is not functional in vivo, as it does not complement the large petal phenotype of the *da1-ko1 dar1-1* double mutant. Transformants expressing 35S::DA1(pep) were scored for petal size and compared with wild-type Col-0 and *da1-ko1 dar1-1*. The values given are means [*n* = 150] ± SE, expressed as percentage of wild-type Col-0 petal areas. Student's *t*-test showed no significant differences between the transformants and the parental *da1-kodar1-1* line. (G) Cleavage of gsGreen-BB is shown in planta in the left panel and in transiently expressed protoplasts in the right panel for comparison. Large-scale protein extracts from transgenic 8-d-old seedlings expressing BB::gsGreen-BB and BB::gsGreen-BB (RING) were purified on a GFP trap. Loading controls used levels of free GFP. The expected size cleavage products (arrows) were observed in plant extracts and protoplasts for comparison.

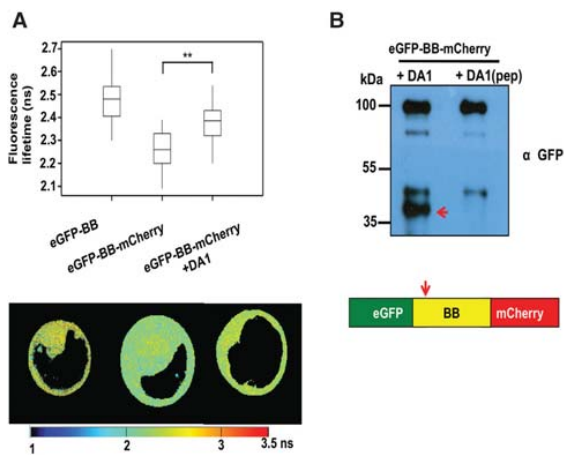


Figure 4. Detection of DA1-mediated cleavage of BB in vivo using FRET. (A) Root protoplasts of *dal1-ko1 dal1-1* plants were transfected with the FRET construct eGFP-BB or a control eGFP-BB-mCherry construct together with DA1 to detect DA1-mediated cleavage of BB. Transfected 2protoplasts were imaged using multiphoton microscopy, and fluorescence half-times of protoplasts ($n = 13$) were captured. The heat map shows fluorescent lifetime values, and typical protoplasts are shown to illustrate lifetime values, and typical protoplasts imaged over the cell. The box plots show significantly increased fluorescence lifetime after DA1 transfection. (***) $P \leq 0.001$, Student's *t*-test. (B) Cleavage of eGFP-BB-mCherry by DA1 in the imaged protoplasts shown in A. The arrow shows the major cleavage product of ~40 kDa expected from DA1 cleavage near the N terminus of BB.

BB stability is dependent on its N terminus and N end rule function

DA1 cleavage products of DA2 were unstable, indicating that one function of DA1 mediated cleavage may be to destabilize proteins (Fig. 3E). This was also observed for BB in cell free degradation assays, in which MY61 BB was unstable compared with wild type BB (Supplemental Fig. S6). To test the role of the neo N terminus of BB on protein stability, 61BB proteins with different N termini (Y, G, and MY) were expressed using the ubiquitin fusion technique (UFT) (Bachmair et al. 1986). HA tagged constructs were translationally coexpressed in a cell free rabbit reticulocyte system with or without MG132 proteasome inhibitor, and translation was stopped by the addition of cycloheximide. Y61 BB was highly unstable, whereas G61 BB was stable (Fig. 5D). Interestingly, the artificial MY61 BB was also highly unstable in a proteasome independent mechanism. The neo N terminal sequence of DA1 cleaved BB starts with YK, a potentially destabilizing sequence of a type II N end rule degron (Varshavsky 2011). The N end rule E3 ligase PRT1 mediates the stability of model N end rule substrates with such aromatic N terminal residues (Potuschak et al. 1998). To assess the potential role of PRT1 in N end rule mediated degradation of BB, we tested the binding of PRT1 to 17 mer peptides representing variants of the neo N termini

of BB on a backbone sequence of an N end rule test substrate in SPOT (synthetic peptide arrays on membrane support technique) assays. Purified recombinant HIS MBP PRT1 protein was incubated with the SPOT array, and binding was visualized by Western blotting. Recombinant PRT1 had a preference for binding to the large aromatic acids tyrosine and phenylalanine, consistent with previously suggested specificity (Fig. 5E; Potuschak et al. 1998; Stary 2003; Faden et al. 2016). To assess whether PRT1 had a role in DA1 mediated BB degradation, BB was expressed with an N terminal ubiquitin fusion and a C terminal luciferase fusion to reveal neo N termini in Col 0 or *prr1* mutant mesophyll protoplasts. BB LUC activity was reduced in wild type protoplasts with a neo N terminal tyrosine, which was not seen in *prr1* mutant protoplasts (Fig. 5F). Neo N terminal glycine BB LUC levels were not altered in either Col 0 or *prr1* mutant protoplasts. This indicated a strong dependence of Tyr 61BB stability on PRT1 activity. In planta evidence supporting the role of DA1 in reducing the growth inhibitory role of BB via N end rule mediated degradation was shown by the suppression of growth reduction in a transgenic 35S::RFP BB overexpression line by overexpression of DA1 (Fig. 5G). Western blots (Fig. 5H) confirmed that 35S::DA1 reduced levels of RFP BB.

Functional analyses of DA1

We showed previously that the *dal1 1* allele of DA1 has a negative interfering phenotype with respect to the closely related family member DAR1 (Li et al. 2008). The peptidase activity of the protein encoded by the *dal1 1* allele, called DA1(R358K), which has an arginine to a lysine residue altered in a highly conserved C terminal region, (Supplemental Fig. S4) was assessed. This mutation did not influence ubiquitylation of Flag DA1(R358K) (Fig. 6A) or create a site for ectopic ubiquitylation of Flag DA1(R358K), as determined by mass spectrometric analysis (Supplemental Fig. S2C). The peptidase activity of ubiquitylated Flag DA1(R358K) was qualitatively assessed in vitro and in vivo (using HA DA1(R358K)) by comparison with wild type DA1 peptidase activity (Fig. 6A,B). Both assays showed that DA1(R358K) had lower peptidase activity compared with DA1, suggesting that regions of the conserved C terminal region are required for peptidase activity and that the *dal1 1* phenotype may be due to reduced peptidase activity. Figure 6B also shows that DA1(4K 4R), which is ubiquitylated (Fig. 2E), had peptidase activity toward BB. This suggested that precise patterns of ubiquitylation are not required for activating DA1 latent peptidase activity.

DAR4, another DA1 family member (Li et al. 2008), encodes a protein with an N terminal TIR NB LRR and has a gain of function *chs3 2d* allele in the conserved C terminal region (Supplemental Fig. S3) that activated constitutive defense responses (Xu et al. 2015). Alignments revealed high similarity to predicted protein sequences from the photosynthetic bacteria *Roseiflexus* sp (Supplemental Fig. S7; Burroughs et al. 2011) that included four pairs of CxxC/H motifs with the potential to bind

Dong et al.

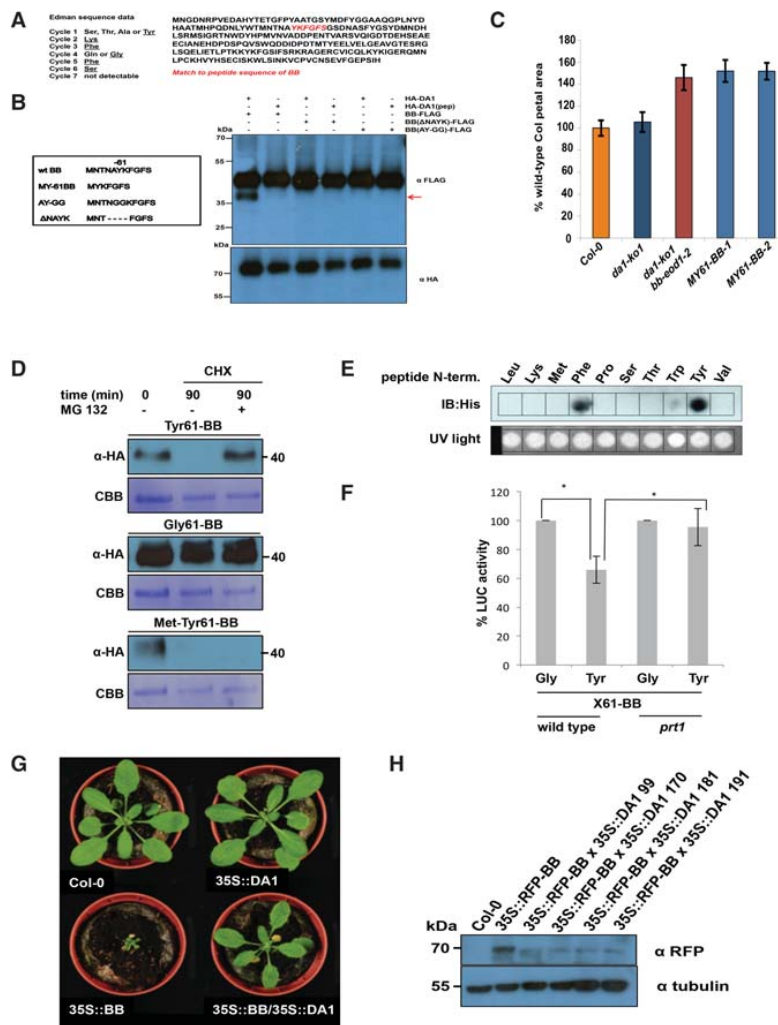


Figure 5. Identification of the DA1 cleavage site in BB and destabilization and functional inactivation of cleaved BB in vivo by the N-end rule. (A) Neo-N-terminal sequences of purified cleaved BB-HIS (left) matched the complete BB protein sequence (right, shown in red). Data from six Edman sequencing cycles are in Supplemental Figure S5. (B) The predicted DA1 cleavage site in BB was mutated by changing the AY amino acids flanking the site to GG (AY-GG) and deleting two amino acids from both sides of the predicted cleavage site (Δ NAYK). BB-Flag, BB (Δ NAYK)-Flag, and BB (AY-GG)-Flag were expressed in *da1-ko1 dar1-1 Arabidopsis* mesophyll protoplasts under the control of the 35S promoter. HA-DA1 did not cleave BB containing mutations in the predicted cleavage site. The bottom panel shows HA-DA1 and HA-DA1(pep) loading. (C) A DA1-cleaved version of BB does not function in planta. A cleaved version of BB, termed MY61-BB, was expressed in *da1-ko1 bb-eod1-2* plants under control of the 35S promoter. The graph compares petal areas in wild-type Col-0, *da1-ko1*, *da1-ko1 bb-eod1-2*, and two independent transgenic lines. Values give are means ($n = 50$) \pm SE, expressed as percentage of wild-type Col-0 petal areas. Student's *t*-test showed no significant differences between the transformants and the parental *da1-ko1 bb-eod1-2* line. (D) In vitro degradation of BB is dependent on N termini. Ubiquitin fusion constructs were expressed in a reticulocyte lysate cell-free system. Samples were incubated for 30 min with or without MG132. Next, cycloheximide (CHX) was added to inhibit translation, and samples were taken 0 and 90 min after CHX addition. Samples were electrophoresed on SDS-PAGE and immunoblotted using HA antibodies to detect BB protein levels. Loading controls were

the CBB-stained membrane. (E) PRT1 binding to synthetic peptides mimicking the neo-N-terminal of 61BB. SPOT assay of a peptide array of synthetic 17-mer peptides incubated with recombinant His8-MBP-tagged PRT1. Peptides were derived from an N-recogin test substrate, and the first amino acid comprised Leu, Lys, Met, Phe, Pro, Ser, The, Trp, Tyr, and Val. His-PRT1 was detected by immunoblotting. Equal peptide loading on the membrane was monitored by UV light prior to PRT1 protein binding. (F) Constructs expressing ubiquitin fusions of 61BB-Luciferase constructs with glycine or tyrosine neo-N termini (Ub-Gly-61-BB-HA-LUC and Ub-Tyr-61-BB-HA-LUC) were transfected into wild-type or *prt1* mutant protoplasts. Transfection efficiency was measured using a pUBC::GUS control. Luciferase activities were normalized to GUS activity, and the luciferase activity of Gly-61-BB-HA-LUC was taken as 100%. The significance of differences was calculated from three independent transformation experiments using Student's *t*-tests (two sites, uncoupled). (*) *P*-value ≤ 0.05 . (G) Overexpression of BB under the control of the 35S promoter leads to strongly reduced growth, and, when crossed with a line overexpressing DA1, this growth inhibition was reversed. This demonstrated that DA1 can reduce the growth inhibitory effect of high levels of BB. (H) Crossing a line overexpressing DA1 into a line expressing 35S::RFP-BB reduced RFP-BB levels. Homozygous progeny of four independent crosses (99, 170, 181, and 191) are shown.

zinc similar to those in canonical LIM domains (Kadmas and Beckerle 2004). The *chs3 2d* mutation changes a cysteine to a tyrosine in the third pair of conserved CxxC/H motifs (Supplemental Figs. S3, S6), suggesting that it may alter a possible LIM like structure. This mutation was introduced into DA1 to create DA1(C274Y), and its

activities were assessed. Figure 6A shows that DA1 (C274Y) was not ubiquitylated by BB and had no peptidase activity toward BB in vitro and in vivo (Fig. 6B). This implicated the putative LIM like domain in DA1 in UIM mediated ubiquitylation and activation of DA1 peptidase activity.

Dong et al.

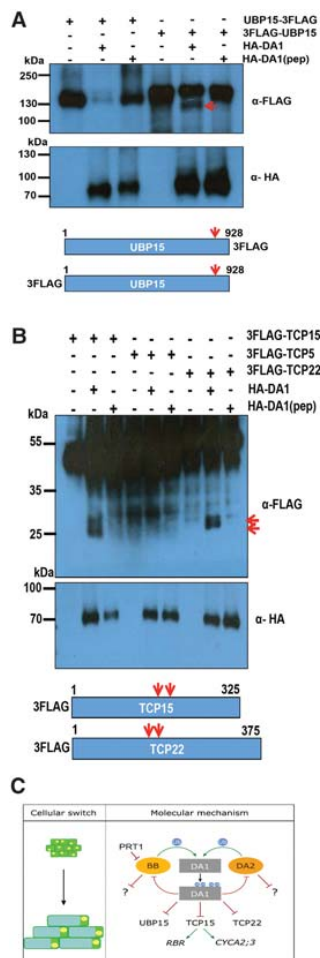


Figure 7. DA1 cleaves UBP15, TCP15, and TCP22 in vivo. (A,B) In vivo cleavage reactions of UBP15-3Flag and 3Flag-UBP15 (A) as well as 3-Flag-TCP15, 3-Flag-TCP22, and 3-Flag TCP5 (a non-cleaved control) (B) using HA-DA1 and HA-DA1(pep). Constructs expressed from the 35S promoter were cotransfected into *da1-ko1 dar1-1* mesophyll protoplasts. UBP15, TCP14, TCP15, and TCP22 cleavage products are shown in the top immunoblots. The bottom immunoblots show HA-DA1 and HA-DA1(pep) protein levels. The approximate locations of DA1 cleavage sites (arrows) are shown in UBP15, TCP15, and TCP22. (C) A model of the proposed transient mechanism of DA1 peptidase activation and the consequences of DA1-mediated cleavage of growth regulators during organ growth. PRT1 activity is shown as degrading BB.

establishing a biochemical foundation for their joint activities in growth control. Zinc metallopeptidases are maintained in an inactive form by a “cysteine switch” (Van Wart and Birkedal Hansen 1990) that coordinates a cysteine residue with the zinc atom at the active site to block it. Conformational changes release this and activate the peptidase.

Ubiquitylation of DA1 has the potential to trigger a conformational change that may release inhibition of pep

tidase activity. Hoeller et al. (2006) showed that UBD and UIM mediated monoubiquitylation of endocytotic proteins, including epsin, led to a conformational change mediated by intramolecular interactions between UBDs/UIMs and *cis* ubiquitin, which regulated endocytosis. The binding of ubiquitin to DA1 UIMs was required for DA1 function in vivo (Fig. 2H), and the UIMs conferred patterns of ubiquitylation on the heterologous protein GST similar to that seen for DA1 (Fig. 2G [for DA1], E,F [for GST UIM1+2]). Related observations were seen in the monoubiquitylation of epsin (Oldham et al. 2002) through coupled monoubiquitylation (Woelk et al. 2006), where UIMs recruit the UIM containing protein to the ubiquitylation machinery by direct interaction with ubiquitin coupled to ubiquitin donor proteins (Haglund and Stenmark 2006). Mutation of Cys274 in the C terminal zinc finger loop of the LIM like domain of DA1 abrogated both ubiquitylation and peptidase activity (Fig. 6A,B), suggesting a functional role for this ancient conserved LIM like domain (Supplemental Fig. S7; Burroughs et al. 2011) in peptidase activation. Analyses of conformational changes caused by DA1 ubiquitylation and their influence on peptidase activity are required to establish this potential mechanism.

DA1 cleavage destabilizes its activating E3 ligases (BB and DA2), and cleavage of BB leads to targeting by the N recognin PRT1

The RING E3 ligases BB and DA2 activate DA1 peptidase by ubiquitylation and are also cleaved by DA1 peptidase (Figs. 3A,B,E,G, 4). Once cleaved, DA2 appeared to be destabilized in transiently expressed protoplasts (Fig. 3E). Identification of the DA1 cleavage site in BB (Fig. 5A,B) revealed Y61 BB at the neo N terminus of cleaved BB. This neo N terminus conferred proteasome mediated degradation in a cell free system (Fig. 5D). This degradation depended on recognition of the neo N terminus by the *Arabidopsis* E3 ligase PRT1 (Fig. 5E,F; Potuschak et al. 1998; Stary 2003), an N recognin catalyzing N end rule mediated degradation (Varshavsky 2011) with a suggested preference for aromatic amino acid N termini. Interestingly, the neo N terminal MY61 BB, which was used to express a cleaved version of BB in planta, conferred strong proteasome independent instability (Fig. 5D) in a mechanism that is not yet clear. The lack of MY61 BB function in vivo (Fig. 5C) supported the observation that DA1 mediated cleavage of BB leads to its loss of function in vivo. Overexpression of BB strongly reduced growth, as expected from its inhibitory role in growth (Disch et al. 2006). The reversal of this inhibition by overexpression of DA1, which reversed growth inhibition (Fig. 5G) and reduced RFP BB levels (Fig. 5H), is consistent with a mechanism involving DA1 mediated reduction of BB activity via peptidase mediated cleavage and subsequent degradation by the N end rule pathway. Such an activation destruction mechanism mediated by BB, DA2, and DA1 may provide a way of tightly controlling peptidase activity. The physiological role of these

mechanisms, which often involve ubiquitylation and proteolytic degradation, is to drive unidirectional cellular processes; for example, in cell cycle progression (Reed 2003). The factors that trigger DA1 ubiquitylation by BB and coordinate the activities of BB and DA2 remain unknown.

DA1 peptidase activity also cleaves diverse growth regulators

We showed previously that *TCP14* and *TCP15* function downstream from DA1 and other family members in controlling organ size in *Arabidopsis*, and reduced function of DA1 family members led to increased *TCP14* and *TCP15* protein levels (Peng et al. 2015). Similarly, levels of *UBP15* protein, which promotes cell proliferation (Liu et al. 2008) and also functions downstream from DA1, were increased in the *da1 1* reduced function mutant (Du et al. 2014). We showed that *TCP15* and the related *TCP22* as well as *UBP15* were cleaved by DA1 peptidase activity (Fig. 7A,B) but could not reliably detect *TCP14* cleavage by DA1 or *DAR1*. DA1 mediated cleavage of *TCP15* and *UBP15* is a plausible mechanism that accounts for these observed reduced protein levels, similar to DA1 mediated inactivation and destabilization of BB by peptidase cleavage. Taken together, these observations suggest a mechanism (Fig. 7C) in which DA1 peptidase, activated transiently by BB or DA2, coordinates a “one way” cessation of cell proliferation and the initiation of endoreduplication through the cleavage and potential inactivation of proteins that promote cell proliferation and inhibit endoreduplication.

Materials and methods

Plant materials, growth conditions, and organ size measurements

A. thaliana Col-0 was the wild-type plant used. Plants were grown in growth rooms at 20°C with 16-h day/8-h dark cycles using either soil or MS medium supplemented with 0.5% glucose. Petal and seed areas were imaged by high-resolution scanning (3600 dpi; Hewlett Packard Scanjet 4370) and analyzed using ImageJ software (<http://rsbweb.nih.gov/ij/>).

In vitro DA1-mediated cleavage assays

Flag-DA1 was ubiquitylated in vitro using either DA2-HIS or BB-HIS as E3 ligases, purified using Flag magnetic beads, and quantified, and 100 ng was added to 100 ng of BB-HIS, DA2-HIS, or BBR-HIS in a 30- μ L reaction in 50 mM Tris HCl (pH 7.4) and 5 mM MgCl₂. Reactions were carried out for 4 h at 30°C and terminated by the addition of SDS sample buffer.

Mass spectrometry analysis

DA1 ubiquitylation patterns were determined from trypsinized proteins purified on SDS-PAGE gels. For liquid chromatography-tandem mass spectrometry analysis, peptides were applied to an LTQ-Orbitrap (Thermo-Fischer) using a nanoAcquity ultraperformance liquid chromatography system (Waters Ltd.). Further details are in the Supplemental Material.

Acknowledgments

We thank Dr. Paul Thomas (Henry Wellcome Laboratory for Cell Imaging, University of East Anglia) for advice and operating the multiphoton microscope, and Dr. Christoph Bücherl (The Sainsbury Laboratory, Norwich) for advice on FRET. We thank Shimadzu Europa GMBH for carrying out Edman sequencing. We thank Andreas Bachmair for the *prt1* EMS allele, and Yukiko Yoshida for the TR-TUBE construct. This work was supported by Biological and Biotechnological Sciences Research Council (BBSRC) grant BB/K017225 and Strategic Programme grant BB/J004588 to M.W.B., and European Commission contract 037704 (AGRONomics) to M.W.B. and D.I. J.D. was supported by a Biotechnology and Biological Sciences Research Council (BBSRC) CASE Studentship, C.N. was supported by a PhD Fellowship from the Landesgraduiertenförderung Sachsen-Anhalt, and N.D. was supported by an Independent Junior Research Group grant from the ScienceCampus Halle-Plant-based Bioeconomy, the Deutsche Forschungsgemeinschaft (DFG; grant DI 1794/3-1), the DFG Graduate Training Centre (GRK1026), and the Leibniz Institute of Plant Biochemistry. Y.L. was supported by the National Natural Science Foundation of China (grants 91417304, 31425004, 91017014, 31221063, and 31100865), the National Basic Research Program of China (grant 2009CB941503), and the Ministry of Agriculture of China (grant 2016ZX08009-003). M. W.B. and Y.L. are in the Chinese Academy of Sciences (CAS)-John Innes Centre (JIC) Centre of Excellence in Plant and Microbial Sciences (CEPAMS). M.W.B., J.D., H.D., F.-H.L., H.V., N.D., Y.L., and D.I. designed the research; H.D., F.-H.L., J.D., R.P., H. V., C.N., M.K., C.S., N.M., L.N., H.V., T.X., L.C., G.S., N.G., and M.S. performed the research and analyzed the data; and M. W.B. wrote the paper.

References

- Andriankaja M, Dhondt S, De Bodt S, Vanhaeren H, Coppens F, De Milde L, Mühlenbock P, Skiryca A, Gonzalez N, Beemster GTS, et al. 2012. Exit from proliferation during leaf development in *Arabidopsis thaliana*: a not-so-gradual process. *Dev Cell* **22**: 64–78.
- Bachmair A, Finley D, Varshavsky A. 1986. In vivo half-life of a protein is a function of its amino-terminal residue. *Science* **234**: 179–186.
- Barry ER, Camargo FD. 2013. The Hippo superhighway: signaling crossroads converging on the Hippo/Yap pathway in stem cells and development. *Curr Opin Cell Biol* **25**: 247–253.
- Breuer C, Ishida T, Sugimoto K. 2010. Developmental control of endocycles and cell growth in plants. *Curr Opin Plant Biol* **13**: 654–660.
- Breuninger H, Lenhard M. 2012. Expression of the central growth regulator BIG BROTHER is regulated by multiple *cis*-elements. *BMC Plant Biol* **12**: 41.
- Burroughs AM, Iyer LM, Aravind L. 2011. Functional diversification of the RING finger and other binuclear treble clef domains in prokaryotes and the early evolution of the ubiquitin system. *Mol Biosyst* **7**: 2261.
- De Veylder L, Larkin JC, Schnittger A. 2011. Molecular control and function of endoreduplication in development and physiology. *Trends Plant Sci* **16**: 624–634.
- Disch S, Anastasiou E, Sharma VK, Laux T, Fletcher JC, Lenhard M. 2006. The E3 ubiquitin ligase BIG BROTHER controls *Arabidopsis* organ size in a dosage-dependent manner. *Curr Biol* **16**: 272–279.
- Du L, Li N, Chen L, Xu Y, Li Y, Zhang Y, Li C, Li Y. 2014. The ubiquitin receptor DA1 regulates seed and organ size by

Dong et al.

- modulating the stability of the ubiquitin-specific protease UBP15/SOD2 in *Arabidopsis*. *Plant Cell* **26**: 665–677.
- Efroni I, Blum E, Goldshmidt A, Eshed Y. 2008. A protracted and dynamic maturation schedule underlies *Arabidopsis* leaf development. *Plant Cell* **20**: 2293–2306.
- Faden F, Ramezani T, Mielke S, Almudi I, Nairz K, Froehlich MS, Höckendorff J, Brandt W, Hoehenwarter W, Dohmen RJ, et al. 2016. Phenotypes on demand via switchable target protein degradation in multicellular organisms. *Nat Commun* **7**: 12202.
- Green AA, Kennaway JR, Hanna AJ, Bangham JA, Coen E. 2010. Genetic control of organ shape and tissue polarity. *PLoS Biol* **8**: e1000537.
- Haglund K, Stenmark H. 2006. Working out coupled monoubiquitination. *Nat Cell Biol* **8**: 1218–1219.
- Haglund K, Di Fiore PP, Dikic I. 2003. Distinct monoubiquitin signals in receptor endocytosis. *Trends Biochem Sci* **28**: 598–603.
- Hicke L, Schubert HL, Hill CP. 2005. Ubiquitin-binding domains. *Nat Rev Mol Cell Biol* **6**: 610–621.
- Hoeller D, Dikic I. 2010. Regulation of ubiquitin receptors by coupled monoubiquitination. *Subcell Biochem* **54**: 31–40.
- Hoeller D, Crosetto N, Blagoev B, Raiborg C, Tikkanen R, Wagner S, Kowanez K, Breitling R, Mann M, Stenmark H, et al. 2006. Regulation of ubiquitin-binding proteins by monoubiquitination. *Nat Cell Biol* **8**: 163–169.
- Husnjak K, Dikic I. 2012. Ubiquitin-binding proteins: decoders of ubiquitin-mediated cellular functions. *Annu Rev Biochem* **81**: 291–322.
- Johnston LA, Gallant P. 2002. Control of growth and organ size in *Drosophila*. *Bioessays* **24**: 54–64.
- Kadmas JL, Beckerle MC. 2004. The LIM domain: from the cytoskeleton to the nucleus. *Nat Rev Mol Cell Biol* **5**: 920–931.
- Kazama T, Ichihashi Y, Murata S, Tsukaya H. 2010. The mechanism of cell cycle arrest front progression explained by a KLUH/CYP78A5-dependent mobile growth factor in developing leaves of *Arabidopsis thaliana*. *Plant Cell Physiol* **51**: 1046–1054.
- Kim H, Chen J, Yu X. 2007. Ubiquitin-binding protein RAP80 mediates BRCA1-dependent DNA damage response. *Science* **316**: 1202–1205.
- Komander D, Rape M. 2012. The ubiquitin code. *Annu Rev Biochem* **81**: 203–229.
- Li Y, Zheng L, Corke F, Smith C, Bevan MW. 2008. Control of final seed and organ size by the DA1 gene family in *Arabidopsis thaliana*. *Genes Dev* **22**: 1331–1336.
- Li Z-Y, Li B, Dong A-W. 2012. The *Arabidopsis* transcription factor AtTCP15 regulates endoreduplication by modulating expression of key cell-cycle genes. *Mol Plant* **5**: 270–280.
- Liu Y, Wang F, Zhang H, He H, Ma L, Deng XW. 2008. Functional characterization of the *Arabidopsis* ubiquitin-specific protease gene family reveals specific role and redundancy of individual members in development. *Plant J* **55**: 844–856.
- Oldham CE, Mohnhey RP, Miller SLH, Hanes RN, O'Bryan JP. 2002. The ubiquitin-interacting motifs target the endocytic adaptor protein epsin for ubiquitination. *Curr Biol* **12**: 1112–1116.
- Pan D. 2010. The hippo signaling pathway in development and cancer. *Dev Cell* **19**: 491–505.
- Peng Y, Chen L, Lu Y, Wu Y, Dumenil J, Zhu Z, Bevan MW, Li Y. 2015. The ubiquitin receptors DA1, DAR1, and DAR2 redundantly regulate endoreduplication by modulating the stability of TCP14/15 in *Arabidopsis*. *Plant Cell* **27**: 649–662.
- Potuschak T, Sary S, Schlögelhofer P, Becker F, Nejminkaia V, Bachmair A. 1998. PRT1 of *Arabidopsis thaliana* encodes a component of the plant N-end rule pathway. *Proc Natl Acad Sci* **95**: 7904–7908.
- Rawlings ND, Barrett AJ, Bateman A. 2012. MEROPS: the database of proteolytic enzymes, their substrates and inhibitors. *Nucleic Acids Res* **40**: D343–D350.
- Reed SI. 2003. Ratchets and clocks: the cell cycle, ubiquitylation and protein turnover. *Nat Rev Mol Cell Biol* **4**: 855–864.
- Sato Y, Yoshikawa A, Mimura H, Yamashita M, Yamagata A, Fukui S. 2009. Structural basis for specific recognition of Lys 63-linked polyubiquitin chains by tandem UIMs of RAP80. *EMBO J* **28**: 2461–2468.
- Sluis A, Hake S. 2015. Organogenesis in plants: initiation and elaboration of leaves. *Trends Genet* **31**: 300–306.
- Stary S. 2003. PRT1 of *Arabidopsis* is a ubiquitin protein ligase of the plant N-end rule pathway with specificity for aromatic amino-terminal residues. *Plant Physiol* **133**: 1360–1366.
- Tholander F, Roques B-P, Fournié-Zaluski M-C, Thunnissen MMGM, Haeggström JZ. 2010. Crystal structure of leukotriene A4 hydrolase in complex with ketolorphan, implications for design of zinc metalloproteinase inhibitors. *FEBS Lett* **584**: 3446–3451.
- van der Krogt GNM, Ogink J, Ponsioen B, Jalink K. 2008. A comparison of donor-acceptor pairs for genetically encoded FRET sensors: application to the Epac cAMP sensor as an example ed. K.-W. Koch. *PLoS One* **3**: e1916.
- Van Wart HE, Birkedal-Hansen H. 1990. The cysteine switch: a principle of regulation of metalloproteinase activity with potential applicability to the entire matrix metalloproteinase gene family. *Proc Natl Acad Sci* **87**: 5578–5582.
- Varshavsky A. 2011. The N-end rule pathway and regulation by proteolysis. *Protein Sci* **20**: 1298–1345.
- Woelk T, Oldrini B, Maspero E, Confalonieri S, Cavallaro E, Di Fiore PP, Polo S. 2006. Molecular mechanisms of coupled monoubiquitination. *Nat Cell Biol* **8**: 1246–1254.
- Xia T, Li N, Dumenil J, Li J, Kamenski A, Bevan MW, Gao F, Li Y. 2013. The ubiquitin receptor DA1 interacts with the E3 ubiquitin ligase DA2 to regulate seed and organ size in *Arabidopsis*. *Plant Cell* **25**: 3347–3359.
- Xu F, Zhu C, Çevik V, Johnson K, Liu Y, Sohn K, Jones JD, Holub EB, Li X. 2015. Autoimmunity conferred by chs3-2D relies on CSA1, its adjacent TNL-encoding neighbour. *Sci Rep* **5**: 8792.

1.3.3 Cysteine dioxygenation enables subsequent arginylation in the N-end rule pathway

We could demonstrate molecular evidence for N-end rule-mediated posttranslational modification of stress-responsive transcription factors that are required for plant survival under low oxygen (hypoxia; [White et al., Nature Comms, 2017](#)). With this, we cemented molecular concepts of the N-end rule pathway which were speculated about for two decades. We show biochemical evidence for the ‘missing link’ in molecular oxygen sensing by ERFVII transcription factors which are essential in response to environmental and developmental stresses caused by hypoxia. This work integrated existing work on various levels with results from our laboratory.

Publication:

White MD, Klecker M, Hopkinson R, Weits D, Mueller C, Naumann C, O’Neill R, Wickens J, Yang J, Brooks-Bartlett JC, Garman EP, Grossmann TN, **Dissmeyer N***, Flashman E*. Plant Cysteine Oxidases are Dioxygenases that Directly Enable Arginyl Transferase-Catalyzed Arginylation of N-End Rule Targets.

Nature Comms. 2017, **8**:14690



ARTICLE

Received 2 Sep 2016 | Accepted 20 Jan 2017 | Published 23 Mar 2017

DOI: 10.1038/ncomms14690

OPEN

Plant cysteine oxidases are dioxygenases that directly enable arginyl transferase-catalysed arginylation of N-end rule targets

Mark D. White¹, Maria Klecker^{2,3}, Richard J. Hopkinson¹, Daan A. Weits⁴, Carolin Mueller^{5,6}, Christin Naumann^{2,3}, Rebecca O'Neill¹, James Wickens¹, Jiayu Yang¹, Jonathan C. Brooks-Bartlett⁷, Elspeth F. Garman⁷, Tom N. Grossmann^{5,6}, Nico Dissmeyer^{2,3} & Emily Flashman¹

Crop yield loss due to flooding is a threat to food security. Submergence-induced hypoxia in plants results in stabilization of group VII ETHYLENE RESPONSE FACTORS (ERF-VIIs), which aid survival under these adverse conditions. ERF-VII stability is controlled by the N-end rule pathway, which proposes that ERF-VII N-terminal cysteine oxidation in normoxia enables arginylation followed by proteasomal degradation. The PLANT CYSTEINE OXIDASES (PCOs) have been identified as catalysts of this oxidation. ERF-VII stabilization in hypoxia presumably arises from reduced PCO activity. We directly demonstrate that PCO dioxygenase activity produces Cys-sulfinic acid at the N terminus of an ERF-VII peptide, which then undergoes efficient arginylation by an arginyl transferase (ATE1). This provides molecular evidence of N-terminal Cys-sulfinic acid formation and arginylation by N-end rule pathway components, and a substrate of ATE1 in plants. The PCOs and ATE1 may be viable intervention targets to stabilize N-end rule substrates, including ERF-VIIs, to enhance submergence tolerance in agriculture.

¹Chemistry Research Laboratory, University of Oxford, 12 Mansfield Road, Oxford OX1 3TA, UK. ²Independent Junior Research Group on Protein Recognition and Degradation, Leibniz Institute of Plant Biochemistry (IPB), Weinberg 3, D 06120 Halle (Saale), Germany. ³ScienceCampus Halle Plant based Bioeconomy, Betty Heimann Strasse 3, D 06120 Halle (Saale), Germany. ⁴Institute of Biology I, RWTH Aachen University, Worringerweg 1, D 52074 Aachen, Germany. ⁵Chemical Genomics Centre of the Max Planck Society, Otto Hahn Strasse 15, D 44227 Dortmund, Germany. ⁶VU University Amsterdam, De Boelelaan 1083, 1081 HV Amsterdam, The Netherlands. ⁷Department of Biochemistry, University of Oxford, South Parks Road, Oxford OX1 3QU, UK. Correspondence and requests for materials should be addressed to N.D. (email: nico.dissmeyer@ipb.halle.de) or to E.F. (email: emily.flashman@chem.ox.ac.uk).

All aerobic organisms require homeostatic mechanisms to ensure O₂ supply and demand are balanced. When supply is reduced (hypoxia), a hypoxic response is required to decrease demand and/or improve supply. In animals, this well characterized response is mediated by the hypoxia inducible transcription factor (HIF), which upregulates genes encoding for vascular endothelial growth factor, erythropoietin and glycolytic enzymes among many others^{1–3}. Hypoxia in plants is typically a consequence of reduced O₂ diffusion under conditions of waterlogging or submergence, or inside of organs such as seeds, embryos or floral meristems in buds where the various external cell layers act as diffusion barriers. Although plants can survive temporary periods of hypoxia, flooding has a negative impact on plant growth and, if sustained, it can result in plant damage or death⁴. This has a major impact on crop yield; for example, flooding resulted in crop loss costing \$3 billion in the United States in 2011 (ref. 5). As climate change results in increased severe weather events including flooding⁴, strategies to address crop survival under hypoxic stress are needed to meet the needs of a growing worldwide population.

The response to hypoxia in rice, *Arabidopsis*, and barley is known to be mediated by the group VII ETHYLENE RESPONSE FACTORS (ERF VIIIs)^{6–11}. It has been found that these transcription factors promote the expression of core hypoxia responsive genes, including those encoding alcohol dehydrogenase and pyruvate decarboxylase that facilitate anaerobic metabolism^{12,13}. Crucially, it was shown, initially in *Arabidopsis*, that the stability of the ERF VIIIs is regulated in an O₂ dependent manner via the Arg/Cys branch of the N end rule pathway, which directs proteins for proteasomal degradation depending on the identity of their amino terminal amino acid^{14–16}. Thus, a connection between O₂ availability and the plant hypoxic response was identified^{11,17,18}. The *Arabidopsis* ERF VIIIs are translated with the conserved N terminal motif MCGGAI/VSDY/F (ref. 4) and co translational N terminal methionine excision, catalysed by Met amino peptidases^{19,20}, leaves an exposed N terminal Cys, which is susceptible to oxidation^{14–16}. N terminally oxidized Cys residues (Cys sulfinic acid or Cys sulfonic acid, Supplementary Fig. 1) are then proposed to render the ERF VII N termini substrates for arginyl transfer RNA transferase (ATE) catalysed arginylation. The subsequent Nt Arg ERF VIIIs are candidates for ubiquitination by the E3 ligase PROTEOLYSIS6 (PRT6) (ref. 21), which promotes targeted degradation via the 26S proteasome. It has also been shown that degradation of ERF VIIIs by the N end rule pathway can be influenced by NO, and that the ERF VIIIs play a role in plant NO mediated stress responses^{22,23}.

The plant hypoxic response mimics the equivalent well characterized regulatory system in animals, whereby adaptation to hypoxia is mediated by HIF. In normoxic conditions, HIF is hydroxylated at specific prolyl residues targeting it for binding to the von Hippel Lindau tumour suppressor protein, the recognition component of the E3 ubiquitin ligase complex, which results in HIF ubiquitination and proteasomal degradation^{1,3}. Thus, although not substrates for the N end rule pathway of protein degradation, HIF levels are regulated by posttranslational modification resulting in ubiquitination, in a manner that is sensitive to hypoxia. HIF prolyl hydroxylation is catalysed by O₂ dependent enzymes, the HIF prolyl hydroxylases 1–3 (ref. 2), which are highly sensitive to O₂ availability^{24,25}. These O₂ sensing enzymes are thus the direct link between O₂ availability and the hypoxic response^{26,27}.

Crucially, a family of five enzymes, the PLANT CYSTEINE OXIDASES (PCO1–5), were identified in *Arabidopsis*²⁸ that were reported to catalyse the O₂ dependent reaction in the plant hypoxic response, specifically the oxidation of the conserved Cys

residue at the N terminus of the *Arabidopsis* ERF VIIIs, RAP2.2, RAP2.12, RAP2.3, HRE1 and HRE2. It was found that overexpression of PCO1 and 2 *in planta* specifically led to depleted RAP2.12 protein levels and reduced submergence tolerance, whereas *pcol pco2* T DNA insertion mutants accumulated RAP2.12 protein. Isolated recombinant PCO1 and PCO2 were shown to consume O₂ in the presence of pentameric peptides CGGAI corresponding to the N termini of various ERF VIIIs (Supplementary Table 1)²⁸. The identification of these enzymes indicates that the hypoxic response in plants is enzymatically regulated²⁸, potentially in a similar manner to the regulation of the hypoxic response in animals by the HIF hydroxylases. The PCOs may therefore act as plant O₂ sensors.

Validation of the chemical steps in the Arg/Cys branch of the N end rule pathway is still limited, both in animals and plants. We therefore sought to provide molecular evidence that the PCOs catalyse the oxidation step in ERF VII proteasomal targeting and to determine whether this step is required for further molecular priming by arginylation. Using mass spectrometry (MS) and nuclear magnetic resonance (NMR) techniques, we confirm that PCO1 and also PCO4 representatives of the two different PCO ‘subclasses’ based on sequence identity and expression behaviour²⁸ catalyse dioxygenation of the N terminal Cys of *Arabidopsis* ERF VII peptide sequences to Cys sulfinic acid (CysO₂). This oxidation directly incorporates molecular O₂. To our knowledge, these are the first described enzymes that catalyse cysteinyl oxidation, as well as being the first described cysteine dioxygenases in plants. We then verify that the Cys sulfinic acid product of the PCO catalysed reactions is a direct substrate for the arginyl tRNA transferase ATE1, demonstrating that PCO activity is relevant and sufficient for the subsequent step of molecular recognition and modification according to the N end rule pathway. This provides the first molecular evidence that Nt Cys sulfinic acid is a *bona fide* substrate for N end rule mediated arginylation. Overall, we thus define the PCOs as plant cysteinyl dioxygenases and ATE1 as an active arginyl transferase, establishing for the first time a direct link between molecular O₂, PCO catalysis and ATE1 recognition and modification of N end rule substrates.

Results

PCOs catalyse O₂ dependent modification of RAP2_{2–11}. N terminally hexahistidine tagged recombinant PCO1 and 4 were purified to ~90% purity, as judged by SDS polyacrylamide gel electrophoresis (Supplementary Fig. 2a). Protein identity was confirmed by comparison of observed and predicted mass by liquid chromatography (LC) MS (PCO1 predicted mass 36,510 Da, observed mass 36,513 Da; PCO4 predicted mass 30,680 Da, observed mass 30,681 Da, Supplementary Fig. 2b). Both PCO1 and PCO4 were found to be monomeric in solution and to co purify with substoichiometric levels of Fe(II) (~0.3 atoms Fe(II) per monomer, Supplementary Fig. 2c e), in line with the reported parameters of recombinant forms of their distant homologues, the cysteine dioxygenases (CDOs)^{28–30}. The activity of the purified PCO1 and PCO4 was tested towards a synthetic 10 mer peptide corresponding to the methionine excised N termini of the ERF VIIIs RAP2.2, RAP2.12 and HRE2 (H₂N CGGAIISDFI COOH, hereafter termed RAP2_{2–11} Supplementary Table 1). Assays comprising RAP2_{2–11} at 100 μM in the presence or absence of PCO1 or PCO4 at 0.5 μM underwent aerobic or anaerobic incubation for 30 min at 30 °C before analysis of the peptide by matrix assisted laser desorption/ionization MS (MALDI MS, Fig. 1a,b). Only under aerobic conditions and in the presence of PCO1 or PCO4 did the spectra reveal the appearance of two species with mass increases of +32 Da and +48 Da, corresponding to two or three added

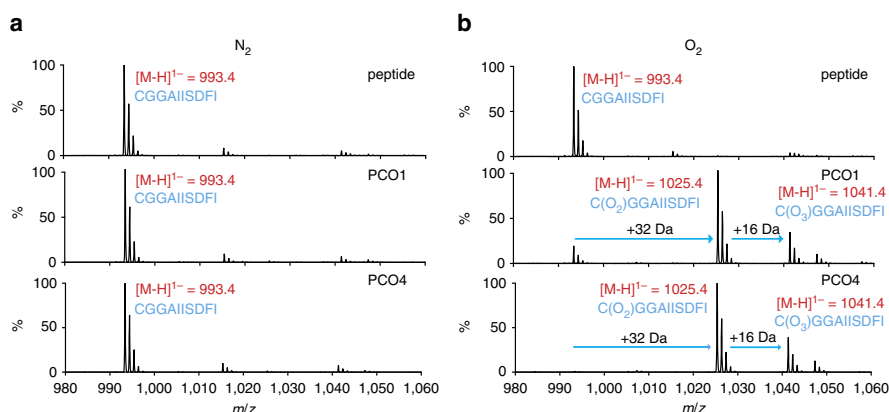


Figure 1 | O₂-dependent Cys-modification of a RAP₂₋₁₁ peptide substrate. MALDI MS spectra showing the RAP₂₋₁₁ peptide species identified following incubation with PCO1 and PCO4 under anaerobic (a) or aerobic (b) conditions. Products with mass increases of +32 Da and +48 Da were only observed in the presence of PCO1 or PCO4 and O₂.

O atoms, suggesting an O₂ dependent reaction for PCOs 1 and 4 (Fig. 1b), as previously shown for PCOs 1 and 2 (it is noteworthy that supplementation of Fe(II) and/or addition of ascorbate was not required for the endpoint PCO1/4 activity assays conducted in this study)²⁸. These mass shifts were deemed to be consistent with enzymatic formation of Cys sulfinic (CysO₂, +32 Da) and Cys sulfonic acid (CysO₃, +48 Da; Supplementary Fig. 1). Although homology between the PCOs and CDOs^{28,30} leads to the predisposition that they will perform similar chemistry (that is, catalyse Cys sulfinic acid formation), both Cys sulfinic and Cys sulfonic acid are proposed to be Arg transferase substrates in the Arg/Cys branch of N end rule mediated protein degradation and therefore both were considered as potential products of the PCO catalysed reaction¹⁴⁻¹⁶.

PCOs catalyse dioxygenation of RAP₂₋₁₁. To ascertain whether the PCOs function as dioxygenases and thus to confirm a direct connection between molecular O₂ and PCO activity, we sought to verify the source of the O atoms in the oxidized RAP₂₋₁₁ by conducting assays in the presence of ¹⁸O₂ as the cosubstrate or H₂¹⁸O as the solvent. To probe O₂ as the source of O atoms in the product, anaerobic solutions of RAP₂₋₁₁ were prepared in sealed vials before addition of PCO4 using a gas tight syringe. The vials were then purged with ¹⁶O₂ or ¹⁸O₂ and the reactions were allowed to proceed at 30 °C for a subsequent 20 min. Upon analysis by MALDI MS, the mass of the products revealed that molecular O₂ was incorporated into the Cys sulfinic acid product (Fig. 2a). The Cys sulfinic acid product had a mass of +32 Da in the presence of ¹⁶O₂ and +36 Da in the presence of ¹⁸O₂, demonstrating addition of two ¹⁸O atoms and indicating that O₂ is the source of O atoms in this product. The Cys sulfonic acid product had a mass of +52 Da in the presence of ¹⁸O₂, indicating a third ¹⁸O atom had not been incorporated into this product. To probe whether the source of the additional mass in the apparent Cys sulfonic acid product was an O atom derived from water, an equivalent reaction was carried out under aerobic conditions in the presence of H₂¹⁸O (H₂¹⁸O:H₂O in a 3:1 ratio). No additional mass was observed in the peak corresponding to the Cys sulfonic acid, raising the possibility that the +48 Da species observed by MALDI MS is not enzymatically formed. Importantly, following incubation in the presence of H₂¹⁸O, no additional mass was observed in the peak corresponding to Cys sulfinic acid, confirming that this species is a product of a reaction where molecular O₂ is a substrate (Fig. 2b).

To further investigate whether the PCO catalysed product species observed at +48 Da is enzymatically produced or an artefact of the MALDI MS analysis method, we turned to LC MS, to analyse the products of the PCO catalysed reactions. Under these conditions, only peptidic product with a mass increase of +32 Da was observed after incubation with both PCO1 and PCO4, corresponding to the incorporation of two O atoms and the formation of Cys sulfinic acid (Fig. 2c), consistent with the products observed using ¹⁸O₂ and H₂¹⁸O (Fig. 2a,b). No product was observed with a mass corresponding to Cys sulfonic acid, which suggested that the +48 Da product detected by MALDI MS was indeed an artefact. When combined with the observation that significant quantities of Cys sulfonic acid were not seen in the no enzyme or anaerobic controls (Fig. 1), it was hypothesized that the Cys sulfinic acid product of the PCO catalysed reaction is non enzymatically converted to Cys sulfonic acid during MALDI MS analysis, potentially as a result of laser exposure. Upon subjecting the products of PCO1 and 4 turnover to MALDI MS analysis with increasing laser intensity, a direct correlation between laser intensity and the ratio of Cys sulfinic acid:Cys sulfonic acid product was observed (Supplementary Fig. 3a). Of note, significant levels of laser induced formation of +32 and +48 Da species upon analysis of unmodified peptide were not observed (Supplementary Fig. 3b). Together, these results confirm that the +48 Da species observed following incubation of the PCOs with RAP₂₋₁₁ are a product of Cys sulfinic acid exposure to the MALDI MS laser and not a product of the PCO catalysed reaction. Overall, these data demonstrate that the PCOs are dioxygenase enzymes, similar to the mammalian and bacterial CDOs to which they show sequence homology^{28,30}.

PCOs catalyse RAP₂₋₁₁ N terminal Cys sulfinic acid formation. Recombinant PCO1 and PCO2 were reported to consume O₂ in the presence of pentameric CGGAI peptides corresponding to the methionine excised N terminus of the *Arabidopsis* ERF VII²⁸. To definitively verify that the N terminal cysteinyl residue of RAP₂₋₁₁ is indeed the target for the PCO catalysed +32 Da modifications, we conducted LC MS/MS analyses on the reaction products. Fragmentation of RAP₂₋₁₁ that had been incubated in the presence and absence of PCO1 and PCO4 revealed *b* and *y* ion series consistent with oxidation of the N terminal Cys residue (Fig. 3a), confirming that PCOs 1 and 4 act as cysteinyl dioxygenases.

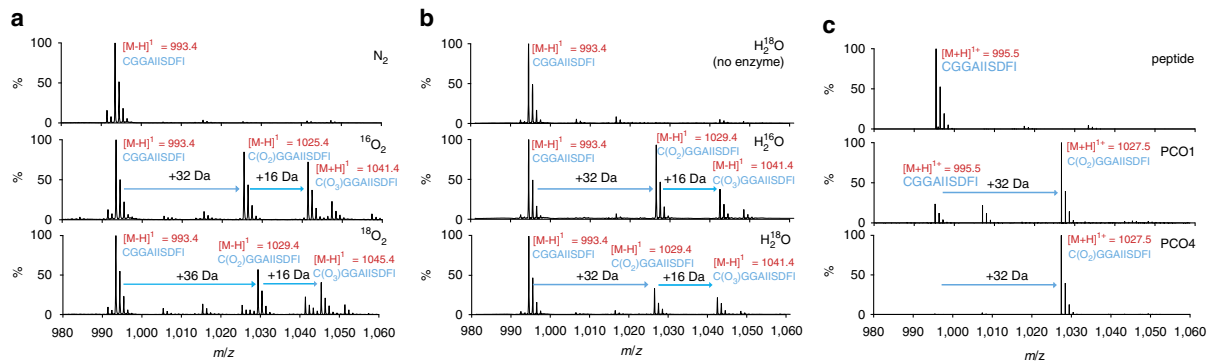


Figure 2 | PCOs catalyse incorporation of molecular O_2 into $RAP2_{2-11}$. (a) MALDI MS spectra showing that PCO4 catalysed reactions carried out in the presence of $^{18}O_2$ result in a +4 Da increase in the mass of the putative Cys sulfinic acid product; however, a +6 Da increase in the size of the putative Cys sulfonic acid product is not observed; (b) MALDI MS spectra showing that PCO4 catalysed reactions carried out in the presence of $H_2^{18}O$ show no additional incorporation of mass compared with products of reactions in the presence of $H_2^{16}O$; (c) LC MS spectra confirm that the +48 Da reaction product is an artefact of MALDI MS analysis (Supplementary Fig. 3) and incubation of PCO1 and PCO4 with $RAP2_{2-11}$ results in formation of a single product with a mass increase of +32 Da, consistent with Cys sulfinic acid formation.

As a final confirmation of the nature of the reaction catalysed by PCO1 and PCO4, their activity was monitored using 1H NMR. Reactions were initiated by adding $5 \mu M$ enzyme to $500 \mu M$ $RAP2_{2-11}$ (in the presence of 10% D_2O) and products of the reaction were analysed using a 600 MHz NMR spectrometer. In the presence of both PCO1 and PCO4, modification to the cysteinyl residues was observed, as exemplified by the disappearance of the 1H resonance corresponding to the β cysteinyl protons (at δ_H 2.88 p.p.m.) and the emergence of a new 1H resonance at δ_H 2.67 p.p.m. (Fig. 3b). The chemical shift of the new resonance is similar to that observed for L Cys conversion to L Cys sulfinic acid by mouse CDO (ref. 31) and also to the chemical shift of an L Cys sulfinic acid standard measured under equivalent conditions to the PCO assays (Supplementary Fig. 4). Therefore, the resonance shift observed upon PCO1/4 reaction was assigned to the β protons of L Cys sulfinic acid. Overall, these results provide confirmation at the molecular level that *Arabidopsis* PCOs 1 and 4 act as plant cysteinyl dioxygenases, catalysing incorporation of O_2 into N terminal Cys residues on a $RAP2$ peptide to form Cys sulfinic acid.

ATE1 arginylates acidic N termini including Cys sulfinic acid.

We next sought to confirm that the PCO catalysed Cys oxidation to Cys sulfinic acid renders a $RAP2$ peptide capable of and sufficient for onward modification by ATE1. Cys sulfinic acid has been proposed as a substrate for ATE1 on the basis of its structural homology with known ATE1 substrates Asp and Glu, but evidence has only been reported to date for arginylation of Cys sulfonic acid^{32,33}. We further sought to validate the role of a plant ATE1: to date ATE1 has been suggested to be responsible for transfer of 3H arginine to bovine α lactalbumin in highly purified plant extracts *in vitro*³⁴ and $RAP2.12$ stabilization in *ate1 ate2* double null mutant plant lines implicates ATE1 as an ERF VII targeting arginyl transferase *in vivo*^{17,18}. To this end, we produced recombinant hexahistidine tagged *Arabidopsis* ATE1 (Supplementary Fig. 5) for use in an arginylation assay, which detects incorporation of radiolabelled ^{14}C Arg into biotinylated peptides. Carboxy terminally biotinylated $RAP2_{2-13}$ peptides (H_2N XGGAIISDFI(PEG)K(biotin) NH_2) where the N terminal residue, X, constitutes Gly, Asp, Cys or Cys sulfonic acid were subjected to the arginylation assay in the presence or absence of PCO1/4 (Fig. 4a). Peptide with an N terminal Gly did

not accept Arg, whereas an N terminal Asp did accept Arg, independent of the presence of PCO1 or 4. A peptide comprising an N terminal Cys sulfonic acid was also shown to be a substrate for ATE1, again independent of the presence of PCO1 or 4, which is in line with proposed steps of the Arg/Cys N end rule pathway and has also recently been reported using a similar assay with mouse ATE1 (refs 14, 16,35). Crucially, in the absence of PCO1/4, $RAP2_{2-13}$ with an N terminal Cys was not an acceptor of arginine transfer by ATE1, yet when either PCO1 or PCO4 was incorporated in the reaction, significant ATE1 transferase activity was observed (Fig. 4a).

To confirm that the increased detection of radiolabelled arginine corresponded to arginyl incorporation at the N termini of the peptides, the experiment was repeated using non radiolabelled arginine in the presence and absence of PCO4 and ATE1, and peptide products subjected to LC MS analysis (Fig. 4c). As with $RAP2_{2-11}$ (Fig. 2c), the Cys initiated $RAP2_{2-13}$ peptide displayed a +32 Da increase in mass upon incubation with PCO4 only (Fig. 4c, red spectrum). Importantly, following incubation of Cys initiated $RAP2_{2-13}$ with both PCO4 and ATE1, a mass increase equivalent to oxidation coupled to arginylation (+188 Da) was observed (Fig. 4c, blue spectrum). Subsequent tandem MS analysis of these product ions revealed fragmentation species consistent with the assumption that oxidation and sequential arginylation occur at the N terminus of PCO4 and ATE1 treated peptides (Fig. 4d, blue spectrum), strongly suggesting that the PCO oxidized N termini of ERF VIIs are rendered N degrens via additional arginylation (Fig. 4b).

A +12 Da mass increase was observed in control assays lacking PCO4 (Fig. 4c,d; purple spectra). This appeared to be related to prolonged incubation in the presence of HEPES and dithiothreitol (DTT) as used in the arginylation assay buffer: The +12 Da modification was not observed if the peptide was dissolved in H_2O (Fig. 4c, black spectrum) or if incubated with HEPES and DTT for just 1 h, but was observed when the peptide was incubated with HEPES and DTT overnight (Supplementary Fig. 6). It is proposed that under these conditions, trace levels of contaminating formaldehyde react with free Nt Cys residues to form thiazolidine N termini³⁶.

These results are in line with proposed arginylation requirements for the Arg/Cys branch of the N end rule pathway¹⁴⁻¹⁶ including the known Cys initiated arginylation targets from mammals^{32,33,35,37}. Importantly, these results demonstrate for the

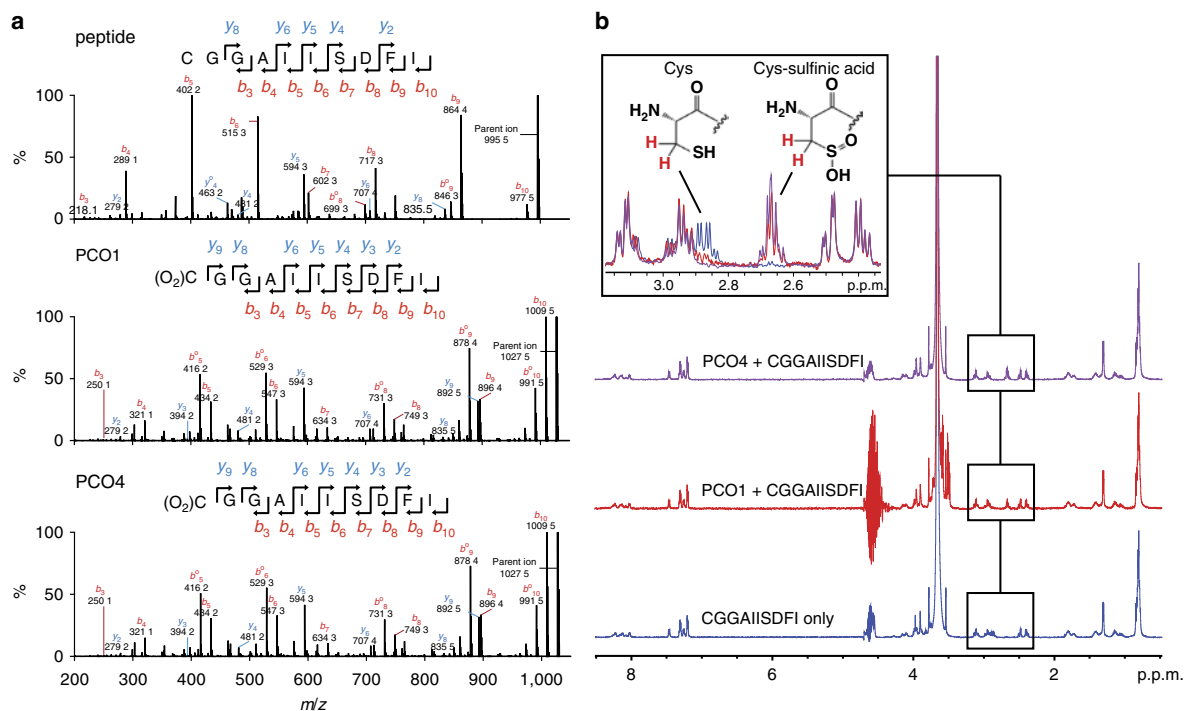


Figure 3 | PCO1 and PCO4 oxidize the N-terminal Cys of RAP2₂₋₁₁ to Cys-sulfonic acid. (a) Peptidic products of PCO catalysed reactions were subjected to LC MS/MS analysis. In the presence of enzyme, fragment assignment was consistent with expected *b* and *y* series ion masses for RAP2₂₋₁₁ with N terminal Cys sulfonic acid. (b) ¹H NMR was used to monitor changes to RAP2₂₋₁₁ (500 μM) upon incubation with enzyme (5 μM). In the presence of PCO1 (red) and PCO4 (purple), the ¹H resonance at δ_H 2.88 p.p.m. (assigned to the β cysteinyl protons of RAP2₂₋₁₁, blue) was observed to decrease in intensity, with concomitant emergence of a resonance at δ_H 2.67 p.p.m. This new resonance was assigned to the β protons of Cys sulfonic based on chemical shift analysis (see Supplementary Fig. 4).

first time Arg transfer mediated by a plant ATE dependent on the N terminal residue of its substrate, and also that both Cys sulfonic acid (the product of PCO catalysis) and Cys sulfonic acid can act as substrates for ATE1. In particular, the arginylation observed with PCO catalysed Cys sulfonic acid supports the assumption that N terminal residues sterically and electrostatically resembling Asp or Glu can serve as Arg acceptors in reactions catalysed by ATEs³³, and also confirms the importance of the PCOs as a connection between the stability of their ERF VII substrates and O₂ availability (Fig. 4b).

Discussion

The PCOs were identified in *Arabidopsis* as a set of five enzymes suggested to catalyse oxidation of N terminal cysteine residues in ERF VII transcription factors and oxygen consumption was demonstrated for reactions with short peptides corresponding to their N termini²⁸. This putative oxidation was associated with destabilization of the ERF VIIs, presumably by rendering them substrates of the Arg/Cys branch of the N end rule pathway^{14,16}. Under conditions of sufficient O₂ availability ERF VII protein levels are decreased, whereas under hypoxic conditions, such as those encountered upon plant submergence or in the context of organ development, ERF VII levels remain high^{17,18}. Importantly, the ERF VII transcription factors are known to upregulate genes which allow plants to cope with or respond to submergence¹³. The PCOs are proposed to act as potential O₂ sensors involved in regulating the plant hypoxic response²⁸.

We sought to biochemically confirm the role of the PCOs in the plant hypoxic response, and present here MS and NMR data

that clearly demonstrate that two enzymes from different ‘subclasses’ of this family, PCOs 1 and 4, are dioxygenases that catalyse direct incorporation of O₂ into RAP2₂₋₁₁ peptides to form Cys sulfonic acid. Their direct use of O₂ supports the proposal that these enzymes may act as plant O₂ sensors²⁸. A relationship has been demonstrated between O₂ concentration and PCO activity²⁸, but it will be of interest to perform detailed kinetic characterization of these enzymes to ascertain their level of sensitivity to O₂ availability, in particular to determine whether their O₂ sensitivity is similar to that of the HIF hydroxylases in animals^{24,25}. Although there is functional homology between the PCOs and the HIF hydroxylases, they are apparently mechanistically divergent: the PCOs show sequence homology to the Fe(II) dependent CDO family of enzymes, which do not require an external electron donor for O₂ activation^{28,30}, whereas the HIF hydroxylases are Fe(II)/2OG dependent oxygenases. They also co purified with Fe(II) as reported for both the CDOs²⁹ and prolyl hydroxylase 2 (ref. 38). Of note, the PCOs are the first identified CDOs in plants. Further, in contrast to the reactions of mammalian and bacterial CDOs, which oxidize free L Cys, the PCOs are also, to our knowledge, the first identified cysteinyl (as opposed to free L Cys) dioxygenases.

According to the Arg/Cys branch of the N end rule pathway, N terminal Cys oxidation is proposed to enable successive arginylation by ATE1 to render proteins as N degrons. Although both Cys sulfonic and Cys sulfonic acid are repeatedly reported as potential arginylation substrates¹⁴⁻¹⁶, detailed evidence has only been presented to date for arginylation of Cys sulfonic acid^{32,33} and this only in a mammalian system. We therefore sought to

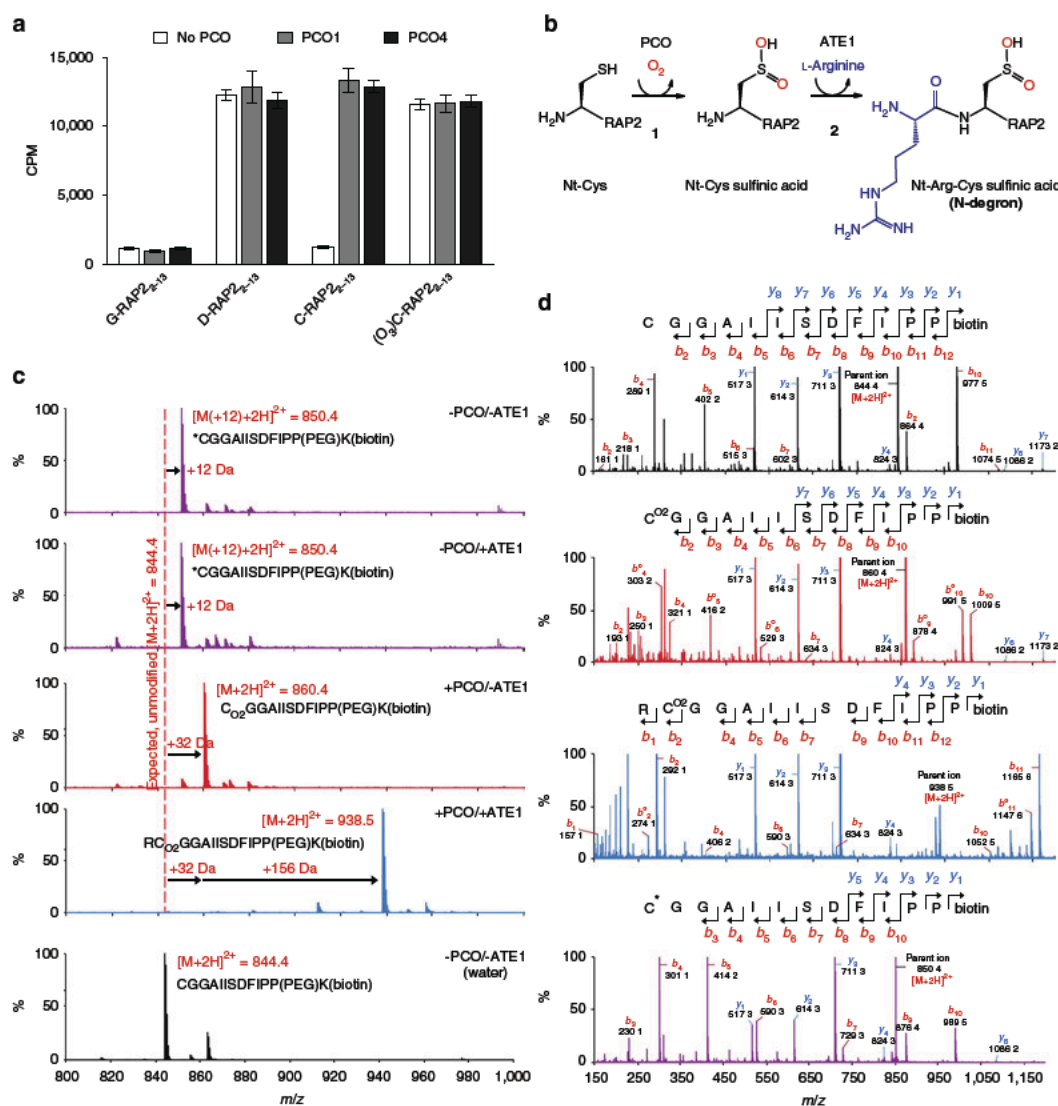


Figure 4 | PCO-catalysed Cys-sulfinic acid formation renders RAP₂₋₁₃ a substrate for ATE1-catalysed arginylation. (a) ¹⁴C Arg incorporation by ATE1 into the 12 mer N terminal ERF VII peptide (H₂N XGGAIISDFIPP(PEG)K(biotin) NH₂, X = Gly, Asp, Cys or Cys sulfonic acid (C(O₃))), was assayed by liquid scintillation counting of immobilized biotinylated peptides after the arginylation reaction and removal of unreacted ¹⁴C Arg (n = 3). In the case of the Cys starting peptide (RAP₂₋₁₃), ATE1 activity was strongly dependent on the presence of PCO1 or PCO4. n = 3, error bars in this panel represent s.e.m. (b) Scheme showing PCO and ATE1 catalysed reactions on Nt Cys of ERF VII, as validated in this study. (c) LC MS spectra of products of equivalent assays with Cys initiated RAP₂₋₁₃ using non radiolabelled Arg, revealing a sequential mass increase of + 32 (corresponding to oxidation) and + 156 Da (corresponding to arginylation) only in the presence of PCO and ATE1 (blue spectrum). The red spectrum shows a + 32Da mass increase for Cys RAP₂₋₁₃ incubated + PCO/ ATE, demonstrating Cys sulfinic acid formation as expected. Purple spectra show + 12Da species formed upon incubation of Cys RAP₂₋₁₃ in the absence of PCO +/ ATE (for explanation of this mass increase see text and Supplementary Fig. 6); the black spectrum shows Cys RAP₂₋₁₃ dissolved in H₂O. (d) b and y ion series spectra generated by MS/MS analysis of Cys RAP₂₋₁₃ only (no incubation; black), Cys RAP₂₋₁₃ incubated + PCO/ ATE (red), Cys RAP₂₋₁₃ incubated + PCO/+ ATE1 (blue) and Cys RAP₂₋₁₃ incubated - PCO/ ATE1 (purple), confirming arginylation only at the N terminus of PCO modified RAP₂₋₁₃.

demonstrate that PCO catalysed ERF VII N terminal Cys oxidation to Cys sulfinic acid promotes arginylation by ATE1. The arginylation assay and MS results we present demonstrate that the PCO catalysed dioxygenation reaction is sufficient to trigger N terminal arginylation of ERF VII, thus probably rendering N termini of ERF VII (at least those comprising the tested N terminal sequence) as N degrons, that is, allowing recognition by PRT6 and other potential E3 ubiquitin

ligases, polyubiquitination and possibly transfer to the 26S proteasome for proteolysis¹⁴⁻¹⁶. Collectively, therefore, we present the comprehensive molecular evidence confirming the Cys oxidation and subsequent arginylation steps of the Arg/Cys branch of the N end rule pathway^{32,33,37}. We also confirm that ATE1 is able to selectively arginylate, as predicted³³, acidic N terminal residues of plant substrates, including Cys sulfonic acid.

Arginylation has been known as a post translational modification since 1963 (ref. 39), to possess a general aminoacyl transferase function in plants (rice and wheat) since 1973 (ref. 40) and to have a speculative involvement in the N end rule pathway since 1988 (refs 41,42). ATE1 is reported as being capable of arginylating proteins at both acidic N termini and midchain acidic side chains via canonical and non canonical peptide bonds, respectively⁴³. Reports of midchain arginylation highlighted a potentially broad involvement of ATEs in posttranslational protein modifications for various functions^{35,43–45} but was only very recently brought into question by ¹⁴C Arg incorporation assays using arrays of immobilized synthetic peptides^{35,43,44}. However, to date only one physiological and two *in vitro* substrates for the Arg/Cys branch of the N end rule pathway have been characterized, namely mammalian regulator of G protein signalling (RGS) 4, and RGS5 and 10, respectively⁴⁶, where Nt Cys oxidation was described (to Cys sulfonic acid) as was Nt Cys arginylation^{33,37}. The first non Cys branch N end rule arginylation target was shown to require posttranslational proteolytic cleavage of a (pre) proprotein. The C terminal fragment of proteolytically cleaved mouse BRCA1 is Asp initiated⁴⁷ and gets degraded in an N end rule dependent manner. Then, the molecular chaperone BiP (GRP78 and HSPA5, heat shock 70kDa protein 5) and the oxidoreductase protein disulphide isomerase, present Glu or Asp after cleavage of their signal peptide, respectively, and were suggested but not shown as putative N end rule substrates⁴⁸. Only very recently, BiP and protein disulphide isomerase were identified in mammalian cell culture together with the Glu initiated calreticulin as arginylation targets with a function in autophagy rather than the N end rule degradation⁴⁹.

Similarly, data regarding the molecular requirements of plant ATEs are limited. Already in 1973, a general aminoacyl transferase activity was found in rice and wheat cell extracts, however, the nature of enzyme, acceptor position and mechanism remained unclear. It was suggested that the N terminus could serve as Arg acceptor⁴⁰.

The first description of a mutant of the single translatable *ATE1* gene in the *Arabidopsis* accession Wassilewskija (Ws 0) highlighted a role of ATEs in plant development. Ws 0 lacks the second *bona fide* ATE, that is, ATE2, due to a single nucleotide polymorphism in *ATE2* causing a premature stop⁵⁰. Developmental functions of the single homologue ATE1 in the moss *Physcomitrella patens* were recently described⁵¹. Interaction partners of the enzyme were found as well as four arginylated peptides immunologically detected by using antibodies directed against peptides mimicking N terminal Arg Asp or Arg Glu⁵². In one case, that is the acylamino acid releasing enzyme PpAARE, which presents for unknown reasons a neo N terminal Asp residue, which was formerly Asp2 and therefore initiated by Met, an N terminal arginylation was found with high confidence. Previously, Arg transferase function of *Arabidopsis* ATE1/2 has been shown using an assay detecting conjugation of ³H Arg to bovine α lactalbumin (bearing an N terminal Glu) in the presence of plant extracts from wild type *Arabidopsis*, and *ate1* and *ate2* single mutants but not from *ate1 ate2* double mutant seedlings³⁴. Therefore, the results we present here demonstrate for the first time Arg transferase activity of a plant ATE towards known plant N end rule substrates.

Interestingly, in combination with O₂, nitric oxide was identified as an RGS oxidizing agent, suggesting a potential role of S nitrosylation in the Arg/Cys branch of the N end rule pathway, albeit non enzymatically controlled³². It has also been reported *in planta* that both NO and O₂ are required for ERF VII degradation, potentially at the Cys oxidation step^{22,23}. Although in N end rule mediated RGS4/5 degradation it has

been proposed that Cys nitrosylation precedes Cys oxidation (also currently considered a non enzymatic process), we find that under the conditions used, the PCO1/4 catalysed reaction does not require either prior Cys nitrosylation or exogenous NO to proceed efficiently. We cannot rule out that NO plays a role in formation of a Cys sulfonic acid product, which is also a substrate for ATE1 as shown in our Arg transfer experiments. Alternatively, NO may have a role in ERF VII degradation *in vivo* via non enzymatic oxidation or via a secondary mechanism. The manner in which NO contributes to Arg/Cys branch of the N end rule pathway therefore remains to be elucidated.

ERF VII stabilization has been shown to result in improved submergence tolerance, elegantly demonstrated in barley by mutation of the candidate E3 ubiquitin ligase *PRT6* (ref. 11), but also in rice containing the *Sub1A* gene; SUB1A is an apparently stable ERF VII that confers particular flood tolerance in certain rare varieties of rice^{9,17}. Overexpression of *Sub1A* in more commonly grown rice varieties has resulted in a 45% increase in yield relative to *sub1a* mutant lines after exposure to flooding⁵³. If ERF VII stabilization is indeed a proficient mechanism for enhancing flood tolerance, then manipulation of PCO or ATE activity may be an efficient and effective point of intervention. This work presents molecular validation of their function, providing the basis for future targeted chemical/genetic inhibition of their activity. It also highlights genetic strategies for breeding via introgression of variants of N end rule pathway components or introduction of alleles of enzymatic components of the N end rule pathway from non crop species into crops. Any of these strategies has the potential to result in stabilized ERF VII levels and increase stress resistance, and may therefore help to address food security challenges.

Methods

Peptide synthesis. All reagents used were purchased from Sigma-Aldrich unless otherwise stated. The 10-mer RAP2_{2–11} peptide (H₂N-CGGAIISDFI-COOH) was purchased from GL Biochem (Shanghai) Ltd, China (Supplementary Table 1). The sequence of the 12-mer RAP2_{2–13} peptides used in the coupled oxidation-arginylation assay is derived from RAP2.2, RAP2.12 and HRE2 (H₂N-X-GGAIISDFIIPP(PEG)K(biotin)-NH₂), and synthesized by Fmoc-based solid-phase peptide synthesis on NovaSyn TGR resin (Merck KGaA, Supplementary Table 2). Fmoc protected amino acids (Iris Biotech GmbH) were coupled using 4 equivalents (eq) of the amino acid according to the initial loading of the resin. 4 eq amino acid was mixed with 4 eq O-(6-chlorobenzotriazol-1-yl)-N,N,N',N'-tetramethyluronium hexafluorophosphate and 8 eq N,N-diisopropylethylamine (Santa Cruz Biotechnology, sc-293894), and added to the resin for 1 h. In a second coupling, the resin was treated with 4 eq of the Fmoc-protected amino acid mixed with 4 eq benzotriazole-1-yl-oxy-tris-pyrrolidino-phosphonium hexafluoro-phosphate and 8 eq 4-methylmorpholine for 1 h. After double coupling a capping step to block free amines was performed using acetanhydride and N,N-diisopropylethylamine in N-methyl-2-pyrrolidinone (1:1:10) for 5 min. The C-terminal Fmoc-Lys(biotin)-OH, the 8-(9-fluorenylmethoxycarbonyl-amino)-3,6-dioxo-octanoic acid (PEG) linker and the different Fmoc protected N-terminal amino acids were coupled manually. The remaining peptide sequence was assembled using an automated synthesizer (Syro II, MultiSynTech GmbH). Fmoc deprotection was performed using 20% piperidine in dimethylformamide (DMF) for 5 min, twice. After each step the resin was washed five times with DMF, methylene chloride (DCM) and DMF, respectively. Final cleavage was performed with 94% trifluoroacetic acid (TFA), 2.5% 1,2-ethanedithiol and 1% triisopropylsilane in aqueous solution for 2 h, twice. The cleavage solutions were combined and peptides were precipitated with diethyl ether (Et₂O) at 20 °C for 30 min. Peptides were solved in water/acetonitrile (ACN) 7:3 and purified by reversed-phase HPLC (Nucleodur C18 column; 10 × 125 mm, 110 Å, 5 µm particle size; Macherey-Nagel) using a flow rate of 6 ml min⁻¹ (A: ACN with 0.1% TFA, B: water with 0.1% TFA). Obtained pure fractions were pooled and lyophilized. Peptide characterization was performed by analytical HPLC (1260 Infinity, Agilent Technology; flow rate of 1 ml min⁻¹, A: ACN with 1% TFA, B: water with 1% TFA) coupled with a mass spectrometer (6120 Quadrupole LC-MS, Agilent Technology) using electrospray ionization (Agilent Eclipse XDB-C18 column, 4.6 × 150 mm, 5 µm particle size). Analytical HPLC chromatograms were recorded at 210 nm (Supplementary Fig. 7). Quantification was performed by HPLC-based comparison (chromatogram at 210 nm) with a reference peptide (Supplementary Table 2).

Protein expression and purification. *Arabidopsis* PCO1 and PCO4 sequences in pDEST17 bacterial expression vectors (Invitrogen) were kindly provided by F. Licausi and J. van Dongen²⁸. Plasmids were transformed into BL21(DE3) *Escherichia coli* cells and expression of recombinant protein carrying an N-terminal hexahistidine tag was induced with 0.5 mM isopropyl- β -D-thiogalactoside and subsequent growth at 18 °C for 18 h. Harvested cells were lysed by sonication and proteins purified using Ni⁺⁺ affinity chromatography, before buffer exchange into 250 mM NaCl/50 mM Tris-HCl (pH 7.5). Analysis by SDS-PAGE and denaturing LC-MS showed proteins with >90% purity and with the predicted molecular weights.

The coding sequence of *Arabidopsis* ATE1 was cloned according to gene annotations at TAIR (www.arabidopsis.org) from complementary DNA. The sequence was flanked by an N-terminal tobacco etch virus recognition sequence for facilitated downstream purification ('tev': ENLYFQ-X) using the primers atel1 tev ss (5'-GCTTAGAGAATCTTTATTTTCAGGGGATGTCTTTGAAAAA CGATGCGAGT-3') and atel1 as (5'-GGGGACCACTTTGTACAAGAAAGCTGG GTATCAGTTGATTCATACACCATTCTCTC-3'). A second PCR using the primers adapter (5'-GGGGACAAGTTTGTACAAAAAAGCAGGCTTAGAGAAT CTTTATTTTCAGGGG-3') and atel1 as was performed to amplify the construct to use it in a BP reaction for cloning into pDONR201 (Invitrogen) followed by an LR reaction into the vector pDEST17 (Invitrogen). The N-terminal hexahistidine fusion was expressed in BL21-CodonPlus (DE3)-RIL *E. coli* cells. The expression culture was induced with 1 mM isopropyl- β -D-thiogalactoside at optical density 0.6 and grown for 16 h at 18 °C. After resuspension in LEW buffer (50 mM NaH₂PO₄ pH 8, 300 mM NaCl and 1 mM DTT), the cells were lysed by incubation with 1.2 mg ml⁻¹ lysozyme for 30 min and underwent subsequent sonification in the presence of 1 mM phenylmethylsulfonyl fluoride. Recombinant protein was purified by Ni⁺⁺ affinity chromatography and subjected to Amicon Ultra-15 (30 K) (Merck Millipore) filtration for buffer exchange to imidazole-free LEW containing 20% glycerol.

PCO activity assays and MALDI analysis. PCO activity assays were conducted under the following conditions, unless otherwise stated: PCO1 or 4 (1 μ M) was mixed with 100 or 200 μ M RAP₂₁₁ peptide in 250 mM NaCl, 1 mM DTT, 50 mM Tris-HCl pH 7.5 and incubated at 30 °C for 30–60 min. Addition of exogenous Fe(II) and/or ascorbate were not required for activity. Assays were stopped by quenching 1 μ l sample with 1 μ l α -cyano-4-hydroxycinnamic acid matrix on a MALDI plate before product mass analysis using a Sciex 4800 TOF/TOF mass spectrometer (Applied Biosystems) operated in negative ion reflection mode. The instrument parameters and data acquisition were controlled by 4000 Series Explorer software and data processing was completed using Data Explorer (Applied Biosystems).

To test the activity of PCO4 in the presence of ¹⁸O₂, 100 μ l of an anaerobic solution of 100 μ M RAP₂₁₁ in 250 mM NaCl/50 mM Tris-HCl pH 7.5 was prepared in a septum-sealed glass vial by purging with 100% N₂ for 10 min at 100 ml min⁻¹ using a mass flow controller (Brooks Instruments), as used for previous preparation of anaerobic samples to determine enzyme dependence on O₂ (ref. 24). PCO4 was then added using a gas-tight Hamilton syringe, followed by purging with a balloon (~0.7 l) of ¹⁶O₂ or ¹⁸O₂ over the course of 10 min at room temperature. Reaction vials were then transferred to 30 °C for a further 20 min before products were analysed by MALDI-MS as described above.

PCO4 activity was additionally tested in the presence of H₂¹⁸O by conducting an assay in 75% H₂¹⁸O, 25% H₂O (with all enzyme/substrate/buffer components comprising a portion of the H₂O fraction). Assays were conducted for 10 min at room temperature followed by 20 min at 30 °C for comparison with assays conducted with ¹⁸O₂. Products were analysed by MALDI-MS, as described above.

UPLC-MS and MS/MS analysis. Ultra-high performance chromatography (UPLC)-MS measurements were obtained using an Acquity UPLC system coupled to a Xevo G2-S Q-ToF mass spectrometer (Waters) operated in positive electrospray mode. Instrument parameters, data acquisition and data processing were controlled by Masslynx 4.1. Source conditions were adjusted to maximize sensitivity and minimize fragmentation while Lockspray was employed during analysis to maintain mass accuracy. Two microlitres of each sample was injected on to a Chromolith Performance RP-18e 100-2 mm column (Merck) heated to 40 °C and eluted using a gradient of 95% deionized water supplemented with 0.1% (v/v) formic acid (analytical grade) to 95% acetonitrile (HPLC grade) and a flow rate of 0.3 ml min⁻¹. Fragmentation spectra of substrate and product peptide ions (MS/MS) were obtained using a targeted approach with a typical collision-induced dissociation energy ramp of 30 to 40 eV. Analysis was carried out with the same source settings, flow rate and column elution conditions as above.

¹H-NMR assay. Reaction components (5 μ M PCO1 or PCO4 and 500 μ M RAP₂₁₁) were prepared to 75 μ l in 156 mM NaCl, 31 mM Tris-HCl (pH 7.5) and 10% D₂O (enzyme added last), in a 1.5 ml microcentrifuge tube before being transferred to a 2 mm diameter NMR tube. ¹H-NMR spectra at 310 K were recorded using a Bruker AVIII 600 (with inverse cryoprobe optimized for ¹H observation and running topspin 2 software; Bruker) and reported in p.p.m.

relative to D₂O (δ _H 4.72). The deuterium signal was also used as internal lock signal and the solvent signal was suppressed by presaturating its resonance.

Arginylation assay. The conditions for arginylation of the 12-mer peptide substrates were modified from ref. 43. In detail, ATE1 was incubated at 10 μ M in the reaction mixture containing 50 mM HEPES pH 7.5, 25 mM KCl, 15 mM MgCl₂, 1 mM DTT, 2.5 mM ATP; 0.6 mg ml⁻¹ *E. coli* tRNA (R1753, Sigma), 0.04 mg ml⁻¹ *E. coli* aminoacyl-tRNA synthetase (A3646, Sigma), 80 μ M (4 nCi μ l⁻¹) ¹⁴C-arginine (MC1243, Hartmann Analytic), 50 μ M C-terminally biotinylated 12-mer peptide substrate and, where indicated, 1 μ M purified recombinant PCO1 or PCO4 in a total reaction volume of 50 μ l. The reaction was conducted at 30 °C for 16–40 h. After incubation, each 50 μ l of avidin agarose bead slurry (20219, Pierce) equilibrated in PBSN (PBS-Nonidet; 100 mM NaH₂PO₄, 150 mM NaCl; 0.1% Nonidet-P40) was added to the samples and mixed with an additional 350 μ l of PBSN. After 2 h of rotation at room temperature, the beads were washed four times in PBSN, resuspended in 4 ml of FilterSafe scintillation solution (Zinsser Analytic) and scintillation counting was performed using a Beckman Coulter LS 6500 Multi-Purpose scintillation counter.

Data availability. The authors declare that all data supporting the findings of this study are available within the manuscript and its Supplementary Information files or are available from the corresponding authors upon request.

References

- Kaelin, J. W. G. & Ratcliffe, P. J. Oxygen sensing by metazoans: the central role of the HIF hydroxylase pathway. *Mol. Cell* **30**, 393–402 (2008).
- Myllyharju, J. Prolyl 4-hydroxylases, master regulators of the hypoxia response. *Acta Physiol. (Oxf)* **208**, 148–165 (2013).
- Semenza, G. L. Oxygen sensing, homeostasis, and disease. *N. Engl. J. Med.* **365**, 537–547 (2011).
- Bailey-Serres, J. *et al.* Making sense of low oxygen sensing. *Trends Plant Sci.* **17**, 129–138 (2012).
- Bailey-Serres, J., Lee, S. C. & Brinton, E. Waterproofing crops: effective flooding survival strategies. *Plant Physiol.* **160**, 1698–1709 (2012).
- Hattori, Y. *et al.* The ethylene response factors SNORKEL1 and SNORKEL2 allow rice to adapt to deep water. *Nature* **460**, 1026–1030 (2009).
- Hinz, M. *et al.* *Arabidopsis* RAP2.2: an ethylene response transcription factor that is important for hypoxia survival. *Plant Physiol.* **153**, 757–772 (2010).
- Licausi, F. *et al.* HRE1 and HRE2, two hypoxia-inducible ethylene response factors, affect anaerobic responses in *Arabidopsis thaliana*. *Plant J.* **62**, 302–315 (2010).
- Xu, K. *et al.* Sub1A is an ethylene-response-factor-like gene that confers submergence tolerance to rice. *Nature* **442**, 705–708 (2006).
- Papdi, T. *et al.* Functional identification of *Arabidopsis* stress regulatory genes using the controlled cDNA overexpression system. *Plant Physiol.* **147**, 528–542 (2008).
- Mendondo, G. M. *et al.* Enhanced waterlogging tolerance in barley by manipulation of expression of the N-end rule pathway E3 ligase PROTEOLYSIS6. *Plant Biotechnol. J.* **14**, 40–50 (2016).
- Lee, S. C. *et al.* Molecular characterization of the submergence response of the *Arabidopsis thaliana* ecotype Columbia. *New Phytol.* **190**, 457–471 (2011).
- Mustroph, A. *et al.* Profiling translomes of discrete cell populations resolves altered cellular priorities during hypoxia in *Arabidopsis*. *Proc. Natl Acad. Sci. USA* **106**, 18843–18848 (2009).
- Varshavsky, A. The N-end rule pathway and regulation by proteolysis. *Protein Sci.* **20**, 1298–1345 (2011).
- Tasaki, T., Sriram, S. M., Park, K. S. & Kwon, Y. T. The N-end rule pathway. *Annu. Rev. Biochem.* **81**, 261–289 (2012).
- Gibbs, D. J., Bacardit, J., Bachmair, A. & Holdsworth, M. J. The eukaryotic N-end rule pathway: conserved mechanisms and diverse functions. *Trends Cell Biol.* **24**, 603–611 (2014).
- Gibbs, D. J. *et al.* Homeostatic response to hypoxia is regulated by the N-end rule pathway in plants. *Nature* **479**, 415–418 (2011).
- Licausi, F. *et al.* Oxygen sensing in plants is mediated by an N-end rule pathway for protein destabilization. *Nature* **479**, 419–422 (2011).
- Ross, S., Giglione, C., Pierre, M., Espagne, C. & Meinnel, T. Functional and developmental impact of cytosolic protein N-terminal methionine excision in *Arabidopsis*. *Plant Physiol.* **137**, 623–637 (2005).
- Giglione, C., Boularot, A. & Meinnel, T. Protein N-terminal methionine excision. *Cell Mol. Life Sci.* **61**, 1455–1474 (2004).
- Garzon, M. *et al.* PRT6/At5g02310 encodes an *Arabidopsis* ubiquitin ligase of the N-end rule pathway with arginine specificity and is not the CER3 locus. *FEBS Lett.* **581**, 3189–3196 (2007).
- Gibbs, D. J. *et al.* Nitric oxide sensing in plants is mediated by proteolytic control of group VII ERF transcription factors. *Mol. Cell* **53**, 369–379 (2014).

23. Gibbs, D. J. *et al.* Group VII ethylene response factors coordinate oxygen and nitric oxide signal transduction and stress responses in plants. *Plant Physiol.* **169**, 23–31 (2015).
24. Tarhonskaya, H. *et al.* Investigating the contribution of the active site environment to the slow reaction of hypoxia-inducible factor prolyl hydroxylase domain 2 with oxygen. *Biochem. J.* **463**, 363–372 (2014).
25. Hiršila, M., Koivunen, P., Gunzler, V., Kivirikko, K. I. & Myllyharju, J. Characterization of the human prolyl 4-hydroxylases that modify the hypoxia-inducible factor. *J. Biol. Chem.* **278**, 30772–30780 (2003).
26. Bruick, R. K. Oxygen sensing in the hypoxic response pathway: regulation of the hypoxia-inducible transcription factor. *Genes Dev.* **17**, 2614–2623 (2003).
27. Epstein, A. C. *et al.* C. *elegans* EGL-9 and mammalian homologs define a family of dioxygenases that regulate HIF by prolyl hydroxylation. *Cell* **107**, 43–54 (2001).
28. Weits, D. A. *et al.* Plant cysteine oxidases control the oxygen-dependent branch of the N-end-rule pathway. *Nat. Commun.* **5**, 3425 (2014).
29. Imsand, E. M., Njeri, C. W. & Ellis, H. R. Addition of an external electron donor to *in vitro* assays of cysteine dioxygenase precludes the need for exogenous iron. *Arch. Biochem. Biophys.* **521**, 10–17 (2012).
30. Joseph, C. A. & Maroney, M. J. Cysteine dioxygenase: structure and mechanism. *Chem. Commun. (Camb)* **32**, 3338–3349 (2007).
31. Li, W. & Pierce, B. S. Steady-state substrate specificity and O₂-coupling efficiency of mouse cysteine dioxygenase. *Arch. Biochem. Biophys.* **565**, 49–56 (2015).
32. Hu, R. G. *et al.* The N-end rule pathway as a nitric oxide sensor controlling the levels of multiple regulators. *Nature* **437**, 981–986 (2005).
33. Kwon, Y. T. *et al.* An essential role of N-terminal arginylation in cardiovascular development. *Science* **297**, 96–99 (2002).
34. Graciet, E. *et al.* The N-end rule pathway controls multiple functions during Arabidopsis shoot and leaf development. *Proc. Natl Acad. Sci. USA* **106**, 13618–13623 (2009).
35. Wadas, B., Piatkov, K. L., Brower, C. S. & Varshavsky, A. Analyzing N-terminal arginylation through the use of peptide arrays and degradation assays. *J. Biol. Chem.* **291**, 20976–20992 (2016).
36. Kallen, R. G. The mechanism of reactions involving Schiff base intermediates. Thiazolidine formation from L-cysteine and formaldehyde. *J. Am. Chem. Soc.* **93**, 6236–6248 (1971).
37. Davydov, I. V. & Varshavsky, A. RGS4 is arginylated and degraded by the N-end rule pathway *in vitro*. *J. Biol. Chem.* **275**, 22931–22941 (2000).
38. McNeill, L. A. *et al.* Hypoxia-inducible factor prolyl hydroxylase 2 has a high affinity for ferrous iron and 2-oxoglutarate. *Mol. Biosyst.* **1**, 321–324 (2005).
39. Kaji, H., Novelli, G. D. & Kaji, A. A soluble amino acid-incorporating system from rat liver. *Biochim. Biophys. Acta* **76**, 474–477 (1963).
40. Manahan, C. O. & App, A. A. An arginyl-transfer ribonucleic acid protein transferase from cereal embryos. *Plant Physiol.* **52**, 13–16 (1973).
41. Ciechanover, A. *et al.* Purification and characterization of arginyl-tRNA-protein transferase from rabbit reticulocytes. Its involvement in post-translational modification and degradation of acidic NH₂ termini substrates of the ubiquitin pathway. *J. Biol. Chem.* **263**, 11155–11167 (1988).
42. Bohley, P., Kopitz, J. & Adam, G. Surface hydrophobicity, arginylation and degradation of cytosol proteins from rat hepatocytes. *Biol. Chem. Hoppe Seyler* **369**, 307–310 (1988).
43. Wang, J. *et al.* Arginyltransferase ATE1 catalyzes midchain arginylation of proteins at side chain carboxylates *in vivo*. *Chem. Biol.* **21**, 331–337 (2014).
44. Eriste, E. *et al.* A novel form of neurotensin post-translationally modified by arginylation. *J. Biol. Chem.* **280**, 35089–35097 (2005).
45. Wong, C. C. *et al.* Global analysis of posttranslational protein arginylation. *PLoS Biol.* **5**, e258 (2007).
46. Lee, M. J. *et al.* RGS4 and RGS5 are *in vivo* substrates of the N-end rule pathway. *Proc. Natl Acad. Sci. USA* **102**, 15030–15035 (2005).
47. Piatkov, K. L., Brower, C. S. & Varshavsky, A. The N-end rule pathway counteracts cell death by destroying proapoptotic protein fragments. *Proc. Natl Acad. Sci. USA* **109**, E1839–E1847 (2012).
48. Hu, R. G. *et al.* Arginyltransferase, its specificity, putative substrates, bidirectional promoter, and splicing-derived isoforms. *J. Biol. Chem.* **281**, 32559–32573 (2006).
49. Cha-Molstad, H. *et al.* Amino-terminal arginylation targets endoplasmic reticulum chaperone BiP for autophagy through p62 binding. *Nat. Cell Biol.* **17**, 917–929 (2015).
50. Yoshida, S., Ito, M., Callis, J., Nishida, I. & Watanabe, A. A delayed leaf senescence mutant is defective in arginyl-tRNA:protein arginyltransferase, a component of the N-end rule pathway in *Arabidopsis*. *Plant J.* **32**, 129–137 (2002).
51. Schuessele, C. *et al.* Spatio-temporal patterning of arginyl-tRNA protein transferase (ATE) contributes to gametophytic development in a moss. *New Phytol.* **209**, 1014–1027 (2016).
52. Hoernstein, S. N. *et al.* Identification of targets and interaction partners of arginyl-tRNA protein transferase in the moss *Physcomitrella patens*. *Mol. Cell Proteomics* **15**, 1808–1822 (2016).
53. Dar, M. H., de Janvry, A., Emerick, K., Raitzer, D. & Sadoulet, E. Flood-tolerant rice reduces yield variability and raises expected yield, differentially benefiting socially disadvantaged groups. *Sci. Rep.* **3**, 3315 (2013).

Acknowledgements

Petra Majovsky, Domenika Thieme and Wolfgang Hoehenwarter from the Proteomics Unit of the Leibniz Institute of Plant Biochemistry (IPB), Halle, are acknowledged for MS of recombinant ATE1. David Staunton from the Biophysical Facility, Department of Biochemistry, University of Oxford, is acknowledged for multi-angle light scatter analysis of PCO1/4. Geoff Grime from the University of Surrey Ion Beam Centre is acknowledged for assistance with the microPIXE data collection. This work was supported by a Biotechnology and Biological Sciences Research Council (U.K.) New Investigator grant (BB/M024458/1) to E.F., a grant for setting up the junior research group of the ScienceCampus Halle-Plant-based Bioeconomy to N.D., by a PhD fellowship of the Landesgraduiertenförderung Sachsen-Anhalt awarded to C.N., by an Engineering and Physical Sciences Research Council (U.K.) studentship (EP/G03706X/1) to J.C.B.-B., a Royal Society Dorothy Hodgkin Fellowship to E.F., a William R. Miller Junior Research Fellowship (St Edmund Hall, Oxford) to R.J.H. and grant DI 1794/3-1 by the German Research Foundation (Deutsche Forschungsgemeinschaft, DFG) to N.D. Financial support came from the Leibniz Association, the state of Saxony-Anhalt, the Deutsche Forschungsgemeinschaft (DFG) Graduate Training Center GRK1026 'Conformational Transitions in Macromolecular Interactions' at Halle, and the Leibniz Institute of Plant Biochemistry (IPB) at Halle, Germany. We thank Professor J. van Dongen (RWTH Aachen University, Germany) and Professor F. Licausi (Scuola Superiore Sant'Anna, Pisa, Italy) for sharing pDEST-PCO plasmids and helpful discussions. The manuscript was deposited as pre-print before publication (<https://doi.org/10.1101/069336>) at bioRxiv—the preprint server for biology, operated by Cold Spring Harbor Laboratory (bioRxiv.org). Publication of this article was funded by the Open Access fund of the Leibniz Institute of Plant Biochemistry (IPB). This work was supported by the network of the European Cooperation in Science and Technology (COST) Action BM1307—European network to integrate research on intracellular proteolysis pathways in health and disease (PROTEOSTASIS).

Author contributions

M.D.W. performed the PCO1/4 activity assays and MALDI/LC-MS/MS analyses. M.K. performed and established arginylation reactions on peptides coupled to biotin pull-down and scintillation measurements and purified ATE1 protein. R.J.H. performed the NMR assays with E.F., D.A.W. prepared the pDEST17-PCO1 and four plasmids. C.M. synthesized the biotinylated peptides, T.N.G. supervised and designed the synthesis and C.N. cloned and established purification and activity assays for ATE1. R.O. conducted LC-MS to analyse +12 Da mass shifts. J.W. performed LC-MS analysis. J.Y. and J.C.B.-B. prepared samples for micro-PIXE analysis, and J.C.B.-B. and E.F.G. collected and analysed micro-PIXE data. E.F. performed the PCO1 and PCO4 protein purification and selected activity assays. E.F., M.D.W., M.K. and N.D. designed the study. E.F. and N.D. wrote the manuscript. M.D.W., M.K., N.D. and E.F. designed the figures. All authors read and approved the final version of this manuscript.

Additional information

Supplementary Information accompanies this paper at <http://www.nature.com/naturecommunications>

Competing financial interests: The authors declare no competing financial interests.

Reprints and permission information is available online at <http://npg.nature.com/reprintsandpermissions/>

How to cite this article: White, M. D. *et al.* Plant cysteine oxidases are dioxygenases that directly enable arginyl transferase-catalysed arginylation of N-end rule targets. *Nat. Commun.* **8**, 14690 doi: 10.1038/ncomms14690 (2017).

Publisher's note: Springer Nature remains neutral with regard to jurisdictional claims in published maps and institutional affiliations.



This work is licensed under a Creative Commons Attribution 4.0 International License. The images or other third party material in this article are included in the article's Creative Commons license, unless indicated otherwise in the credit line; if the material is not included under the Creative Commons license, users will need to obtain permission from the license holder to reproduce the material. To view a copy of this license, visit <http://creativecommons.org/licenses/by/4.0/>

© The Author(s) 2017

1.4 OUTLOOK PART I – BIOLOGY

We are currently evaluating a forward genetics suppressor screen of N-end rule-mediated protein degradation via mapping-by-sequencing to identify novel enzymatic components or interactors of the plant N-end rule (in collaboration with the Genome Center, Max Planck Institute for Plant Breeding Research, Cologne and Andreas Bachmair, Max F. Perutz Laboratories, Vienna). Together with synthetic chemists (Bernhard Westermann, IPB Halle), we designed activity-based protein profiling (ABPP) strategies to capture N-end rule enzymes by using substrate-analogous decoys, click-chemistry and IP-MS (with Wolfgang Hoehenwarter, IPB Halle).

A project on structural elucidation of N-end rule-mediated substrate recognition is ongoing with Andrea Sinz (Institute of Pharmacy, University of Halle) and Jochen Balbach (Institute of Physics, University of Halle). Here, we try to solve the structure of E3 ligase PRT1 with the help of cross-linked substrate peptides.

Characterization of *bona fide* substrates such as RIN4 (RESISTANCE TO P. SYRINGAE PV MACULICOLA 1 (RPM1) INTERACTING PROTEIN 4) and other targets of the bacterial protease AvrRpt2, cleaved ETHYLENE INSENSITIVE 2 (EIN2) or those proteins identified to be upregulated in N-end rule mutants by differential proteomics takes place in my lab according to a well-established experimental algorithm *in vitro* and *in vivo*. In my lab, we are creating and implementing novel inducible vector systems to set up an optimized substrate identification pipeline and have started to analyze SENESCENCE-ASSOCIATED GENE 101 (SAG101) as potential N-end rule target (in collaboration with Johannes Stuttmann, University of Halle). A number of substrate candidates are amongst the proven and hypothesized targets of the *Pseudomonas syringae* protease AvrRpt2, amongst targets of the protease DA1 which are transcription factors and other regulators of cell differentiation (TEOSINTE BRANCED 1/CYCLOIDEA/PCF 15 (TCP15) and TCP22, with Mike Bevan, Norwich, UK and Emmanuelle Graciet, Maynooth, Ireland).

Two of the candidate targets that came up in our comparative proteomics screens as upregulated on protein level in N-end rule mutants were GLYCINE-RICH RNA-BINDING PROTEIN 7 and 8 (GRP7/8) which links the proteolysis machinery to RNA metabolism, stability, environmental stress and gene expression. We have followed up this work with help of Dorothee Staiger, University of Bielefeld.

In two newly established collaborations with the Medical Faculties of the University of Halle (Thorsten Pfirrmann, Institute of Physiological Chemistry) and Magdeburg (Martin Zenker, Institute of Human Genetics), we address two novel branches of the N-end rule in mammalian systems.

2 PART II – BIOTECHNOLOGY OF THE N-END RULE

2.1 INTRODUCTION PART II – BIOTECHNOGY

Targeted and conditional gene expression and conditional modulation of biological processes play key roles in basic and applied research. Modulating concentrations of proteins of interest can be achieved on various levels via a multitude of approaches. Manipulating target protein levels and activity can be altered by transcriptional, post-transcriptional, translational and posttranslational control. Most of these techniques rely on the specific half-life of the target protein and its turn-over. According to experience from my lab, modulation of protein abundance can therefore be best accomplished directly on the protein level.

2.1.1 Conditional expression and degradation as genetic tools

Here, recent advances in targeted protein depletion and accumulation and also other techniques in modulating expression levels are reviewed and discussed. Methods and protocols discussed here include inducible and tissue specific promoter systems as well as portable degrons. The techniques discussed in this chapter are mostly established in yeast, cell culture and *in vitro* systems and some successful applications in multicellular organisms are highlighted. The major goal was to link current concepts of conditionally modulating expression levels of proteins in living, multicellular organisms.

Publication:

Faden F, Mielke S, Lange D, **Dissmeyer N***. Generic tools for conditionally altering protein abundance and phenotypes on demand.
Biol Chem. 2014, **395**:737-62

Review

Frederik Faden, Stefan Mielke, Dieter Lange and Nico Dissmeyer*

Generic tools for conditionally altering protein abundance and phenotypes on demand

Abstract: Conditional gene expression and modulating protein stability under physiological conditions are important tools in biomedical research. They led to a thorough understanding of the roles of many proteins in living organisms. Current protocols allow for manipulating levels of DNA, mRNA, and of functional proteins. Modulating concentrations of proteins of interest, their post-translational processing, and their targeted depletion or accumulation are based on a variety of underlying molecular modes of action. Several available tools allow a direct as well as rapid and reversible variation right on the spot, i.e., on the level of the active form of a gene product. The methods and protocols discussed here include inducible and tissue-specific promoter systems as well as portable degrons derived from instable donor sequences. These are either constitutively active or dormant so that they can be triggered by exogenous or developmental cues. Many of the described techniques here directly influencing the protein stability are established in yeast, cell culture and *in vitro* systems only, whereas the indirectly working promoter-based tools are also commonly used in higher eukaryotes. Our major goal is to link current concepts of conditionally modulating a protein of interest's activity and/or abundance and approaches for generating cell and tissue types on demand in living, multicellular organisms with special emphasis on plants.

Keywords: conditional mutants; degron; expression control; inducible phenotypes; N-end rule pathway; targeted protein degradation.

DOI 10.1515/hsz-2014-0160

Received March 4, 2014; accepted May 15, 2014

Introduction

For several decades, conditional methods for manipulating genes or their products have been very fruitful in basic biomedical research (e.g., by using temperature-sensitive mutants; Hartwell 1967; Hartwell et al., 1970). In numerous studies, altered phenotypes of systems resulting from an induced absence of a protein's function or, vice versa, from its accumulation *on demand*, have been successfully used. Systems that allow a conditional activation/inactivation of a gene of interest (GOI) or depletion/accumulation of the corresponding protein of interest (POI) helped to shed light on normal cellular functions of the modified components.

Several methods for gene and protein shut-off are available for use in single-cell and multicellular organisms, based on diverse mechanisms of molecular actions. These tools and protocols are – depending on their mode of operation – directed either on the level of transcription, translation, or later. Conditional methods, however, may be able to change the abundance of a POI either completely or partially on demand, i.e., by applying an exogenous trigger or exploiting endogenous processes such as developmental events. These highly useful tools for studying protein function and requirement are so powerful because they – in the ideal case – directly impinge on the pool of functional POI by restricting its presence in its functional form or by removing it from its normal environment.

Established protocols rely on turning on or off transcription or tuning translation of GOIs, and by selectively sequestering, cleaving, or degrading POIs (excellent overviews are given in Nishimura et al., 2009; Taxis et al., 2009; Caussin et al., 2012; further helpful reviews are Prabha et al., 2012, and Kanemaki, 2013). The outstanding advantage of numerous conditional systems is that, ideally, they respond rapidly to the trigger but may also be

*Corresponding author: Nico Dissmeyer, Independent Junior Research Group on Protein Recognition and Degradation, Leibniz Institute of Plant Biochemistry (IPB), Weinberg 3, D-06120 Halle/Saale, Germany; and ScienceCampus Halle – Plant-based Bioeconomy, D-06120 Halle/Saale, Germany, e-mail: nico.dissmeyer@ipb-halle.de

Frederik Faden, Stefan Mielke and Dieter Lange: Independent Junior Research Group on Protein Recognition and Degradation, Leibniz Institute of Plant Biochemistry (IPB), Weinberg 3, D-06120 Halle/Saale, Germany; and ScienceCampus Halle – Plant-based Bioeconomy, D-06120 Halle/Saale, Germany

used reversibly. In multicellular organisms, e.g., sectors on cellular level can be created by eliminating or enhancing POI function in certain tissue or cell types. This can then be used to generate a highly topical effect of the POI which might, for example, be cytotoxic or dominant negative. Under these circumstances, sectors of ‘normal’ development or cellular function neighboring the manipulated area can be induced.

Regulation of POI abundance, or finally POI activity and function, can be accomplished at different levels. Broadly used protocols rely on gene disruption and mutation, RNA interference (RNAi) or artificial micro RNAs (amiRNAs), promoter shut-off, temperature-sensitive alleles, activation or inactivation by small molecules, and several ways of induced protein degradation, which we review here in the following sections.

In many different experimental systems, such as in animals (e.g., Paddison et al., 2002; Boutros et al., 2004; Perrimon et al., 2010) and plants (see this review and references herein), conditional knockout/knockdown systems are controlled at the DNA or mRNA levels. Firstly, we review methods applicable in multicellular organisms with focus on model plant species. Some protocols such as gene deletions are not reversible in many systems, and RNA-mediating protocols or chemical inhibitors often comprise silencing or strong off-target effects, such as in the case of hormones. In plants, many gene disruption (T-DNA) mutants may offer several initially unexpected features, such as read-through or knockdown instead of a complete knockout (Ülker et al., 2008). These can be exploited for example as an allelic series of mutants with varying levels of reduced expression.

Moreover, in many of these conditional systems, protein depletion or accumulation and therefore the desired loss- or gain-of-function is indirect and depends on the translation and maturation speed and half-life of the POI itself. In many cases, a phenotypic response both on the molecular (proteomic) but especially on the macromolecular or developmental level is a slow process. This ‘phenotypic lag’, which may occur between the activation of the conditional system and the emergence or establishment of a relevant phenotype, represents a major limitation (discussed in Varshavsky, 2005). Another frequent problem related to conditional phenotypes is the leakiness of a system that can be caused by residual activity of a POI in its OFF state or between translation and inactivation, its incomplete elimination from its natural context, or a basal activity of the promoters.

In practice, it can be very difficult to achieve these switchable effects in eukaryotes, unless an inhibitor has been developed for the target protein or a recognition

domain described that could be used, e.g., in a proteolysis targeting chimeric molecule (PROTAC) approach (Sakamoto et al., 2001; Schneekloth et al., 2004; Carmony and Kim, 2012) or via mutated chimeric F-box proteins (Zhou et al., 2000, 2005; Zhang et al., 2003; and others; see section ‘Inducible systems for protein destabilization’).

It can be difficult to very selectively induce protein shut-off or function on demand in specific cells or tissues only. This might be required even in a certain developmental stage, especially when working in multicellular organisms. Because of the aforementioned constraints, many conditional systems are applied in order to generate conditional mutants of essential proteins. Most widely, they are used in *Saccharomyces cerevisiae* (budding yeast) as well as in *in vitro* cell cultures of different mammalian or avian origin, see sections ‘Inducible systems for protein destabilization’ and ‘N-end rule-based systems’. They offer powerful tools to control protein expression and induce phenotypes *on demand*. In contrast, the application of these techniques *in vivo* is often difficult or impossible or never leads to published results.

Recently, several more sophisticated systems for induction of transgene expression in multicellular organisms, especially in plants, have been described and successfully applied. A number of gene shut-off tools is broadly applicable *in vitro* and *in vivo* (see the section ‘Classically inducible systems on DNA and mRNA levels’, reviewed in Moore et al., 2006). In plants, inducible systems were used mainly in *Arabidopsis thaliana* (mouse-ear cress, e.g., Love et al., 2000; Zhou et al., 2000; Padidam et al., 2003; Craft et al., 2005), *Nicotiana tabacum* (tobacco, e.g., Gatz et al., 1992; Caddick et al., 1998; Müller et al., 2014), *Oriza sativa* rice (e.g., Ouwerkerk et al., 2001; Kubo et al., 2013), and *Solanum lycopersicum* (tomato) (e.g., Sweetman et al., 2002; Garoosi et al., 2005). A comprehensive list of commonly used approaches and model organisms is given in Table 1.

Several examples given below represent a combinatorial approach, e.g., inducible or cell-type specific promoters controlling either genes for interfering with mRNA stability or leading to a destabilization of chimeric proteins containing degradation cassettes. In our review, we also compare available methods for conditional and non-conditional (constitutive) gene or protein manipulation, which can be used as genetic tools. We give an overview of successful applications of various techniques that are based on different underlying molecular modes of action and influence different levels of a gene’s or a protein’s function, either pre-, co-, or post-translationally. Focus, however, is (i) on the regulation of the actual function of a GOI and thus on the level of the activity of the POI it encodes for, (ii) to link conditional gene/protein shut-on/

off with *in vivo* phenotypes that are the result of manipulating POI abundance and function, and (iii) to discuss advantages of conditional phenotypes (phenotypes *on demand*) in multicellular organisms with focus on plants.

In this section ‘Conclusion and Perspectives’, we discuss the possible combination of several of the mentioned tools that could be used in order to, for example, engineer and target a specific biosynthetic pathway to a compartment, a cell, or a tissue. For example, such a potential ‘cascade’ of intertwined methods can, in our eyes, be realized by using one method to mutate a GOI, a second method to conditionally restore the protein function (in case of, e.g., a developmentally essential function), and a third method to implement a desired biosynthetic pathway. The activity of the latter could be hosted in the mentioned compartments, which serve as pre-defined containments.

Successfully establishing some of these tools, for example in plants, has strong potential not only for basic research and applications in genetics and cell biology but also for biotechnology.

Classically inducible systems on DNA and mRNA levels

One possibility to regulate the abundance of a POI in eukaryotic cells is to control its expression on the DNA or mRNA level, e.g., via inducible gene expression systems or post-transcriptional gene silencing. Inducible systems allow the regulation of expression levels at particular developmental stages or in particular tissues of interest, and eventually in specific cells only. Ideally, these on demand methods allow the promotion of local changes in expression levels without causing gross alterations to the entire individual, if applied in multicellular organisms such as in plants.

In the field of inducible gene expression systems, chemically inducible protocols are very relevant today. For successful application, they need to fulfill certain conditions, as they should be characterized by (i) no or a very low basal expression level preceding induction (leakiness), (ii) a high specificity of the inducer, (iii) a strong induction below toxic levels of the inducer, (iv) absence of endogenous inducer analogs or related compounds, (v) a simple application of the inducing agents, and (vi) a rapid transcriptional and/or translational response after treatment.

In plants, chemically inducible expression systems are generally based on transcriptional activation, although there are some systems mediating de-repression and inactivation of gene transcription. All these systems consist of two transcription units (Figure 1A). The first one is a

chimeric, chemical-binding transcription factor, mostly under control of a constitutive promoter, e.g., the cauliflower mosaic virus (CaMV) 35S promoter (35S). The second component is a minimal plant promoter, which is usually a truncated 35S promoter, containing multiple transcription factor binding sites to control the expression of the GOI. The chimeric transcription factor can then activate or inactivate transcription by the promoter, but only after induction by the respective chemical. Since the early 1990s, many chemically inducible systems have been characterized and successfully applied in different species (Table 1).

Tetracycline

A first de-repressive system was developed using the bacterial Tet repressor protein (TetR). This binds to the *tet*-operator (*tetO*) in absence of the antibiotic tetracycline and thereby prevents target gene expression by repressing the promoter. By supplying tetracycline, the promoter can be de-repressed resulting in expression of the GOI (Gatz et al., 1992). However, the system has its drawbacks and limitations that prevented widespread use, one being the limited half-life of tetracycline. Although the TetR system can be successfully used in *Nicotiana tabacum*, it has not yet been shown to work reliably in other plant species such as *Arabidopsis*. In another approach, the TetR repressor was converted into an activator by fusing it with an activation domain of the *Herpes simplex* virus protein 16 (VP16). The obtained tTA (tetracycline transactivator) system mediates tetracycline-induced inactivation of transgene expression in tobacco (Weinmann et al., 1994). Again, one limiting factor is the instability of tetracycline. That is why it is crucial to apply fresh inducer frequently in order to prevent gene expression.

Copper

Most chemically inducible expression systems in plants are based on transcriptional activation. One of the first activation systems described was the copper-inducible ACE1 (activating copper-metallothionein expression 1) system based on the ACE1 transcription factor of *S. cerevisiae* metallothionein (Mett et al., 1993). However, this system was reported to be not effective in plants, as it failed to induce green fluorescent protein (GFP) expression in the tobacco standard cell line BY-2 (Granger and Cyr, 2000). Recently a promising improvement of the system was reported by both fusing ACE1 to the VP16 activation domain in order to increase expression efficiency, and by insertion of the

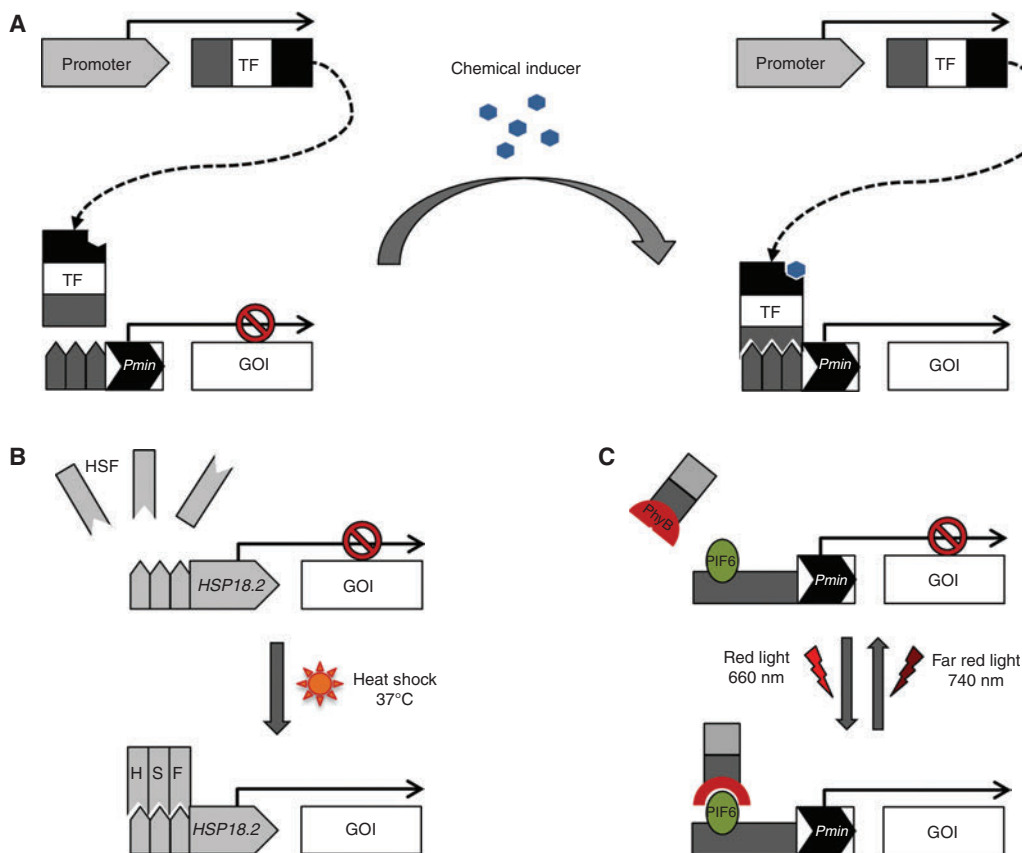


Figure 1 Simplified scheme of different inducible gene expression systems for plants.

(A) Most chemically inducible gene expression systems are based on chimeric transcription factors (TF), which comprise a DNA-binding and a chemical-binding site and controlled by either a constitutive (e.g., the strong cauliflower mosaic virus (CaMV) 35S promoter) or a cell- or tissue-specific promoter. The gene of interest (*GOI*) is usually under control of a plant minimal promoter (*Pmin*) that contains multiple transcription factor binding sites. The TF can activate the *Pmin* and therefore the transcription of the *GOI* but only after induction via the respective chemical/small-molecule inducer. (B) The heat-shock inducible gene expression system using the *HSP18.2* promoter is based on the widely conserved heat-shock response in living cells. Transcription of the *GOI* is induced by a heat-shock, resulting in the trimerization of endogenous plant heat-shock factors (HSF), which then activate the *HSP18.2* promoter. (C) A chimeric split transcription factor containing PHYTOCHROME B (PHYB) and the PHYTOCHROME-INTERACTING FACTOR 6 (PIF6), both expressed under the control of CaMV 35S, is the basis of the red light responsive gene expression system. Red light illumination activates PhyB and induces heterodimerization with PIF6, which results in activation of *Pmin* and transcription of the *GOI*. The process can be reversed via illumination with far-red light.

To71 sequence of tomato mosaic virus upstream of the *GOI* to reduce basal expression (Saijo and Nagasawa, 2014). As copper is a naturally occurring trace element in the soil, the applicability of this system remains limited. In addition, increased concentrations of copper are highly cytotoxic when accumulated in plant tissues.

Hormones

Another way to achieve chemically regulated transgene expression is the use of hormone receptor-based systems

by application of dexamethasone (DEX), β -estradiol or ecdysone analogs. Some of these make use of the ligand-binding domain of the rat glucocorticoid receptor (GR) and are induced by the glucocorticoid dexamethasone. Currently, two major systems of relevance exist: i) the GVG system (GAL4-VP16-GR), where the GAL4 DNA-binding domain is fused to the VP16 activation domain and to GR (Aoyama and Chua, 1997), and ii) the LhGR system (LacI-GAL4-GR), where the *Escherichia coli* lac repressor is fused to the yeast GAL4 transactivation domain and GR (Craft et al., 2005). Although there is a widespread use of both systems, it is noteworthy that dexamethasone can cause

Table 1 Inducible systems in plants and examples for conditional phenotypes.

System	Inducer	Applied in ^a	Reference(s)	Induction speed ^b	Conditional phenotype ^c
De-repressible TetR	Tetracycline	<i>N. tabacum</i>	Gatz et al. (1992)	48 h mRNA (<i>N. tabacum</i>)	n.a.
Inactivatable tTa	Tetracycline	<i>N. tabacum</i> <i>Arabidopsis</i>	Weinmann et al. (1994) Love et al. (2000)	1 h mRNA decrease (<i>N. tabacum</i>)	n.a.
Activatable ACE1	Copper (Cu ²⁺)	<i>N. tabacum</i> <i>Arabidopsis</i>	Mett et al. (1993) Saijo and Nagasawa (2014)	1 h mRNA (<i>Arabidopsis</i>)	Floral induction in <i>Arabidopsis</i> [Saijo and Nagasawa (2014)]
GVG	Dexamethasone	<i>Arabidopsis</i> <i>N. tabacum</i> <i>Lotus japonicus</i> [legume (Fabaceae)] <i>Oryza sativa</i> (rice)	Aoyama and Chua (1997) Andersen et al. (2003) Ouwkerk et al. (2001)	3 h mRNA [<i>Arabidopsis</i> ; Moore et al. (2006)]; 1 h mRNA (<i>N. tabacum</i>)	Floral induction system [Gómez-Mena et al. (2005); Wellmer et al. (2006)]
LhGR	Dexamethasone	<i>Arabidopsis</i> <i>N. tabacum</i>	Craft et al. (2005) Samalova et al. (2005)	2 h mRNA (<i>Arabidopsis</i>); 1 h mRNA (<i>N. tabacum</i>)	Control of cutin biosynthesis in <i>Arabidopsis</i> [Kannangara et al. (2007)]
AlcR	Ethanol/ Acetaldehyde	<i>N. tabacum</i> <i>Arabidopsis</i> <i>Solanum lycopersicum</i> (tomato) <i>Solanum tuberosum</i> (potato) <i>Brassica napus</i> (rapeseed/ oilseed rape)	Caddick et al. (1998) Roslan et al. (2001) Garooosi et al. (2005) Sweetman et al. (2002)	1–2 h mRNA [<i>Arabidopsis</i> ; Moore et al. (2006)]	Manipulation of carbon metabolism in <i>N. tabacum</i> [Caddick et al. (1998)]
GVGE	Tebufenozide/ methoxyfenozide	<i>N. tabacum</i>	Martinez et al. (1999)	~5 h GUS activity (no information on mRNA or protein levels)	n.a.
GVE	Tebufenozide/ methoxyfenozide	<i>Arabidopsis</i> <i>N. tabacum</i> <i>S. lycopersicum</i>	Padidam et al. (2003) Gallie (2010)	n.a.	Regulation of fruit ripening in <i>S. lycopersicum</i> [Gallie (2010)]
VGE	Tebufenozide/ methoxyfenozide	<i>Arabidopsis</i> <i>Brassica juncea</i> (leaf mustard)	Koo et al. (2004) Yang et al. (2012)	6 h mRNA (<i>Arabidopsis</i>)	n.a.
XVE	β-estradiol	<i>Arabidopsis</i> <i>N. tabacum</i> <i>S. lycopersicum</i> <i>O. sativa</i> <i>Physcomitrella patens</i> [moss (bryophyte)]	Zuo et al. (2000) Pedley and Martin (2004) Sreekala et al. (2005) Kubo et al. (2013)	0.5 h mRNA (<i>Arabidopsis</i>)	Lobed leaf formation in <i>Arabidopsis</i> [Brand et al. (2006)]
HSP18.2	Heat shock (37 °C)	<i>Petunia</i> <i>Arabidopsis</i> <i>N. tabacum</i> cell culture (cultivar Bright Yellow-2 BY-2) of the tobacco plant	Takahashi and Komeda (1989) Takahashi et al. (1992) Yoshida et al. (1995)	0.25 h mRNA (<i>N. tabacum</i> , BY-2 cells)	Induced photobleaching and growth arrest in <i>Arabidopsis</i> [Masclaux et al. (2004)]
PhyB/PIF6	Red light	<i>N. tabacum</i> <i>P. patens</i>	Müller et al. (2014)	~ 5 h LUC activity (<i>N. tabacum</i>)	n.a.

^aOnly a few examples are given here; ^bFor *Arabidopsis thaliana* and *Nicotiana tabacum*, if mentioned in the reference(s); n.a. not indicated; ^cn.a.; only data for artificial reporter systems available such as GFP or GUS.

growth defects in plants and induce defense-related genes (Kang et al., 1999). Furthermore, when using the LhGR system, crossings of activator lines with reporter lines are required.

As another alternative there is a system available that is based on the human estrogen receptor (ER). The XVE system (LexA-VP16-ER) is driven by a chimeric transcription factor, where the ER is fused to the DNA-binding domain of the bacterial repressor LexA and to the VP16 activation domain (Zuo et al., 2000). The XVE is activated at low concentrations of the human steroid hormone β -estradiol. Phytoestrogens are not reported to be able to activate the system in *Arabidopsis*, while in soy bean unspecific activation was observed (Zuo and Chua, 2000). Both of these inducers, dexamethasone and β -estradiol, are steroids, which need to be used in a controlled environment. Thus these systems are not suitable for field application.

In addition to the examples described before, there are systems exploiting the ligand-binding domain of the ecdysone receptor (EcR) from *Heliothis virescens*. GOI expression in these systems is induced by non-steroidal ecdysone analogues like methoxyfenozide or tebufenozide, therefore they are promising candidates for field application. Currently there are three different systems, which are i) the GVGE system (GR^{act}-VP16-GR^{bind}-EcR), where the EcR is fused to the binding and activating domains of the human GR and the VP16 activation domain (Martinez et al., 1999), ii) the GVE system (GAL4-VP16-EcR), where the EcR is fused to VP16 and the GAL4 DNA-binding domain (Padidam et al., 2003), and iii) the VGE system (VP16-GAL4-EcR), representing a reconfigured version of the GVE system (Koo et al., 2004).

Ethanol

The AlcR transcription factor and its responsive promoter *alcA* from the filamentous fungus *Aspergillus nidulans* are utilized to control the expression of target genes in plants using ethanol as an inducer (Caddick et al., 1998). As ethanol is readily available, cheap, easily supplied to plants and rapidly taken up, this system has many advantages and is widely used in different plant species. Ethanol can be supplied via soil drenching and foliar spraying (Salter et al., 1998), as well as using ethanol vapor (Roslan et al., 2001; Sweetman et al., 2002). However, higher ethanol concentrations during induction have to be avoided, as it is cytotoxic. Because of the volatility of ethanol, a localized induction of the AlcR system is difficult and can rather be achieved by using acetaldehyde

as an inducer, as shown in transgenic tobacco plants (Schaarschmidt et al., 2004). The inducer of the AlcR system is in fact acetaldehyde, which is a product of the ethanol metabolism. Acetaldehyde is also formed during low oxygen conditions, which is why it can also act as an endogenous inducer of the AlcR system in cell suspension cultures (Roberts et al., 2005).

Nonchemical inducers

Apart from chemically inducible gene expression, there are also many systems that are induced by other stimuli or stresses (Table 1). One example is the heat-inducible expression system using the *HSP18.2* promoter of *Arabidopsis* (Takahashi and Komeda, 1989), which has been used successfully in different plant species. The system exploits the heat-shock response, which is highly conserved in living cells. Under normal growth conditions, the promoter is repressed. In order to activate the promoter and induce gene expression, a brief heat shock of 37°C is necessary (Figure 1B). After induction, plants have to be returned to lower temperature, as ongoing heat-shock stress can cause for example male sterility in *Arabidopsis* (Kim et al., 2001). As this system requires a specific temperature for induction, it remains limited to be used in a controlled environment.

Yet another approach using red light as an inducer was recently described (Müller et al., 2014). This system is based on the phytochrome B (PhyB) and the phytochrome-interacting factor 6 (PIF6), which interact in a red/far-red light-dependent manner and are both part of a synthetic split transcription factor (Figure 1C). The resulting synthetic switch is able to induce gene expression under red light conditions (660 nm) as well as to induce transcriptional shut-off under far-red light conditions (740 nm).

Downstream effectors reducing gene expression

Inducible gene expression systems can also be used to exploit the biological process of RNA interference (RNAi), in which small RNA molecules inhibit gene expression by triggering the degradation of homologous mRNA. These small RNAs are referred to as silencing RNAs (sRNAs), which include small interfering RNAs (siRNAs) and microRNAs (miRNAs). In plants, conditional RNAi can be achieved by expressing a hairpin RNA (hpRNA)-encoding transgene under the control of a chemically inducible gene expression system. After induction, a double-stranded RNA molecule is obtained

and processed into siRNAs which target degradation of the respective mRNA. The first construct for chemically inducible RNAi was developed from the β -estradiol-inducible XVE system and tested in *Arabidopsis* (Guo et al., 2003). Furthermore, inducible RNAi was successfully used via the dexamethasone inducible LhGR system (Wielopolska et al., 2005), the ethanol inducible AlcR system (Chen et al., 2003; Ketelaar et al., 2004), the methoxyfenozide inducible VGE system (Dietrich et al., 2008), as well as the heat-shock inducible *HSP18.2* system (Masclaux et al., 2004). Another example for conditional RNAi techniques are artificial micro RNAs (amiRNAs), which can specifically target genes activity after induction. A first inducible amiRNA system for *Arabidopsis* was based on the ethanol inducible AlcR system (Schwab et al., 2006).

Tissue and cell-type specific expression

Because of the use of constitutive promoters, most inducible systems described above are ubiquitously active in the plant. Under certain circumstances, a POI needs to be expressed in a specific tissue or cell type. Another reason is that constitutive misexpression of RNAi and related strategies can mask tissue-specific effects, cause cell death or lead to other severe developmental defects. A solution is to use cell- or tissue-specific promoters, which are only active in specific types of tissues or cells, such as leaf hair (trichome) cells. As it is highly desirable to control gene expression spatially as well as temporally, it would be useful to combine a cell-/tissue-specific promoter with an inducible gene expression system. However, GOIs in these systems are usually under the control of a plant minimal promoter containing the essential transcription factor binding sites. Therefore a remaining possibility is to clone the transcription factor itself under the control of a tissue- or cell-specific promoter. Such systems were reported to work successfully in *Arabidopsis* when cloning the ethanol inducible AlcR transcription factor under the control of different tissue-specific promoters such as those of *LEAFY (LFY)*, *UNUSUAL FLOWER ORGANS (UFO)*, and *CLAVATA3 (CLV3)*; Deveaux et al., 2003; Maizel and Weigel, 2004). Furthermore this strategy was also successfully applied to the XVE system in *Arabidopsis* (Brand et al., 2006) as well as to the VGE system in both *Arabidopsis* and *Brassica juncea* (Yang et al., 2012). In plant research, a variety of cell- and tissue-specific promoters has been described, but it is noteworthy that many of these promoters are not necessarily exclusively active in one single-cell type or tissue. Mostly, they have also minor activity in other cells or tissues, which is important to consider when, for example, expressing toxic proteins.

Combinatorial approaches for tissue or cells on demand

Tissue or developmental stage specific promoters or inducible promoters can also be used to drive POIs, causing a switch in an entire developmental signaling cascade. An excellent example for this is the floral induction system (Gómez-Mena et al., 2005; Wellmer et al., 2006). In a well-described example, *Arabidopsis* transcription factor *APETALA1 (AP1)*, which controls the onset of flower development, was translationally fused to the hormone binding domain of the rat GR and transformed into the loss-of-function *ap1 cauliflower* double mutant (Wellmer et al., 2006; Ó'Maoiléidigh et al., 2013). *CAULIFLOWER (CAL)* is an AP1 paralog. Induction with dexamethasone activates the function of the AP1-GR fusion protein by mediating its relocation into the nucleus. The subsequent phenotype is a massive formation of inflorescence-like meristems a few days after treatment. This method has been used successfully in genomic and proteomic approaches (Wellmer et al., 2006). A similar protocol was developed using the homeotic gene *AGAMOUS (AG)* instead of AP1 in a GR fusion protein (*AG-GR*) in *ap1 cal* mutants (Gómez-Mena et al., 2005). This also led to steroid-inducible stamen and carpel development.

A second example for tissue formation on demand is conditional trichome induction. In *Arabidopsis*, wildtype trichomes are single-celled with large endoreplicating nuclei comprising a high metabolic activity (Schillmiller et al., 2008). Misexpression of *CYCLIN B1;2* under control of the trichome-specific *GLABRA2 (GL2)* promoter induces mitotic divisions which results in the formation of trichome clusters and multicellular trichomes (Schnittger et al., 2002). Overexpression of *MIXTA*, an MYB-related regulator controlling conical cell formation in snapdragon (*Antirrhinum majus*), or *MIXTA*-like genes trigger enhanced trichome formation in *Antirrhinum* (Glover et al., 1998), tobacco (Payne et al., 1999), woody nightshade (*Solanum dulcamara*; Glover et al., 2004), and petunia (*Petunia hybrida*; Avila et al., 1993). In tomato (*Solanum lycopersicum*), the mutation *Woolly (Wo)* induces enhanced trichome formation (Yang et al., 2011) and trichomes can be induced by misexpressing cotton (*Gossypium arboreum*) *GaMYB2* in normally glabrous, trichome-free *Arabidopsis* seeds (Wang et al., 2004). A remarkable, albeit not yet conditionally tested, trichome induction occurs in *Arabidopsis* triple mutants lacking the function of the small MYB proteins and trichome initiation factors *ENHANCER OF TRY AND CPC1 (ETC1)*, *TRIPTYCHON (TRY)*, and *CAPRICE (CPC)*; Kirik et al., 2004). A mutation for *etc1* can be replaced by *etc2* or *etc3* and still leads to a dramatic

overproduction of trichomes covering the entire upper leaf surface (Wester et al., 2009).

Summarizing the systems described here for protein expression control at DNA/mRNA level, we can state that on the one hand most of them are able to tightly control temporal and spatial protein accumulation and therefore are potential tools for generating conditional phenotypes (see Table 1 for examples); while on the other hand, protein depletion and thus the loss of protein function, which is mostly critical to the user, are not actively regulated and the time for POI depletion depends on its *in vivo* half-life. Thus, POI abundance can only be indirectly modulated by downstream gene expression and, in order to overcome this limitation, protein accumulation and depletion rather need to be controlled at protein level to allow a rapid change in phenotypes. Several widely used approaches are discussed in the following.

Inducible systems for protein destabilization

In this section, we will discuss and compare different amino acid tags as degrons derived from different organisms that are not related to a specific N-terminal or C-terminal protein recognition and degradation mechanism. A ‘degron’ (Varshavsky, 1991) is a sequence, a motif or a domain that can be recognized by the protein degradation machinery and is therefore sufficient for the recycling of the respective substrate. It can be constitutively active, dormant, or regulated in a cell-type or -phase specific fashion. Degron establishment may also involve post-translational processing such as phosphorylation or proteolytic cleavage or other conformational transitions. Its function is independent of the protein it is attached to, and this is its central property exploited in the following methods.

Auxin-inducible degron

The mechanisms by which different eukaryotic cells and organisms induce protein degradation are very diverse, therefore several of these pathways have been exploited for conditional protein knockdown methods. One frequently used approach is the auxin-inducible degron (AID; Figure 2; Table S1; Nishimura et al., 2009). It is based on the response signaling to the plant hormone auxin (indole-3-acetic acid or IAA), which includes the destruction of a transcriptional repressor of auxin response factors, called

IAA17 (Gray et al., 2001). Upon binding of auxin to TRANSPORT INHIBITOR RESPONSE1 (TIR1), a subunit of the SCF (Skp-Cullin1-F-Box) E3 ubiquitin (Ub) ligase complex, TIR1 binds to IAA17 to recruit it to the SCF E3 Ub ligase complex, which triggers its quick polyubiquitinylation followed by proteasomal degradation. Nishimura et al. (2009) transplanted TIR1 firstly into *S. cerevisiae* and fused IAA17 to a POI, which altogether induces its degradation upon addition of auxin acting as a molecular glue very similar to its natural function in hormone sensing by facilitating the assembly of the SCF E3 ubiquitin ligase complex. This general mechanism has been demonstrated to be portable into a number of different non-plant organisms, albeit only on an *in vitro* cell culture level and in single-celled organisms (Table 2), as the SCF E3 Ub ligase complexes and their components are widely conserved in eukaryotes. Limitations noted by the authors were possible cytotoxicity, i.e., membrane and DNA damage of auxin when oxidized by peroxidases (Folkes et al., 1999), and the difficulty of manipulating an endogenous essential GOI when homologous recombination is not feasible.

Naturally, because of its origin, this system cannot be used in plants as it can be used in other organisms. However, it might prove useful for tracking endogenous hormone levels in a cell or tissue-specific manner by measuring the stability of a reporter-degron fusion protein.

JAZ1 degron

Another recently developed approach is based on the sensing mechanism of the plant hormone jasmonate, which is quite similar to the auxin sensing described above. Here, (3R,7S)-jasmonoyl-L-isoleucine (JA-Ile) functions as a molecular glue between the F-box protein CORONATINE INSENSITIVE 1 (COI1) and the transcription repressor JASMONATE ZIM-DOMAIN 1 (JAZ1). These factors, and inositol pentakisphosphate (InsP5) as a cofactor, form the jasmonate sensing complex that triggers recruitment of JAZ1 to the SCF E3 Ub ligase complex and its subsequent polyubiquitinylation and proteasomal degradation (Chini et al., 2007; Thines et al., 2007; Yan et al., 2007). A short C-terminal peptide from JAZ1 is sufficient to obtain formation of the complex (Table 2; Table S1; Sheard et al., 2010). This peptide can serve as a tag to induce temporally controlled degradation of a fused POI. As for the AID system, heterologous COI1 expression and administration of JA-Ile and InsP5 is required to trigger degradation. The advantageous fact as highlighted by the authors is the small size of the degradation tag (3.2 kDa compared to 27 kDa of the IAA17 protein). The JAZ1 degron has so far

DE GRUYTER

F. Faden et al.: On demand phenotypes by conditional protein expression — 745

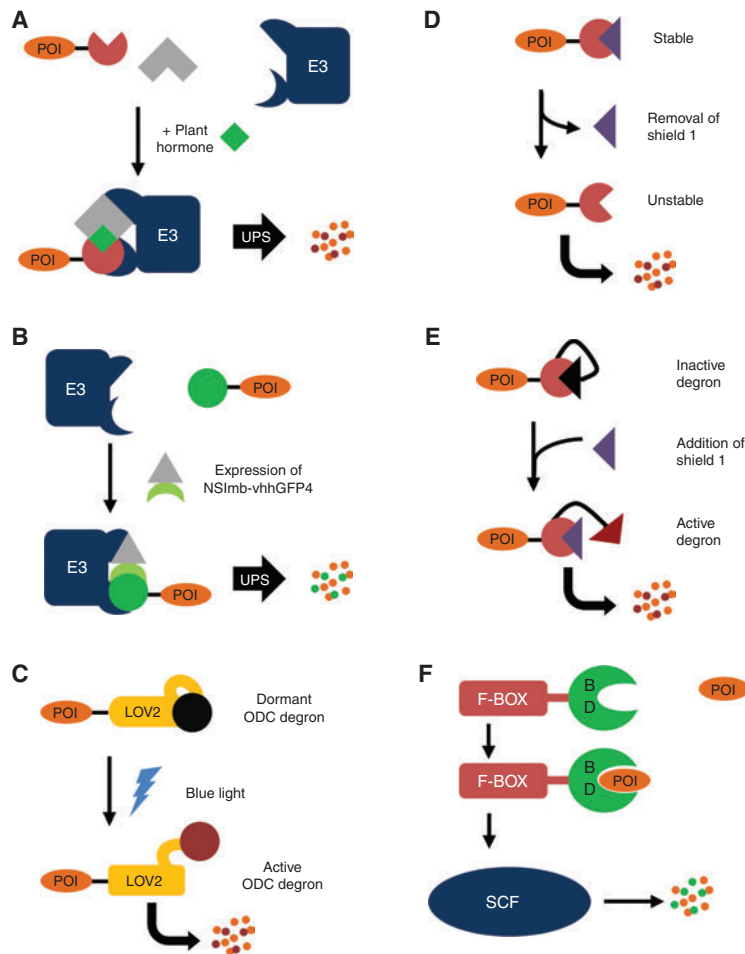


Figure 2 Schematic representations of (inducible) systems for protein destabilization.

(A) AID and JAZ1 system. Addition of the respective plant hormone (green) triggers the recruitment of the degron (red) to the E3 Ub ligase via a scaffold protein (gray), which leads to target protein degradation via the UPS. (B) deGradFP. GFP (green) is recognized by an anti-GFP antibody fragment (light green) fused to Slmb (gray), a scaffold protein which recruits the GFP-target protein fusion to an E3 Ub ligase. (C) Photosensitive degron. The LOV2 domain masks the cODC degron unless it undergoes a conformational change triggered by blue light. (D) and (E) DD- and LID-FKBP system. Addition of Shield 1 (violet triangle) stabilizes DD-FKBP (red), while it destabilizes LID-FKBP. (F) Modified F-box proteins. A binding domain (BD) fused to an F-box protein recruits an endogenous protein to the SCF complex.

been characterized concerning its affinity to COI1 in the presence of coronatine, a jasmonate analog from the plant pathogen *Pseudomonas syringae*. Its feasibility in fusion with a reporter protein in *S. cerevisiae* and its degradation kinetics are currently still to be investigated.

Degrade green fluorescent protein (deGradFP)

A similar, though more unconventional method is the deGradFP system. Here, a GFP moiety has been turned

into a degron. The F-box domain of Slmb, a *Drosophila* F-box protein, was fused to a single-domain antibody fragment (Table S1; Caussin et al., 2012). Upon expression of this fusion protein named NSlmb-vhhGFP4, it recognizes the GFP moiety of a GFP-POI fusion protein (Figure 2). Then, the GFP-POI fusion protein is recruited to SCF E3 Ub ligase complex, polyubiquitinated, and degraded. The universality and efficiency of this system has been proven in human HeLa cells as well as *Drosophila* cell culture and entire embryos. It should therefore be possible to establish this system in a plant model as well. In addition, as degradation is induced by heterologous

Table 2 Portable systems for targeted protein degradation.

System	Nature of degron (molecular weight)	Inducer	Applied in (organism and conditional phenotype)	N- or C-terminal fusion	Time required for degradation (reference and species)
Auxin-inducible degron (AID)	AUX/IAA-ARF domain of rice IAA17 (27 kDa)	Auxin	<ul style="list-style-type: none"> – <i>S. cerevisiae</i> [cell-cycle defective; Nishimura et al. (2009); Watase et al. (2012)] – <i>S. pombe</i> [DNA replication and cell-cycle defective; Kanke et al. (2011)] – mammalian and vertebrate cells [cell-cycle defective; Nishimura et al. (2009)] – Human cells [cell-cycle and chromosome maintenance defective; Nishimura et al. (2009); Holland et al. (2012)] – <i>P. falciparum</i> [Kreidenweiss et al. (2013)] 	Both	>30 min [Nishimura et al. (2009), in all species used]
DD-FKBP	Human FKBP with F36V and L106P (12 kDa)	Removal of Shd1	<ul style="list-style-type: none"> – Mouse and human cells [cell-cycle defective, cell morphology; Banaszynski et al. (2006)] – Living mice [tumor reduction, muscle dystrophy, alteration of fatty acid metabolism; Banaszynski et al. (2008); Berdeaux et al. (2007); Rodriguez and Wolfgang (2012)], – <i>Toxoplasma gondii</i> [growth defect; Herm-Götz et al. (2007)] – <i>Plasmodium falciparum</i> [swollen food vacuole; Armstrong and Goldberg (2007)] 	Both	4 h [Banaszynski et al. (2006), mouse NIH3T3 cells]
LID-FKBP	Human DD-FKBP with an additional C-terminal 19-AA-peptide (red, 13 kDa)	Addition of Shd1	<ul style="list-style-type: none"> – Mouse NIH3T3 cells [reprogramming into pluripotent cells; Bongner et al. (2011)] 	C-terminal	2–3 h [Bongner et al. (2011), NIH3T3 mouse cells]
deGradFP	GFP (27 kDa)	Expression of modified F-box protein NSlmb-vhhGFP4	<ul style="list-style-type: none"> – Human HeLa cells, <i>Drosophila melanogaster</i> cells and embryos [defects in dorsal closure and wing formation; Caussinus et al. (2012)] 	Both	2.5 h [Caussinus et al. (2012), <i>Drosophila</i> embryos]
Photosensitive degron	<i>Arabidopsis</i> LOV2-cODC1 (20 kDa)	Blue light	<ul style="list-style-type: none"> – <i>S. cerevisiae</i> [cell-cycle defective, adenine auxotrophy; Renicke et al. (2013a)] 	C-terminal	1.5–2 h [Renicke et al. (2013a), <i>S. cerevisiae</i>]
JAZ1-degron	<i>Arabidopsis</i> JAZ1 peptide, Sheard et al. (2010)	JA-ile	To be reported	To be reported	To be reported
Cyclin destruction boxes (DBs)	N-terminal domain e.g., from tobacco CYCLIN B1;1, Genschik et al. (1998)	None (exposure sufficient) and passage through mitosis, is stable before and until G2/M-phase transition of the cell-cycle	– <i>Arabidopsis</i> [Schmittger et al. (2002); Jakoby et al. (2006)]	Both	n.a.

(Table 2 Continued)

System	Nature of degron (molecular weight)	Inducer	Applied in (organism and conditional phenotype)	N- or C-terminal fusion	Time required for degradation (reference and species)
cODC1	37 C-terminal residues	None (exposure sufficient)	– <i>S. cerevisiae</i> [Jungbluth et al. (2010); Renicke et al. (2013a)]	C-terminal	2–4 h [<i>S. cerevisiae</i> ; Jungbluth et al. (2010)]
New York 1 virus (NY-1V) glycoprotein G1 tail	30 residues hydrophobic C-terminal domain	None (exposure sufficient)	– African green monkey, <i>Cercopithecus aethiops</i> , fibroblast-like kidney cells, COS7; Geimonen et al. (2003); Sen et al. (2007)]	C-terminal	n.a.
Andes virus (ANDV) glycoprotein G1 tail	30 residues hydrophobic C-terminal domain	None (exposure sufficient)	– COS7 cells [Sen et al. (2007)]	C-terminal	n.a.
Hantaan virus (HTNV) glycoprotein G1 tail	30 residues hydrophobic C-terminal domain	None (exposure sufficient)	– COS7 cells [Sen et al. (2007)]	C-terminal	n.a.
Mutated Prospect Hill virus (PHV) glycoprotein G1 fragment	30 residues hydrophobic C-terminal domain	None (exposure sufficient)	– COS7 cells [Sen et al. (2007)]	C-terminal	n.a.
RESISTANCE TO <i>P. SYRINGAE</i> PV <i>MACULICOLA</i> 1 (RPM1) INTERACTING PROTEIN 4 (RIN4)	First 30 amino acids of wildtype RIN4	None (exposure sufficient)	– <i>Nicotiana benthamiana</i> (close relative of tobacco, used mainly for transient expression systems by leaf transformation) – GFP fluorescence in epidermal cells of <i>N. benthamiana</i> leaves bombarded with RIN4-30N:GFP after addition of bacterial protease AvrRpt2 from the plant pathogen <i>Pseudomonas syringae</i> [Takemoto and Jones (2005)]	N-terminal	n.a.
Group VII ETHYLENE RESPONSE FACTORS (ERFs)	First seven amino acids including a Met-Cys N-terminal	None (exposure sufficient)	– <i>Arabidopsis</i> , <i>Hordeum vulgare</i> [Barley, Gibbs et al. (2014)]	N-terminal	n.a.

expression of a protein, there are many possibilities for the precise method of induction. Caussin et al. (2012) even succeeded in resolving the dorsal closure in *Drosophila* embryos in greater detail by activating the degradation of Sqh, the myosin II regulatory light chain, cell- and tissue-specifically.

DD-FKBP – Shield-1 system

Yet another approach has been pursued by Banaszynski et al. (2006), who mutated the human FK506 binding protein 12 (FKBP12) until they found a version that was constitutively unstable. This degradation domain (DD) was found to also confer instability to any other POI fused to it. Stabilization of the protein occurs after addition of Shield-1, a derivative of the immunosuppressant drug rapamycin (Banaszynski et al., 2006). Shield-1 is membrane permeable and its control of FKBP abundance is rapid and concentration dependent and therefore well tunable. Although it has already been applied in a wide range of organisms (mouse, human, *Plasmodium* and *Toxoplasma*; Table 2 and references therein), it has been shown that it does not work in *S. cerevisiae* (Rakhit et al., 2011). Its applicability in plants remains to be elucidated.

LID-FKBP

A modification of the DD-FKBP system is LID (ligand-induced degradation)-FKBP. Bongers et al. (2011) discovered an additional 19 amino acid peptide that, when fused to the C-terminus of DD-FKBP, occupies the Shield-1 binding site via intramolecular binding in the absence of the ligand (Table S1, additional peptide sequenced highlighted in bold). When Shield-1 is added, it replaces the peptide in its binding site, and thereby unmasks the degron activity of the peptide. In this way, the role of Shield-1 could be reversed in comparison to the original system, meaning that its administration confers instability, rather than stability, to the fusion protein. The artificial peptide can also be used as a degradation tag independent from FKBP and was found to trigger rapid and efficient ubiquitylation (Table 2, Melvin et al., 2013).

Photosensitive and light-dependent degrons

Renicke et al. (2013) developed a system that depends on a much more common factor: light. LOV2 (LIGHT OXYGEN

VOLTAGE 2) is a domain of *Arabidopsis* PHOTOTROPIN 1 (PHOT1) which activates the kinase domain of PHOT1 upon irradiation with blue light (Christie et al., 2002). This includes a conformational change of the LOV2 domain (Harper et al., 2003), a property that has already been exploited in a wide variety of experiments to manipulate protein synthesis or the conformational or chemical state of proteins (Mills and Truong, 2013). The authors of this method could show that this conformational change can be used to unmask a cryptic degron derived from mODC [mouse ornithine decarboxylase (Renicke et al., 2013a)]. mODC contains a CysAla-motif in its 37 C-terminal amino acid degradation signal composed of residues 425–461 at its C-terminal (cODC; Table 2; Table S1), which confers instability to the protein via its Ub-independent association to the 26S proteasome complex, whereas the identity of the other amino acids within the degron is irrelevant (Takeuchi et al., 2008). mODC was shown to have an extremely short half-life of 12 min (Dice and Goldberg, 1975).

In *S. cerevisiae*, the system used originally, it provides effective depletion of a protein and very tight control over a corresponding phenotype, which, for example, made it even possible to capture an image on a cell layer of a conditional *ade2*-mutant strain. Here, the conditional depletion of Ade2 resulted in the likewise conditional accumulation of an intermediate product of purine metabolism forming a red pigment. However the kinetics of the system were reported to be not as rapid as e.g., for the AID technique.

Destruction boxes of mitotic cyclins

For a mitotic cell-cycle, the anaphase promoting complex/cyclosome (APC/C), an E3 Ub ligase complex composed of more than ten subunits, is of crucial importance (Carroll and Morgan, 2002, Passmore et al., 2003). APC/C has a fundamental role in separation of chromosomes and exit from mitosis (Peters, 2006; Pesin and Orr-Weaver, 2008) as it facilitates the degradation of mitotic cyclins. These are complex partners of cyclin-dependent kinases (Cdks) and confer substrate specificity, whereas the Cdk itself is the active subunit required for phosphotransfer (Dissmeyer et al., 2007, 2009; Dissmeyer and Schnittger, 2011). Thus, cyclin degradation contributes to the establishment of a phase of low Cdk activity and is accomplished by APC/C which is able to mediate the degradation of destruction (D)-box-containing substrates such as cyclin B (Fang et al., 1999; Pesin and Orr-Weaver, 2008). It has been shown that the D-box pathway is conserved in plants (Genschik et al., 1998).

If an N-terminal fragment of a mitotic cyclin such as CYCLIN B1;1 (CYCB1;1), containing the destruction box (DB) motif, is grafted onto otherwise stable proteins such as β -glucuronidase (GUS) or yellow fluorescent protein (YFP), those become unstable in late mitosis because they are recognized as a substrate for APC/C and marked for the rapid degradation by the 26S proteasome. For cloning, parts of the genomic coding sequence of CYCB1;1 can be used which are translated into a small fragment containing the nine residues RQVLGDIGN, which represent the actual DB motif (Table S1; Jakoby et al., 2006). In previous studies, DB-fusions have been successfully applied to monitor a dynamic expression pattern. Chimeric reporter proteins such as Cyclin B-DB:GUS or YFP:DB allow monitoring of the transcriptional activity and the dynamics of the promoter with a high temporal and spatial resolution. For instance, it was shown that after GUS staining, a ProCYCB1;2::DB:GUS fusion has the characteristic ‘salt and pepper’ expression pattern of a cell-cycle-regulated gene, i.e., a patchy pattern of reporter signal due to cell-cycle dependent protein degradation (Schnittger et al., 2002). Thus, a YFP:DB fusion allows the *in vivo* analysis of promoter activity with a high temporal resolution because the carry-over of the reporter to the daughter cells after mitosis is precluded (e.g., King et al., 1996; Genschik et al., 1998; Schnittger et al., 2002). A ProCDKA;1::YFP:DB has successfully served as positive control showing the *in planta* action of the proteasome inhibitor MG132 (Jakoby et al., 2006). To exclude that the addition of the CYCB1;1 part affects the properties of POIs *per se*, the appropriate control is a mutated DB motif from 30-RxxLxxIxN-38 to 30-GxxVxxIxN-38. This gives rise to a ‘DB-dead’ nondegradable variant (Weingartner et al., 2004).

Viral transferrable degron sequences

Hantaviruses are members of the *Bunyaviridae* family and can be split up into several pathogenic and non-pathogenic species. The tails of G1 glycoproteins derived from the pathogenic NY-1 virus (NY-1V) (Geimonen et al., 2003), from Andes (ANDV) and Hantaan viruses (HTNV, Sen et al., 2007) contain intervening hydrophilic residues within the C-terminal hydrophobic domain called the ‘G1 tail’. These residues were found to confer instability to the domain. However, those amino acids are not found in nonpathogenic hantaviruses such as Prospect Hill virus (PHV). The G1 tail of PHV is therefore stable. Interestingly their G1 tails can be mutated to act as destabilizing sequences by introducing amino acid substitutions corresponding to the residues present in G1 tails of e.g., NY-1V.

As a result from adding hydrophilic side chains to PHV G1, a reporter protein fused to this peptide could be directed to proteasomal degradation (Table 2; Table S1; Sen et al., 2007).

Taken together, the techniques described above provide a wide variety of approaches for rapid on demand protein depletion *in vitro* and *in vivo*, including the possibility of conditional phenotypes (Table 2). The induction of many of the hitherto reported degron systems is related to a small molecule (auxin, JA-Ile, or Shield-1), others depend on the expression of a factor that recognizes the degron (deGradFP) or are constitutively active (viral degrons). Some degrons are even recognized only in a specific stage of the cell-cycle (cyclin DB) or depend on an exogenous factor like blue light. Still, the currently most established methods use small molecules as inducers. Nevertheless, there are still more approaches on the scene that exploit another widely conserved degradation mechanism, the so-called N-end rule, as described in detail in the following section.

Engineering the UPS for targeting endogenous proteins

All the systems reviewed in this article use attachable protein sequences as degradation signals to target non-endogenous proteins for degradation via the ubiquitin-proteasome system (UPS). This method, by design, does not allow for the manipulation of endogenous proteins within an organism. In plants, especially in the model plant *Arabidopsis* this problem can be circumvented by complementing a knockout mutant with a degron-fused version of the protein. However, this possibility does not exist in all organisms and also does not allow for the influence of specific sub-populations of a given protein e.g., post-translationally modified vs. unmodified.

Aside from the formerly mentioned PROTAC-approach (proteolysis targeting chimeric molecule; Sakamoto et al., 2001; Schneekloth et al., 2004; Carmony and Kim, 2012), where a chemically synthesized target protein-binding molecule is fused to an E3-recognized peptide, engineered F-box proteins represent another way of using the UPS for the degradation of endogenous proteins (Figure 2F).

Zhou et al. (2000) showed that a 35 amino acid stretch of the human papillomavirus type 16 protein E7 (E7N), that can complex with the retinoblastoma protein pRb, can efficiently target this protein for degradation via the SCF complex in yeast as well as in human cancer cell lines when it is fused to the F-box/WD-40 domains of Cdc4p (for yeast) or β TrCP (for human cell lines). Within the

SCF machinery, the F-box is important for the interaction with the SCF complex, whereas the WD-40 repeats confer substrate binding. Additionally they showed that an engineered β TrCP-E7N can target endogenous p107 in human cervical carcinoma cells (CAC33) rendering it a substrate for the UPS.

Zhang et al. (2003) further refined the method in human cell lines by structurally engineering the WD-40 domains of β TrCP-E7N to shift its affinity towards the desired cellular target p107 by abolishing the original target specificity without disturbing the overall structure of the chimeric protein. Furthermore they demonstrated that the effect of the chimeric F-box protein is dosage-dependent, meaning the titer of the target protein can be set to new steady-state levels, depending on the amount of introduced chimeric F-box protein. Also it exhibits a strong preference for the hypophosphorylated version of p107 leaving the hyperphosphorylated version as well as *in vivo* bound proteins untouched.

Cong et al. (2003) used the β -catenin binding domain of E-cadherin fused to the C-terminal of β TrCP (F-TrCP-Ecad) to downregulate a pool of cytosolic β -catenin, which acts as a transcription factor and is involved in tumor formation. Even though β -catenin is an endogenous target of β TrCP, it requires phosphorylation to be recognized. The authors showed that the chimeric F-TrCP-Ecad can subject a pool of non-phosphorylated cytosolic β -catenin to degradation. Su et al. (2003) used a similar approach to target the cytosolic version of β -catenin. However instead of using the Ecad-domain of E-cadherin, they used four repeats of a 15 amino acid stretch of the APC (adenomatous polyposis coli) protein they showed strongly to bind β -catenin with almost no affinity towards the E-cadherin bound pool. This domain was fused to different versions of the C-terminal of h-TrCP. The fusion proteins showed efficient affinity and subsequent ubiquitinylation and destruction of unbound β -catenin in human cancer cell lines.

Cohen et al. (2004) used this approach in an *in vivo* situation to study the role of c-Myc, a transcription factor of the MYC-family important for the control of proliferation, metabolism, growth, apoptosis, and differentiation. Knockout mice of this protein exhibit embryonic lethality, thus its function in later development cannot be studied. In this study they used *in utero* transfection via an adenovirus to knockout c-Myc via an engineered F-box protein consisting of the C-terminus of β TrCP fused to a domain of Max, a protein known to interact with c-Myc. They could show that the targeted knockdown by an engineered β TrCP yielded similar results as an approach using the introduction of an antisense gene.

Hannah and Zhou (2011) presented a double knock-down method, which was able to improve ablation of the target protein pRb. To this end they combined ubiquitin ligase-mediated protein knockout using a β TrCP-E7N construct as well as transcript targeting RNAi using an anti-*RBI* shRNA construct, to target ectopically expressed pRB in human SAOS-2 cells. Furthermore they demonstrated a more rapid protein ablation by targeting endogenous p107 with either anti-*RBL1* siRNA or β TrCP-E7N. The results confirmed that this combinatorial approach is more effective than using either the ubiquitin ligase-mediated protein knockout or RNAi alone.

In conclusion, this method represents a powerful tool for targeting endogenous (sub-) populations of a protein. However, a strong limiting factor is the availability of suitable binding domains for target specificity. Also the application of the chimeric F-box proteins is non-reversible. Still, they have advantages in comparison with the PROTAC-approach, namely that they can be delivered easier into the systems e.g., via a virus based system because they do not have to cross the membrane in a constituted form.

N-end rule-based systems

The following section will give an overview over the current state and uses of different N-degrons in the eukaryotic field. An overview of the general features on assembly options for the discussed degrons can be found in Figure 3. A summary of publications using N-degrons on a variety of different target proteins and enzymes is given in Table 3.

N-degrons

N-degrons represent a class of degradation signals that can be fused to the N-terminus of a target protein. They contain a specific N-terminal, which is a destabilizing residue of the N-end rule pathway of protein degradation (NERD).

The N-end rule relates the half-life of a protein to the identity of its N-terminal residue. It was first formulated after the discovery that *E. coli* β -gal containing an N-terminal fragment of the *lac repressor* may confer instability and degradation via the 26S proteasome in *S. cerevisiae*. This destabilization/stabilization effect depends on the identity of its N-terminal amino acid (Bachmair et al., 1986; Bachmair and Varshavsky, 1989). NERD determines

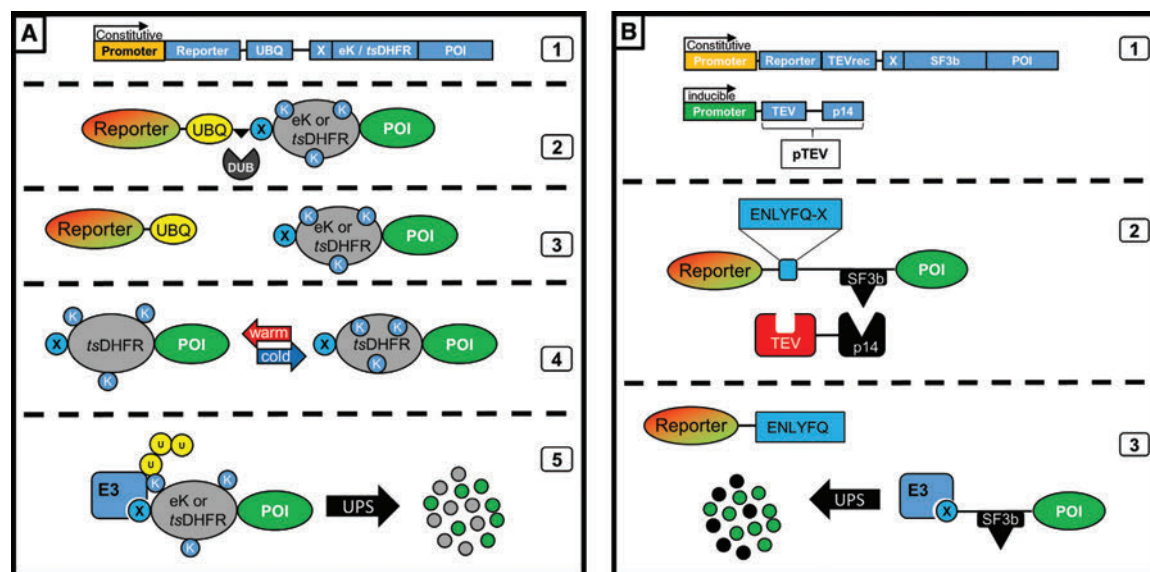


Figure 3 Assembly and mechanisms of different NERD degrons.

(A) The e^k /ts-degron. (1) Assembly of the fusion protein on DNA level. (2) Co-translational cleavage of ubiquitin fusion (UBQ) by endogenous deubiquitinating enzymes (DUBs), following exposure of the destabilizing residue ‘X’ at the N-terminus of the fusion protein (ubiquitin fusion technique). (3) Presence of protein of interest (POI) and reporter. For regulation of the ts-DHFR, see step 4, for use of e^k as a degron, see step 5. (4) Temperature shift for ts-degron. Upon shift to restrictive temperature (‘warm’), conformational changes within the ts-DHFR lead to an increased accessibility of otherwise shielded Lysine residues (K) at permissive temperatures (‘cold’). (5) Recognition and ubiquitinylation via N-recognins (E3, Ub ligase) and subsequent degradation via the 26S-proteasome under warm conditions (ts-DHFR) or temperature independent (e^k). (B) The TIPI degron. (1) Assembly on DNA level. POI and pTEV are encoded on different constructs under the control of different promoters. (2) Upon induction of pTEV expression, the TEV cleaves between reporter and POI. Affinity of the TEV to the TEV cleavage site (TEVrec) is increased by the interactions of a sequence of the protein SF3b and the protein p14. (3) Cleavage reveals a dormant destabilizing residue (X) which can be recognized by N-recognins (Ubr1 in yeast) leading to proteasomal degradation; modified after Taxis et al. (2009).

the degradation rate of the protein with half-lives ranging between a few minutes (e.g., 2–3 min for arginine, phenylalanine, and aspartic acid) up to 420 h (e.g., serine or methionine; Bachmair et al., 1986; Mogk et al., 2007).

One of the major advantages of exploiting the NERD is the fact that it is thought to be conserved over all kingdoms. It has been described to function in mammals, bacteria, yeast (Varshavsky, 2011) and also plants (Bachmair et al., 1993; Graciet et al., 2010), however, in bacteria, because of their lack of ubiquitin, its general functionality is altered (Dougan et al., 2010).

All approaches using N-degrons require processing the N-terminal of the degron-protein fusion after translation to expose the desired destabilizing residue. This can be achieved e.g., by applying the ubiquitin fusion technique (UFT, Bachmair et al., 1986; Varshavsky, 2005) or an actively induced cleavage of the N-terminal, e.g., by a tobacco etch virus (TEV) protease in order to activate a dormant degron such as in case of the TEV protease induced protein inactivation (TIPI) system (Taxis et al., 2009) as described below.

e^k and alternative degron sequences

The e^k (lysines [Ks] containing extension [e]) sequence is a 45 amino acid sequence derived from a stretch of the *E. coli lac* repressor (Bachmair et al., 1986; Bachmair and Varshavsky, 1989) and has mainly been used to generate artificial NERD substrates to be used as *in vivo* degradation reporters. The stability of the sequence is highly dependent on the N-terminal but also on a specific KRK (Lys-Arg-Lys) motif that is available for ubiquitinylation in a defined distance from the N-terminal amino acid (Bachmair and Varshavsky, 1989). This allows specific modifications within the e^k sequence that can alter its general features (Bachmair and Varshavsky, 1989; Suzuki and Varshavsky 1999). For example, an introduction of additional KRK motifs results in a lower stability (Suzuki and Varshavsky, 1999). The first protein having been destabilized by a fusion to the e^k sequence was the protein β -gal (β -galactosidase) from *E. coli* shown to be unstable in *S. cerevisiae*, dependent on its N-terminal amino acid (Bachmair et al., 1986).

Table 3 NERD-based systems (N-degrons) with examples for target proteins and organisms.

Active sequence	Organism	Target protein/application	References	E.C. number (if applicable)
ts-DHFR	<i>S. cerevisiae</i>	Cdc28p (cyclin-dependent kinase)	Dohmen et al. (1994)	2.7.11.22
ts-DHFR	<i>S. cerevisiae</i>	Oaf1–1p (oleate-activated transcription factor),		
		Orc-1p (origin recognition complex)	Hardy (1996)	
ts-DHFR	<i>S. cerevisiae</i>	Cdc28p (cyclin-dependent kinase)	Amon (1997)	2.7.11.22
ts-DHFR	<i>S. cerevisiae</i>	Act5p (Arp1p, actin-related protein)	Muhua et al. (1998)	
ts-DHFR	<i>S. cerevisiae</i>	Tfb4p (transcription factor B subunit 4)	Feaver et al. (1999)	
ts-DHFR	<i>S. cerevisiae</i>	Cdc45p (cell division cycle)	Tercero et al. (2000)	
ts-DHFR	<i>S. cerevisiae</i>	Mcm2–7p (minichromosome maintenance)	Labib et al. (2000)	
ts-DHFR	<i>S. cerevisiae</i>	Duo1p (death upon overproduction)	Cheeseman et al. (2001b)	
ts-DHFR	<i>S. cerevisiae</i>	Ask1p (associated with spindles and kinetochores),	Cheeseman et al. (2001a)	
		Dad2p (Duo1 and Dam1 interacting)		
ts-DHFR	<i>S. cerevisiae</i>	Mif2p (mitotic fidelity of chromosome transmission),	Gardner et al. (2001)	
		Cep3p (Centromere protein),		
		Cse4p (chromosome segregation),		
		Skp1p (suppressor of kinetochore protein mutant),		
		Ndc10p (Cbf2, centromere-binding factor),		
		Ctf13p (chromosome transmission fidelity)		
ts-DHFR	<i>S. cerevisiae</i>	Noc3p (Nucleolar complex associated)	Zhang et al. (2002)	
ts-DHFR	<i>S. cerevisiae</i>	Esp1p (extra spindle pole bodies)	Stegmeier et al. (2002)	3.4.22.49
ts-DHFR	<i>S. pombe</i>	Mcm4 (minichromosome maintenance)	Lindner et al. (2002)	
ts-DHFR	<i>S. pombe</i>	Cdc23p (cell division cycle)	Gregán et al. (2003)	
ts-DHFR	<i>Drosophila</i>	eGFP (enhanced green fluorescent protein)	Speese et al. (2003)	
ts-DHFR	<i>S. cerevisiae</i>	Cdc101p, 102p, 105p (cell division cycle),	Kanemaki et al. (2003)	
		Mcm4p (minichromosome maintenance)		
ts-DHFR	<i>S. pombe</i>	Bir1p (baculoviral IAP repeat-containing protein)	Rajagopalan et al. (2004)	
ts-DHFR	<i>S. cerevisiae</i>	Cdc48p (cell division cycle)	Fu et al. (2003)	3.6.4.6/7
ts-DHFR	<i>S. cerevisiae</i>	Erg11p (ERGosterol biosynthesis)	Parsons et al. (2004)	1.14.13.70
ts-DHFR	<i>S. cerevisiae</i>	Cdc13p (cell division cycle),	Vodenicharov and Wellinger (2006)	
		Stn1p (suppressor of cdc Thirteen)		
ts-DHFR	Chicken cells	Rad51 (RADiation sensitive)	Su et al. (2008)	
ts-DHFR	<i>S. cerevisiae</i>	several essential genes	Ben-Aroya et al. (2008)	
ts-DHFR	<i>S. cerevisiae</i>	Tif51Ap (Hyp2, HYPusine-containing protein)	Saini et al. (2009)	
ts-DHFR	<i>S. pombe</i>	Smnp (survival of motoneurons)	Campion et al. (2010), Piazzon et al. (2012)	
ts-DHFR	Chicken cells	Orc6p (origin recognition complex subunit 6)	Bernal and Venkitaraman (2011)	
ts-DHFR	<i>S. cerevisiae</i>	Scs3p (Irr, IRRegular),	Kulemzina et al. (2012)	
		Pds5p (precocious dissociation of sisters)		
ts-DHFR	<i>S. cerevisiae</i>	Bir1p (baculoviral IAP repeat-containing protein)	Ren et al. (2012)	
e ^k	<i>S. cerevisiae</i>	β-Gal (β-galactosidase)	Bachmair et al. (1986)	3.2.1.23
e ^k	<i>S. cerevisiae</i>	β-Gal (β-galactosidase),	Bachmair and Varshavsky (1989)	3.2.1.23
		DHFR (dihydrofolate reductase)		
e ^k	Reticulocyte lysate (rabbit)	β-Gal (β-galactosidase)	Gonda et al. (1989)	3.2.1.23
e ^k	<i>Arabidopsis</i>	DHFR (dihydrofolate reductase)	Bachmair et al. (1993)	1.5.1.3
e ^k (engineered)	<i>S. cerevisiae</i>	β-Gal (β-galactosidase), screen for altered properties	Suzuki and Varshavsky (1999)	3.2.1.23
e ^k	<i>D. discoideum</i>	β-Gal (β-galactosidase)	Detterbeck et al. (1994)	3.2.1.23
e ^k (engineered)	<i>S. cerevisiae</i>	CFP (cyan fluorescent protein)	Hackett et al. (2006)	
e ^k (engineered)	<i>S. cerevisiae</i>	GFP (green fluorescent protein)	Houser et al. (2012)	

(Table 3 Continued)

Active sequence	Organism	Target protein/application	References	E.C. number (if applicable)
e ^K	<i>S. cerevisiae</i>	β-Gal (β-galactosidase)	Hwang et al. (2010)	3.2.1.23
C-terminal Scc1	<i>S. cerevisiae</i>	<i>in vivo</i> pulse-chase	Choi et al. (2010)	
pTEV	<i>S. cerevisiae</i>	CDC14p (TIPI), DON1p (DONut)	Taxis et al. (2009)	
pTEV	<i>S. cerevisiae</i>	C- and N-terminally destabilized reporter (TIPI)	Jungbluth et al. (2010)	
pTEV	<i>S. cerevisiae</i>	Met4p, 31p (METHionine requiring)	Mclsaac et al. (2011)	

ts-DHFR, mouse dihydrofolate reductase carrying point mutations for temperature sensitivity; e^K, lysine containing sequence; Scc1, C-terminus of the yeast protein mitotic chromosome determinant (Mcd1p); pTEV, TEV protease from tobacco etch virus enhanced in proteolytic activity.

The e^K sequence has been used to prime proteins for rapid degradation. Park et al. (1992) fused the sequence to *ARD1* (ARrest defective 1), a subunit of the N-terminal acetyltransferase A (NatA), monitoring its turnover depending on the stability of the fusion protein conferred by its N-terminal. Here, the observed half-life of a destabilized Ard1p was just 3 min. Hackett et al. (2006) used modified versions of the e^K sequence to design CFP (cyan fluorescent protein) reporter constructs with specific degradation times of 5, 50, and 70 min to monitor cellular protein turnover. Houser et al. (2012) again applied the destabilizing abilities of the e^K sequence to generate GFP fusions with a degradation time of 7 min to use them as temporal indicators of gene expression *in vivo*. However, the e^K sequence has also been used in other organisms, such as: in a rabbit reticulocyte lysate, indicating that it is also applicable in mammals (Gonda et al., 1989); in the slime mold (*Mycetozoum*) *Dictyostelium discoideum* (Detterbeck et al., 1994); and also in the model plant *Arabidopsis*, where Bachmair et al. (1993) used an e^K-fused murine dihydrofolate reductase (DHFR) with a destabilizing N-terminal in a forward genetics screen to identify mutants deficient in N-terminal protein degradation (Potuschak et al., 1998; Stary et al., 2003).

Another example for a protein fragment following the N-end rule is the 33 kDa C-terminal cleavage product of *S. cerevisiae* Scc1p (Mcd1p, mitotic chromosome determinant). This peptide has been described by Rao et al. (2001) and has also been used as a stability and affinity reporter for the investigation of *S. cerevisiae* Ubr1p substrate binding (Choi et al., 2010).

Additionally, the e^K tag has been used as an adapter sequence for the recognition and discovery of new E3 ligases of NERD via peptide arrays on membrane support (SPOT) assays (Hwang et al., 2010; Kim et al., 2014). Another sequence used in this context is the N-terminal part of the Sindbis virus RNA polymerase nsP4. De Groot

and coworkers (1991) showed that this protein follows the N-end rule. Since then it has been used as an adapter in peptide-based pull-downs of endogenous NERD E3 ligases (Tasaki et al., 2005), and thus, because of the similar behavior of the e^K and the nsP4 sequences, it seems likely that the nsP4 sequence might as well be used as a constitutive N-terminal degradation signal.

Potentially applicable portable N-degrons are emerging in the plant field. Takemoto and Jones (2005) showed that cleavage products of the *Arabidopsis* RPM1 INTERACTING PROTEIN 4 (RIN4) are recognized and degraded via the NERD. Also the N-terminal domain of the B-2 subfamily of group VII ETHYLENE RESPONSE FACTORS (ERFs), such as from RAP2.12 (RELATED TO APETALA 2.12) transcription factors, were described as *in vitro* and *in vivo* NERD targets (Gibbs et al., 2011, 2014; Licausi et al., 2011). These transcription factors are initiated by a highly conserved MCGGAIL (single letter amino acid code) sequence motif that starts with the residues Met1-Cys2 (MC). However, so far, these sequences have not yet been used in a different application-based background and need to be further characterized before they can be used as portable N-degrons.

TEV protease induced protein inactivation (TIPI)

Taxis et al. (2009) introduced a different type of N-terminal processing in order to create an N-degron. Instead of exposing the desired N-terminus by non-adjustable co-translational cleavage of an N-terminal ubiquitin as in the UFT, (see above) they use an inducible TEV protease, which cleaves a protein sequence at a defined point, therefore exposing a dormant N-degron. They also showed that in the usually used, most efficient and

‘classical’ TEV recognition site ENLYFQG/S the terminal glycine can be replaced by a phenylalanine or an aspartic acid, both leading to efficient cleavage and degradation. The initial work uses a GAL1 driven TEV protease. However, the authors showed that dependent on the expression strength of the protein fusion destined for degradation, various versions of the TEV that differ in proteolytic efficiency (pTEV) had to be used. To further increase the affinity of TEV to its target sequence it is fused to the human protein p14, which recognizes a stretch of the SF3b protein contained within the spacer region between the N-terminus and the target protein. Within the fusion construct a C-terminal reporter protein, e.g., GFP, can also be included. Upon cleavage at the TEV recognition site, the reporter remains stable while the POI is being degraded and consequently serves as an expression control. Renicke et al. (2013b) demonstrated a new version of TEV protease with an almost completely abolished specificity for the amino acid at position P1’ therefore allowing for an even broader variety of N-terminals to be exposed via cleavage.

McIsaac and coworkers (2011) modified the system to increase the reaction time upon inducing the TEV. Instead of directly triggering the TEV expression they used the chimeric transcriptional activator Gal4dbd.ER.VP16 (GEV). Upon induction with β -estradiol the cytoplasmic GEV relocates into the nucleus where it activates a promoter containing GAL4p consensus sequences, which drives the TEV expression. Because of large amounts of GEV relocating to the nucleus at once upon induction, the reaction time of the system – until a substrate is degraded – lays in the range of just 20 min. Another modification of the TIPI system has been introduced by Jungbluth et al. (2010). To further increase the applicability, they introduced a second C-terminal degron upstream of the TEV recognition site. Hence, upon cleavage two differentially destabilized fragments are created.

Temperature-sensitive degron

It was shown that a point-mutated and N-terminally altered version of the DHFR follows the N-end rule in a temperature-dependent manner (Dohmen et al., 1994; Dohmen and Varshavsky, 2005). According to the original work, described as the ts-degron or td method (temperature-sensitive degron), the DHFR unfolds upon a temperature shift from 16°C to 28°C exposing internal lysine residues that can be ubiquitinated therefore priming the entire fusion construct for degradation. Since its first appearance, the ts-degron has been extensively used in *S. cerevisiae* to generate temperature-sensitive mutants. The

regulating temperatures rest hereby within the range of 25°C (permissive temperature) and 37°C (restrictive temperature), respectively (Dohmen et al., 1994; Dohmen and Varshavsky, 2005). Many different classes of proteins have been shown to function with a ts-degron fusion, including Ask1p (associated with spindles and kinetochores), Dad2p (Duo1 and Dam1 interacting) (Cheeseman et al., 2001a), and Duo1p (death upon overproduction) (Cheeseman et al., 2001b) which are subunits of the Dam1p (Duo1 And Mps1 interacting) complex, or Bir1p (Baculoviral IAP repeat-containing protein) as part of the CPC (subunit of chromosomal passenger complex; Ren et al., 2012). Unexpectedly, in the case of Bir1p, a degradation of the mRNA was reported as well, leading to a much more efficient target depletion by an unknown mechanism. To further improve efficiency, the ts-alleles are not expressed in wildtype cells but rather in an Ubr1p overexpressing background of *S. cerevisiae*. This strain has been used first by Kanemaki and coworkers (2003).

Also in *Schizosaccharomyces pombe* (fission yeast) the ts-degron has been shown to function. Lindner et al. (2002) created a tsMcm4 (minichromosome maintenance) expressing strain. A tsCdc23p-strain was constructed by Gregán et al. (2003) and Rajagopalan et al. (2004) also destabilized Bir1p. The method to create ts-alleles in *S. pombe* is described in the protocol by Kearsy and Grégan (2009).

Despite the fact that the ts-degron seems to function with many different target proteins (Table 3) it does not work in every case. For example, Campion et al. (2010) and Piazzon et al. (2012) reported problems working with a ts-allele of *SMN1* (survival of motoneurons). *S. pombe* cells carrying the gene already exhibited growth defects at the permissive temperature of 25°C.

Besides the yeasts *S. cerevisiae* and *S. pombe*, the ts-degron has also been used in avian cell cultures as well as in the fruit fly *Drosophila melanogaster* (Speese et al., 2003) where it served in a GFP fusion as a test substrate for localized UPS-dependent protein degradation. Su and coworkers (2008) used the ts-degron to elucidate the function of the avian RAD51, a protein involved in homologous DNA recombination and repair of double-strand breaks in an avian DT40 cell line. As a proof of concept they also showed the possible regulation of a ts-degron-eGFP (enhanced GFP) fusion. Using the same techniques and cell lines, Bernal and Venkitaraman (2011) worked on the function of the avian ORC6 protein, a subunit of the origin recognition complex (ORC) using a ts-degron fusion. However, it is noteworthy that the ts-degron regulating temperatures differ greatly in the DT40 cells compared to yeast cells. While

in yeast a temperature of 25°C leads to stabilization and a temperature of 37°C to degradation of the degron-fusion protein, this range is shifted in the DT40 cells to 35°C and 42°C, respectively. This is surprising because a degradation of a ts-degron fused to Duo1p was also observed at 34°C resulting in death of the transformed yeast cells (Cheeseman et al., 2001b).

As the degradation mechanistic of many NERD substrates have been characterized, more *bona fide* substrates discussed (Varshavsky, 2011; Piatkov et al., 2012), and after the discovery of totally new branches of the NERD (Hwang et al., 2010; Kim et al., 2014; Gibbs et al., 2014; Weits et al., 2014) it is likely that N-terminal sequences of target proteins could be used as recognition motifs for NERD and thus lead to the destruction of C-terminally fused POIs. However, as many powerfully destabilizing sequences exist, especially in yeast and mammalian cell cultures, the applicability and necessity of even more and in this context, yet poorly described degrons needs to be discussed beforehand.

Still, to this point the e^k sequence together with the ts-degron remain the most widely used and most extensively studied portable N-terminal degradation signal.

Conclusion and perspectives

Conditional systems based on protein accumulation or degradation

Small-molecule reagents used in promotor induction or stabilization/destabilization of fusion proteins as well as protein inhibitors address several required issues of conditionality. Similarly, nonchemical inducers such as light or temperature can work with high success in many experimental setups.

However, many of them are prone to strong off-target effects or simply cannot be used in a subset of target organisms, due to specific toxicity or involvement of the exogenic small molecules in endogenous processes. For example, in the case of using the plant hormone auxin, which would not be applicable in plants both because of the endogenous levels of the compound and potential strong interference with plant development, if exogenously added in higher doses. In addition, the potentially high costs of exogenously applied small-molecule inhibitors must be taken into account when considering using them to trigger responses in multicellular organisms.

The application of N-degrons has been long established. They do provide a quick and invasion minimized

way to study protein turnover and degradation, also offering inducibility in some cases and therefore improved control over the desired experiment. The ts-degron (td method) is able to eliminate or reduce phenotypic lags, because the activation of N-degrons results in rapid disappearance of the chimeric protein fusion and by this directly reducing the abundance of functional POI (Varshavsky, 2005). One major constraint is, of course, the need of temperature-shifts or growing cells or plants at constitutively permissive or restrictive temperatures. These – if not optimized to the system of investigation – may simply be too low or high for normal growth and metabolism and cause phenotypic differences *per se*. The different types of N-degrons have mainly, with few exceptions, been used in single-cellular organisms or cell cultures. This still leaves a lot of room for methods improvement and establishing the techniques in more complicated multicellular organisms. However, due to the high conservation of the N-end rule pathway, they offer tremendous possibilities for inducible phenotypes *in vivo*.

However, a general drawback of all of these techniques is to overcome the barrier of specifically manipulating a GOI in the respective genome, if an endogenous one is to be studied. This is especially problematic in organisms not amenable to homologous recombination. Here, genome editing tools as zinc finger nucleases (ZNFs), transcription activator-like effector endonucleases (TALENs) or the recently introduced CRISPR-Cas system might be assayed (Gaj et al., 2013; Fichtner et al., 2014).

Conditional phenotypes in multicellular organisms

A possible future focus of the use of portable conditional degrons is their use in biotechnological applications in order to generate beneficial phenotypes, e.g., for the manufacture of plant-based industrials or pharmaceuticals.

Studies have demonstrated that these systems can be functional under complex circumstances such as in the case of inducing specific cell or tissue types in multicellular organisms (floral induction system; Gómez-Mena et al., 2005; Wellmer et al., 2006). Conditional phenotypes might also emerge from switchable trichomes by using inducible promoters driving trichome-specific developmental factors, as discussed here. For example, using a conditional N-degron regulating the presence and function of trichome- or flower-specific transcription factors might lead to the formation of metabolically highly active areas in a plant. Both the floral induction systems and inducible trichomes highlight the availability of tools for

beneficially manipulating endogenous reserves and metabolic potential of eukaryotes to form conditional organs. Eventually, these not yet established approaches might pave the way towards a biotechnological system of conditional reaction compartments or bioreactors to harbor biosynthetic pathways.

Acknowledgments: We thank Maria Klecker and Pavel Reichman for comments on the manuscript. The Independent Junior Research Group is funded by a grant of the ScienceCampus Halle – Plant-based Bioeconomy (SCH) to N.D., a graduate fellowship by the Landesgraduiertenförderung Sachsen-Anhalt to F.F. Support comes from the Deutsche Forschungsgemeinschaft (DFG) Graduate Training Center GRK1026 ‘Conformational Transitions in Macromolecular Interactions’ at Halle, Germany and the Leibniz Institute of Plant Biochemistry (IPB) at Halle, Germany.

References

- Amon, A. (1997). Regulation of B-type cyclin proteolysis by Cdc28-associated kinases in budding yeast. *EMBO J.* *16*, 2693–2702.
- Andersen, S.U., Cvitanich, C., Hougaard, B.K., Roussis, A., Gronlund, M., Jensen, D.B., Frokjaer, L.A., and Jensen, E.O. (2003). The glucocorticoid-inducible GVG system causes severe growth defects in both root and shoot of the model legume *Lotus japonicus*. *Mol. Plant Microbe Interact.* *16*, 1069–1076.
- Aoyama, T. and Chua, N.H. (1997). A glucocorticoid-mediated transcriptional induction system in transgenic plants. *Plant J.* *11*, 605–612.
- Armstrong, C.M. and Goldberg, D.E. (2007). An FKBP destabilization domain modulates protein levels in *Plasmodium falciparum*. *Nat. Methods* *4*, 1007–1009.
- Avila, J., Nieto, C., Canas, L., Benito, M.J., and Paz-Ares, J. (1993). *Petunia hybrida* genes related to the maize regulatory C1 gene and to animal myb proto-oncogenes. *Plant J.* *3*, 553–562.
- Bachmair, A. and Varshavsky, A. (1989). The degradation signal in a short-lived protein. *Cell* *56*, 1019–1032.
- Bachmair, A., Finley, D., and Varshavsky, A. (1986). *In vivo* half-life of a protein is a function of its amino-terminal residue. *Science* *234*, 179–186.
- Bachmair, A., Becker, F., and Schell, J. (1993). Use of a reporter transgene to generate *Arabidopsis* mutants in ubiquitin-dependent protein degradation. *Proc. Natl. Acad. Sci. USA* *90*, 418–421.
- Banaszynski, L.A., Chen, L.C., Maynard-Smith, L.A., Ooi, A.G., and Wandless, T.J. (2006). A rapid, reversible, and tunable method to regulate protein function in living cells using synthetic small molecules. *Cell* *126*, 995–1004.
- Banaszynski, L.A., Sellmyer, M.A., Contag, C.H., Wandless, T.J., and Thorne, S.H. (2008). Chemical control of protein stability and function in living mice. *Nat. Med.* *14*, 1123–1127.
- Ben-Aroya, S., Coombes, C., Kwok, T., O'Donnell, K.A., Boeke, J.D., and Hieter, P. (2008). Toward a comprehensive temperature-sensitive mutant repository of the essential genes of *Saccharomyces cerevisiae*. *Mol. Cell* *30*, 248–258.
- Berdeaux, R., Goebel, N., Banaszynski, L., Takemori, H., Wandless, T., Shelton, G.D., and Montminy, M. (2007). SIK1 is a class II HDAC kinase that promotes survival of skeletal myocytes. *Nat. Med.* *13*, 597–603.
- Bernal, J.A. and Venkitaraman, A.R. (2011). A vertebrate N-end rule degron reveals that Orc6 is required in mitosis for daughter cell abscission. *J. Cell Biol.* *192*, 969–978.
- Bonger, K.M., Chen, L.C., Liu, C.W., and Wandless, T.J. (2011). Small-molecule displacement of a cryptic degron causes conditional protein degradation. *Nat. Chem. Biol.* *7*, 531–537.
- Boutros, M., Kiger, A.A., Armknecht, A., Kerr, K., Hild, M., Koch, B., Haas, S.A., Heidelberg Fly Array Consortium, Paro, R., and Perrimon, N. (2004). Genome-wide RNAi analysis of growth and viability in *Drosophila* cells. *Science* *303*, 832–835.
- Brand, L., Horler, M., Nuesch, E., Vassalli, S., Barrell, P., Yang, W., Jefferson, R.A., Grossniklaus, U., and Curtis, M.D. (2006). A versatile and reliable two-component system for tissue-specific gene induction in *Arabidopsis*. *Plant Physiol.* *141*, 1194–1204.
- Caddick, M.X., Greenland, A.J., Jepson, I., Krause, K.P., Qu, N., Riddell, K.V., Salter, M.G., Schuch, W., Sonnewald, U., and Tomsett, A.B. (1998). An ethanol inducible gene switch for plants used to manipulate carbon metabolism. *Nat. Biotechnol.* *16*, 177–180.
- Campion, Y., Neel, H., Gostan, T., Soret, J., and Bordonne, R. (2010). Specific splicing defects in *S. pombe* carrying a degron allele of the Survival of Motor Neuron gene. *EMBO J.* *29*, 1817–1829.
- Carmony, K.C. and Kim, K.B. (2012). PROTAC-induced proteolytic targeting. *Methods Mol. Biol.* *832*, 627–638.
- Carroll, C.W. and Morgan, D.O. (2002). The Doc1 subunit is a processivity factor for the anaphase-promoting complex. *Nat. Cell Biol.* *4*, 880–887.
- Causinus, E., Kanca, O., and Affolter, M. (2012). Fluorescent fusion protein knockout mediated by anti-GFP nanobody. *Nat. Struct. Mol. Biol.* *19*, 117–121.
- Cheeseman, I.M., Brew, C., Wolyniak, M., Desai, A., Anderson, S., Muster, N., Yates, J.R., Huffaker, T.C., Drubin, D.G., and Barnes, G. (2001a). Implication of a novel multiprotein Dam1p complex in outer kinetochore function. *J. Cell Biol.* *155*, 1137–1145.
- Cheeseman, I.M., Enquist-Newman, M., Muller-Reichert, T., Drubin, D.G., and Barnes, G. (2001b). Mitotic spindle integrity and kinetochore function linked by the Duo1p/Dam1p complex. *J. Cell Biol.* *152*, 197–212.
- Chen, S., Hofius, D., Sonnewald, U., and Bornke, F. (2003). Temporal and spatial control of gene silencing in transgenic plants by inducible expression of double-stranded RNA. *Plant J.* *36*, 731–740.
- Chini, A., Fonseca, S., Fernandez, G., Adie, B., Chico, J.M., Lorenzo, O., Garcia-Casado, G., Lopez-Vidriero, I., Lozano, F.M., Ponce, M.R., et al. (2007). The JAZ family of repressors is the missing link in jasmonate signalling. *Nature* *448*, 666–671.
- Choi, W.S., Jeong, B.C., Joo, Y.J., Lee, M.R., Kim, J., Eck, M.J., and Song, H.K. (2010). Structural basis for the recognition of N-end rule substrates by the UBR box of ubiquitin ligases. *Nat. Struct. Mol. Biol.* *17*, 1175–1181.
- Christie, J.M., Swartz, T.E., Bogomolni, R.A., and Briggs, W.R. (2002). Phototropin LOV domains exhibit distinct roles in regulating photoreceptor function. *Plant J.* *32*, 205–219.

- Cohen, C., Scott, D., Miller, J., Zhang, J., Zhou, P., and Larson, J.E. (2004). Transient *in utero* knockout (TIUKO) of C-MYC affects late lung and intestinal development in the mouse. *BMC Devel. Biol.* 4, 4.
- Cong, F., Zhang, J., Pao, W., Zhou, P., and Varmus, H. (2003). A protein knockdown strategy to study the function of β -catenin in tumorigenesis. *BMC Mol. Biol.* 4, 10.
- Craft, J., Samalova, M., Baroux, C., Townley, H., Martinez, A., Jepson, I., Tsiantis, M., and Moore, I. (2005). New pOp/LhG4 vectors for stringent glucocorticoid-dependent transgene expression in Arabidopsis. *Plant J.* 41, 899–918.
- de Groot, R.J., Rumenapf, T., Kuhn, R.J., Strauss, E.G., and Strauss, J.H. (1991). Sindbis virus RNA polymerase is degraded by the N-end rule pathway. *Proc. Natl. Acad. Sci. USA* 88, 8967–8971.
- Detterbeck, S., Morandini, P., Wetterauer, B., Bachmair, A., Fischer, K., and MacWilliams, H.K. (1994). The ‘prespore-like cells’ of *Dictyostelium* have ceased to express a prespore gene: analysis using short-lived beta-galactosidases as reporters. *Development* 120, 2847–2855.
- Deveaux, Y., Peaucelle, A., Roberts, G.R., Coen, E., Simon, R., Mizukami, Y., Traas, J., Murray, J.A., Doonan, J.H., and Laufs, P. (2003). The ethanol switch: a tool for tissue-specific gene induction during plant development. *Plant J.* 36, 918–930.
- Dice, J.F. and Goldberg, A.L. (1975). Relationship between *in vivo* degradative rates and isoelectric points of proteins. *Proc. Natl. Acad. Sci. USA* 72, 3893–3897.
- Dietrich, C.R., Han, G., Chen, M., Berg, R.H., Dunn, T.M., and Cahoon, E.B. (2008). Loss-of-function mutations and inducible RNAi suppression of *Arabidopsis* LCB2 genes reveal the critical role of sphingolipids in gametophytic and sporophytic cell viability. *Plant J.* 54, 284–298.
- Dissmeyer, N. and Schnittger, A. (2011). The age of protein kinases. *Methods Mol. Biol.* 779, 7–52.
- Dissmeyer, N., Nowack, M.K., Pusch, S., Stals, H., Inze, D., Grini, P.E., and Schnittger, A. (2007). T-loop phosphorylation of *Arabidopsis* CDKA;1 is required for its function and can be partially substituted by an aspartate residue. *Plant Cell* 19, 972–985.
- Dissmeyer, N., Weimer, A.K., Pusch, S., De Schutter, K., Alvim Kamei, C.L., Nowack, M.K., Novak, B., Duan, G.L., Zhu, Y.G., De Veylder, L., et al. (2009). Control of cell proliferation, organ growth, and DNA damage response operate independently of dephosphorylation of the *Arabidopsis* Cdk1 homolog CDKA;1. *Plant Cell* 21, 3641–3654.
- Dohmen, R.J. and Varshavsky, A. (2005). Heat-inducible degron and the making of conditional mutants. *Methods Enzymol.* 399, 799–822.
- Dohmen, R.J., Wu, P., and Varshavsky, A. (1994). Heat-inducible degron: a method for constructing temperature-sensitive mutants. *Science* 263, 1273–1276.
- Dougan, D.A., Truscott, K.N., and Zeth, K. (2010). The bacterial N-end rule pathway: expect the unexpected. *Mol. Microbiol.* 76, 545–558.
- Fang, G., Yu, H., and Kirschner, M.W. (1999). Control of mitotic transitions by the anaphase-promoting complex. *Philos. Trans. R. Soc. Lond. B Biol. Sci.* 354, 1583–1590.
- Feaver, W.J., Huang, W., and Friedberg, E.C. (1999). The TFB4 subunit of yeast TFIIH is required for both nucleotide excision repair and RNA polymerase II transcription. *J. Biol. Chem.* 274, 29564–29567.
- Fichtner, F., Urrea Castellanos, R., and Ulker, B. (2014). Precision genetic modifications: a new era in molecular biology and crop improvement. *Planta* 239, 921–939.
- Folkes, L.K., Dennis, M.F., Stratford, M.R., Candeias, L.P., and Wardman, P. (1999). Peroxidase-catalyzed effects of indole-3-acetic acid and analogues on lipid membranes, DNA, and mammalian cells *in vitro*. *Biochem. Pharmacol.* 57, 375–382.
- Fu, X., Ng, C., Feng, D., and Liang, C. (2003). Cdc48p is required for the cell cycle commitment point at Start via degradation of the G1-CDK inhibitor Far1p. *J. Cell Biol.* 163, 21–26.
- Gaj, T., Gersbach, C.A., and Barbas, C.F. (2013). ZFN, TALEN, and CRISPR/Cas-based methods for genome engineering. *Trends Biotechnol.* 31, 397–405.
- Gallie, D.R. (2010). Regulated ethylene insensitivity through the inducible expression of the Arabidopsis *etr1-1* mutant ethylene receptor in tomato. *Plant Physiol.* 152, 1928–1939.
- Gardner, R.D., Poddar, A., Yellman, C., Tavormina, P.A., Monteagudo, M.C., and Burke, D.J. (2001). The spindle checkpoint of the yeast *Saccharomyces cerevisiae* requires kinetochore function and maps to the CBF3 domain. *Genetics* 157, 1493–1502.
- Garooi, G.A., Salter, M.G., Caddick, M.X., and Tomsett, A.B. (2005). Characterization of the ethanol-inducible *alc* gene expression system in tomato. *J. Exp. Bot.* 56, 1635–1642.
- Gatz, C., Froberg, C., and Wendenburg, R. (1992). Stringent repression and homogeneous de-repression by tetracycline of a modified CaMV 35S promoter in intact transgenic tobacco plants. *Plant J.* 2, 397–404.
- Geimonen, E., Fernandez, I., Gavrilovskaya, I.N., and Mackow, E.R. (2003). Tyrosine residues direct the ubiquitination and degradation of the NY-1 hantavirus G1 cytoplasmic tail. *J. Virol.* 77, 10760–10868.
- Genschik, P., Criqui, M.C., Parmentier, Y., Derevier, A., and Fleck, J. (1998). Cell cycle-dependent proteolysis in plants. Identification of the destruction box pathway and metaphase arrest produced by the proteasome inhibitor mg132. *Plant Cell* 10, 2063–2076.
- Gibbs, D.J., Lee, S.C., Isa, N.M., Gramuglia, S., Fukao, T., Bassel, G.W., Correia, C.S., Corbinau, F., Theodoulou, F.L., Bailey-Serres, J., et al. (2011). Homeostatic response to hypoxia is regulated by the N-end rule pathway in plants. *Nature* 479, 415–418.
- Gibbs, D.J., Md Isa, N., Movahedi, M., Lozano-Juste, J., Mendiondo, G.M., Berckhan, S., Marin-de la Rosa, N., Vicente Conde, J., Sousa Correia, C., Pearce, S.P., et al. (2014). Nitric oxide sensing in plants is mediated by proteolytic control of group VII ERF transcription factors. *Mol. Cell* 53, 369–379.
- Glover, B.J., Perez-Rodriguez, M., and Martin, C. (1998). Development of several epidermal cell types can be specified by the same MYB-related plant transcription factor. *Development* 125, 3497–3508.
- Glover, B.J., Bunnewell, S., and Martin, C. (2004). Convergent evolution within the genus *Solanum*: the specialised anther cone develops through alternative pathways. *Gene* 331, 1–7.
- Gómez-Mena, C., de Folter, S., Costa, M.M., Angenent, G.C., and Sablowski, R. (2005). Transcriptional program controlled by the floral homeotic gene *AGAMOUS* during early organogenesis. *Development* 132, 429–438.
- Gonda, D.K., Bachmair, A., Wunning, I., Tobias, J.W., Lane, W.S., and Varshavsky, A. (1989). Universality and structure of the N-end rule. *J. Biol. Chem.* 264, 16700–16712.

- Graciet, E., Mesiti, F., and Wellmer, F. (2010). Structure and evolutionary conservation of the plant N-end rule pathway. *Plant J.* *61*, 741–751.
- Granger, C.L. and Cyr, R.J. (2000). Microtubule reorganization in tobacco BY-2 cells stably expressing GFP-MBD. *Planta* *210*, 502–509.
- Gray, W.M., Kepinski, S., Rouse, D., Leyser, O., and Estelle, M. (2001). Auxin regulates SCF(TIR1)-dependent degradation of AUX/IAA proteins. *Nature* *414*, 271–276.
- Gregán, J., Van Laer, L., Lieto, L.D., Van Camp, G., and Kearsley, S.E. (2003). A yeast model for the study of human DFNA5, a gene mutated in nonsyndromic hearing impairment. *Biochim. Biophys. Acta* *1638*, 179–186.
- Guo, H.S., Fei, J.F., Xie, Q., and Chua, N.H. (2003). A chemical-regulated inducible RNAi system in plants. *Plant J.* *34*, 383–392.
- Hackett, E.A., Esch, R.K., Maleri, S., and Errede, B. (2006). A family of destabilized cyan fluorescent proteins as transcriptional reporters in *S. cerevisiae*. *Yeast* *23*, 333–349.
- Hannah, J. and Zhou, P.B. (2011). Maximizing target protein ablation by integration of RNAi and protein knockout. *Cell Res.* *21*, 1152–1154.
- Hardy, C.F. (1996). Characterization of an essential Orc2p-associated factor that plays a role in DNA replication. *Mol. Cell. Biol.* *16*, 1832–1841.
- Harper, S.M., Neil, L.C., and Gardner, K.H. (2003). Structural basis of a phototropin light switch. *Science* *301*, 1541–1544.
- Hartwell, L.H. (1967). Macromolecule synthesis in temperature-sensitive mutants of yeast. *J. Bacteriol.* *93*, 1662–1670.
- Hartwell, L.H., Culotti, J., and Reid, B. (1970). Genetic control of the cell-division cycle in yeast. I. Detection of mutants. *Proc. Natl. Acad. Sci. USA* *66*, 352–359.
- Herm-Göltz, A., Agop-Nersesian, C., Munter, S., Grimley, J.S., Wandless, T.J., Frischknecht, F., and Meissner, M. (2007). Rapid control of protein level in the apicomplexan *Toxoplasma gondii*. *Nat. Methods* *4*, 1003–1005.
- Holland, A., Fachinetti, D., Han, J., and Cleveland, D.W. (2012). Inducible, reversible system for the rapid and complete degradation of proteins in mammalian cells. *Proc. Natl. Acad. Sci. USA* *109*, E3350–E3357.
- Houser, J.R., Ford, E., Chatterjea, S.M., Maleri, S., Elston, T.C., and Errede, B. (2012). An improved short-lived fluorescent protein transcriptional reporter for *Saccharomyces cerevisiae*. *Yeast* *29*, 519–530.
- Hwang, C.S., Shemorry, A., and Varshavsky, A. (2010). N-terminal acetylation of cellular proteins creates specific degradation signals. *Science* *327*, 973–977.
- Jakoby, M.J., Weinl, C., Pusch, S., Kuijt, S.J., Merkle, T., Dissmeyer, N., and Schnittger, A. (2006). Analysis of the subcellular localization, function, and proteolytic control of the *Arabidopsis* cyclin-dependent kinase inhibitor ICK1/KRP1. *Plant Physiol.* *141*, 1293–1305.
- Jungbluth, M., Renicke, C., and Taxis, C. (2010). Targeted protein depletion in *Saccharomyces cerevisiae* by activation of a bidirectional degron. *BMC Syst. Biol.* *4*, 176.
- Kanemaki, M.T. (2013). Frontiers of protein expression control with conditional degrons. *Pflugers Arch.* *465*, 419–425.
- Kanemaki, M., Sanchez-Diaz, A., Gambus, A., and Labib, K. (2003). Functional proteomic identification of DNA replication proteins by induced proteolysis *in vivo*. *Nature* *423*, 720–724.
- Kang, H.G., Fang, Y., and Singh, K.B. (1999). A glucocorticoid-inducible transcription system causes severe growth defects in *Arabidopsis* and induces defense-related genes. *Plant J.* *20*, 127–133.
- Kanke, M., Nishimura, K., Kanemaki, M., Kakimoto, T., Takahashi, T.S., Nakagawa, T., and Masukata, H. (2011). Auxin-inducible protein depletion system in fission yeast. *BMC Cell Biol.* *12*, 8.
- Kannangara, R., Branigan, C., Liu, Y., Penfield, T., Rao, V., Mouille, G., Hofte, H., Pauly, M., Riechmann, J.L., and Broun, P. (2007). The transcription factor WIN1/SHN1 regulates Cutin biosynthesis in *Arabidopsis thaliana*. *Plant Cell* *19*, 1278–1294.
- Kearsley, S.E. and Grégan, J. (2009). Using the DHFR heat-inducible degron for protein inactivation in *Schizosaccharomyces pombe*. *Methods Mol. Biol.* *521*, 483–492.
- Ketelaar, T., Allwood, E.G., Anthony, R., Voigt, B., Menzel, D., and Hussey, P.J. (2004). The actin-interacting protein AIP1 is essential for actin organization and plant development. *Curr. Biol.* *14*, 145–149.
- Kim, S.Y., Hong, C.B., and Lee, I. (2001). Heat shock stress causes stage-specific male sterility in *Arabidopsis thaliana*. *J. Plant Res.* *114*, 301–307.
- Kim, H.K., Kim, R.R., Oh, J.H., Cho, H., Varshavsky, A., and Hwang, C.S. (2014). The N-terminal methionine of cellular proteins as a degradation signal. *Cell* *156*, 158–169.
- King, R.W., Deshaies, R.J., Peters, J.M., and Kirschner, M.W. (1996). How proteolysis drives the cell cycle. *Science* *274*, 1652–1659.
- Kirik, V., Simon, M., Wester, K., Schiefelbein, J., and Hulskamp, M. (2004). ENHANCER of TRY and CPC 2 (ETC2) reveals redundancy in the region-specific control of trichome development of *Arabidopsis*. *Plant Mol. Biol.* *55*, 389–398.
- Koo, J.C., Asurmendi, S., Bick, J., Woodford-Thomas, T., and Beachy, R.N. (2004). Ecdysone agonist-inducible expression of a coat protein gene from tobacco mosaic virus confers viral resistance in transgenic *Arabidopsis*. *Plant J.* *37*, 439–448.
- Kreidenweiss, A., Hopkins, A.V., and Mordmuller, B. (2013). 2A and the auxin-based degron system facilitate control of protein levels in *Plasmodium falciparum*. *PLoS One* *8*, e78661.
- Kubo, M., Imai, A., Nishiyama, T., Ishikawa, M., Sato, Y., Kurata, T., Hiwatashi, Y., Reski, R., and Hasebe, M. (2013). System for stable β -estradiol-inducible gene expression in the moss *Physcomitrella patens*. *PLoS One* *8*, e77356.
- Kulemzina, I., Schumacher, M.R., Verma, V., Reiter, J., Metzler, J., Failla, A.V., Lanz, C., Sreedharan, V.T., Ratsch, G., and Ivanov, D. (2012). Cohesin rings devoid of Scc3 and Pds5 maintain their stable association with the DNA. *PLoS Genet.* *8*, e1002856.
- Labib, K., Tercero, J.A., and Diffley, J.F. (2000). Uninterrupted MCM2–7 function required for DNA replication fork progression. *Science* *288*, 1643–1647.
- Licausi, F., Kosmacz, M., Weits, D.A., Giuntoli, B., Giorgi, F.M., Voesenek, L.A., Perata, P., and van Dongen, J.T. (2011). Oxygen sensing in plants is mediated by an N-end rule pathway for protein destabilization. *Nature* *479*, 419–422.
- Lindner, K., Grégan, J., Montgomery, S., and Kearsley, S.E. (2002). Essential role of MCM proteins in premeiotic DNA replication. *Mol. Biol. Cell* *13*, 435–444.
- Love, J., Scott, A.C., and Thompson, W.F. (2000). Technical advance: stringent control of transgene expression in *Arabidopsis thaliana* using the Top10 promoter system. *Plant J.* *21*, 579–588.
- Maizel, A. and Weigel, D. (2004). Temporally and spatially controlled induction of gene expression in *Arabidopsis thaliana*. *Plant J.* *38*, 164–171.

- Martinez, A., Sparks, C., Hart, C.A., Thompson, J., and Jepson, I. (1999). Ecdysone agonist inducible transcription in transgenic tobacco plants. *Plant J.* 19, 97–106.
- Masclaux, F., Charpentreau, M., Takahashi, T., Pont-Lezica, R., and Galaud, J.P. (2004). Gene silencing using a heat-inducible RNAi system in *Arabidopsis*. *Biochem. Biophys. Res. Commun.* 321, 364–369.
- McIsaac, R.S., Silverman, S.J., McClean, M.N., Gibney, P.A., Mac-inskas, J., Hickman, M.J., Petti, A.A., and Botstein, D. (2011). Fast-acting and nearly gratuitous induction of gene expression and protein depletion in *Saccharomyces cerevisiae*. *Mol. Biol. Cell* 22, 4447–4459.
- Melvin, A.T., Woss, G.S., Park, J.H., Dumberger, L.D., Waters, M.L., and Allbritton, N.L. (2013). A comparative analysis of the ubiquitination kinetics of multiple degrons to identify an ideal targeting sequence for a proteasome reporter. *PLoS One* 8, e78082.
- Mett, V.L., Lochhead, L.P., and Reynolds, P.H. (1993). Copper-controllable gene expression system for whole plants. *Proc. Natl. Acad. Sci. USA* 90, 4567–4571.
- Mills, E. and Truong, K. (2013). Photoswitchable protein degradation: a generalizable control module for cellular function? *Chem. Biol.* 20, 458–460.
- Mogk, A., Schmidt, R., and Bukau, B. (2007). The N-end rule pathway for regulated proteolysis: prokaryotic and eukaryotic strategies. *Trends Cell Biol.* 17, 165–172.
- Moore, I., Samalova, M., and Kurup, S. (2006). Transactivated and chemically inducible gene expression in plants. *Plant J.* 45, 651–683.
- Muhua, L., Adames, N.R., Murphy, M.D., Shields, C.R., and Cooper, J.A. (1998). A cytokinesis checkpoint requiring the yeast homologue of an APC-binding protein. *Nature* 393, 487–491.
- Müller, K., Siegel, D., Rodriguez Jahnke, F., Gerrer, K., Wend, S., Decker, E.L., Reski, R., Weber, W., and Zurbriggen, M.D. (2014). A red light-controlled synthetic gene expression switch for plant systems. *Mol. Biosyst.* Epub 12 Dec 2013. doi:10.1039/C3MB70579J.
- Nishimura, K., Fukagawa, T., Takisawa, H., Kakimoto, T., and Kanemaki, M. (2009). An auxin-based degron system for the rapid depletion of proteins in nonplant cells. *Nat. Methods* 6, 917–922.
- Ó'Maoiléidigh, D.S., Wuest, S.E., Rae, L., Raganelli, A., Ryan, P.T., Kwasniewska, K., Das, P., Lohan, A.J., Loftus, B., Graciet, E., et al. (2013). Control of reproductive floral organ identity specification in *Arabidopsis* by the C function regulator AGAMOUS. *Plant Cell* 25, 2482–2503.
- Ouwerkerk, P.B., de Kam, R.J., Hoge, J.H., and Meijer, A.H. (2001). Glucocorticoid-inducible gene expression in rice. *Planta* 213, 370–378.
- Paddison, P.J., Caudy, A.A., and Hannon, G.J. (2002). Stable suppression of gene expression by RNAi in mammalian cells. *Proc. Natl. Acad. Sci. USA* 99, 1443–1448.
- Padidam, M., Gore, M., Lu, D.L., and Smirnova, O. (2003). Chemical-inducible, ecdysone receptor-based gene expression system for plants. *Transgenic Res.* 12, 101–109.
- Park, E.C., Finley, D., and Szostak, J.W. (1992). A strategy for the generation of conditional mutations by protein destabilization. *Proc. Natl. Acad. Sci. USA* 89, 1249–1252.
- Parsons, A.B., Brost, R.L., Ding, H., Li, Z., Zhang, C., Sheikh, B., Brown, G.W., Kane, P.M., Hughes, T.R., and Boone, C. (2004). Integration of chemical-genetic and genetic interaction data links bioactive compounds to cellular target pathways. *Nat. Biotechnol.* 22, 62–69.
- Passmore, L.A., McCormack, E.A., Au, S.W., Paul, A., Willison, K.R., Harper, J.W., and Barford, D. (2003). Doc1 mediates the activity of the anaphase-promoting complex by contributing to substrate recognition. *EMBO J.* 22, 786–796.
- Payne, T., Clement, J., Arnold, D., and Lloyd, A. (1999). Heterologous myb genes distinct from GL1 enhance trichome production when overexpressed in *Nicotiana tabacum*. *Development* 126, 671–682.
- Pedley, K.F. and Martin, G.B. (2004). Identification of MAPKs and their possible MAPK kinase activators involved in the Pto-mediated defense response of tomato. *J. Biol. Chem.* 279, 49229–49235.
- Perrimon, P., Ni, J.-Q., and Perkins, L. (2010). In vivo RNAi: Today and Tomorrow. *Cold Spring Harb. Perspect. Biol.* 2, a003640. Epub 2010 Jun 9. doi: 10.1101/cshperspect.a003640.
- Pesin, J.A. and Orr-Weaver, T.L. (2008). Regulation of APC/C activators in mitosis and meiosis. *Annu. Rev. Cell Dev. Biol.* 24, 475–499.
- Peters, J.M. (2006). The anaphase promoting complex/cyclosome: a machine designed to destroy. *Nat. Rev. Mol. Cell Biol.* 7, 644–656.
- Piatkov, K.I., Brower, C.S., and Varshavsky, A. (2012). The N-end rule pathway counteracts cell death by destroying proapoptotic protein fragments. *Proc. Natl. Acad. Sci. USA* 109, E1839–E1847.
- Piazzon, N., Schlotter, F., Lefebvre, S., Dodre, M., Mereau, A., Soret, J., Besse, A., Barkats, M., Bordonne, R., Branlant, C., et al. (2012). Implication of the SMN complex in the biogenesis and steady state level of the signal recognition particle. *Nucleic Acids Res.* 41, 1255–1272.
- Potuschak, T., Stary, S., Schlogelhofer, P., Becker, F., Nejmiskaia, V., and Bachmair, A. (1998). PRT1 of *Arabidopsis thaliana* encodes a component of the plant N-end rule pathway. *Proc. Natl. Acad. Sci. USA* 95, 7904–7908.
- Prabha, C.R., Mukherjee, S., Raman, R., and Kulkarni, S. (2012). The ends and means of artificially induced targeted protein degradation. *Appl. Microbiol. Biotechnol.* 96, 1111–1123.
- Rajagopalan, S., Liling, Z., Liu, J., and Balasubramanian, M. (2004). The N-degron approach to create temperature-sensitive mutants in *Schizosaccharomyces pombe*. *Methods* 33, 206–212.
- Rakhit, R., Edwards, S.R., Iwamoto, M., and Wandless, T.J. (2011). Evaluation of FKBP and DHFR based destabilizing domains in *Saccharomyces cerevisiae*. *Bioorg. Med. Chem. Lett.* 21, 4965–4968.
- Rao, H., Uhlmann, F., Nasmyth, K., and Varshavsky, A. (2001). Degradation of a cohesin subunit by the N-end rule pathway is essential for chromosome stability. *Nature* 410, 955–959.
- Ren, Q., Liou, L.C., Gao, Q., Bao, X., and Zhang, Z. (2012). Bir1 deletion causes malfunction of the spindle assembly checkpoint and apoptosis in yeast. *Front. Oncol.* 2, 93.
- Renicke, C., Schuster, D., Usherenko, S., Essen, L.O., and Taxis, C. (2013a). A LOV2 domain-based optogenetic tool to control protein degradation and cellular function. *Chem. Biol.* 20, 619–626.
- Renicke, C., Spadaccini, R., and Taxis, C. (2013b). A tobacco etch virus protease with increased substrate tolerance at the P1' position. *PLoS One* 8, e67915.

- Roberts, G.R., Garoosi, G.A., Koroleva, O., Ito, M., Laufs, P., Leader, D.J., Caddick, M.X., Doonan, J.H., and Tomsett, A.B. (2005). The alc-GR system: a modified alc gene switch designed for use in plant tissue culture. *Plant Physiol.* **138**, 1259–1267.
- Rodriguez, S. and Wolfgang, M. (2012). Targeted chemical-genetic regulation of protein stability in vivo. *Chem. Biol.* **19**, 391–398.
- Roslan, H.A., Salter, M.G., Wood, C.D., White, M.R., Croft, K.P., Robson, F., Coupland, G., Doonan, J., Laufs, P., Tomsett, A.B., et al. (2001). Characterization of the ethanol-inducible alc gene-expression system in *Arabidopsis thaliana*. *Plant J.* **28**, 225–235.
- Saijo, T. and Nagasawa, A. (2014). Development of a tightly regulated and highly responsive copper-inducible gene expression system and its application to control of flowering time. *Plant Cell Rep.* **33**, 47–59.
- Saini, P., Eyler, D.E., Green, R., and Dever, T.E. (2009). Hypusine-containing protein eIF5A promotes translation elongation. *Nature* **459**, 118–121.
- Sakamoto, K.M., Kim, K.B., Kumagai, A., Mercurio, F., Crews, C.M., and Deshaies, R.J. (2001). Protacs: chimeric molecules that target proteins to the Skp1-Cullin-F box complex for ubiquitination and degradation. *Proc. Natl. Acad. Sci. USA* **98**, 8554–8559.
- Salter, M.G., Paine, J.A., Riddell, K.V., Jepson, I., Greenland, A.J., Caddick, M.X., and Tomsett, A.B. (1998). Characterisation of the ethanol-inducible alc gene expression system for transgenic plants. *Plant J.* **16**, 127–132.
- Samalova, M., Brzobohaty, B., and Moore, I. (2005). pOp6/LhGR: a stringently regulated and highly responsive dexamethasone-inducible gene expression system for tobacco. *Plant J.* **41**, 919–935.
- Schaarschmidt, S., Qu, N., Strack, D., Sonnewald, U., and Hause, B. (2004). Local induction of the alc gene switch in transgenic tobacco plants by acetaldehyde. *Plant Cell Physiol.* **45**, 1566–1577.
- Schilmiller, A.L., Last, R.L., and Pichersky, E. (2008). Harnessing plant trichome biochemistry for the production of useful compounds. *Plant J.* **54**, 702–711.
- Schneekloth, J.S. J., Fonseca, F.N., Koldobskiy, M., Mandal, A., Deshaies, R., Sakamoto, K., and Crews, C.M. (2004). Chemical genetic control of protein levels: selective *in vivo* targeted degradation. *J. Am. Chem. Soc.* **126**, 3748–3754.
- Schnittger, A., Schobinger, U., Stierhof, Y.D., and Hulskamp, M. (2002). Ectopic B-type cyclin expression induces mitotic cycles in endoreduplicating *Arabidopsis* trichomes. *Curr. Biol.* **12**, 415–420.
- Schwab, R., Ossowski, S., Riester, M., Warthmann, N., and Weigel, D. (2006). Highly specific gene silencing by artificial microRNAs in *Arabidopsis*. *Plant Cell* **18**, 1121–1133.
- Sen, N., Sen, A., and Mackow, E.R. (2007). Degrons at the C terminus of the pathogenic but not the nonpathogenic hantavirus G1 tail direct proteasomal degradation. *J. Virol.* **81**, 4323–4330.
- Sheard, L.B., Tan, X., Mao, H., Withers, J., Ben-Nissan, G., Hinds, T.R., Kobayashi, Y., Hsu, F.F., Sharon, M., Browse, J., et al. (2010). Jasmonate perception by inositol-phosphate-potentiated CO11-JAZ co-receptor. *Nature* **468**, 400–405.
- Speese, S.D., Trotta, N., Rodesch, C.K., Aravamudan, B., and Broadie, K. (2003). The ubiquitin proteasome system acutely regulates presynaptic protein turnover and synaptic efficacy. *Curr. Biol.* **13**, 899–910.
- Sreekala, C., Wu, L., Gu, K., Wang, D., Tian, D., and Yin, Z. (2005). Excision of a selectable marker in transgenic rice (*Oryza sativa* L.) using a chemically regulated Cre/loxP system. *Plant Cell Rep.* **24**, 86–94.
- Stary, S., Yin, X.J., Potuschak, T., Schlogelhofer, P., Nizhynska, V., and Bachmair, A. (2003). PRT1 of *Arabidopsis* is a ubiquitin protein ligase of the plant N-end rule pathway with specificity for aromatic amino-terminal residues. *Plant Physiol.* **133**, 1360–1366.
- Stegmeier, F., Visintin, R., and Amon, A. (2002). Separase, polo kinase, the kinetochore protein Slk19, and Spo12 function in a network that controls Cdc14 localization during early anaphase. *Cell* **108**, 207–220.
- Su, Y., Ishikawa, S., Kojima, M. and Liu, B. (2003). Eradication of pathogenic β -catenin by Skp1/Cullin/F box ubiquitination machinery. *Proc. Natl. Acad. Sci. USA* **100**, 12729–12734.
- Su, X., Bernal, J.A., and Venkitaraman, A.R. (2008). Cell-cycle coordination between DNA replication and recombination revealed by a vertebrate N-end rule degron-Rad51. *Nat. Struct. Mol. Biol.* **15**, 1049–1058.
- Suzuki, T. and Varshavsky, A. (1999). Degradation signals in the lysine-asparagine sequence space. *EMBO J.* **18**, 6017–6026.
- Sweetman, J.P., Chu, C., Qu, N., Greenland, A.J., Sonnewald, U., and Jepson, I. (2002). Ethanol vapor is an efficient inducer of the alc gene expression system in model and crop plant species. *Plant Physiol.* **129**, 943–948.
- Takahashi, T. and Komeda, Y. (1989). Characterization of two genes encoding small heat-shock proteins in *Arabidopsis thaliana*. *Mol. Gen. Genet.* **219**, 365–372.
- Takahashi, T., Naito, S., and Komeda, Y. (1992). The *Arabidopsis* HSP18.2 promoter/GUS gene fusion in transgenic *Arabidopsis* plants – a powerful tool for the isolation of regulatory mutants of the heat-shock response. *Plant J.* **2**, 751–761.
- Takemoto, D. and Jones, D.A. (2005). Membrane release and destabilization of *Arabidopsis* RIN4 following cleavage by *Pseudomonas syringae* AvrRpt2. *Mol. Plant Microbe Interact.* **18**, 1258–1268.
- Takeuchi, J., Chen, H., Hoyt, M.A., and Coffino, P. (2008). Structural elements of the ubiquitin-independent proteasome degron of ornithine decarboxylase. *Biochem J.* **410**, 401–407.
- Tasaki, T., Mulder, L.C., Iwamatsu, A., Lee, M.J., Davydov, I.V., Varshavsky, A., Muesing, M., and Kwon, Y.T. (2005). A family of mammalian E3 ubiquitin ligases that contain the UBR box motif and recognize N-degrons. *Mol. Cell Biol.* **25**, 7120–7136.
- Taxis, C., Stier, G., Spadaccini, R., and Knop, M. (2009). Efficient protein depletion by genetically controlled deprotection of a dormant N-degron. *Mol. Syst. Biol.* **5**, 267.
- Tercero, J.A., Labib, K., and Diffley, J.F. (2000). DNA synthesis at individual replication forks requires the essential initiation factor Cdc45p. *EMBO J.* **19**, 2082–2093.
- Thines, B., Katsir, L., Melotto, M., Niu, Y., Mandaokar, A., Liu, G., Nomura, K., He, S.Y., Howe, G.A., and Browse, J. (2007). JAZ repressor proteins are targets of the SCF(CO1) complex during jasmonate signalling. *Nature* **448**, 661–665.
- Ülker, B., Peiter, E., Dixon, D.P., Moffat, C., Capper, R., Bouché, N., Edwards, R., Sanders, D., Knight, H., and Knight, M.R. (2008). Getting the most out of publicly available T-DNA insertion lines. *Plant J.* **56**, 665–677.

- Varshavsky, A. (1991). Naming a targeting signal. *Cell* *64*, 13–15.
- Varshavsky, A. (2005). Ubiquitin fusion technique and related methods. *Methods Enzymol.* *399*, 777–799.
- Varshavsky, A. (2011). The N-end rule pathway and regulation by proteolysis. *Protein Sci.* *20*, 1298–1345.
- Vodenicharov, M.D. and Wellinger, R.J. (2006). DNA degradation at unprotected telomeres in yeast is regulated by the CDK1 (Cdc28/Clb) cell-cycle kinase. *Mol. Cell* *24*, 127–137.
- Wang, S., Wang, J.W., Yu, N., Li, C.H., Luo, B., Gou, J.Y., Wang, L.J., and Chen, X.Y. (2004). Control of plant trichome development by a cotton fiber MYB gene. *Plant Cell* *16*, 2323–2334.
- Watae, G., Takisawa, H., and Kanemaki, M.T. (2012). Mcm10 plays a role in functioning of the eukaryotic replicative DNA helicase, Cdc45-Mcm-GINS. *Curr. Biol.* *22*, 343–349.
- Weingartner, M., Criqui, M.C., Meszaros, T., Binarova, P., Schmit, A.C., Helfer, A., Derevier, A., Erhardt, M., Bogre, L., and Genschik, P. (2004). Expression of a nondegradable cyclin B1 affects plant development and leads to endomitosis by inhibiting the formation of a phragmoplast. *Plant Cell* *16*, 643–657.
- Weinmann, P., Gossen, M., Hillen, W., Bujard, H., and Gatz, C. (1994). A chimeric transactivator allows tetracycline-responsive gene expression in whole plants. *Plant J.* *5*, 559–569.
- Weits, D.A., Giuntoli, B., Kosmacz, M., Parlanti, S., Hubberten, H.M., Riegler, H., Hoefgen, R., Perata, P., van Dongen, J.T., and Licausi, F. (2014). Plant cysteine oxidases control the oxygen-dependent branch of the N-end-rule pathway. *Nat. Commun.* *6*, 3425. doi: 10.1038/ncomms4425.
- Wellmer, F., Alves-Ferreira, M., Dubois, A., Riechmann, J.L., and Meyerowitz, E.M. (2006). Genome-wide analysis of gene expression during early *Arabidopsis* flower development. *PLoS Genet.* *2*, e117.
- Wester, K., Digiuni, S., Geier, F., Timmer, J., Fleck, C., and Hulskamp, M. (2009). Functional diversity of R3 single-repeat genes in trichome development. *Development* *136*, 1487–1496.
- Wielopolska, A., Townley, H., Moore, I., Waterhouse, P., and Helliwell, C. (2005). A high-throughput inducible RNAi vector for plants. *Plant Biotechnol. J.* *3*, 583–590.
- Yan, Y., Stolz, S., Chetelat, A., Reymond, P., Pagni, M., Dubugnon, L., and Farmer, E.E. (2007). A downstream mediator in the growth repression limb of the jasmonate pathway. *Plant Cell* *19*, 2470–2483.
- Yang, C., Li, H., Zhang, J., Luo, Z., Gong, P., Zhang, C., Li, J., Wang, T., Zhang, Y., Lu, Y. et al. (2011). A regulatory gene induces trichome formation and embryo lethality in tomato. *Proc. Natl. Acad. Sci. USA* *108*, 11836–11841.
- Yang, J., Ordiz, M.I., Semenyuk, E.G., Kelly, B., and Beachy, R.N. (2012). A safe and effective plant gene switch system for tissue-specific induction of gene expression in *Arabidopsis thaliana* and *Brassica juncea*. *Transgenic Res.* *21*, 879–883.
- Yoshida, K., Kasai, T., Garcia, M.R., Sawada, S., Shoji, T., Shimizu, S., Yamazaki, K., Komeda, Y., and Shinmyo, A. (1995). Heat-inducible expression system for a foreign gene in cultured tobacco cells using the HSP18.2 promoter of *Arabidopsis thaliana*. *Appl. Microbiol. Biotechnol.* *44*, 466–472.
- Zhang, Y., Yu, Z., Fu, X., and Liang, C. (2002). Noc3p, a bHLH protein, plays an integral role in the initiation of DNA replication in budding yeast. *Cell* *109*, 849–860.
- Zhang, J., Zheng, N., and Zhou, P. (2003). Exploring the functional complexity of cellular proteins by protein knockout. *Proc. Natl. Acad. Sci. USA* *100*, 14127–14132.
- Zhou, P. (2005). Targeted protein degradation. *Curr. Opin. Chem. Biol.* *9*, 51–55.
- Zhou, P., Bogacki, R., McReynolds, L., and Howley, P.M. (2000). Harnessing the ubiquitination machinery to target the degradation of specific cellular proteins. *Mol. Cell* *6*, 751–756.
- Zuo, J.R. and Chua, N.H. (2000) Chemical-inducible systems for regulated expression of plant genes. *Curr. Opin. Biotechnol.* *11*, 146–151.
- Zuo, J., Niu, Q.W., and Chua, N.H. (2000). Technical advance: an estrogen receptor-based transactivator XVE mediates highly inducible gene expression in transgenic plants. *Plant J.* *24*, 265–273.

Supplemental Material: The online version of this article (DOI 10.1515/hsz-2014-0160) offers supplementary material, available to authorized users.

2.1.2 Manipulation of biological processes via conditional proteolysis

In my lab, we have introduced the low-temperature degron (It-degron) to various intact multicellular organisms which allows to control target protein levels and therefore function and activity directly on the level of active protein. The It-degron uses a combination of Ubiquitin-fusion technique linking target protein degradation to the N-end rule pathway of targeted proteolysis coupled to the use of cell- and tissue-specific promoters.

Publication:

Dissmeyer N. Conditional modulation of biological processes by low-temperature degrons.

Methods Mol Biol. In print.

Chapter 30

Conditional Modulation of Biological Processes by Low-Temperature Degrons

Nico Dissmeyer

Abstract

Conditional modulation of biological processes plays key roles in basic and applied research and in translation. It can be achieved on various levels via a multitude of approaches. One of the directions is manipulating target protein levels and activity by transcriptional, posttranscriptional, translational, and posttranslational control. Because in most of these techniques, the synthesis of the target proteins is adjusted to the needs, they all rely on the specific half life of the target protein and its turn over. Therefore, their time of action, in direct correlation to the desired reprogramming of molecular phenotypes caused by altering the target levels, is fixed and determined by the naturally inherent properties. We have introduced the low temperature degron (lt degron) to various intact multicellular organisms which allows to control target protein levels and herefore function and activity directly on the level of active protein. The lt degron uses a combination of Ubiquitin fusion technique linking target protein degradation to the N end rule pathway of targeted proteolysis coupled with the use of cell and tissue specific promoters.

Key words Conditional allele, Conditional genetics, Protein degradation, Proteostasis, N end rule, Ubiquitination

1 Introduction

The lt-degron can be used to conditionally accumulate, deplete, or tune levels of target proteins in vivo in multicellular organisms and to conditionally complement mutants (Fig. 1) [1]. Especially the latter possibility makes it a prime tool for dissection of gene and protein function in contexts which are otherwise hard or impossible to address, for example, lethal mutations of essential genes or those genes which are expressed in a cell-type or spatiotemporally specific manner [2].

In our experience, the lt-degron worked reliably for a broad number of proteins of interest (POIs) such as transcription factors, kinases, hydrolases, decarboxylases, proteases, highly active enzymes, and very stable proteins in various host systems and multicellular organisms like plants, insects, yeast, and cell cultures [1].

Nico Dissmeyer

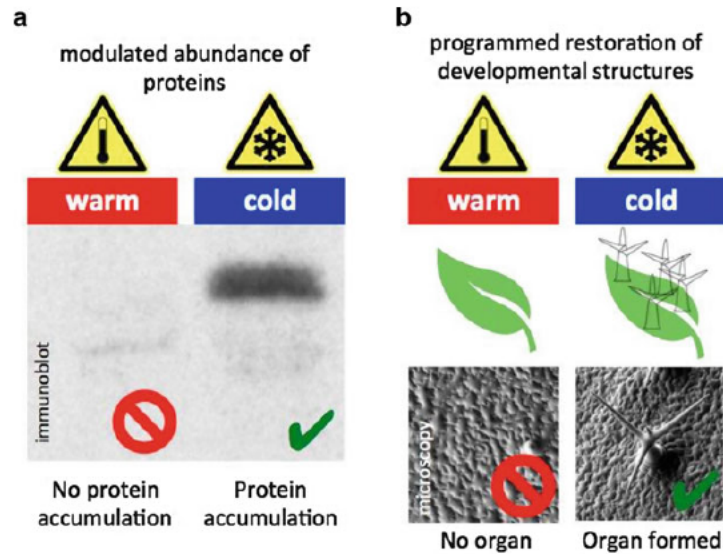


Fig. 1 Application of the It-degron system. (a) Production of proteins in conditional alleles and (b) example for the establishment of phenotypes on demand in vivo

However, several precautions are to be taken into account in terms of target selection. The POI needs to be at least transiently located in one of the compartments with an active N-end rule pathway and Ubiquitin proteasome system, i.e., the nucleus and the cytosol.

Depending on the POI, intrinsic factors such as aggregation and oligomerization might play a role in final degradation dynamics and lead to longer protein half-lives. Highly active enzymes, cytotoxic proteins, or those with a high “biological” activity such as certain transcription factors might require special handling and tuning of the It-degron system as a slow response of the system or a leakiness will lead to a failure of the conditionality. Last but not least, potential interferences of the relatively small N-terminal It-degron tag which mainly consists of a thermolabile mouse dihydrofolate reductase (DHFR, 22 kDa) and linker sequences, need to be taken into account (Fig. 2). Steric hindrance might – as in each and every fusion protein – cause structural problems such as conformational errors and in the end loss of function of the It-degron fusion. The temperature might interfere with desired effects such as protein function, enzyme activity, or development of the tissue or cell type of interest which shall be modulated via this technique.

Once a testable system is generated, that is either a stably transformed line or a transiently transformed or transfected tissue or cell culture, the restrictive and permissive temperatures need to

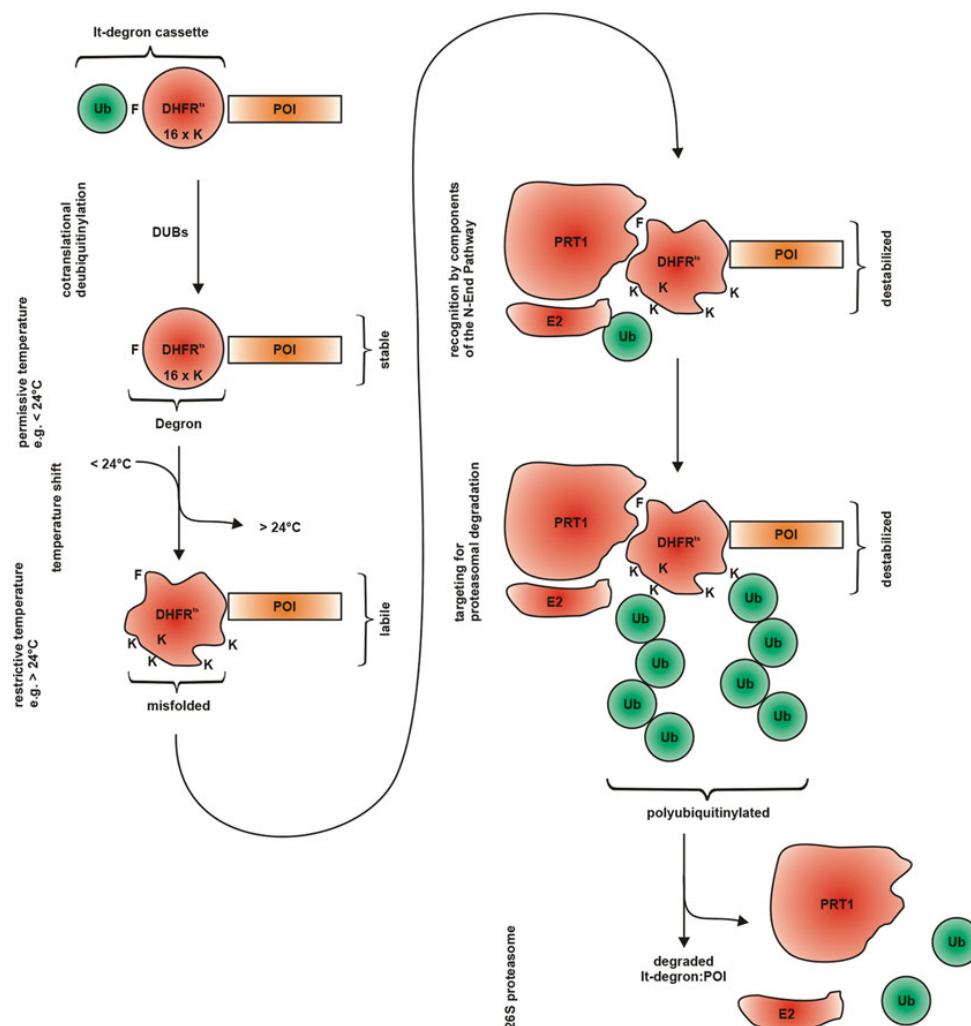


Fig. 2 The It-degron approach. Low temperature (It)-degron constructs contain an N-terminal degron cassette starting with a sequence encoding one single ubiquitin (Ub; Ub-fusion technique) followed by mouse dihydrofolate reductase (DHFR) with the first triplet coding for a destabilizing residue (here the bulky hydrophobic amino acid phenylalanine; F). The protein of interest (POI) is fused to the amino-terminal end of the cassette. The It-degron fusion protein consists of an N-terminal Ub (76 amino acids, 8.5 kDa) and the destabilizing residue preceding the temperature-sensitive (ts) variant of mouse DHFR (22 kDa). DHFR contains 16 Lys (K) residues that can be partially exposed to the surface at restrictive temperatures. The Ub-fusion technique (UFT) is based on the cotranslational deubiquitylation by deubiquitylating enzymes (DUBs) and Ub-specific processing proteases (Ubps) or deubiquitinating enzymes (DUBs) revealing the actual N-degron which is (partially) inactive at permissive temperature (up to 25 °C in Arabidopsis, tobacco, Drosophila an cell cultures). A shift to restrictive temperature (above 25 °C using our low-temperature (It)-degron) promotes DHFRts flexibility and exposure of internal Lys residues. The destabilizing N-terminal residue (F) is recognized by the N-recogin PROTEOLYSIS1 (PRT1), an E3 ligase, which represents the initial N-end rule pathway recognition component (Mot et al. 2017). E1 Ub-activating enzyme and E2 Ub-conjugating enzyme prime Ub for transfer to the DHFR moiety of the fusion protein. Polyubiquitylation targets the entire fusion protein for degradation by the 26S proteasome

Nico Dissmeyer

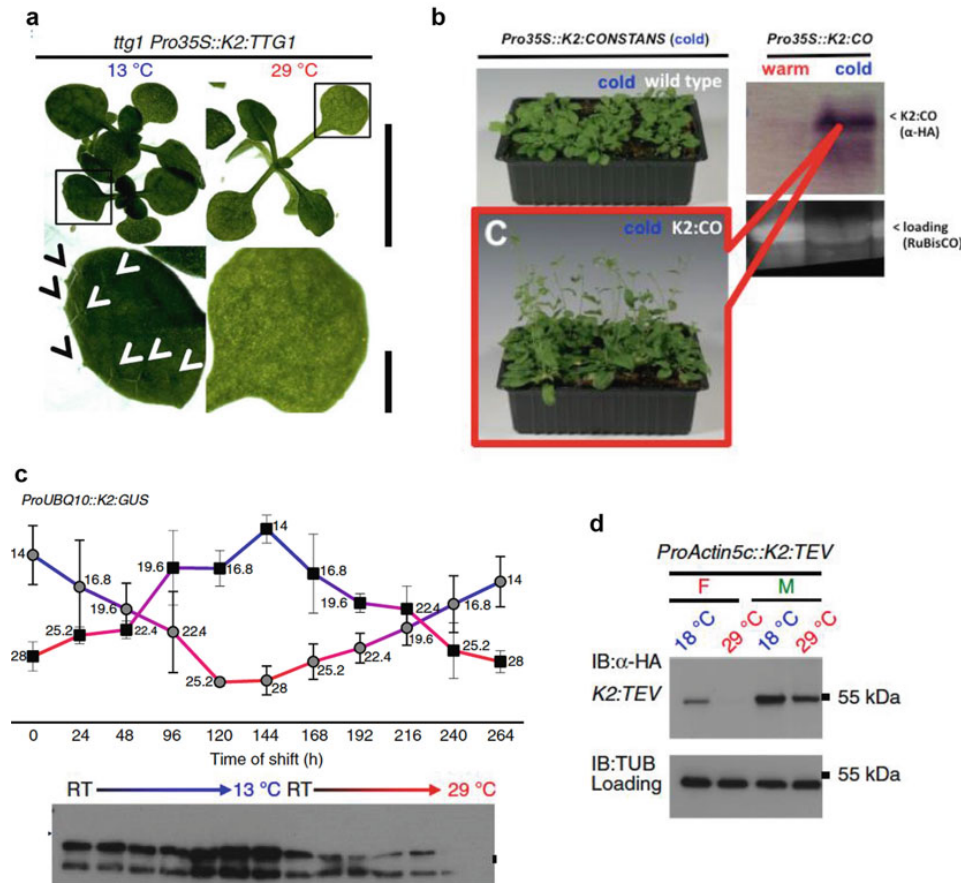


Fig. 3 Examples for use of the It-degron in *Arabidopsis* and *Drosophila*. (a) Conditional protein depletion/accumulation causes developmental phenotypes on demand in vivo and can be used to develop trichome cells in *Arabidopsis*. (b) Switchable flower meristems by conditional accumulation of It-CONSTANS transcription factor by low temperature. (c) In vivo depletion of proteins and inactivation of enzymes as new tool for tuning of activity levels via conditional protein degradation of It-degron fusion proteins. (d) Conditional protein depletion in living *Drosophila* flies. Modified from Faden et al. (2016), *Nature Communications*

be individually determined as they depend on POI, organism or system, and equipment (for examples, see Fig. 3) [1].

2 Materials

2.1 Cloning of It-degron Constructs

1. It-degron containing plasmid pEN-L1-K2-L2 (Addgene plasmid # 80684; [1]) (see Note 1).
2. Transformation system (vector) containing promoters of choice, e.g., cell- or tissue-specific or ubiquitously active such

Phenotypes on Demand by Low-Temperature Degrons

as ProUBQ10 (Addgene plasmid # 79751) or Pro35S (pLEELA; Addgene plasmid # 79752) (*see Note 2*).

3. Standard cloning equipment.

2.2 Selection of It-degron Lines

1. Standard selection media or solutions depending on the transformation vectors used such as Kanamycin or DL-Phosphinotricin (ammonium glufosinate, Basta; Santa Cruz Biotechnology).

2. Anti-HA epitope (hemagglutinin epitope tag) antibody: mouse monoclonal Anti-HA.11 Epitope Tag, Mouse IgG1, Clone: 16B12, MMS-101R, BioLegend or HISS (*see Note 3*); in a 1:1000 dilution in standard Tris-buffered saline with Tween 20 (TBST) 5% milk.

3. Optional: anti-DHFR (human dihydrofolate reductase) antibody: mouse monoclonal DHFR A-4 (sc-74593, Santa Cruz Biotechnology); 1:1000 dilution in TBST 5% milk.

4. Optional: Criterion Dodeca Cell (Bio-Rad) (*see Note 4*).

5. Optional: methotrexate (Santa Cruz Biotechnology).

6. Optional: Arabidopsis *prt1-1* mutant as control (*see Note 5*).

2.3 Application of It-degron Lines

1. Growth cabinets.

2. Temperature logger (*see Note 6*).

3. If applicable, specific needs for selection tailored to targeted POI.

3 Methods

3.1 Cloning of It-degron Constructs

Standard assembly techniques are used here such as PCR and gateway cloning or construct can be optimized for Modular Cloning such as via Golden Gate Assembly or GoldenBraid (*see Note 7*).

3.2 Selection of It-degron Lines

Selection can be done under restrictive or permissive or both temperatures and in case of stable transformation, the aim is to discard most of the lines where the conditional phenotype does not occur or is difficult to isolate. At the same time, those individuals can be collected with the desired phenotype or phenotypic range to use for further characterization. This phenotype can be investigated on macro- and microscopical as well as on molecular level, including identification of the levels of It-degron fusion protein and the activity of the POI, if applicable (e.g., when working with a conditional enzyme) (*see Note 8*).

1. Start off with choosing the appropriate experimental environment for the selection of It-degron lines, this can be growth cabinets with highly controlled environments, growth

Nico Dissmeyer

chambers with controlled environment, or standard growth rooms and greenhouses.

2. If only one growth compartment is available, initially, only one temperature condition will be able for selection; choose between restrictive or permissive temperature depending on the expected read-out of the It-degron function and the associated feasibility of screening (see above).
3. If possible from the growth and cultivation infrastructure, choose the restrictive or permissive temperatures as “extreme” as possible, that is restrictive as high as 30 °C or permissive as low as 8–10 °C [1].
4. If working with two temperature conditions for selection in parallel, continue as described previously but in two different growth environments.
5. Allow the plants to grow like under standard greenhouse conditions except by keeping them at different temperatures, if this growth regime is not conflicting the function or selection of the chosen POI.
6. If the characteristics of the chosen POI, e.g., when cytotoxic or triggering a developmental phenotype, require specific spatio-temporal induction of the expression of the It-degron:POI fusion, then this algorithm needs to be adjusted by reducing the time of growth at either restrictive or permissive temperature. If there are no conflicts for growth performance or selectivity are expected, the first round of selection should be done starting after germination to fully grown plants to also observe late phenotypes.
7. Collect, e.g., leaf samples of plants grown at restrictive and/or permissive temperature to compare levels of It-degron:POI by Western blot or other assays, if other read-outs are expected such as enzymatic activities or fluorescence, *see* Subheading 3.3.2.
8. The restrictive and permissive temperatures should later on be adjusted upon identification of responding lines. Lowering the restrictive and increasing the permissive temperatures will lead to better growth and reduced stress for the specimen which will be beneficial for the experiments and lead to an optimized work and assay flow.

3.3 Application of It-degron Lines

3.3.1 Developmental Phenotypes on Demand

If a developmental phenotype such as ablation or overproduction of a cell type or target-dependent triggering of a phenotype are envisaged, it could be feasible to plant the identification of functional lines with the bare eye or by using microscopical or histological methods for analysis.

Phenotypes on Demand by Low-Temperature Degrons

3.3.2 *Molecular
Phenotypes on Demand*

If molecular phenotypes are expected such as enzyme activity or subcellular phenotypes due to structural changes in a cell, it will be difficult at first to identify functional lines with the methods suggested previously in Subheading 3.3.1. These phenotypes simply cannot be easily monitored. We therefore suggest screening on protein levels, i.e., by using large- or high-throughput Western blotting.

1. The easiest way to compare levels of It-degron:POI is via a side-by-side comparative Western blot using normal or high-throughput gel running and blotting systems, *see* Subheading 2.2.
2. Collect plant material grown, e.g., at two different conditions, here at restrictive versus permissive temperatures, extract total protein and treat as for standard SDS-PAGE and Western blotting.
3. If processing many samples at a time, plan the experiment beforehand carefully to avoid loss of samples, e.g., during loading of multiple gels and make sure to have the capacity to blot all samples either on one semi-dry transfer system or in one wet blotter to exclude artifacts of uneven protein transfer during the blotting procedure. This will inevitably lead to misinterpretation of the results because you will be watching out for strong protein abundance versus low protein abundance in the same experiment. It is advisable to load samples of restrictive and permissive conditions side-by-side to immediately observe potential effects of degradation versus accumulation and identify responding lines.
4. After pre-screening, identified lines need to be verified by subsequent Western blotting and responding standard lines isolated and ideally propagated to a non-segregating homozygous situation.
5. Another possibility to use the It-degron is in the context of transient expression. If this is preferred, two populations of transformed plants should be risen in parallel under similar general growth conditions under various – at least two – temperatures representing the extreme permissive and restrictive temperatures (*see* Note 9).

3.3.3 *Controls*

Two possible negative controls are conceivable, namely the use of a nondegradable control fusion protein and a mutant background with disturbed N-end rule pathway. For the first option, the codon for the critical neo-N-terminal Phe residue needs to be altered to a Met or Ala. By this, the fusion protein undergoes the same post-translational processing with regard to cleavage of the ubiquitin fusion but cannot be recognized by the E3 ligase PROTEOLYSIS1 (PRT1) [3–7] which is required to initiate It-degron degradation

Nico Dissmeyer

[1]. One problem became apparent during the last years when the technique was established in various laboratories. The possible high variability in expression of the It-degron fusions is directly linked to the copy number in the transformed organism and also to half-life or detectable protein levels and/or active POI. Therefore, in *Arabidopsis*, where N-end rule pathway mutants are available, we strongly recommend to use the *prt1* mutant background introgressed into the It-degron lines of choice wherever possible. However, in the specific case of the It-degron, naturally, every single transgenic line or transformation/transfection setup already represents its own control because the restrictive temperature is the restrictive one leading to protein degradation and the control condition is the permissive temperature causing protein accumulation.

4 Notes

1. This plasmid is a Gateway-compatible Entry clone containing L1 and L2 recombination sites. It can be used in single and multiple Gateway reactions and as template for PCR fusion constructs.
The linker at the N-terminus of the It-degron cassette “K2” may not be altered as functionality might be impaired by exchanging, deleting, or introducing amino acid coding sequences here.
2. These plasmids are Gateway-compatible Destination vectors containing R1 and R2 recombination sites. They can be used in single Gateway reactions to create binary plant expression vectors.
3. This monoclonal antibody is produced from raw ascites fluid derived from the clone 16B12 and available from a multitude of suppliers such as from Covance. There is no need to use the purified version (MMS-101P), it is sufficient to use the “non-purified” MMS-101R.
4. Vertical midi-format electrophoresis cell, includes buffer tank with built-in cooling coil, lid with power cables, 12 gel capacity. Depending on the experience of the experimenter and the comb size, several hundred samples can be run in parallel with this setup.
5. This mutant *Arabidopsis thaliana* line can be used to generate controls that constitutively accumulate the It-degron:POI fusion protein due to impaired N-end rule-mediated protein degradation. If *prt1* is introgressed in the background of the It-degron:POI expressing line, the fusion protein cannot be degraded, irrespective of the temperature.

Phenotypes on Demand by Low-Temperature Degrons

6. Consult, e.g., the website of the German Controlled Environment User Group (www.gceug.de) for further instructions on diverse aspects of controlled plant growth environments from technology to plant growth parameters. This web resource raises awareness for details that need to be considered in instrument and equipment acquisition from measurement devices and growth cabinets to walk-in chambers and whole facilities.
7. Cave! The linker at the N-terminus of the It-degron cassette “K2” may not be altered as functionality might be impaired by exchanging, deleting, or introducing amino acid coding sequences here.
8. Data logging of growth and selection conditions is very much encouraged. This holds true for both standard greenhouse as well as controlled environment such as in growth chambers or cabinets. According to our experience, only this allows to both identify and document the exact conditions (especially temperatures) the selection and isolation experiments were done at and assist to identify possible interferences by technical problems that might disturb the outcome and influence the selection of lines for the actual follow-up experiments.
9. Extreme permissive and restrictive temperatures should be used for initial screens to quickly eliminate non-functional lines. We made very good experience with temperatures such as 16 °C and 27 °C. But also screens at as low as 8 °C and as high as 30 °C were done in our lab. This all depends strongly on the available infrastructure, the planned time-frame, and the POI.

Acknowledgements

This work was supported by a grant for setting up the junior research group of the *ScienceCampus Halle – Plant-based Bioeconomy* to N.D., a Ph.D. scholarship from the DAAD (Deutscher Akademischer Austauschdienst) to P.R., by DI 1794/3-1 of the German Research Foundation (DFG) to N.D., and by grant LSP-TP2-1 of the Research Focus Program “*Molecular Biosciences as a Motor for a Knowledge-Based Economy*” from the European Regional Development Fund (EFRE) to N.D. Financial support came from the Leibniz Association, the state of Saxony Anhalt, the DFG Graduate Training Center GRK1026 “*Conformational Transitions in Macromolecular Interactions*” at Halle, and the Leibniz Institute of Plant Biochemistry (IPB) at Halle, Germany. N.D. lab is participant of the European Cooperation in Science and Technology (COST) Action BM1307 – “*European network to integrate research on intracellular proteolysis pathways in health and disease (PROTEOSTASIS)*”.

283
284
285

Nico Dissmeyer

References

1. Faden F, Ramezani T, Mielke S, Almudi I, Nairz K, Froehlich MS, Hockendorff J, Brandt W, Hoehenwarter W, Dohmen RJ, Schnittger A, Dissmeyer N (2016) Phenotypes on demand via switchable target protein degradation in multicellular organisms. *Nat Commun* 7:12202
2. Faden F, Mielke S, Lange D, Dissmeyer N (2014) Generic tools for conditionally altering protein abundance and phenotypes on demand. *Biol Chem* 395:737–762
3. Bachmair A, Becker F, Schell J (1993) Use of a reporter transgene to generate arabidopsis mutants in ubiquitin dependent protein degradation. *Proc Natl Acad Sci U S A* 90:418–421
4. Potuschak T, Stary S, Schlogelhofer P, Becker F, Nejnskaia V, Bachmair A (1998) PRT1 of *Arabidopsis thaliana* encodes a component of the plant N end rule pathway. *Proc Natl Acad Sci U S A* 95:7904–7908
5. Stary S, Yin X, Potuschak T, Schlogelhofer P, Nizhynska V, Bachmair A (2003) PRT1 of *Arabidopsis* is a ubiquitin protein ligase of the plant N end rule pathway with specificity for aromatic amino terminal residues. *Plant Physiol* 133:1360–1366
6. Dong H, Dumenil J, Lu FH, Na L, Vanhaeren H, Naumann C, Klecker M, Prior R, Smith C, McKenzie N, Saalbach G, Chen L, Xia T, Gonzalez N, Seguela M, Inze D, Dissmeyer N, Li Y, Bevan MW (2017) Ubiquitylation activates a peptidase that promotes cleavage and destabilization of its activating E3 ligases and diverse growth regulatory proteins to limit cell proliferation in *Arabidopsis*. *Genes Dev* 31:197–208
7. Mot AC, Prell E, Klecker M, Naumann C, Faden F, Westermann B, Dissmeyer N (2017) Real time detection of PRT1 mediated ubiquitination via fluorescently labeled substrate probes. *New Phytol.* doi:10.1111/nph.14497

2.2 OBJECTIVES PART II – BIOTECHNOLOGY

I have a strong interest in application and translational science and one focus is therefore on utilizing our knowledge about the N-end rule degradation pathway in such translational approaches. In this chapter, I will describe how we generated tools for genetic and biotechnological applications, namely an N-end rule-based switchable system for protein activity and ‘*phenotypes on demand*’ in living multicellular organisms. This work, the so-called ‘low-temperature (lt) degron’ approach has implications for *Synthetic Biology* and *Molecular Farming*. Key of the lt-degron is a temperature-sensitive portable degradation signal (degron; [Faden et al., Nature Comms, 2016](#)).

2.3 RESULTS PART II – BIOTECHNOLOGY

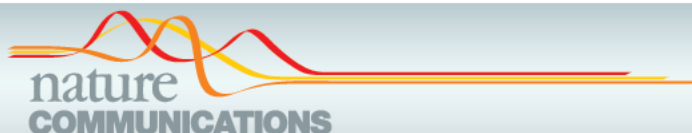
I have designed a portable protein fusion cassette which allows to conditionally destabilize or accumulate proteins of interest in cell culture, insects and plants by simply using a temperature shift. The method relies on a Ubiquitin fusion technique and the N-end rule pathway and requires function of PRT1. This so-called ‘low temperature (lt) degron’ approach directly addresses proteins on the level of their function by their conditional expression, stabilization and accumulation and can be used to switch the function of transcription factors, developmental regulator proteins, and a number of different highly active enzymes such as hydrolases, proteases and kinases ([Faden et al., Nature Comms, 2016](#)). We implemented this technique to switch the formation of specific cell types to produce small molecular compounds by harboring their biosynthetic reaction cascades within these cell types. The cell types serve as ‘driver line’ and the reaction cascade as ‘effector line’ or ‘effector construct’ which is introgressed into the genetic background of the switchable cell system. The lt-degron can be used as a platform for different approaches in *Synthetic Biology* and *Molecular Farming* ([Faden et al., Biol Chem, 2014](#); [Görner et al., in preparation](#)) in collaboration with Thomas Vogt and Sylvestre Marillonnet, IPB Halle as well as Hans-Peter Mock and Jochen Kumlehn, IPK Gatersleben). The lt-degron is patented ([Dissmeyer and Schnittger, 2016, Rapid depletion and reversible accumulation of proteins in vivo. Patent No. EP3061820 A1](#)).

2.3.1 Phenotypes on demand via switchable target protein degradation in multicellular organisms

Here, we could successfully demonstrate the use of a temperature-sensitive portable degron to be used as a protein degradation method in multicellular organisms. An N-terminal protein destabilization tag was used to conditionally accumulate various target proteins and enzymes in different model species to generate conditional alleles for genetics and developmental biology as well as achieve robust protein stabilization for biotechnology.

Publication:

Faden F, Ramezani T, Mielke S, Almudi I, Nairz K, Froehlich MS, Hoeckendorf J, Hoehenwarter W, Brandt W, Dohmen RJ, Schnittger A, **Dissmeyer N***. Phenotypes on demand via switchable target protein degradation in multicellular organisms. ***Nature Comms.*** 2016, **7**:12202



ARTICLE

Received 12 Jan 2016 | Accepted 10 Jun 2016 | Published 22 Jul 2016

DOI: 10.1038/ncomms12202

OPEN

Phenotypes on demand via switchable target protein degradation in multicellular organisms

Frederik Faden^{1,2}, Thomas Ramezani^{3,4,†}, Stefan Mielke^{1,2}, Isabel Almudi^{5,†}, Knud Nairz^{5,†}, Marceli S. Froehlich^{6,†}, Jorg Hockendorff^{6,†}, Wolfgang Brandt⁷, Wolfgang Hoehenwarter⁸, R. Jurgen Dohmen⁶, Arp Schnittger^{3,4,9,†} & Nico Dissmeyer^{1,2,3,4,9}

Phenotypes on-demand generated by controlling activation and accumulation of proteins of interest are invaluable tools to analyse and engineer biological processes. While temperature-sensitive alleles are frequently used as conditional mutants in microorganisms, they are usually difficult to identify in multicellular species. Here we present a versatile and transferable, genetically stable system based on a low-temperature-controlled N-terminal degradation signal (It-degron) that allows reversible and switch-like tuning of protein levels under physiological conditions *in vivo*. Thereby, developmental effects can be triggered and phenotypes on demand generated. The It-degron was established to produce conditional and cell-type-specific phenotypes and is generally applicable in a wide range of organisms, from eukaryotic microorganisms to plants and poikilothermic animals. We have successfully applied this system to control the abundance and function of transcription factors and different enzymes by tunable protein accumulation.

¹Independent Junior Research Group on Protein Recognition and Degradation, Leibniz Institute of Plant Biochemistry (IPB), Weinberg 3, D 06120 Halle (Saale), Germany. ²ScienceCampus Halle Plant based Bioeconomy, Betty Heimann Strasse 3, D 06120 Halle (Saale), Germany. ³University Group at the Max Planck Institute for Plant Breeding Research (MIPZ), Max Delbrück Laboratory, Carl von Linné Weg 10, D 50829 Cologne, Germany. ⁴University of Cologne, Institute of Botany III, Biocenter, Zülpicher Str. 47 b, D 50674 Cologne, Germany. ⁵Institute of Molecular Systems Biology (IMSB), Swiss Federal Institute of Technology (ETH), Wolfgang Pauli Strasse 16, CH 8093 Zurich, Switzerland. ⁶Institute for Genetics, Biocenter, University of Cologne, Zülpicher Straße 47a, D 50674 Cologne, Germany. ⁷Computational Chemistry, Department of Bioorganic Chemistry, Leibniz Institute of Plant Biochemistry (IPB), Weinberg 3, D 06120 Halle (Saale), Germany. ⁸Proteomics Unit, Leibniz Institute of Plant Biochemistry (IPB), Weinberg 3, Halle (Saale) D 06120, Germany. ⁹Département Mécanismes Moléculaires de la Plasticité Phénotypique, Institut de Biologie Moléculaire des Plantes du CNRS, IBMP CNRS, Unité Propre de Recherche 2357, Conventionné avec l'Université de Strasbourg, 12, rue du Général Zimmer, Strasbourg F 67000, France. † Present addresses: The Queen's Medical Research Institute, MRC Centre for Inflammation Research, The University of Edinburgh, 47 Little France Crescent, Edinburgh EH16 4TJ, UK (T.R.); Andalusian Centre for Developmental Biology (CABD), Universidad Pablo de Olavide, Ctra. Utrera Km. 1, 41013 Seville, Spain (I.A.); Novino Slowdrink GmbH, Blümlisalpstrasse 31, CH 8006 Zürich, Switzerland and Inselspital Bern, Freiburgstrasse 10, CH 3010 Bern, Switzerland (K.N.); Grüenthal Innovation Early Clinical Development, Grüenthal GmbH, Zieglerstraße 6, D 52078 Aachen, Germany (M.S.F.); UCB BIOSCIENCES GmbH, Alfred Nobel Straße 10, D 40789 Monheim, Germany (J.H.); Department of Developmental Biology, Biozentrum Klein Flottbek, University of Hamburg, Ohnhorststrasse 18, D 22609 Hamburg, Germany (A.S.). Correspondence and requests for materials should be addressed to N.D. (email: nico.dissmeyer@ipb.halle.de).

The classical way to generate temperature sensitive alleles comprises random mutagenesis followed by large scale screens at different temperatures. This procedure is usually limited to fast growing single celled organisms where mutant populations can be analysed simultaneously at restrictive and permissive temperatures. Major problems in using temperature sensitive alleles are their generation, identification, establishment and leakiness. An alternative way to generate heat sensitive mutants is to use a temperature inducible N degron (td), where a protein of interest (POI) is fused to a portable N terminal degradation cassette¹. However, to date this technique has been solely used in unicellular eukaryotes in a temperature range impractical for most multicellular organisms. We show how to efficiently circumvent these limitations by using a novel portable td fusion protein to render the levels of active POIs conditional.

Generally, degradation signals within a protein sequence that make it short lived *in vivo* or *in vitro* are called 'degrons'², and an 'N degron'³ is an amino terminal (N terminal) degron, which relates the metabolic stability of a protein to the identity of its amino terminal residue depending on the N end rule pathway⁴. The N end rule pathway is part of the ubiquitin (Ub)/proteasome system and has been shown to be active in yeast, animals and plants^{5–9}. It maintains proteostasis as a protein quality control mechanism by removing cleaved, damaged or misfolded proteins from the cell^{7,10,11}. N degrons comprise several determinants to target a substrate to the N end rule pathway. First, they must contain a destabilizing N terminal amino acid that can be recognized by N end rule pathway specific E3 Ub ligases (N recognins). Second, another crucial factor is a certain flexibility and accessibility of the N terminal amino acid enabling a proper recognition of the substrate¹². Third, substrates need to contain at least one internal Lys in appropriate distance to the N terminus, which may serve as polyubiquitination site³. The N end rule pathway targets both cytosolic and nuclear substrates but also proteins localized in the membrane¹³.

Conditional protein expression via heat sensitive N degrons was designed as a genetic tool to generate conditional, temperature inducible alleles in budding yeast¹. The system is based on rapid, reversible depletion or accumulation of POIs and targets the entire protein for proteasome dependent proteolysis at a restrictive temperature. Therefore, it can be used as a rapid ON/OFF system for reversible accumulation of active proteins (Fig. 1a,b and Supplementary Fig. 1). Here an N degron serves as a destabilizing N terminal tag (26 kDa) fused to the POI as a portable td cassette. It consists of three vital parts: (1) Ub that is co translationally removed from the fusion by deubiquitinating enzymes (Ub fusion technique¹⁴); (2) a thermo labile mouse dihydrofolate reductase (*DHFR^{ts}*) that triggers protein degradation at the restrictive (high) temperature; and (3) a destabilizing N terminal residue at the *Ub DHFR^{ts}* junction, which is exposed after deubiquitination of the full fusion construct, which serves as dormant N degron and can be recognized by N end rule E3 Ub ligases (Supplementary Fig. 1).

Even if a potential degron (that is, a motif theoretically recognized by a N end rule pathway E3 Ub ligase) is present on the surface of a target, its conformational rigidity may prevent its recognition due to steric hindrance. A conformationally destabilized protein may contain formerly buried (cryptic) surface degrons (that is, dormant degrons), which were masked in a stabilized version of the protein¹⁵. In the classical yeast td degron, both happens according to the presented model¹: a previously rigid surface degron (N terminal) undergoes conformational relaxation and previously buried degrons, such as internal Lys side chains, are exposed.

However, to date, this system has only been used at the single cell level in yeast and cell culture where it requires restrictive

temperatures of 37 or 42 °C (refs 1,16,17). These high temperatures are beyond the physiological range of many multicellular organisms, including animals and plants¹⁸. Although there are alternative methods for conditional protein shut off via degradation, for example, the protease mediated TIPI¹⁹, the destabilizing domain (DD) systems²⁰ and the auxin inducible degron (AID)²¹, their use is also limited to cells in culture²². The latter two systems require the addition of exogenous compounds to trigger the response (Supplementary Note 1).

To fill the gap of a conditional protein accumulation system for multicellular systems under physiological conditions, we constructed a low temperature (lt) N degron and show its general applicability by studying seven POIs in five different model systems (that is, two plant species (*Arabidopsis thaliana* and *Nicotiana benthamiana* (tobacco)), *Drosophila melanogaster* (fruit fly), *Drosophila* cell culture and *Saccharomyces cerevisiae* (budding yeast)). The design of the lt degron not only allowed *in vivo* inactivation and depletion of proteins and enzymes but also tuning of protein levels and enzyme activity. Depending on the POI, we demonstrated triggering of developmental processes on demand. We define the temporal requirement of a transcriptional regulator protein mandatory for the formation of trichomes, which belong to the prime model cells in plant developmental genetics. Moreover, we made use of a developmental switch by stabilizing a transcription factor causing flowering on demand, triggered protein accumulation in *N. benthamiana* (tobacco), conditionally depleted proteins in cell culture and *Drosophila* flies. Therefore, the link to in depth applications in developmental studies is addressed as well as the proof of concept for applications of the lt degron in biotechnologically relevant contexts.

Results

N degron functionality in multicellular organisms. To assess N degron functionality in multicellular organisms, we chose easily scorable, quantitative and irreversible biological read outs after temperature shifts *in vivo*, like the development of *Arabidopsis* trichomes (leaf hairs) and flower induction. We first asked whether the established yeast td degron containing the single mutated *DHFR^{P67L}* (termed 'K1'), exhibiting a restrictive temperature of 37–42 °C (refs 1,16,17,23) is functional in plants. Our *DHFR* was initiated by phenylalanine (Phe), a strongly destabilizing residue in plants, which is presumably recognized by the bona fide N end rule E3 Ub ligase PROTEOLYSIS1 (PRT1)^{24–26}. As the first test system, we used the formation of *Arabidopsis* trichomes, which are a well established model in cell and developmental biology^{27–29}, and an attractive target for plant metabolic engineering.³⁰ WD40 protein TRANSPARENT TESTA GLABRA1 (TTG1) is an essential regulator for trichome development³¹, *ttg1* mutants are devoid of trichomes (Figs 1c and 2a) but the mutant phenotype can be rescued by expressing *TTG1* under control of the constitutive cauliflower mosaic virus (CaMV) 35S promoter (*Pro35S*)³². In this evaluation system, the read out for a functional N degron is the number of trichomes formed per leaf after the shift from permissive to restrictive temperature. Under permissive conditions, the degron is non functional, that is, the POI will accumulate and form trichomes, whereas under restrictive conditions, the degron is active and leads to the degradation of the fusion protein, and leaves will be devoid of trichomes.

To this end, transgenic *ttg1* mutant *Arabidopsis* plants were generated that expressed TTG1 fused to degron cassette K1 (Supplementary Fig. 2). We set the presumptive maximal restrictive temperature treatment to 29 °C, which is near but not above the upper end of the physiological temperature range of

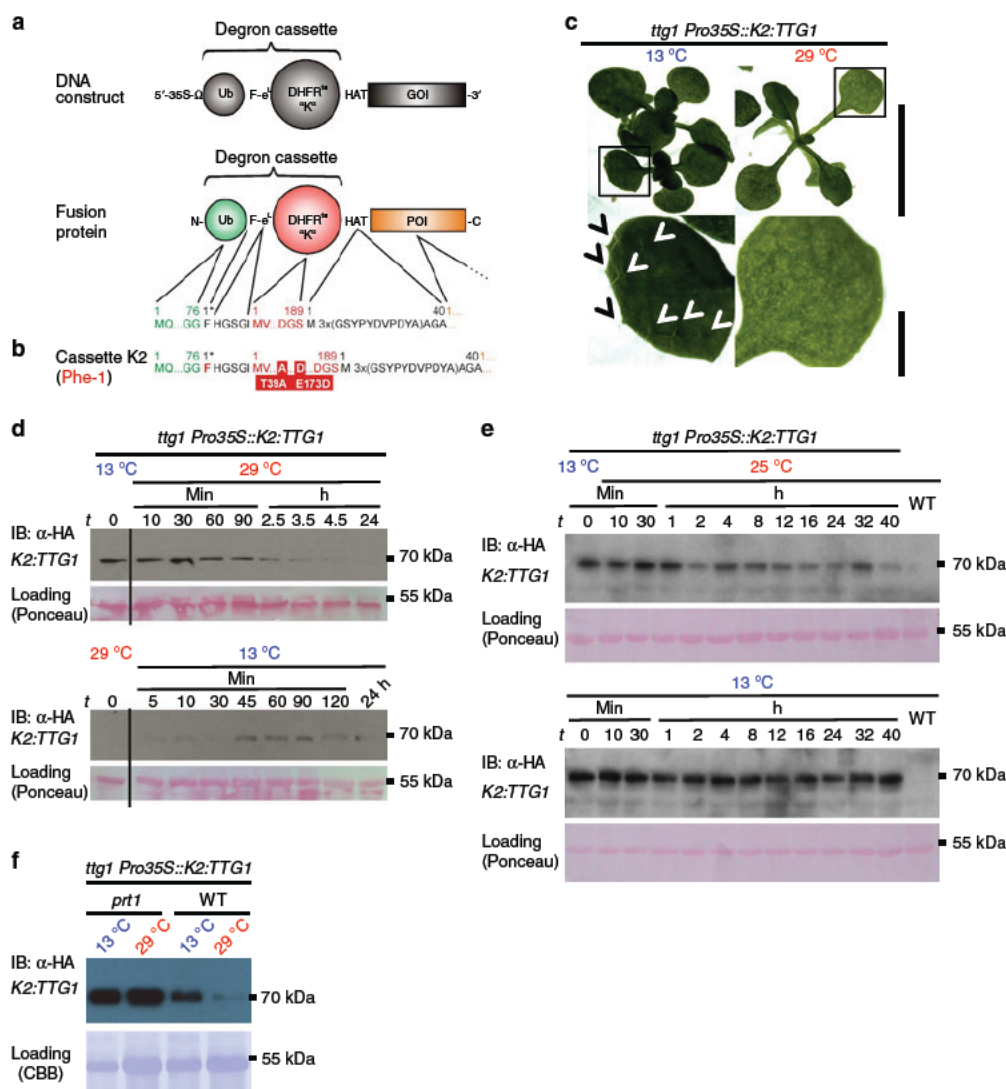


Figure 1 | Conditional protein depletion/accumulation cause developmental phenotypes on demand *in vivo* and can be used to develop trichome cells. (a,b) Lt degron architecture. The mechanism of conditional N degron containing protein depletion is shown in Supplementary Fig. 1, degron construct design is shown in Supplementary Fig. 2. (c) *ttg1 K2:TTG1* plants grown at permissive or restrictive temperatures. Arrow heads indicate trichomes in inlets. Scale bar, 1 cm, 5 mm (inlet). (d) *In vivo* protein depletion time course of *K2:TTG1* from transgenic *ttg1 Pro35S::K2:TTG1* mutant plants. (e) *In vivo* dimming of *K2:TTG1* levels by application of semi permissive temperatures. Plants were subjected to temperature shift experiments from 13 to 25 °C. Western blots of plants shifted to semi restrictive (25 °C) and kept at constitutively permissive temperature (13 °C) are shown. Plants were shifted at *t* = 0 from 13 to 25 °C (upper panel) or kept at 13 °C (lower panel). (f) Stabilization of *K2:TTG1* in *prt1*. The *K2:TTG1* fusion protein stabilizes in the *prt1* mutant background under restrictive temperature indicating that the E3 ligase PRT1 is the principal component responsible for *K2* degradation. *K2:TTG* also partially accumulates under permissive temperatures in the *prt1* mutant background compared with the WT indicating that also here, the fusion protein is not fully stabilized. All samples derived from the same experiment, processed in parallel and leaves of the same developmental stage were compared. Data were confirmed by analysis of at least three biological replicates. Equal loading was further confirmed by Ponceau S staining of blotted and immunostained membranes.

*Arabidopsis*¹⁸ and found that *K1:TTG1* stably transformed plants developed trichomes also at this temperature indicating that the fusion protein is not sufficiently destabilized (Supplementary Table 1).

To lower the restrictive temperature, we generated an N degron variant containing a triple mutated *DHFR*^{T39A/P67L/E173D} (*K3*) with two additional substitutions (*T39A/E173D*). We had previously identified the latter mutations in a yeast mutagenesis

screen for destabilizing point mutations within *DHFR* (Supplementary Note 2)³³. However, *ttg1* mutants containing *K3:TTG1* never formed trichomes under any tested conditions. The protein appeared to be unstable after growing the plants at constitutively permissive or restrictive temperatures or shifting them between the two conditions (Supplementary Fig. 3 and Supplementary Table 1). Lack of trichomes under low temperatures correlated with levels of *K3:TTG1* protein undetectable by western blot

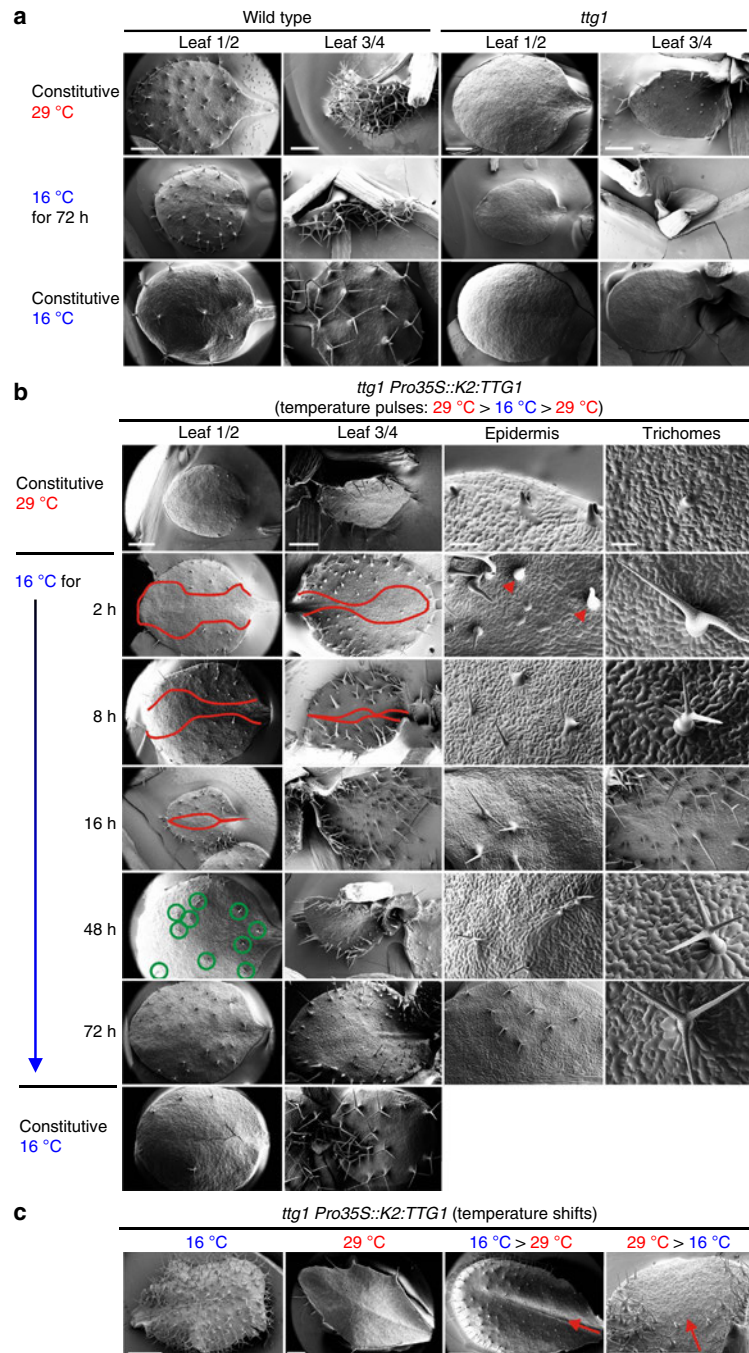


Figure 2 | Spatiotemporal development of trichomes as test system for conditional protein accumulation. (a) Phenotype of *ttg1* mutants compared with the WT. Cryo scanning electron micrographs were taken from 4 week old plants grown constitutively at 29 or 16 °C. Scale bar, 1 mm. (b,c) Conditional complementation of *ttg1* with *K2:TTG1* depending on temperature and time. SEMs of 4 week old *ttg1 K2:TTG1* plants. (b) Temperature pulsing of *K2:TTG1* protein in *ttg1* by short shifts from the restrictive to the permissive temperature (16 °C). Control plants were grown constitutively at restrictive (29 °C, upper row) or permissive (16 °C, bottom row) temperatures. Centre: plants grown at restrictive and shifted to permissive temperature for the time indicated (2–48 h). Red lines: borders of trichome initiation zone moving from lateral to medial with duration of the *K2:TTG1* pulse. Green circles: fully mature trichomes and epidermal patterning appearing after 48 h. Arrow heads: loped circumference at trichome bases. Scale bars, 1 mm (left), 500 μm (second and third columns) and 100 μm (right). (c) WT and *ttg1* like glabrous leaves of *ttg1 K2:TTG1* grown at permissive and restrictive temperatures (left two panels) or after temperature up and downshifts during leaf development (right two panels). Arrows: direction of proximo distal leaf development highlighting the sector affected by the temperature shift. A phenotypic comparison of different degron variants is shown in Supplementary Fig. 3, expression levels of all degron fusion genes under restrictive and permissive conditions are presented in Supplementary Fig. 4. Molecular dynamics simulations and models of the DHFR variants used are presented in Supplementary Fig. 5.

analysis although its transcript was found (Supplementary Fig. 3). These findings indicated that proteins carrying the *K3* degron are too unstable at lower temperatures to provide a permissive phenotype.

Novel It N degron for *in vivo* application. Finally, we fused *TTG1* to *DHFR*^{*T39A/E173D*} (*K2*), which only contains the two destabilizing point mutations *T39A/E173D* identified in the mutagenesis screen. The expression of *K2:TTG1* caused a conditional (that is, temperature dependent) restoration of trichomes in the *ttg1* mutant background (Figs 1c and 2b,c, Supplementary Fig. 3 and Supplementary Table 1). In time course experiments, decreasing and increasing levels of *K2:TTG1* protein could be tracked as a consequence of temperature up or downshifts causing depletion versus accumulation (Fig. 1d). Neither the endogenous *TTG1* protein without the It degron nor the *K2:TTG1* transcript levels responded to the temperature shifts when tested in a transgenic *ttg1 TTG1 HA* complementation line (Supplementary Figs 3a and 4a).

For the classical temperature induced yeast N degron, it was hypothesized that after heat induction, a dormant N terminal degron becomes active after conformational changes and that internal Lys side chains get exposed¹. We tested this hypothesis for the point mutations present in the sequences of the *DHFR* variants of the classical td (*K1*) and our novel It degron (*K2*) by stability predictions and molecular dynamics simulations (Supplementary Table 2 and Supplementary Note 3). Modelling of the point mutations within the *DHFR* crystal structure suggested that *E173D* contributes to a higher conformational flexibility and increases the exposure of Lys side chains on the surface under elevated temperatures. This may lead to a better accessibility to the ubiquitination machinery (Supplementary Fig. 5a d).

N terminal accessibility and N end rule requirements. We hypothesized that a possible hyper destabilization of *K3:TTG1* could be due to the flexibility introduced by the short linker e^L (2 His Gly Ser Gly Ile 6; Supplementary Figs 2,3) between *DHFR* and the destabilizing Phe residue compared with the classical yeast degron³⁴. By deleting e^L from the degron cassettes and thus making the destabilizing N terminal Phe less accessible for the N end rule Ub ligases, we tested if a conditional phenotype can now be observed as a way to further optimize, that is, decrease, the restrictive temperature of the system. However, transgenic plants expressing *K3:TTG1* lacking e^L showed very similar phenotypes as the previously tested e^L containing versions. Similarly, only expression of *K2:CO* containing the linker led to a temperature dependent response, the constructs lacking the linker did not (Supplementary Table 1 and Supplementary Fig. 3).

As control, cassette *K4* was engineered. It contains the same *DHFR* variant as *K2* but starts with a methionine and can therefore not be recognized by N end rule E3 ligases due to the lacking destabilizing N terminal residue (Supplementary Figs 2 and 3). The *T39A* and *E173D* mutations were previously shown to cause degradation by a protein quality control pathway at higher temperatures (30 °C)³³. The *K4:TTG1* phenotypes were highly variable but not temperature dependent as expected from a conditionally stable *TTG1 td* (Supplementary Fig. 3c,d and Supplementary Table 1). *K4:TTG1* plants developed trichomes regardless of the growth temperature. These data demonstrated that the destabilizing N terminal Phe residue is a critical feature of the conditional It *K2* degron.

Tuning of protein levels. Indeed, protein accumulation by this novel It degron containing the *K2* cassette was even tuneable

and allowed fading out the POI to achieve intermediate levels at semi restrictive temperatures (Fig. 1e). For this experiment, plants were shifted at *t* = 0 from 13 to 25 °C or kept at 13 °C. Protein degradation appeared slower when shifted to 25 °C compared with restrictive temperature (Fig. 1d), and low levels of POI were still detectable after 40 h. The decrease of It protein over time could be observed reaching a level lower than at permissive but higher than at restrictive temperatures. To test for the requirement of a functional N end rule pathway in the host organism to efficiently degrade the Phe initiated It degron, we introgressed *ttg1 K2:TTG* into the *prt1* mutant. Proteins with initiating Phe at their N terminus are expected to be recognized by one of the two known plant N recognins, namely *PRT1*. We observed that the fusion protein is stable in the *prt1* mutant background also at restrictive temperature (Fig. 1f).

Triggering trichome induction on demand. The tunability of *K2:TTG1* and the conditional induction of trichomes in the mutant background allowed us to perform previously impossible experiments, that is, to dissect the temporal requirement of *TTG1* function during trichome establishment and maturation in great detail (Fig. 2b,c). Taking the pattern of wild type (WT) trichome distribution into account³⁵, we found that a pulse of *K2:TTG1* protein is needed for at least 2 h to establish a trichome fate during the initial induction phase (Fig. 2b,c). After a pulse of 2 h at permissive temperature of 16 °C, the front of the trichome initiation sites started to move proximal to the midvein and trichomes began to differentiate (branching). Notably, initiation sites develop proximal to the mid vein as spots with enlarged precursor cells, suggesting that different leaf areas have a differential predisposition to form trichomes. After 8 h, further branch points are formed and few three branched, albeit not fully developed, trichomes appeared. Many trichomes formed a loped circumference, which is typical for de differentiation if initial maintenance of cell fate is not completed³⁶. After 16 h, a spacing pattern was formed indicating robust trichome maintenance. Forty eight hours of *TTG1* function were needed for developing WT like three branched trichomes. Expansion and partial restoration of a WT like distribution pattern, as well as morphology of trichomes, is fully accomplished after 72 h of *TTG1* action (Fig. 2b). Here the It degron allowed us to determine the temporal requirement of *TTG1* in the context of the development of a highly specific cell type.

Switching floral induction on demand. As a second test system with an easily scorable biological read out, we chose WT *Arabidopsis* plants that conditionally overexpress the transcription factor *CONSTANS* (*CO*), a key regulator of flowering time³⁷. Overexpressing *CO* causes a rapid shift from the vegetative to reproductive growth mode and thereby an early flowering^{38,39}. Thus, at permissive temperatures, plants expressing a functional degron *CO* fusion protein (*CO td*) were expected to flower earlier than plants grown under the restrictive temperature. The read out is hence the days till flowering at permissive temperature in comparison with the WT. Similarly to the *TTG1 td* constructs, neither *K1:CO* nor *K3:CO* showed a temperature dependent phenotype (Supplementary Table 1). In contrast, the It degron system very efficiently worked as expression of *K2:CO* at the permissive temperature caused early floral induction. Here the inducible formation of flower meristems occurred about 14 days earlier than in the WT when grown at the same permissive temperature (Fig. 3a). No differences were found when plants were grown at the restrictive temperature as in a time course experiment, the onset of flowering was observed from day 15 onwards for both WT and *K2:CO* plants (Supplementary Fig. 6).

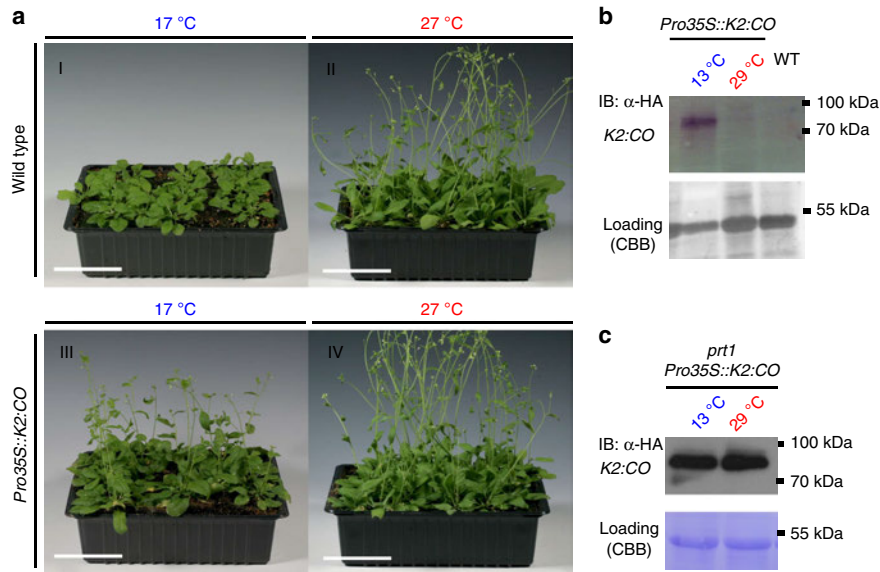


Figure 3 | Switchable flower meristems by conditional accumulation of CO-td. (a) Conditional expression of CO *td* fusion leads to premature flowering *in vivo*. Four week old (I and II) WT and (III and IV) K2:CO transgenic plants grown under permissive and restrictive temperatures and short day conditions. (III) In transgenic K2:CO plants, plants bolted earlier than in the WT (I). Scale bars, 5 cm. (b) K2:CO protein levels from transgenic plants grown at permissive or restrictive temperature. (c) Stabilization of K2:CO in *prt1*. The K2:CO fusion protein stabilizes in the *prt1* mutant background under restrictive temperature indicating that the E3 ligase PRT1 is required for K2 degradation. For details on N degron technology, see Supplementary Fig. 1; for construct layout, see Supplementary Fig. 2. For transcript levels under restrictive and permissive conditions, see Supplementary Fig. 4. A developmental time course experiment for CO *td* is shown in Supplementary Fig. 6.

This phenotype correlates with decreased levels of K2:CO under restrictive conditions while transcript levels remained unchanged (Fig. 3b and Supplementary Fig. 4b). K2:CO introgressed into *prt1* lead to stabilization of the fusion protein also at restrictive temperature (Fig. 3c). Here conditionally stable CO *td*, enabled us to control the onset of flowering and to generate floral meristem cells, that is, specialized cell types, on demand.

In vivo inactivation and depletion of proteins and enzymes. To further assess the application spectrum of the It degron in plants, we chose green fluorescent protein (GFP), β glucuronidase (GUS) and tobacco etch virus protease (TEV) as additional target proteins to be tested when stably transformed in *Arabidopsis*. K2:GFP robustly followed the accumulation/depletion regime (Fig. 4a,b and Supplementary Fig. 4c). Moreover, for K2:GFP, we have designed two different It degron cassettes to test for degradation via two known branches of the N end rule pathway. We used either the previously mentioned Phe or, as another potentially destabilizing residue, Arg, which results as neo N terminal after deubiquitination of the translated K2:GFP fusion protein. These residues are expected to be recognized by the two known N recognins, that is, Arg via PRT6 and Phe via PRT1. The response of these two constructs was compared under standard growth conditions (Supplementary Fig. 4c) and in time course experiments (Supplementary Fig. 4d) to demonstrate robustness. Both destabilizing N termini gave comparable, strongly temperature dependent results and revealed that the It degron is functional by both branches of the N end rule pathway.

Histological staining for K2:GUS revealed activity of the fusion protein *in vivo* at permissive and a significantly reduced activity at restrictive temperature (Fig. 4c). K2:GUS protein levels and activity were strongly decreased for individuals grown constitutively at restrictive temperature (Fig. 4d,e) with transcript levels unchanged (Supplementary Fig. 4e). In time course experiments,

K2:GUS protein levels increased and correlated with high enzyme activity after shift to permissive temperature and vice versa if shifted to restrictive conditions (Fig. 4f,g). K2:GUS western blots showed two bands of different sizes (Fig. 4d,f). To identify the K2:GUS population with a temperature dependent hydrolase activity, which accumulates at permissive temperature, we analysed the bands by mass spectrometry (Supplementary Fig. 7). This revealed that only the K2:GUS population, which accumulated at the permissive temperature contains the It degron part and is highly active (Fig. 4e,g). At the same time, K2:GUS is stabilized also at restrictive temperature after the addition of proteasome inhibitor indicating the degradation of the fusion protein via the Ub/proteasome system (Supplementary Fig. 4f).

Tuning of activity levels. To further strengthen our claim on the temperature dependent tunability of the It degron system, we performed temperature shift assays with *ProUBQ10::K2:GUS* addressing temperature dependent changes in both protein and activity levels at various temperatures (Fig. 4h). In contrast to the *in vivo* dimming of K2:TTG1 (Fig. 1e), this represents a more appropriate tuning experiment because here, the activity of the conditional It POI could be quantified in relation to the It POI protein levels and total protein content of the sample. The levels of active K2:GUS fusion protein were stabilized and its activity, as monitored by the quantitative GUS assay, followed the increased or decreased protein levels according to the applied temperatures in the permissive to restrictive range. Moreover, K2:GUS activity levels can be efficiently regulated by means of different temperatures. All of this indicated a high flexibility of the It degron regardless of temperature adjustment from permissive to restrictive temperature or vice versa.

Application of It degrons in *N. benthamiana*. Next, we applied our low temperature approach to TEV as a target, which is widely

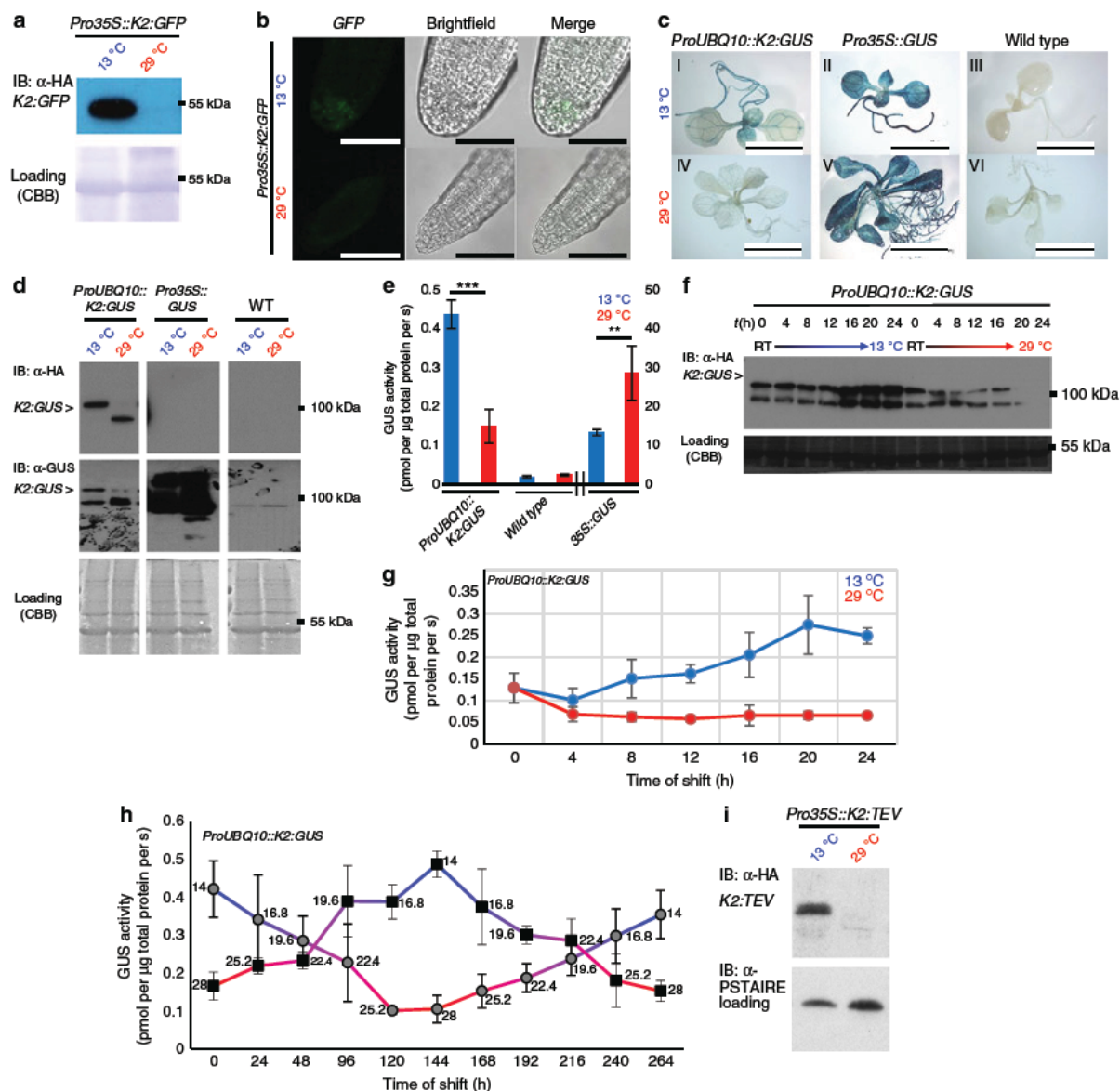


Figure 4 | Conditional molecular phenotypes are linked with protein degradation and deactivation of It-degron fusion proteins. (a) Conditional accumulation of *K2:GFP* fusion protein in whole seedlings and (b) functionality of *K2:GFP* in root tips. Also Arg initiated *K2:GFP* is conditionally depleted (Supplementary Fig. 4c). Scale bar, 50 μm. (c) *In vivo* hydrolase activity of transgenic *ProUBQ10::K2:GUS* compared with *Pro35S::GUS*, overexpression lines and the WT constitutively grown at permissive or restrictive temperature. Scale bar, 1 cm. (d) *K2:GUS* protein levels of seedlings constitutively grown at the indicated temperatures. Membranes were immunostained with α HA antibody followed by a second staining with α GUS antibody after stripping. The asterisk indicates *K2:GUS* protein. (e) Quantitative GUS assays of plants constitutively grown at 13 versus 29 °C. Six biological replicates were performed for *K2:GUS* and three biological replicates for WT and *35S::GUS*. All samples were measured as three technical replicates. *P* values for Student's *t* test (two sided *t* test, type 3) are *K2:GUS*: 6.44766×10^{-7} (***); *35S::GUS*: 0.004365663 (**). All error bars in this panel represent s.d., asterisk: significant. (f) Western blots of *ProUBQ10::K2:GUS* seedlings constitutively grown at ambient temperature (room temperature (RT)) shifted to permissive or restrictive temperature. (g) Quantitation of enzyme activity of f. Seedlings were grown under standard long day conditions (16 h light, 8 h dark, 21 °C) aseptically on MS plates. One week old seedlings were shifted to permissive or restrictive conditions, respectively. In all, 5 10 individual seedlings were collected and pooled every 4 h. Three biological replicates were performed with two technical replicates each. All error bars in this panel represent s.d. (h) Degron tuning assay monitoring *K2:GUS* activity through temperature shift. Plants expressing *ProUBQ10::K2:GUS* were grown at cold (permissive) or warm (restrictive) temperature and then shifted to the respective opposite temperature and back over the course of 10 days. Samples were taken every 24 h, followed by a temperature shift of 2.8 °C. Activity of the *K2:GUS* fusion protein clearly follows the temperature shift. The numbers next to the data points represent the sampling temperature, *n* = 3. All error bars in this panel represent s.d. MS analysis of *K2:GUS* populations is documented in Supplementary Fig. 7. (i) *K2:TEV* in stably transformed *Arabidopsis* plants. Western blot of material collected from seedlings grown at permissive and restrictive temperatures. Equal loading was further confirmed by staining of blotted membranes with Coomassie Brilliant Blue G225 after immunostaining or α PSTAIRE antibody detecting CYCLIN DEPENDENT KINASE A,1 (CDKA;1). For transcript levels under restrictive and permissive conditions, see Supplementary Fig. 4.

used for cleaving proteins *in vitro* and *in vivo*. The protease can be expressed for site specific protein cleavage in many different host organisms without causing adverse effects⁴⁰. In *Arabidopsis*, *K2:TEV* transcript levels were unaffected by temperature shifts (Supplementary Fig. 4g), but the fusion protein accumulated exclusively at permissive temperature (Fig. 4i).

N. benthamiana (tobacco) plants are widely used expression hosts for plant made pharmaceuticals and high value proteins. Therefore, we tested the It degron in tobacco, which was transiently transformed with *K2:TEV*. The fusion protein was depleted from plants shifted to 29 °C and accumulated in individuals grown at 13 °C (Fig. 5a). A conditional TEV offers opportunities for downstream processing of recombinant proteins by intracellular cleavage. In addition to *K2:TEV*, *K2:GUS* and a fusion of *K2* with the agriculturally important herbicide resistance proteins phosphinothricin *N* acetyltransferase (*PAT*) were also expressed in a conditional manner in tobacco (Fig. 5b,c). Together these findings established that the It degron approach was also suitable for the manipulation of tobacco and therefore is likely applicable for many more plant species.

Conditional protein depletion in *S. cerevisiae*. To test whether the It degron system is also functional outside of plant species, we used orotidine 5' phosphate decarboxylase (*URA3*) as a reporter in *S. cerevisiae*. *URA3* functionality and half life were tested at 17.5 and 27 °C in the WT, in *ubr1 Δ* lacking the functional N end rule pathway E3 Ub ligase *UBR1* and in *ump1 Δ*, with impaired proteasome function (Fig. 6a). Experiments in WT (*JD47 13C*), *ubr1 Δ* (*JD55*) and *ump1 Δ* (*JD59*) strains revealed that *K1* and *K2* confer uracil prototrophic growth in the *ubr1 Δ* and *ump1 Δ* mutants at all temperatures that were generally growth permissive for these strains, and at lower temperatures in WT cells (Supplementary Fig. 2c). Increasing the temperature, however, resulted in growth inhibition of the WT strain expressing these constructs on media lacking uracil. Moreover, in WT cells, a strong decrease of fusion protein was observed 30 min following a shift to 27 °C (Fig. 6b). Thus, the It degron allows a significantly lower restrictive temperature by about 10 °C compared with the classical temperature controlled *DHFR*^{P67L} variant.

Conditional protein depletion in *Drosophila*. We then tested the It degron in *D. melanogaster* using *K2:GFP* and *K2:TEV* as model POIs. *K2:GFP* was destabilized after a shift from stabilizing 15 to 29 °C in embryonic Kc cells subjected to a temperature shift

for 4 h (Fig. 7a,b). *K2:TEV* was depleted from macrophage like Schneider 2 (S2) cells after a shift from 16 to 29 °C (Fig. 7c). A stable transgenic *Drosophila* line expressing *K2:TEV* under the control of the *Actin5c* promoter proved the principle *in vivo*. After shifting the living flies from the permissive (18 °C) to the restrictive (29 °C) temperature, we observed that *K2:TEV* becomes unstable (Fig. 7d). This revealed that the It degron has a broad spectrum of applications and can be used to modulate protein abundance not only in plants and yeast but also in animal cell culture and living insects.

Discussion

Tight modulation of protein activities is still a major challenge, especially in multicellular organisms. We introduce here a transferable It degron for obtaining conditional mutants coupled to tunable protein accumulation in entire plants, insects and cell culture. The It system allows a rapid and reversible modulation of protein function and enzymatic activities. This was demonstrated in the case of seven different targets in five model systems, suggesting that it is generic and versatile.

Pronounced and unique technical advantages of the method over comparable systems include non invasive functionality in a wide range of multicellular organisms, the lack of technically difficult or costly applications of exogenous chemical triggers, the possibility of the formation of cell and tissue types on demand by direct action on protein activity, and the perspective of applicability in large scale, for example, in entire growth containments, as the trigger is temperature.

In today's age of recent technological advances where site specific gene inactivation is becoming routine, clearly methods for the re introduction of tightly and rapidly controllable conditional genes will allow additional functional analyses. In combination with CRISPR/Cas9, ZFNs or TALENs, our method allows directed generation of novel conditional alleles of genes, including essential ones, at the organismal and tissue specific level. The It degron is technically well suited for the application in poikilothermal animals such as fishes, amphibians, reptiles, insects and other invertebrates, facilitating the design of conditional knockout animals in many model systems to dissect, for example, developmental programmes.

We recently discussed the classical heat inducible N degron with other techniques for conditionally altering protein abundance and generating phenotypes on demand (Supplementary

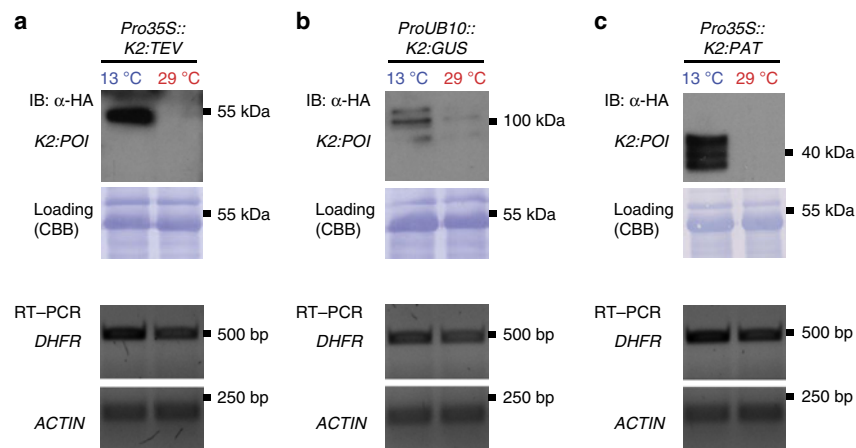


Figure 5 | The It-degron in *N. benthamiana* as a protein accumulation system. (a) Stability and transcript levels of *K2:TEV* in transiently transformed *N. benthamiana* (tobacco) plants. (b) Conditional expression of *K2:GUS* and (c) of *K2:PAT*. Equal loading was confirmed by staining of blotted membranes with Coomassie Brilliant Blue G225 after immunostaining.

Note 1)²². In contrast, the system presented here is expected to work for many proteins under physiological conditions in multicellular, intact organisms, however, different aspects have

to be taken into consideration when adopting this technique: (1) POIs must tolerate N terminal fusions of about 26 kDa, a C terminal fusion is not feasible; (2) POIs must at least

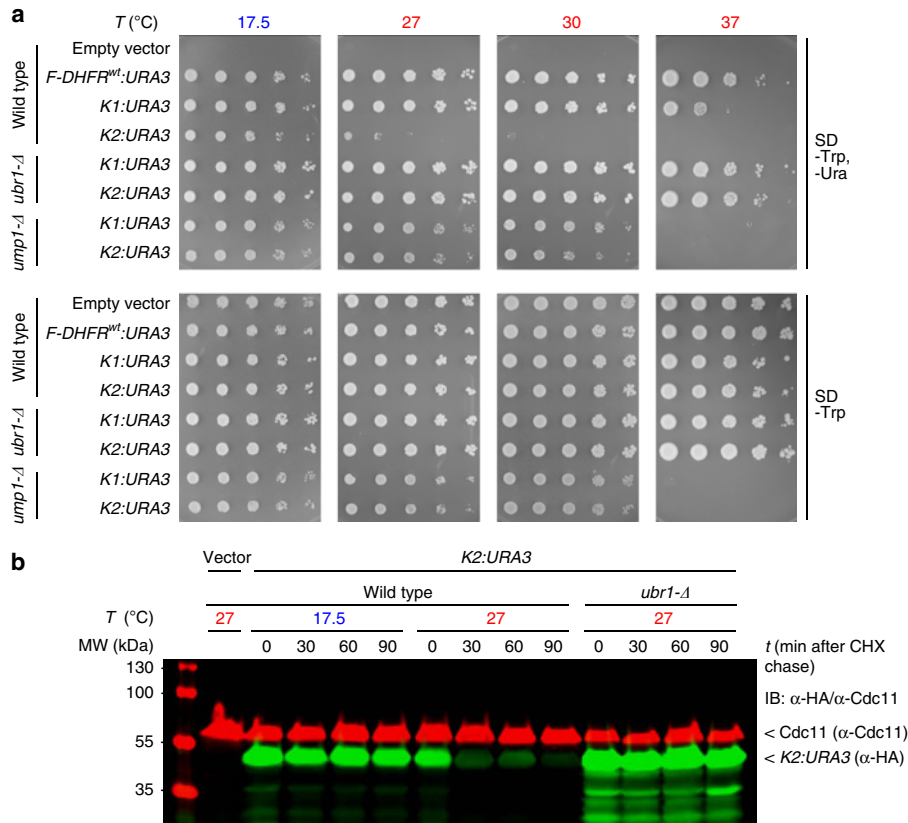


Figure 6 | The It-degron significantly lowers the restrictive temperature for conditional alleles in *S. cerevisiae*. (a,b) Modulation of enzyme activity and protein degradation in *S. cerevisiae*. Yeast cells were transformed with *F-DHFR^{mt}:URA3*, *K1:URA3*, *K2:URA3* under control of the copper inducible P_{CUP1} promoter. (a) Spot tests of WT, *ubr1 Δ* or *ump1 Δ* cells in serial (1:5) dilutions grown for 3 days at the indicated temperatures. Plates were grown at 17.5 °C for 5 days. *ump1 Δ* shows a general growth defect at elevated temperature. (b) Cycloheximide (CHX) chase of *K2:URA3*. Equal loading was confirmed by simultaneously probing against Cdc11 (red signal).

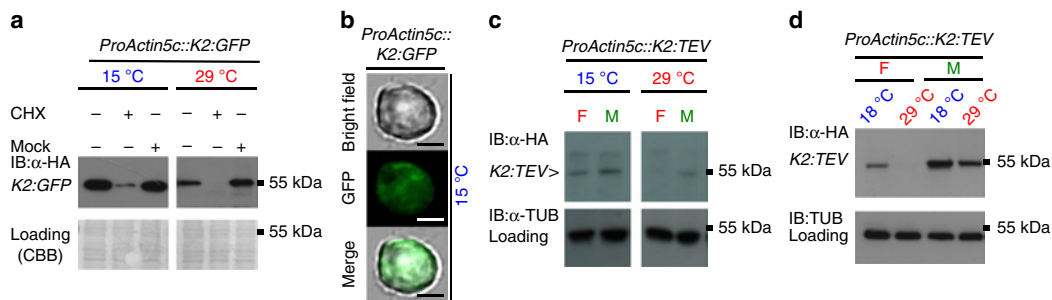


Figure 7 | Conditional protein depletion in cell culture and living *Drosophila* flies. (a d) Modulation of protein abundance in *D. melanogaster*. Two of the most commonly used *Drosophila* cell lines, as well as stably transformed living flies were used as follows. (a) *K2:GFP* stability in embryonic *Drosophila* Kc cells with 24 h recovery after transfection and after a temperature shift for 4 h from permissive (15 °C) to restrictive temperature (29 °C). CHX chase was performed with 100 μg ml⁻¹ in DMSO. (b) *K2:GFP* functionality detected as green fluorescence at permissive temperature. Scale bar, 2 μm. (c,d) Depletion of *K2:TEV* depending on a destabilizing N terminal residue (F: phenylalanine) according to the N end rule. Methionine (M) as control. (c) Transfection into *Drosophila* Schneider 2 (S2) cells with 24 h recovery after transfection and 60 h post transfection temperature shift from 16 to 29 °C. (d) *Drosophila* flies were stably transformed with *K2:TEV* initiated by a Phe (F) residue or a Met (M) *K2:TEV* control. Flies were subjected to shifts to permissive (18 °C) and restrictive temperatures (29 °C). Equal loading was further confirmed by staining of blotted membranes with probing against tubulin. CBB, Coomassie Brilliant Blue.

temporally localize to the nucleus or cytosol, the compartments with high activity of the N end rule pathway or in case for membrane localized proteins have accessible N termini¹³; (3) a pre selection via phenotype and/or western blotting after transformation helps to identify lines responding to the temperature alterations. The functionality of the system in organelles other than the cytosol or the nucleus where the action of the N end rule pathway is unclear such as endoplasmic reticulum and other membrane systems, mitochondria and chloroplasts is still to be determined.

Plant growth and development are known to be influenced by temperature^{18,41–44} and these topics are in the focus of current research. Detrimental side effects of temperature treatment may represent a downside of a temperature induced approach, the impact of 29 °C as a restrictive temperature on plant growth was documented (Figs 1 and 2, and Supplementary Figs 3 and 6). Effects of the plant high temperature adaptation responses such as hypocotyl and petiole elongation, increased leaf size and earlier flowering have to be taken into consideration. Effects of elevated temperature on plant development and genetic control of plant thermomorphogenesis are currently matter of intense research⁴⁵. However, all tested organisms were able to degrade the *K2* fusion proteins at restrictive temperature, and transcript levels remained stable over permissive and restrictive conditions. This suggests a low vulnerability of our *It* degron system to side effects related to growth differences caused by temperature.

In this study, the *It* degron enabled us to determine the temporal requirement of the transcriptional regulator *TTG1* in the context of trichome development. With a switchable CO transcription factor, we controlled timing of flowering and generated specialized cell types and meristematic tissue of the flower on demand. An engineered conditional TEV protease offers opportunities for, for example, a facilitated downstreaming of recombinant proteins by intracellular self cleavage directly in the expression host. *K2:GUS* temperature shift experiments coupled to GUS activity measurements revealed that the *It* degron opens completely new avenues by, for example, testing the influence of various levels or pulses of conditionally accumulated proteins of interest in one stable genetic background without the need to generate a plethora of transgenic events.

Trichomes are very well studied specialized model cells²⁹ present on the surfaces of many plants and capable of synthesizing and either storing or secreting large amounts of specialized metabolites³⁰. The use of the intrinsic metabolic capacity of trichomes to produce secondary metabolites or to enhance transcript levels of genes encoding enzymes required for biosynthesis of small molecules within trichomes has been discussed^{46–49}.

A special feature of using the heat inducible N degron system in living organisms is that it allows conditional build up of this cellular trichome compartment in the *K2:TTG1* system. This could be used as a genetic background to globally switch ON/OFF a regulatory protein and establish a specific cellular reaction compartment or micro reactor. Such a cell population or tissue could harbour an enzymatic reaction cascade needed to build up a molecule of interest, which is not necessarily a protein, which could potentially directly be influenced by the fusion to the *It* degron. Compartment specific expression can be achieved by using compartment specific promoters. Thus, the manufacture of biomolecules represents a possible scalable technical application as a production platform in the context of synthetic biology. We are convinced that the *It* degron is a powerful tool both for fundamental research in cell biology and developmental genetics but also has strong potential in biotechnological contexts like molecular farming of proteins or for metabolic engineering of small molecules. The conditional formation of trichomes in a

trichome lacking mutant or induced development of flowering tissue can be regarded as the design of a reaction compartment on demand, a tool to possibly form *in vivo* bioreactors.

Methods

Plant work. *A. thaliana* (L.) Heynh. plants were sown on soil mixture 1 (eight bags of MiniTray (70 l per bag, Balster Einheitserdewerk); add 50 l of water containing 800 ml Osmocote Start (Scotts International) and 250 g BioMukk (Sautter and Stepper)), or on steamed (pasteurized for at least 3 h at 90 °C) soil mixture 2 (Einheitserde Classic Kokos (45% white peat, 20% clay, 15% block peat, 20% coco fibres; 10-00800-40, Einheitserdewerke Patzer); 25% Vermiculite (grain size 2–3 mm; 29.060220, Gartnerbedarf Kamlot) and 300–400 g Exemptor per m³ soil substrate (100 g kg⁻¹ thiacloprid, 802288, Hermann Meyer). After stratification of 4 to 5 days at 4 °C in the dark, seeds were germinated and plants grown under standard long-day (16/8 h light/dark) or short-day (8/16 h light/dark) greenhouse conditions between 18 and 25 °C. *N. benthamiana* (tobacco) plants were grown on soil mixture 2.

For strictly controlled development such as during temperature-shift experiments, plants were grown either in growth cabinets (AR-66L2 and AR-66L3, Percival Scientific, CLF PlantClimatics) or in walk-in phyto chambers (Johnson Controls, equipped with ESC 300 software interface) at a humidity of 60% depending on the requirements, and watered with pre-warmed or pre-cooled tap water.

Seeds were plated either on soil or aseptically *in vitro* on plastic Petri dishes under long-day regime (16/8 h light/dark) on 0.5% Murashige & Skoog (MS; Duchefa Biochemicals, M0221) containing 1% sucrose and 8 g l⁻¹ phytoagar (Duchefa Biochemicals, P10031) in growth cabinets. For aseptic culture, dry seeds were sterilized with chlorine dioxide gas produced from 75% *Eau de Javel* (Floreale Haagen) and 25% HCl. Selective MS media contained 10 mg l⁻¹ DL-phosphinotricin (PPT, Basta, glufosinate-ammonium, Duchefa Biochemicals), 50 mg l⁻¹ kanamycin sulfate, 5.25 mg l⁻¹ sulfadiazine sodium salt (Sigma-Aldrich, S6387) or 20 mg l⁻¹ hygromycin B (Duchefa Biochemicals, H0192). Basta-resistant plants were selected *in solium* in cotyledon stage by spraying 150 ml per tray of a 1:1,000 dilution of Basta (contains 200 g l⁻¹ glufosinate-ammonium; Bayer CropScience) in tap water, which was repeated three times in a 2-day interval.

Plants used in this study were all in the background of the Columbia-0 accession (Col-0) and either WT plants, T-DNA insertion mutants for *TTG1* (*ttg1*, GABI 580A05, NASC stock ID: N455589, kindly provided by the GABI-Kat⁵⁰ team via NASC—The European Arabidopsis Stock Centre, arabidopsis.info), ethyl methanesulfonate mutants for *PRT1* (*prt1* HygS or *prt1-1*, kind gift of Andreas Bachmair, Max F. Perutz Laboratories, Vienna, Austria)^{24, 26} and '*TTG1-HA*' is *ttg1-13 Pro35S::TTG1-3xHA* (kind gift of Martina Pesch, University of Cologne, Germany). *ttg1-13* is a deletion line from fast-neutron bombardment, originally isolated from David Oppenheimer, University of Alabama, Tuscaloosa³¹), which carries the *TTG1* CDS in the backbone of *pAM-PAT-GW-3xHA* (see below for plasmid details) under control of the *CaMV* 35S promoter (*Pro35S*) and carrying the *bar* resistance marker (Laurent D. Noel and Jane Parker, Max Planck Institute for Plant Breeding Research, Cologne, Germany)), which was used as a negative control for a temperature-dependent destabilization of *TTG1*. Leaves 3/4 of the *ttg1* mutant show few undifferentiated stichel-like trichomes or initiation sites at the rim of the leaf, but neither initiation sites proximal to the midvein nor further differentiated trichomes (Figs 1c and 2a). The central parts remain glabrous³¹. All plant strains used are listed in Supplementary Table 3.

For cryo scanning electron micrographs (SEMs), 5- to 7-day-old plants (pulses; Fig. 2b or 2-week-old plants (shifts; Fig. 2c) were treated for the indicated time. First, leaves were not yet visible at the time of the pulse experiments. Before protein isolation, transgenic plants were subjected to temperature shifts by removing the potted plants constantly grown at the indicated starting temperature (16 °C in Fig. 2b or 29 °C in Fig. 2c) and shifting them to the corresponding destination temperature (29 °C in Fig. 2b or 16 °C in Fig. 2c). To achieve a rapid acclimatization, plants were immediately watered with water pre-warmed or pre-cooled to the final temperature.

DNA work and degron construct design. DNA cloning was performed following standard procedures using *Escherichia coli* strain DH5 α (Invitrogen). The constructs were generated by fusion PCR (*Pfu* polymerase, fermentas) using the primer combinations according to Supplementary Table 4. All individual constructs designed for this study are schematically represented in Supplementary Fig. 2. DNA amplicons were purified with ExoSap-IT (USB) preceding fusion PCRs. All fusions were flanked by Gateway *attB1/attB2* sites and recombined by BP reactions into *pDONR201* (Invitrogen).

Constructs *K1–K3* start with the strong *CaMV* 35S promoter, a 3'-tobacco Omega (Ω) leader sequence for translation enhancing followed by a sequence encoding for a synthetic codon-optimized *Ub*, a triplet for the destabilizing bulky and hydrophobic amino acid Phe (F), a short linker peptide (e¹; translates to HGSGI)²⁴ to further expose the N-terminal residue, one of the three different temperature-sensitive mouse dihydrofolate reductase sequences (*DHFR*⁴⁵) triggering the protein unfolding response, a triple hemagglutinin (HA)-tag (HAT)

for immunodetection and the gene of interest. All plant degron cassettes carry Phe as destabilizing N-terminal residue, because it was shown to be recognized by the *Arabidopsis* N-end rule pathway^{24, 26} but to also represent a strongly destabilizing N-terminal in other model systems^{6, 9, 25, 26} (Fig. 1a,b and Supplementary Fig. 1).

Cassettes *K1–K3* were based on a 5'-synthetic human *Ub* gene⁵¹ and an Ω leader sequence from *pRTUB8*, a derivative of *pRTUB1* (refs 24,52). The leader contains the 20 nucleotides upstream of the start codon of tobacco mosaic virus strain U1 (ref. 53) HAT was amplified from *pSKTag3SUM6* (kind gift of Andreas Bachmair). The differences of the three *DHFR* variants in *K1–K3* were as follows.

For construct *K1*, the yeast N-degron cassette, the mouse *DHFR*^{P67L} variant^{1,23}, was amplified from *pKL187* of the *S. cerevisiae* 'DEGRON-KIT' ('Kit for making *CUP1* t.s. degrons by PCR', EUROSCARF, EUROpean *Saccharomyces cerevisiae* ARchive for Functional Analysis (web.uni-frankfurt.de/fb15/mikro/euroscarf/))^{54,55}. Ω leader and *Ub* were amplified from *pRTUB8* with ND70/ND71, *DHFR*^{P67L} from *pKL187* with ND72/ND73 and HAT from *pSKTag3SUM6* with ND74/N138 (*K1:CO*) or N172 (*K1:TTG1*) introducing a *NotI* site. The short linker *e^L* (translates to HGSGI) was adapted from previous studies on protein half-life³⁴ and used to further expose the N-terminal Phe. The TTC triplet introducing Phe (F) at the *Ub–DHFR* junction and the sequence encoding *e^L* were included in ND71/ND72. Final fusion PCRs were always accomplished using the most distal primer pairs. Cloning and sequencing primers are listed in Supplementary Table 4 and Supplementary Fig. 2.

K2 is derived from *pJH10^{mut}* (*pJH23*), containing a mutated mouse *DHFR*^{T39A,E173D}, which was isolated in the yeast mutagenesis screen (Supplementary Note 2)³³. The fusion partner fragments were generated analogously to construct *K1*, that is, Ω leader and *Ub* were amplified with ND70/ND78, *DHFR*^{T39A,E173D} from *pJH10^{mut}* with ND79/ND80 and HAT with ND81/ND75 (*K2:TTG1*) or N138 (*K2:CO*). A point mutation within the *DHFR*^{T39A,E173D} was corrected by site-directed mutagenesis using N158/N159 and PfuTurbo polymerase (Stratagene). *TTG1* of *K2:TTG1* contains two silent point mutations (A555G and C567T).

An Entry clone containing *K2:TTG1* was used as a template for further *K2:POIs*. A Gateway-compatible Entry clone *pEN-L1-K2-L2* containing the *K2* degron cassette including Ω to HAT was generated to construct *K2:POI* fusions by Gateway LR reactions. *K2* was amplified from the previously described *K2:PAT* using primers 21/22 containing *attB1/attB2* recombination sites.

K3 contains a triple-mutated mouse *DHFR*. All degron constructs containing cassette *K3* are derived from the Entry vectors harbouring *K2:TTG1/CO*, which were used as templates in site-directed mutagenesis (PfuTurbo, Stratagene) using ND68/ND69 introducing the additional mutation *P67L*. *DHFR* of *K3* carries the two newly isolated mutations *DHFR*^{T39A,E173D} plus *P67L*, the original mutation from the *S. cerevisiae* N-degron¹.

K4 starts with the native *DHFR* and an N-terminal Met residue and is based on *pJH10^{mut}* (*DHFR*^{T39A,E173D}) from the yeast screen (Supplementary Note 2)³³. *DHFR* was amplified with ND82/ND80 and HAT with ND81/N138 (*K4:CO*) or N172 (*K4:TTG1*). *K2* and *K3* lacking the N-terminal HGSGI linker following the destabilizing Phe residue were based on the corresponding *K2* and *K3* fusions with *TTG1* and *CO*. To alter the *Ub–Phe–DHFR* junction, TR01 and TR02 were designed for fusion PCR.

Plant expression constructs. *Arabidopsis* *TTG1* and *CO* cDNAs (AT5G24520 and AT5G15840; kind gifts of Daniel Buoyer, University of Cologne, and Laurent Corbesier, Max Planck Institute for Plant Breeding Research, Cologne) were amplified with N173/ND77 (*K1:TTG1* and *K4:TTG1*), with ND76/ND77 (*K2:TTG1* and *K3:TTG1*) and with N139/N140 (*K1:CO*, *K2:CO*, *K3:CO* and *K4:CO*).

These *degron:POI* fusion proteins were subcloned into *pDONR201* (Invitrogen) and the Entry clones sequenced (Supplementary Table 5). For stable expression in transgenic plants, Entry clones were recombined in an LR reaction into the *attR* site-containing binary Gateway destination vector *pLEELA* (ref. 56), containing a double *CaMV* 35S promoter fused to the first *WRYKY33* intron or into *pAM-PAT-GW-ProUBQ10* (generated and kindly provided by Stefan Pusch, Deutsches Krebsforschungszentrum, Heidelberg). These Gateway-compatible Destination vectors are derived from *pAM-PAT-MCS* (multiple cloning site; GenBank accession number AY436765), derivative of *pPAM* (GenBank accession number AY027531)⁵⁷. These backbones carry the *Streptomyces hygroscopicus bar* gene that translates to phosphinothricin-N-acetyltransferase (*PAT*) as plant selection marker conferring resistance towards PPT. The vector backbone of *pAM-PAT-GW-ProUBQ10* contains an insertion of 132 bp between the *UBQ10* promoter and the *attR1* site. The insertion is part of the promoter of *TOO MANY MOUTHS* (AT1G80080) and located after the 5'-XhoI site used to insert the *UBQ10* promoter into the *pAM-PAT-GW* backbone. The insertion does not result in alternative translation products since it includes stop codons in all reading frames.

For *K2:GFP*, *pEN-L1-K2-L2* was recombined with *pAM-Kan-35S-GW-GFP* (kind gift of Jane Parker), also a derivative of *pAM-PAT-MCS*.

K2:GUS was assembled by amplifying *K2* with ND70/TR08 from *K2:TTG1*, as well as by TR07/TR06, which amplifies *GUS* from *pENTR-gus* (*uidA* CDS⁵⁸ in *pDONR201* (carries a Val(GtC)2Leu(TtA) and a silent Gaa > Caa substitution for Glu279)). *K2:GUS* was fused using ND70/TR06 and introduced into *pAM-PAT-GW-ProUBQ10* by LR.

For *K2:TEV*, *K2* was amplified from *K2:TTG1* with primers 41/36. *TEV* was isolated from *pCT190-6* (ref. 19) with primers 46/29, generating linker sequence 'L4' comprising HAT and hexahistidine tags. *pCT190-6* carries a *TEV*-containing

fusion protein in *pRS416*, *TEV* is a more stable, autoinhibition-resistant mutated (S219V) catalytic domain variant⁵⁹. *K2* and *TEV* were fused with primers 41/29, and *Taq* was added for a final 15-min adenylation step at 72 °C. The *K2:TEV* product was incompatible with Gateway ENTR vectors suggesting that the *TEV* sequence interferes with plasmid stability. Thus, *K2:TEV* was cloned into *pCRII-TOPO* (Invitrogen) by TOPO cloning between the XhoI and SpeI.

To construct a binary plant expression vector, *K2:TEV* was then cloned into *pAM-PAT-MCS* using the 5'- and 3'-EcoRI sites from *pCRII-TOPO*.

K2 for *K2:PAT* was amplified from *K2:TTG1* with ND70/TR11, *bar* (encodes *PAT*) from *pLEELA* with TR10/TR09, and fused with ND70/TR09. To receive a kanamycin-selectable binary plant expression vector, *K2:PAT* was recombined into *pJan33* (double *CaMV* 35S promoter fused to the first *WRYKY33* intron, selectable marker *NPTII*; kind gift of Marc Jakoby, University of Cologne).

S. cerevisiae constructs. Plasmids are derivatives of *pRS314* (*CEN-ARS-TRP1*) or *pRS315* (*pJH10*, *CEN-ARS-LEU2*)⁶⁰. *DHFR-HA-URA3* was assembled by inserting copper-inducible promoter *P_{CUP1}* as a *NotI–EcoRI* fragment, *Ub-F-DHFR* as *EcoRI–BamHI* fragment from *pJH10* (WT *DHFR*), *DHFR*^{P67L} (same as in *K1*), *pJH10^{mut}C33* containing the *DHFR*^{T39A,E173D} variant (same as in *K2*; Supplementary Note 2) and *HA-URA3* as *BamHI–KpnI* fragment into the polylinker of *pRS314* serving as templates for *pJD646* (*Ub-F-DHFR-wt*), *pJD647* (*Ub-F-DHFR-P67L K1*) and *pJD648* (*Ub-F-DHFR-T39A, E173D K2*). Yeast strains used are listed in Supplementary Table 3. Standard media were YPD medium and ammonia-based synthetic complete (SC) dextrose.

For spot growth assays, yeast cultures were grown overnight in liquid culture and exponentially growing cells serially diluted to 5,000/1,000/200/40/8 cells per μ l (1.5 steps). A volume of 1 μ l of the suspension was spotted with a pin-frogger onto plates containing yeast standard minimal medium/synthetic defined (SD) and grown for 3–5 days.

For cycloheximide (CHX) chase experiments, exponentially growing yeast cultures were supplemented with 100 μ g ml⁻¹ CHX; samples collected at different time-points, pelleted, washed and frozen in liquid N₂. The cells were lysed by incubating them in Laemmli loading buffer at 100 °C for 5 min. Extracts were analysed by SDS-polyacrylamide gel electrophoresis (SDS-PAGE) and two-colour western blotting using the Odyssey Infrared Imaging System (Li-Cor). Mouse monoclonal anti-HA epitope tag antibody (HA.11, clone 16B12, MMS-101R, BioLegend) in combination with an IRDye 800-coupled rat anti-mouse IgG (Rockland) was used for detecting tagged *DHFR-HA-URA3* proteins. A rabbit polyclonal anti-Cdc11 antibody (γ -415: sc-7170, Santa Cruz Biotechnology) was used for detecting CDC11 in combination with an Alexa Fluor 680-coupled goat anti-rabbit IgG antibody (Biomol), which served as an internal protein-loading control⁶¹.

Drosophila constructs. For expression of *K2:GFP* in *Drosophila* cell culture, *K2* from *pEN-L1-K2-L2* was introduced into *pAWG* (*Drosophila* Genomics Resource Center (DGRC), Indiana University, Bloomington, USA; https://dgrc.cgb.indiana.edu/product/View?product_1072; Stock Number: 1072; Murphy, T.D. et al., Construction and application of a set of Gateway vectors for expression of tagged proteins in *Drosophila*, unpublished data) via a Gateway LR reaction. *pAWG* contains an *Actin5c* promoter upstream of the Gateway cassette and a C-terminal *eGFP* tag. *ProActin5c::K2:TEV* for cell culture transfection and transformation of flies contains *DHFR*^{T39A,E173D}, amplified from *K2:TTG1* using primers 36/37 (*Phe-K2*) or 36/38 (*Met-K2*). *Ub* from *S. cerevisiae*⁴ was used and amplified with primers 9/39 (*Phe-K2*) or 9/40 (*Met-K2*). The fragments were fused to *Ub:X-DHFR*^{T39A,E173D} with primers 9/36. *TEV* was amplified from *pCT190-6* with primers 46/29 and *K2* fused with primers 9/29. *Taq* polymerase was added for a final 15-min adenylation step at 72 °C. The construct was subcloned in *pCRII-TOPO*. *K2:TEV* was incompatible with Gateway recombination and the construct prepared as XhoI–SpeI fragment, which was partially cut to leave an internal SpeI site unaffected. The fragment was ligated into *pAW* (DGRC; https://dgrc.cgb.indiana.edu/product/View?product_1127; Stock Number: 1127). *pAW* contains the *Actin5c* promoter upstream of the Gateway cassette and was cut with XhoI and NheI to lose the Gateway cassette and yield the *Actin5c*-driven fly expression vector.

Stable plant transformation and selection of transformants. The binary plant expression vectors were retransformed into *Agrobacterium tumefaciens* *GV3101-pMP90RK* (C58C1 *Rif^r Gm^r Km^r*)⁶² to obtain a bacterial transformation suspension. The identity of the *Agrobacterium* strains was verified by backtransformation of isolated plasmid into *E. coli* DH5 α and at least three independent analytical digestions. All constructs were transformed by a modified version of the floral dip method⁶³.

Individual T1 (generation 1 after transformation) transgenic plant lines were pre-selected with Basta or kanamycin as described above. To exclude lines showing position effects, for example, by disrupting essential genes by the construct T-DNA, the number of insertion loci was determined in a segregation analysis in the T2 generation and only transgenic plants carrying one single insertion locus were further used. Standard lines were established by isolating T3 plants homozygous for the transgene. Independent representative reference lines displaying a typical conditional phenotype on temperature up- and downshifts were used in the final

experiments. Standard lines were established by isolating T3 plants homozygous for the transgene.

To identify responsive transgenic lines, we prescreened *TTG1-td*, *CO-td*, *GUS-td* and *PAT-td* by developmental and histological phenotype and *TEV-td* and *GFP-td* by western blotting.

Transient transfection of *N. benthamiana*. For transient transformation of tobacco, leaves of 4-week-old plants were infiltrated with *Agrobacterium* GV3101-*pMP90RK*, carrying binary plant expression vectors. *Agrobacterium* were grown to the stationary phase overnight in 10 ml of YEB medium and pelleted at 5,000g at room temperature. The pellet was washed once in 10 ml of infiltration buffer (10 mM MES (pH 5.6), 10 mM MgSO₄, 100 μM acetosyringone (D134406, Sigma)) and subsequently resuspended in 10 ml of the same buffer. *Agrobacterium* strains were co-infiltrated with *p19*, an *A. tumefaciens* strain based on GV3101 carrying *pBIN6Ip19* containing the *p19* protein of tomato bushy stunt virus to suppress post-transcriptional gene silencing and increase ectopic gene expression⁹⁴. Before infiltration, bacteria suspensions were adjusted to an OD₆₀₀ of 0.5. Desired bacteria suspensions were then mixed with *p19* bacteria suspension to a final OD₆₀₀ value of 0.25 for both components. Bacteria suspensions were then infiltrated into the epidermis on the lower side of the tobacco leaf. Infiltrated areas were marked on the upper side of the leaf with a permanent marker. For an easier infiltration procedure, plants were watered and transferred to standard greenhouse long-day conditions the day before to allow plant stomata to open. To allow efficient transformation and expression, plants were kept for 48 h in the greenhouse, before applying temperature shift experiments by transferring them into a growth cabinet at either permissive or restrictive growth conditions. For one data point, 15–20 leaf discs of 5 mm diameter were collected from infiltrated areas and snap-frozen in liquid nitrogen. Extraction was performed using radioimmunoprecipitation assay (RIPA) buffer as mentioned below.

Drosophila cell culture work. *D. melanogaster* Kc embryonic tissue culture cells⁶⁵ or Schneider 2 (S2) cells⁶⁶ (Invitrogen) were grown at 24 °C in 3 ml of Schneider's medium (Gibco) supplemented with 10% fetal bovine serum. Cells were passaged into fresh media every 5 days in a 1:10 dilution. Transfection was carried out in a 12-well dish using the Effectene transfection kit (Qiagen) according to the manufacturer's protocol for adherent cells. Temperature treatments and shifts from 24 °C to the desired temperature were carried out at 15 or 16 °C versus 29 °C. The details of the temperature-shift experiments are indicated in the figure legend. CHX chase was performed with 100 μg ml⁻¹ in dimethylsulfoxide (DMSO).

Drosophila transformation and characterization. Vectors carrying *Actin5c::Phe-K2:TEV* (F-K2:TEV) or *Actin5c::Met-K2:TEV* (M-K2:TEV) were injected in ZH-attP-2A or ZH-attP-51D embryos according to the phic31 recombinase transgenesis system⁶⁷. In brief, 1-h-old embryos were collected, placed on slides and immersed in injection oil. The plasmids were injected in the posterior region of the embryo aiming at the area where the pole cells would develop. Hatched larvae were collected and placed on standard *Drosophila* medium based on a mixture of cornmeal, yeast, agar, sucrose, soy flour and water. Transformants were grown at 25 °C standard conditions. Adult flies were shifted either to 18 or 29 °C. After 24 h, total protein extracts were obtained from whole flies homogenized in standard lysis buffer (20 mM Tris-Cl (pH 7.5), 200 mM NaCl, 2 mM EDTA, 10% glycerol, 1% Nonidet P-40 and EDTA-free Complete Protease Inhibitor Cocktail (Roche Diagnostics)).

Protein extraction and western blot analysis. Plant tissue (*Arabidopsis*: leaf or seedlings, tobacco: leaf discs) was collected in a standard 2 ml reaction tube containing three Nirosta stainless steel beads (3.175 mm; 75306, Muhlmeier), snap-frozen in liquid N₂ and stored at -80 °C. Material was ground frozen using a bead mill (Retsch, MM400; 45 s, 30 Hz) in collection microtube blocks (adaptor set from TissueLyser II, 69984, Qiagen).

For *K2:TTG1* time courses, per time point, one leaf was ground in 200 μl of extraction buffer (50 mM Tris-Cl (pH 7.6), 150 mM NaCl, 5 mM EDTA, 0.1% SDS, 0.1% β-mercaptoethanol and EDTA-free Complete Protease Inhibitor Cocktail). Alternatively, tissue was lysed using RIPA buffer (50 mM Tris-Cl (pH 8), 120 mM NaCl, 20 mM NaF, 1 mM EDTA, 6 mM EGTA, 1 mM benzamidine hydrochloride, 15 mM Na₄P₂O₇ and 1% Nonidet P-40 supplemented with EDTA-free Complete Protease Inhibitor cocktail added freshly).

Extraction of *K2:TEV* was done in 25 mM Tris-Cl (pH 7.5), 75 mM NaCl, 15 mM MgCl₂, 15 mM EGTA (pH 8.0), 0.1% Tween 20, 0.1% Triton X-100, 5 mM dithiothreitol and EDTA-free Complete Protease Inhibitor Cocktail in a chilled cooling block at 4 °C, 800 r.p.m. for 30 min. Insoluble cell debris was pelleted via centrifugation for 20 min at 4 °C, 20,000g. The protein content of the samples was determined using a DirectDetect infrared spectrophotometer (MerckMillipore).

Drosophila cells were transferred into a standard 1.5 ml reaction tube and collected via centrifugation at 4 °C for 5 min, 300g. The pellet was washed once with ice-cold PBS and cells lysed using RIPA buffer. Following steps were carried out as described above.

Drosophila pupae were lysed as described above and western blots performed with rabbit polyclonal anti-HA epitope tag antibody (Y-11: sc-805, Santa Cruz

Biotechnology) or rabbit polyclonal α-Tubulin antibody (H-300: sc-5546, Santa Cruz Biotechnology) and detected by enhanced chemiluminescence (ECL).

S. cerevisiae cells were grown at 30 °C to logarithmic growth phase, and CHX added to the cultures to a final concentration of 100 mg l⁻¹. Strains were expanded at 25 °C and incubated at 37 °C for 30 min before CHX addition. Proteins were extracted from 5 to 50 ml of exponentially growing suspension culture (OD₆₀₀ 0.8–1.2) by centrifugation and grinding with glass beads (5 min, IKA Vibra-VXR, Janke und Kunkel) at 4 °C in 150–300 μl Native lysis buffer (50 mM Na-HEPES (pH 7.5); 150 mM NaCl, 5 mM EDTA, 1% Triton X-100, containing EDTA-free Complete Protease Inhibitor Cocktail, 20 μM MG132) followed by a second centrifugation (4 °C, 10 min, 20,000g). Proteins were separated by SDS-PAGE and analysed by quantitative western blotting⁶¹ using an LAS1000 system (Fuji).

Equal protein amounts were resolved by 10% (GUS) or 12% (all others) SDS-PAGE. Blotting of TTG1 and CO samples was done on nitrocellulose transfer membrane by wet blot in a tank blotter (SCIE-PLAS EB10)⁶³. All other samples were blotted onto polyvinylidene fluoride transfer membrane by semi-dry blot using a Trans-Blot SD semi-dry electrophoretic transfer cell (170-3940, Bio-Rad).

Equal loading and general protein abundance was confirmed by staining of the blotted and probed membranes after immunostaining with Ponceau S (sodium salt) or Coomassie Brilliant Blue G250 (CBB G150). All antibodies used including parameters are listed in Supplementary Table 6. All degen constructs can be detected with mouse monoclonal anti-DHFR antibody (A-4: sc-74593, Santa Cruz Biotechnology) and mouse monoclonal anti-HA epitope tag antibody (HA.11, clone 16B12: MMS-101R, BioLegend), or rat monoclonal anti-HA epitope tag antibody (High Affinity, clone 3F10: 11 867 423 001, Roche Diagnostics). Horseradish peroxidase-conjugated secondary antibodies (Supplementary Table 6) were detected by ECL using ECL SuperSignal West Pico or Femto (34087 or 34096, Pierce) followed by exposure on autoradiography film. Colorimetric detection of alkaline phosphatase-labelled antibody (Supplementary Table 6) via the nitroblue tetrazolium chloride/5-bromo-4-chloro-3-indolyl phosphate *p*-toluidine (NBT/BCIP) substrate system by tetrazolium precipitation with NBT/BCIP reaction buffer (100 mM Tris-Cl (pH 9.5), 100 mM NaCl, 50 mM MgCl₂, 400 μM NBT (75 mg ml⁻¹ stock in 70% DMSO) and 400 μM BCIP salt (50 mg ml⁻¹ stock in DMSO). Staining was done until colour developed and the reaction stopped in 20 mM EDTA in tris-buffered saline (TBS) (pH 8.0) and by washing for three times in water. Western data were confirmed by analysis of at least three biological replicates. Full blot and gel images are provided in Supplementary Fig. 8.

In situ glucuronidase histology. Two- to three-week-old plants were collected and submerged in GUS staining solution (1 mM X-Gluc (X-glucuronide sodium salt))⁶⁸. After vacuum infiltration for 30 min, samples were incubated overnight at 37 °C, fixed and cleared in GUS fixation solution (9:1 ethanol/glacial acetic acid for 4 h/room temperature) and stored in 70% ethanol.

Quantification of glucuronidase activity. At least five seedlings/sample were collected, pooled and snap-frozen in liquid N₂. Proteins from 2-week-old *K2:GUS* seedlings were extracted in GUS extraction buffer (50 mM Na-phosphate, 10 mM EDTA, 0.1% SDS, 0.1% Triton X-100 and freshly added 10 mM β-mercaptoethanol and EDTA-free protease inhibitor cocktail)⁶⁸. A volume of 196 μl assay solution (1 mM 4-methylumbelliferyl-β-D-glucuronide (4-MUG)) were mixed with 4 μl of protein extract in a white 96-well plate (Nunc FluoroNunc, Thermo Scientific) for the assay. Fluorometric measurements were done at 37 °C in a spectrophotometer (M1000, Tecan) for 60 min, one data point was taken per minute. Hydrolysis of 4-MUG by GUS generates the aglycone 4-methylumbelliferone (4-MU), which gives a detectable fluorescent emission at 455 nm after excitation at 365 nm. Owing to the online fluorescence measurement of increasing 4-MU, the reaction samples did not have to be separately stopped with 0.2 M Na₂CO₃ after 60 min as described in the original protocol. Samples were measured for a total of 60 min with one data point taken every minute and normalized to a 4-MU standard. Activity was determined as pmol 4-MU per min and mg of total protein. Control plants expressing *Pro35S::GUS* from the binary plasmid *pBI121* (ref. 69) were a kind gift of Diana Schmidt (Leibniz Institute of Plant Biochemistry, Halle).

Degen tuning assay. For the time-course *K2:GUS* experiment, plants were grown aseptically on MS-containing Petri dishes (see above) including 10 mg l⁻¹ PPT for 2 weeks at either permissive or restrictive temperatures. A first sample (at least five seedlings) was taken and snap-frozen in liquid N₂. Then, the temperature was increased or decreased by 2.8 °C, depending on the design of the time course (warm-cold-warm or cold-warm-cold), and kept for 24 h. Every 24 h, samples were taken before the new temperature change. The time frame allowed plants to run one complete day/night cycle, acclimatize and appropriately express/stabilize protein. The activity was measured as indicated above, all three biological replicates (*n* = 3) consisting of independent plant material were individually measured as three technical replicates.

Immunoprecipitation for mass spectrometry. *K2:GUS* plants were grown on plates on 0.5% MS containing PPT at permissive temperature (13 °C) for 2 weeks, collected and frozen in liquid N₂. After milling (see above), plant material was lysed

and proteins extracted with extraction buffer containing phosphatase inhibitors and cleared twice by centrifugation (4 °C, 20,000g)^{70,71}. Per sample, two microcentrifuge tubes were prepared, each containing 250 µl of lysate at a concentration of 1.5 µg total protein per µl. Preclearing of sepharose matrix (nProtein A Sepharose 4 Fast Flow, GE Healthcare Life Sciences) was performed for 2 h on a rotating wheel at 4 °C with 100 µl of 50% bead slurry/reaction. After a centrifugation step (4 °C, 5 min, 20,000g), the supernatant was transferred into a new tube and 50 µl of anti-DHFR antibody (A-4: sc-74593, Santa Cruz Biotechnology) were added per reaction. Samples were incubated overnight on a rotating wheel at 4 °C. A volume of 250 µl of 50% bead slurry were then added and incubated for 3 h rotating at 4 °C. Beads were centrifuged (4 °C, 400g, 2 min) and washed 3 times with 1 ml of bead buffer^{70,71}. Beads were boiled for 15 min in 30 µl of 5 × SDS loading dye, centrifuged (5 min, 20,000 g) and the supernatants of two reactions pooled. A volume of 5 µl of the supernatant were loaded on a 6% PAGE gel and subjected to western blotting with rabbit anti-HA antibody (HA.11, clone 16B12: MMS-101R, BioLegend) to confirm running parameters of the different K2:GUS bands. The rest of the supernatant was separated via SDS–PAGE and silver-stained using an MS compatible staining protocol in an overall volume of 25 ml per gel. The gel was incubated twice for 20 min in aqueous fixing solution (40% methanol and 10% glacial acetic acid), pretreated for 30 min in 0.8 mM Na₂S₂O₃, 0.8 M CH₃COONa and 30% methanol, washed for three times in water for 5 min, stained for 20 min in 12 mM AgNO₃, developed for maximum 5 min in 0.2 M NaCO₃, 0.04% formaldehyde, stopped for 10 min in 0.3 M Na₂-EDTA and washed for two times in water for 10 min. The stained gel can be conserved overnight or longer in 25% ethanol, 3% glycerol and 72% water. Three lanes were excised (Supplementary Fig. 7). Liquid chromatography–mass spectrometric (LC–MS) analysis was carried out as follows.

LC–MS analysis. Cysteine side chains were reduced and alkylated, proteins digested with trypsin overnight and peptides extracted and dried in a concentrator. Peptides were dissolved in 5% acetonitrile and 0.1% trifluoroacetic acid, and injected into an EASY nano-LCII chromatography system (Thermo Fisher). Reverse phase chromatography was performed using an EASY column SC200 (10 cm, inner diameter: 75 µm, particle size: 3 µm) using a pre-column (EASY column SC001, 2 cm, inner diameter: 100 µm, particle size: 5 µm) and a mobile phase gradient from 5 to 40% acetonitrile, 0.1% trifluoroacetic acid in water in 150 min (flow rate of 300 nl min⁻¹, all from Thermo Fisher). Peptides were electrosprayed on-line into an LTQ-Orbitrap Velos Pro mass spectrometer (Thermo Fisher; spray voltage of 1.9 kV). Orbitrap (Fourier transform, FT) and ion trap (IT) injection waveforms were enabled, one micro scan acquired for all scan types, FT master scan preview and charge state screening enabled; singly charged ions were rejected in data-dependent acquisition (DDA) analysis. The mass spectrometer was calibrated with *m/z* of 445.120024 Th. Data-dependent MS/MS spectral acquisition of the 20 most abundant ion signals was performed in the full scan. SwissProt protein sequence database (535,248 sequences; 189,901,164 residues) was searched with MS/MS spectra using Mascot (matrix Science, Proteome Discoverer v.1.4; Thermo Fisher) to identify Ub, DHFR and GUS peptides. The enzyme was set to trypsin, two missed cleavages tolerated, precursor tolerance set to 7 p.p.m., fragment ion tolerance to 0.8 Th, and the family-wise error rate controlled using a 1% peptide false discovery rate.

Proteasome inhibitor experiments. Seedlings were grown in liquid culture in 50-ml Erlenmeyer flasks in 20 ml of 0.5% MS including vitamins (Duchefa Biochemicals, M0222), 0.25% sucrose, 500 mg l⁻¹ MES (2-(N-Morpholino)-ethane sulfonic acid, Carl Roth, 4256) and 10 mg l⁻¹ PPT for 2 weeks at permissive or restrictive temperature. Before treatment, seedlings were transferred into 12-well microplates (Greiner) into 5 ml of medium and treated with 5 µM of MG132 (UBPbio) in DMSO (5 µl of a 50 mM stock per 5 ml medium). Mock-treated samples were supplemented with an equivalent volume of DMSO. Plates were incubated for 5 h, collected, frozen in liquid N₂ and proteins extracted with RIPA buffer. After protein quantification with bicinchoninic acid assay (Thermo Scientific), 20 µg of total protein were loaded per lane, separated on a 10% SDS–PAGE, blotted and probed as described above.

RNA work and RT–PCR. Two-week-old seedlings were collected and snap-frozen. After milling, about 50 mg of tissue was used for RNA extraction with RNeasy Plant Mini Kit (Qiagen). RNA was measured with a spectrophotometer and quality assessed via agarose gel electrophoresis. For first-strand cDNA synthesis, 500 ng of total RNA were used with an equimolar mixture of four oligo(dT) primers (CDSIII–NotIA/C/G/T, Supplementary Table 7) and RevertAid H Minus Reverse Transcriptase (Thermo Scientific). A volume of 1 µl of cDNA was used for PCR analysis using self-made *Taq* in two reactions per sample; one with generic degron-specific primers (DHFR frw/DHFR rev) to test transcript levels of the transgene and one with intron-spanning primers EF1ss/EF1as for *ELONGATION FACTOR 1 (EF1)* as a housekeeping gene (amplicon sizes: genomic 810 bp; cDNA 709 bp). Both PCRs were run for 30 cycles. Oligonucleotide primers used for RT–PCR are listed in Supplementary Table 7.

Microscopy. SEM was done with a SUPRA 40VP (Carl Zeiss MicroImaging) equipped with a K1250X Cryogenic SEM Preparation System (EMITECH), a CPD

030 critical point dryer (Bal-Tec) and a SC 7600 sputter coater (Polaron) at the on-campus microscopy core facility Zentrale Mikroskopie (CeMic) of the Max Planck Institute for Plant Breeding Research, Cologne. Light and confocal laser scanning microscopy was performed with an LSM710 system (Carl Zeiss MicroImaging). K2:GFP fluorescence was observed in root tips of plants that were aseptically grown for 2 weeks under long-day conditions at either constitutively restrictive or permissive temperatures on 0.5 MS medium containing 50 mg l⁻¹ kanamycin sulfate. Photographs of *in vitro* cultures and histological stainings were taken with a stereo microscope (Stemi 2000-C) equipped with a Zeiss CL 6000 LED illumination unit, and a video adapter 60 C including an AxioCam ERC 5s digital camera (all from Carl Zeiss MicroImaging).

Data availability. The authors declare that the data supporting the findings of this study are available within the article and its Supplementary Information files or are available from the corresponding author on request.

References

- Dohmen, R. J., Wu, P. & Varshavsky, A. Heat-inducible degron: a method for constructing temperature-sensitive mutants. *Science* **263**, 1273–1276 (1994).
- Varshavsky, A. Naming a targeting signal. *Cell* **64**, 13–15 (1991).
- Johnson, E. S., Gonda, D. K. & Varshavsky, A. cis-trans recognition and subunit-specific degradation of short-lived proteins. *Nature* **346**, 287–291 (1990).
- Bachmair, A., Finley, D. & Varshavsky, A. *In vivo* half-life of a protein is a function of its amino-terminal residue. *Science* **234**, 179–186 (1986).
- Graciet, E., Mesiti, F. & Wellmer, F. Structure and evolutionary conservation of the plant N-end rule pathway. *Plant J.* **61**, 741–751 (2010).
- Graciet, E. & Wellmer, F. The plant N-end rule pathway: structure and functions. *Trends Plant Sci.* **15**, 447–453 (2010).
- Varshavsky, A. The N-end rule pathway and regulation by proteolysis. *Protein Sci.* **20**, 1298–1345 (2011).
- Tasaki, T., Sriram, S. M., Park, K. S. & Kwon, Y. T. The N-end rule pathway. *Annu. Rev. Biochem.* **81**, 261–289 (2012).
- Gibbs, D. J., Bacardit, J., Bachmair, A. & Holdsworth, M. J. The eukaryotic N-end rule pathway: conserved mechanisms and diverse functions. *Trends Cell Biol.* **24**, 603–611 (2014).
- Heck, J. W., Cheung, S. K. & Hampton, R. Y. Cytoplasmic protein quality control degradation mediated by parallel actions of the E3 ubiquitin ligases Ubr1 and San1. *Proc. Natl Acad. Sci. USA* **107**, 1106–1111 (2010).
- Nillegoda, N. B. et al. Ubr1 and Ubr2 function in a quality control pathway for degradation of unfolded cytosolic proteins. *Mol. Biol. Cell* **21**, 2102–2116 (2010).
- Levy, F., Johnston, J. A. & Varshavsky, A. Analysis of a conditional degradation signal in yeast and mammalian cells. *Eur. J. Biochem.* **259**, 244–252 (1999).
- Wittke, S., Lewke, N., Muller, S. & Johnsson, N. Probing the molecular environment of membrane proteins *in vivo*. *Mol. Biol. Cell* **10**, 2519–2530 (1999).
- Baker, R. T., Smith, S. A., Marano, R., McKee, J. & Board, P. G. Protein expression using cotranslational fusion and cleavage of ubiquitin. Mutagenesis of the glutathione-binding site of human Pi class glutathione S-transferase. *J. Biol. Chem.* **269**, 25381–25386 (1994).
- Parsell, D. A. & Sauer, R. T. The structural stability of a protein is an important determinant of its proteolytic susceptibility in *Escherichia coli*. *J. Biol. Chem.* **264**, 7590–7595 (1989).
- Su, X., Bernal, J. A. & Venkitaraman, A. R. Cell-cycle coordination between DNA replication and recombination revealed by a vertebrate N-end rule degron-Rad51. *Nat. Struct. Mol. Biol.* **15**, 1049–1058 (2008).
- Bernal, J. A. & Venkitaraman, A. R. A vertebrate N-end rule degron reveals that Orc6 is required in mitosis for daughter cell abscission. *J. Cell Biol.* **192**, 969–978 (2011).
- Larkindale, J., Hall, J. D., Knight, M. R. & Vierling, E. Heat stress phenotypes of *Arabidopsis* mutants implicate multiple signaling pathways in the acquisition of thermotolerance. *Plant Physiol.* **138**, 882–897 (2005).
- Taxis, C., Stier, G., Spadaccini, R. & Knop, M. Efficient protein depletion by genetically controlled deprotection of a dormant N-degron. *Mol. Syst. Biol.* **5**, 267 (2009).
- Banaszynski, L. A., Chen, L. C., Maynard-Smith, L. A., Ooi, A. G. & Wandless, T. J. A rapid, reversible, and tunable method to regulate protein function in living cells using synthetic small molecules. *Cell* **126**, 995–1004 (2006).
- Nishimura, K., Fukagawa, T., Takisawa, H., Kakimoto, T. & Kanemaki, M. An auxin-based degron system for the rapid depletion of proteins in nonplant cells. *Nat. Methods* **6**, 917–922 (2009).
- Faden, F., Mielke, S., Lange, D. & Dissmeyer, N. Generic tools for conditionally altering protein abundance and phenotypes on demand. *Biol. Chem.* **395**, 737–762 (2014).
- Dohmen, R. J. & Varshavsky, A. Heat-inducible degron and the making of conditional mutants. *Methods Enzymol.* **399**, 799–822 (2005).
- Bachmair, A., Becker, F. & Schell, J. Use of a reporter transgene to generate *Arabidopsis* mutants in ubiquitin-dependent protein degradation. *Proc. Natl Acad. Sci. USA* **90**, 418–421 (1993).

25. Potuschak, T. *et al.* PRT1 of *Arabidopsis thaliana* encodes a component of the plant N-end rule pathway. *Proc. Natl Acad. Sci. USA* **95**, 7904–7908 (1998).
26. Stary, S. *et al.* PRT1 of *Arabidopsis* is a ubiquitin protein ligase of the plant N-end rule pathway with specificity for aromatic amino-terminal residues. *Plant Physiol.* **133**, 1360–1366 (2003).
27. Marks, M. D. Molecular genetic analysis of trichome development in *Arabidopsis*. *Annu. Rev. Plant Physiol. Plant Mol. Biol.* **48**, 137–163 (1997).
28. Oppenheimer, D. G. Genetics of plant cell shape. *Curr. Opin. Plant Biol.* **1**, 520–524 (1998).
29. Hulskamp, M. Plant trichomes: a model for cell differentiation. *Nat. Rev. Mol. Cell Biol.* **5**, 471–480 (2004).
30. Schilmiller, A. L., Last, R. L. & Pichersky, E. Harnessing plant trichome biochemistry for the production of useful compounds. *Plant J.* **54**, 702–711 (2008).
31. Walker, A. R. *et al.* The TRANSPARENT TESTA GLABRA1 locus, which regulates trichome differentiation and anthocyanin biosynthesis in *Arabidopsis*, encodes a WD40 repeat protein. *Plant Cell* **11**, 1337–1350 (1999).
32. Bouyer, D. *et al.* Two-dimensional patterning by a trapping/depletion mechanism: the role of TTG1 and GL3 in *Arabidopsis* trichome formation. *PLoS Biol.* **6**, e141 (2008).
33. Gowda, N. K., Kandasamy, G., Froehlich, M. S., Dohmen, R. J. & Andreasson, C. Hsp70 nucleotide exchange factor Fes1 is essential for ubiquitin-dependent degradation of misfolded cytosolic proteins. *Proc. Natl Acad. Sci. USA* **110**, 5975–5980 (2013).
34. Bachmair, A. & Varshavsky, A. The degradation signal in a short-lived protein. *Cell* **56**, 1019–1032 (1989).
35. Chien, J. C. & Sussex, I. M. Differential regulation of trichome formation on the adaxial and abaxial leaf surfaces by gibberellins and photoperiod in *Arabidopsis thaliana* (L.) Heynh. *Plant Physiol.* **111**, 1321–1328 (1996).
36. Bramsiepe, J. *et al.* Endoreplication controls cell fate maintenance. *PLoS Genet.* **6**, e1000996 (2010).
37. Putterill, J., Robson, F., Lee, K., Simon, R. & Coupland, G. The CONSTANS gene of *Arabidopsis* promotes flowering and encodes a protein showing similarities to zinc finger transcription factors. *Cell* **80**, 847–857 (1995).
38. Simon, R., Igeno, M. I. & Coupland, G. Activation of floral meristem identity genes in *Arabidopsis*. *Nature* **384**, 59–62 (1996).
39. Onouchi, H., Igeno, M. I., Perilleux, C., Graves, K. & Coupland, G. Mutagenesis of plants overexpressing CONSTANS demonstrates novel interactions among *Arabidopsis* flowering-time genes. *Plant Cell* **12**, 885–900 (2000).
40. Volkmann, G., Volkmann, V. & Liu, X. Q. Site-specific protein cleavage *in vivo* by an intein-derived protease. *FEBS Lett.* **586**, 79–84 (2012).
41. Gray, W. M., Ostin, A., Sandberg, G., Romano, C. P. & Estelle, M. High temperature promotes auxin-mediated hypocotyl elongation in *Arabidopsis*. *Proc. Natl Acad. Sci. USA* **95**, 7197–7202 (1998).
42. Koini, M. A. *et al.* High temperature-mediated adaptations in plant architecture require the bHLH transcription factor PIF4. *Curr. Biol.* **19**, 408–413 (2009).
43. Kumar, S. V. & Wigge, P. A. H2A.Z-containing nucleosomes mediate the thermosensory response in *Arabidopsis*. *Cell* **140**, 136–147 (2010).
44. Franklin, K. A. *et al.* Phytochrome-interacting factor 4 (PIF4) regulates auxin biosynthesis at high temperature. *Proc. Natl Acad. Sci. USA* **108**, 20231–20235 (2011).
45. Quint, M. *et al.* Molecular and genetic control of plant thermomorphogenesis. *Nat. Plants* **2**, 15190 (2016).
46. Tissier, A. Glandular trichomes: what comes after expressed sequence tags? *Plant J.* **70**, 51–68 (2012).
47. Lange, B. M. & Turner, G. W. Terpenoid biosynthesis in trichomes—current status and future opportunities. *Plant Biotechnol. J.* **11**, 2–22 (2013).
48. Kliebenstein, D. J. Making new molecules—evolution of structures for novel metabolites in plants. *Curr. Opin. Plant Biol.* **16**, 112–117 (2013).
49. Pattanaik, S., Patra, B., Singh, S. K. & Yuan, L. An overview of the gene regulatory network controlling trichome development in the model plant, *Arabidopsis*. *Front. Plant Sci.* **5**, 259 (2014).
50. Kleinboelting, N., Huep, G., Kloetgen, A., Viehoveer, P. & Weisshaar, B. GABI-Kat SimpleSearch: new features of the *Arabidopsis thaliana* T-DNA mutant database. *Nucleic Acids Res.* **40**, D1211–D1215 (2012).
51. Ecker, D. J. *et al.* Gene synthesis, expression, structures, and functional activities of site-specific mutants of ubiquitin. *J. Biol. Chem.* **262**, 14213–14221 (1987).
52. Bachmair, A., Becker, F., Masterson, R. V. & Schell, J. Perturbation of the ubiquitin system causes leaf curling, vascular tissue alterations and necrotic lesions in a higher plant. *EMBO J.* **9**, 4543–4549 (1990).
53. Gallie, D. R., Sleat, D. E., Watts, J. W., Turner, P. & Wilson, T. M. A comparison of eukaryotic viral 5'-leader sequences as enhancers of mRNA expression *in vivo*. *Nucleic Acids Res.* **15**, 8693–8711 (1987).
54. Kanemaki, M., Sanchez-Diaz, A., Gambus, A. & Labib, K. Functional proteomic identification of DNA replication proteins by induced proteolysis *in vivo*. *Nature* **423**, 720–724 (2003).
55. Sanchez-Diaz, A., Kanemaki, M., Marchesi, V. & Labib, K. Rapid depletion of budding yeast proteins by fusion to a heat-inducible degron. *Sci. STKE* **2004**, PL8 (2004).
56. Jakoby, M. J. *et al.* Analysis of the subcellular localization, function, and proteolytic control of the *Arabidopsis* cyclin-dependent kinase inhibitor ICK1/KRP1. *Plant Physiol.* **141**, 1293–1305 (2006).
57. Rademacher, T. *et al.* An engineered phosphoenolpyruvate carboxylase redirects carbon and nitrogen flow in transgenic potato plants. *Plant J.* **32**, 25–39 (2002).
58. Kertbundit, S., De Greve, H., Deboeck, F., Van Montagu, M. & Hernalsteens, J. P. *In vivo* random beta-glucuronidase gene fusions in *Arabidopsis thaliana*. *Proc. Natl Acad. Sci. USA* **88**, 5212–5216 (1991).
59. Lucast, L. J., Batey, R. T. & Doudna, J. A. Large-scale purification of a stable form of recombinant tobacco etch virus protease. *Biotechniques* **30**, 544–556 (2001).
60. Sikorski, R. S. & Hieter, P. A system of shuttle vectors and yeast host strains designed for efficient manipulation of DNA in *Saccharomyces cerevisiae*. *Genetics* **122**, 19–27 (1989).
61. Kurian, L., Palanimurugan, R., Godderz, D. & Dohmen, R. J. Polyamine sensing by nascent ornithine decarboxylase antizyme stimulates decoding of its mRNA. *Nature* **477**, 490–494 (2011).
62. Koncz, C. & Schell, J. The promoter of TL-DNA gene 5 controls the tissue-specific expression of chimaeric genes carried by a novel type of *Agrobacterium* binary vector. *Mol. Gen. Genet.* **204**, 383–396 (1986).
63. Dissmeyer, N. & Schnittger, A. Use of phospho-site substitutions to analyze the biological relevance of phosphorylation events in regulatory networks. *Methods Mol. Biol.* **779**, 93–138 (2011).
64. Voinnet, O., Rivas, S., Mestre, P. & Baulcombe, D. An enhanced transient expression system in plants based on suppression of gene silencing by the p19 protein of tomato bushy stunt virus. *Plant J.* **33**, 949–956 (2003).
65. Echaler, G. & Ohanessian, A. Isolement, en cultures *in vitro*, de lignées cellulaires diploïdes de *Drosophila melanogaster*. *C. R. Acad. Sci. (Paris)* **268**, 1771–1773 (1969).
66. Schneider, I. Cell lines derived from late embryonic stages of *Drosophila melanogaster*. *J. Embryol. Exp. Morphol.* **27**, 353–365 (1972).
67. Bischof, J., Maeda, R. K., Hediger, M., Karch, F. & Basler, K. An optimized transgenesis system for *Drosophila* using germ-line-specific phiC31 integrases. *Proc. Natl Acad. Sci. USA* **104**, 3312–3317 (2007).
68. Kim, K. W., Franceschi, V. R., Davin, L. B. & Lewis, N. G. Beta-glucuronidase as reporter gene: advantages and limitations. *Methods Mol. Biol.* **323**, 263–273 (2006).
69. Jefferson, R. A., Kavanagh, T. A. & Bevan, M. W. GUS fusions: beta-glucuronidase as a sensitive and versatile gene fusion marker in higher plants. *EMBO J.* **6**, 3901–3907 (1987).
70. Dissmeyer, N. *et al.* T-loop phosphorylation of *Arabidopsis* CDKA;1 is required for its function and can be partially substituted by an aspartate residue. *Plant Cell* **19**, 972–985 (2007).
71. Dissmeyer, N. *et al.* Control of cell proliferation, organ growth, and DNA damage response operate independently of dephosphorylation of the *Arabidopsis* Cdk1 homolog CDKA;1. *Plant Cell* **21**, 3641–3654 (2009).

Acknowledgements

This work was supported by a grant for a Junior Research Group of the ScienceCampus Halle—Plant-based Bioeconomy to N.D.; by a PhD fellowship of the Landesgraduiertenförderung Sachsen-Anhalt and a grant of the German Academic Exchange Service (DAAD) awarded to F.F.; grants from the EMBO Young Investigator Programme (YIP) and the Action Thématique et Incitative sur Programme (ATIP) from the Centre National de la Recherche Scientifique (CNRS) to A.S. Financial support comes from the state of Saxony Anhalt, the Deutsche Forschungsgemeinschaft (DFG), Graduate Training Center GRK1026 ‘Conformational Transitions in Macromolecular Interactions’ at Halle and the Leibniz Institute of Plant Biochemistry (IPB) at Halle, Germany. The GABI-Kat project (German Plant Genomics Program—Köln *Arabidopsis* T-DNA lines) provided the *ttg1* T-DNA line via NASC—The European *Arabidopsis* Stock Centre. We thank Dieter Lange for assistance in western blotting, Petra Majovsky for LC–MS analyses, Hugo Stocker for his advice and Angela Baer and Anna Maria Strässle Eugster for technical support during the fly work. We are thankful to Petra Jansen, Sabine Voigt and Philipp Plato for their excellent greenhouse support at Halle. We thank Annika K. Weimer for constant support; Andreas Bachmair for the *prt1* mutant and initial discussions; Luz Irina A. Calderón Villalobos, Moritz K. Nowack, Nikolay Rozhkov, Christof Taxis, Michael Knop, Masato Kanemaki and the members of N.D.’s lab for advice and comments on the manuscript. The publication of this article was funded by the Open Access fund of the Leibniz Association.

Author contributions

N.D. and A.S. planned the project and N.D. wrote the manuscript and compiled the display items; N.D. designed the degron cassettes, tested and identified the functional It-degron cassette and performed plant and protein work for TTG1 and CO together with T.R.; F.F. contributed the GUS, TEV and GFP work in *Arabidopsis*; S.M. and

F.F. contributed protein work in tobacco and transcript analyses; N.D. contributed the developmental and protein analysis of TTG1 and CO. K.N. prepared and performed experiments in cell culture together with F.F.; K.N. prepared and performed experiments in *Drosophila* flies together with I.A.; M.S.F., J.H. and R.J.D. contributed mutant DHFR variants; R.J.D. planned and tested the *S. cerevisiae* constructs; W.H. analysed protein samples by LC-MS; W.B. modelled the DHFR variants. All authors discussed the results and contributed in the finalization of the manuscript. Responsibility for figures and related experiments: Figs 1a,b,c,e, 2a,b and 3b, and Supplementary Figs 1, 2, 3b,c,d,f,g, 5 and 7, N.D.; Figs 1f, 3c, 4, 5 and 7a–c, and Supplementary Figs 3e, 4, 6 and 7a,b, F.F.; Figs 1d, 2c and 3a, and Supplementary Figs 3a,b, T.R.; Fig. 5 and Supplementary Figs 3e and 4a–c,e.g, S.M.; Fig. 6, R.J.D., M.S.F., J.H.; Fig. 7d, I.A., K.N.; Supplementary Fig. 5a–c,e–i, W.B.; Supplementary Fig. 7c, W.H.

Additional information

Supplementary Information accompanies this paper at <http://www.nature.com/naturecommunications>

Competing financial interests: The Technology Offices at the Leibniz Institute of Plant Biochemistry (IPB) and at the Centre national de la recherche scientifique (CNRS) have

filed a patent application on behalf of N.D. and A.S. based on the findings described in this manuscript. The remaining authors declare no competing financial interests.

Reprints and permission information is available online at <http://npg.nature.com/reprintsandpermissions/>

How to cite this article: Faden, F. *et al.* Phenotypes on demand via switchable target protein degradation in multicellular organisms. *Nat. Commun.* 7:12202 doi: 10.1038/ncomms12202 (2016).



This work is licensed under a Creative Commons Attribution 4.0 International License. The images or other third party material in this article are included in the article's Creative Commons license, unless indicated otherwise in the credit line; if the material is not included under the Creative Commons license, users will need to obtain permission from the license holder to reproduce the material. To view a copy of this license, visit <http://creativecommons.org/licenses/by/4.0/>

© The Author(s) 2016

2.4 OUTLOOK PART II – BIOTECHNOLOGY

We aim to further find genetic and biotechnological applications or in conditional genetics where the It-degron technology can be used. We will apply the It-degron to generate conditional alleles in investigating lethal or developmentally impaired mutations and for novel genetic tools lifting conditional genetics in plants to a new level. Examples that we have generated in this context are conditional alleles for core cell division regulators, namely CDKA;1 and cyclins, epigenetics (FERTILIZATION INDEPENDENT ENDOSPERM, FIE), core flower development transcription factors LEAFY and AGAMOUS and also a conditional ribonuclease BARNASE. The conditional cytotoxic alleles are also tested heterologously in relevant strains of *Saccharomyces cerevisiae* including N-end rule mutants and can be used in living plants to generate genetic sectors by directed, tissue type-specific cell ablation. In a collaboration with John Doonan, Aberystwyth University, UK, we investigate conditional restoration of mutants of EUKARYOTIC TRANSLATION INITIATION FACTOR 4A1 (EIF4A1) with switchable CDK alleles.

We are generating plant lines harboring conditional CRISPR-Cas9 by engineering a switchable Cas9, conditional synthetic TALE effectors (dTALE). These enabling technologies have the potential to tune genome editing tools and the It-degron is an ideal method to conditionally complement null mutants generated by CRISPR-Cas9 or TALENs.

We use '*conditional reaction compartments*' such as It-degron-inducible trichomes as microfactories for small molecules and a novel modular tool in *Synthetic Biology*. We also aim to transfer the conditional protein accumulation technique to tomato and tobacco to harness their glandular trichomes as microfactories and to tobacco and barley to use leaf or endosperm tissue for target protein production.

A good example for combining our research in the local research landscape of the University of Halle is our recently funded Landesschwerpunkt project on genetic reprogramming by using temperature-inducible artificial alleles of transcription factors, core cell cycle regulators and proteasome subunits. In an industry collaboration with PlantForm Corporation, Ontario, Canada, it links conditional genetics via modulated proteolysis with biotechnological applications (co-PI Sacha Baginsky, Halle).

3 CONCLUSION

A key question in plants is to understand the roles of proteome dynamics, especially how the regulation of protein stability contributes to developmental processes and to the response of plants to environmental signals. In recent years, the N-end rule pathway has emerged as a key player in these different processes. However, in particular, the N-terminal proteome (N-terminome) with a potentially direct influence on protein half-life and therefore protein functions is underexplored, partially due to the lack of tools, methods and protocols.

Genetic approaches have revealed a wide range of functions of the N-end rule pathway in plants. Despite this major advance, which includes the discovery of the ERFVII transcription factors as the first substrates of this pathway, the number of potential N-end rule substrates identified remains small. This is largely the result of technical limitations of proteomics approaches, the possible restricted spatial and temporal accumulation of N-end rule substrates, as the generation of these substrates often requires specific endogenous or exogenous triggers such as a stress or developmental cues that lead to endoproteolytic cleavage by proteases, and the lack of knowledge of protease cleavage sites in plants and the identity of the neo-N-termini. In other words, 'conditional' substrates could remain invisible under standard conditions due to dormant N-degrons.

Current bottlenecks are the completeness of databases, their accurateness, and their interpretation in terms of the certainty of the described neo-N-termini. Besides that, systematic and in-depth identification and quantification of co- and posttranslational N-terminal protein modifications are lacking albeit represent the key for regulation of protein homeostasis (proteostasis).

In the future, improvements in proteomics techniques aimed at analyzing N-terminal residues and their modifications (N-terminomics), will contribute to the identification of N-end rule substrates and hence to our understanding of the molecular mechanisms underlying many of the new functions of the N-end rule pathway. For example, the only known function of the N-recognin PRT1 is related to the regulation of plant-pathogen responses, but the substrates responsible for the increased susceptibility of *prt1* mutants remain unknown.

In summary, the N-end rule pathway represents a central field of investigation to understand the role of protein degradation in plants. It has strong implications for our understanding of proteome dynamics and has an impact on traits relevant for agronomy. The pathway is a target for plant breeding as altering substrates and enzymes levels can positively influence environmental stress tolerance (e.g. tolerance to waterlogging) and increase plant growth and yield .

Furthermore, easy manipulation of turn-over rates of recombinant target proteins by using temperature-inducible N-degrons indicates that the N-end rule pathway is also a valuable tool for biotechnological approaches. Several substrate candidates with highly diverse biological roles exist but we do not know if, how and why they are degraded.

We will continue integrating these fragments into a global picture of plant proteolysis networks and exploit the experimental systems established in my lab and in collaborations as well as the scientific networks that have been built. We have readily set up

all experimental approaches covering the identification and characterization of N-end rule enzymes and substrates as well as towards application of the degron tool in synthetic biology to manufacture pharmaceuticals, diagnostics or industrials on protein and small compound level.

REFERENCES

- Dissmeyer, N., and Schnittger, A.** (2016). Rapid depletion and reversible accumulation of proteins *in vivo*. **Patent No. EP3061820 A1**
- Dissmeyer, N., Rivas, S., and Graciet, E.** (2017). Life and death of proteins after protease cleavage: protein degradation by the N-end rule pathway. *New Phytol.*
- Dong, H., Dumenil, J., Lu, F.H., Na, L., Vanhaeren, H., Naumann, C., Klecker, M., Prior, R., Smith, C., McKenzie, N., Saalbach, G., Chen, L., Xia, T., Gonzalez, N., Seguela, M., Inze, D., Dissmeyer, N., Li, Y., and Bevan, M.W.** (2017). Ubiquitylation activates a peptidase that promotes cleavage and destabilization of its activating E3 ligases and diverse growth regulatory proteins to limit cell proliferation in *Arabidopsis*. *Genes Dev* **31**, 197-208.
- Faden, F., Eschen-Lippold, L., and Dissmeyer, N.** (2016a). Normalized Quantitative Western Blotting Based on Standardized Fluorescent Labeling. *Methods Mol Biol* **1450**, 247-258.
- Faden, F., Mielke, S., Lange, D., and Dissmeyer, N.** (2014). Generic tools for conditionally altering protein abundance and phenotypes on demand. *Biol Chem* **395**, 737-762.
- Faden, F., Ramezani, T., Mielke, S., Almudi, I., Nairz, K., Froehlich, M.S., Hockendorff, J., Brandt, W., Hoehenwarter, W., Dohmen, R.J., Schnittger, A., and Dissmeyer, N.** (2016b). Phenotypes on demand via switchable target protein degradation in multicellular organisms. *Nat Commun* **7**, 12202.
- Klecker, M., and Dissmeyer, N.** (2016). Peptide Arrays for Binding Studies of E3 Ubiquitin Ligases. *Methods Mol Biol* **1450**, 85-94.
- Majovsky, P., Naumann, C., Lee, C.W., Lassowskat, I., Trujillo, M., Dissmeyer, N., and Hoehenwarter, W.** (2014). Targeted proteomics analysis of protein degradation in plant signaling on an LTQ-Orbitrap mass spectrometer. *J Proteome Res* **13**, 4246-4258.
- Mot, A.C., Prell, E., Klecker, M., Naumann, C., Faden, F., Westermann, B., and Dissmeyer, N.** (2017). Real-time detection of N-end rule-mediated ubiquitination via fluorescently labeled substrate probes. *New Phytol.*
- Naumann, C., Mot, A.C., and Dissmeyer, N.** (2016). Generation of Artificial N-end Rule Substrate Proteins In Vivo and In Vitro. *Methods Mol Biol* **1450**, 55-83.
- Potuschak, T., Stary, S., Schlogelhofer, P., Becker, F., Nejnskaia, V., and Bachmair, A.** (1998). PRT1 of *Arabidopsis thaliana* encodes a component of the plant N-end rule pathway. *Proc Natl Acad Sci U S A* **95**, 7904-7908.
- Stary, S., Yin, X., Potuschak, T., Schlogelhofer, P., Nizhynska, V., and Bachmair, A.** (2003). PRT1 of *Arabidopsis* is a ubiquitin protein ligase of the plant N-end rule pathway with specificity for aromatic amino-terminal residues. *Plant Physiol* **133**, 1360-1366.

Venne, A.S., Solari, F.A., Faden, F., Paretti, T., Dissmeyer, N., and Zahedi, R.P. (2015). An improved workflow for quantitative N-terminal charge-based fractional diagonal chromatography (ChaFRADIC) to study proteolytic events in *Arabidopsis thaliana*. *Proteomics* **15**, 2458-2469.

White, M.D., Klecker, M., Hopkinson, R.J., Weits, D.A., Mueller, C., Naumann, C., O'Neill, R., Wickens, J., Yang, J., Brooks-Bartlett, J.C., Garman, E.F., Grossmann, T.N., Dissmeyer, N., and Flashman, E. (2017). Plant cysteine oxidases are dioxygenases that directly enable arginyl transferase-catalysed arginylation of N-end rule targets. *Nat Commun* **8**, 14690.

ACKNOWLEDGEMENT

I would like to thank the funding organizations who have supported research in my lab, especially the German Research Foundation (DFG) and the ScienceCampus Halle – Plant-based Bioeconomy. I want to thank the IPB – the Leibniz Institute of Plant Biochemistry for supporting us over the years with the luxury of an own, fully equipped, independent laboratory and the marvelous core infrastructure at the IPB ranging from its plant growth facilities, the proteomics service, the instrumentation, an efficient administration and funds for inviting many exciting speakers in frame of the ‘IPB Seminar Series in Plant Biochemistry’.

The work, however, would never have been so exciting and fruitful without my collaborators whom I mentioned earlier on and – especially – my students in the lab, at the forefront Frederik Faden, Christin Naumann, Maria Klecker, Pavel Reichman and Stefan Mielke.

Thank you.

ERKLÄRUNG

Versicherung an Eides Statt

Ich, Dr. Nico Dissmeyer, versichere hiermit an Eides Statt durch meine Unterschrift, dass ich meine Habilitationsschrift selbständig und ohne fremde Hilfe verfasst, andere als die angegebenen Quellen und Hilfsmittel nicht benutzt und die den benutzten Werken wörtlich oder inhaltlich entnommenen Stellen als solche kenntlich gemacht habe.

Ich versichere an Eides Statt, dass ich die vorgenannten Angaben nach bestem Wissen und Gewissen gemacht habe und dass die Angaben der Wahrheit entsprechen und ich nichts verschwiegen habe.

Die Strafbarkeit einer falschen eidesstattlichen Versicherung ist mir bekannt, namentlich die Strafandrohung gemäß § 156 StGB bis zu drei Jahren Freiheitsstrafe oder Geldstrafe bei vorsätzlicher Begehung der Tat bzw. gemäß § 163 Abs.1 StGB bis zu einem Jahr Freiheitsstrafe oder Geldstrafe bei fahrlässiger Begehung.

Seoul, 5. Juli 2017

Dr. Nico Dissmeyer

CURRICULUM VITAE

NAME: Nico Dissmeyer, Dr. rer. nat.
CURRENT POSITION: Independent Junior Research Group Leader
OFFICE ADDRESS: Leibniz Institute of Plant Biochemistry (IPB)
Independent Junior Research Group on
Protein Recognition and Degradation
Weinberg 3
D-06120 Halle (Saale), Germany
DATE OF BIRTH: May 11, 1979 in Detmold, Germany
FAMILY STATUS: one son, Veit Enno, * July 6, 2014 in Halle (Saale)
PRIVATE ADDRESS: Burgstrasse 2, D-06114 Halle (Saale), Germany
NATIONALITY: German

EDUCATION & PROFESSIONAL POSITIONS

since 2011 Principal Investigator, Head of Independent Junior Research Group
"Protein Recognition and Stability", Leibniz Institute of Plant Biochemis-
try, Halle, Germany
2009 – 2010 Postdoctoral Researcher, Cell and Developmental Biology, Institut de
Biologie Moléculaire des Plantes (IBMP) du CNRS, Strasbourg, France
2005 – 2009 Graduate (Ph.D.) Student, Max Planck Institute for Plant Breeding Re-
search, Cologne; 10/2009 *Dr. rer. nat.* (biochemistry), University of Co-
logne, Germany
2004 – 2005 Graduate Student (Diplom), Max Planck Institute for Plant Breeding
Research; 05/2005 "Diplom-Biochemiker", Free University of Berlin,
Germany
2000 – 2003 Graduate Research Assistant, Dept. of Biochemistry and Biophysics,
Oregon State University, Corvallis, USA; Undergraduate Research As-
sistant, Center for Plant Molecular Biology (ZMBP), Eberhard Karls Uni-
versity of Tübingen, Germany
1999 – 2005 Biochemistry and biophysics, Eberhard Karls University of Tübingen,
Germany; Oregon State University, Corvallis, USA; Free University of
Berlin, Germany

Halle (Saale), 7/5/2017

Nico Dissmeyer

